UNIVERSITY OF LONDON

Imperial College of Science and Technology
Royal College of Science
Department of Physics
Applied Optics Section

THE ANALYSIS OF SURFACE TEXTURE BY GONIOSPECTROPHOTOMETRY

by

Michael Peter Wassall

Thesis submitted for the degree of Doctor of Philosophy of the University of London.

1972

ABSTRACT.

Methods, both physical and subjective in nature, for assessing the effect of surface texture of materials on their light reflecting properties are discussed and colorimetric techniques of analysing such data considered.

Since the appreciation of surface texture is essentially a visual phenomenon, the variation of reflected light with angle must convey much of this information. In this context it is held that such variations may be considered to be basically in colour and luminance.

The latter two parameters are investigated both over angular ranges and at various locations upon the surface of naturally occurring specimens of differing texture. In particular the effects on colorimetric properties of both randomly rough and periodically rough sample surfaces are considered, together with variations in gloss content.

Data from the investigation are used to assess the capability of colour media to reproduce with accuracy the parameters responsible for faithful texture appreciation, and a useful method of assessment is quantitatively considered with respect to reversal and negative colour photography.

Further treatment of the angular light reflecting properties from a material can only be considered with extremely detailed knowledge of the specimen construction. The Morpho butterfly wing provides a natural material of outstanding colour properties and texture. The results of recent scanning electron microscope studies on the insect

are used to provide a detailed explanation of the angular chromaticity and luminance distributions measured on the material with reference to interference and diffraction theory. Other structural colours are discussed to obtain further information on such iridescent samples.

CONTENTS.

Chapter 1.	Colour Specification and Measuring Techniques.	4.
Chapter 2.	Background and Aims of the Present Work.	25.
Chapter 3.	Sources of Error and Their Treatment.	45.
Chapter 4.	The Effect of Surface Roughness on Goniospectrophotometric Data.	65.
Chapter 5.	Colorimetric Aspects of Surface Texture.	106.
Chapter 6.	The Colour Reproduction of Surface Texture.	143.
Chapter 7.	The Colorimetric and Physical Properties of a Particular Surface Texture and Structure The Morpho Butterfly Wing.	177.
Chapter 8.	Theoretical Interpretations of The Morpho Wing Structure.	219.
	Appendix.	271.
	References.	282.
	Acknowledgements.	286.

CHAPTER ONE.

COLOUR SPECIFICATION AND MEASURING TECHNIQUES.

1.1 Colour Specification.

The number of possible colours discernable by the normal human eye is very large, and in an attempt to specify any particular colour sensation with both accuracy and ease it is necessary to reduce this information to a few variables. The analysis is greatly simplified since any given colour may be represented by three variables, this being attributed to the presence of three receptive channels in the human visual system with different spectral sensitivities. The variables may, for example, be three primary stimuli upon which few restrictions are placed and could therefore be spectral distributions of light obtained from filters or pure spectral colours. To express this quantitatively using vector notation, a particular colour $\underline{C}_1$ is given by

$$\underline{C}_1 = R_1\underline{R} + G_1\underline{G} + B_1\underline{B} \qquad \text{.....(1.1)}$$

where $\underline{R}$, $\underline{G}$ and $\underline{B}$ are the unit vector quantities of the three primaries in this so called ($\underline{RGB}$) system. It is then customary to give the name tristimulus values to the quantities R_1, G_1 and B_1. Similarly a second colour $\underline{C}_2$ may be expressed as a match of the same primaries in different proportions, so that

$$\underline{C}_2 = R_2\underline{R} + G_2\underline{G} + B_2\underline{B} \qquad \text{.....(1.2)}$$

It is possible to specify the quantities $\underline{R}$, $\underline{G}$ and $\underline{B}$ in normal photometric units such as lumens, but in order to

simplify further work a somewhat different approach may be used. A suitable white light is normally specified such as an equal energy spectrum, and since this conveys the idea of a 'colourless' object the tristimulus values are made equal for this colour by suitable scaling of $\underline{R}$, $\underline{G}$ and $\underline{B}$.

Experiments on mixing three coloured lights were summarised by Grassmann (1853), (Judd and Wyszecki, 1963) in laws which form the basis of all modern colorimetry, and from which the concept of additivity follows. That is if the colour $\underline{C}_1$ in equation (1.1) above, with tristimulus values R_1, G_1, B_1, is added to colour $\underline{C}_2$, tristimulus values R_2, G_2, B_2, a third colour, $\underline{C}_3$, is obtained

$$\underline{C}_3 = \underline{C}_1 + \underline{C}_2 = R_3\underline{R} + G_3\underline{G} + B_3\underline{B} \qquad \ldots\ldots(1.3)$$

whose tristimulus values are the sums of the corresponding tristimulus values of the two component colours, so that

$$R_3 = R_1 + R_2$$
$$G_3 = G_1 + G_2$$
$$\text{and } B_3 = B_1 + B_2$$

In general this will hold for more than two colour mixtures so that

$$R = \sum_{i=1}^{n} R_i \qquad \text{etc.}$$

This is only applicable when using foveal fields of 2° angular subtense or less, and breaks down under conditions of very high or very low luminance.

The tristimulus values may now be reduced to a two dimensional representation by the normalising process, thus

$$r = R \;/\; (R+G+B)$$

$$g = G / (R+G+B)$$

$$b = B / (R+G+B)$$

and so

$$r + g + b = 1$$

This linear relationship means that only two quantities are necessary and sufficient to specify uniquely any colour $\underline{C}$ and so information must therefore have been lost in the process concerning actual magnitudes. This now enables a two dimensional plot to be made of say r versus g in rectangular coordinates, and any given colour will occupy an exact point in this diagram. The quantities r, g and b are then referred to as the chromaticity coordinates of a particular colour and the diagram in which they are plotted, the chromaticity diagram. It follows from the law of additivity that any mixture of two colours will lie on a straight line joining the two colours in such a diagram, the exact point being determined directly by the proportions of each in the mixture.

Since there are many possible sets of primaries it is most important to be able to perform transformations between different sets. In order to do this the relationships

$$\underline{R} = x_R\underline{X} + y_R\underline{Y} + z_R\underline{Z}$$

$$\underline{G} = x_G\underline{X} + y_G\underline{Y} + z_G\underline{Z}$$

$$\underline{B} = x_B\underline{X} + y_B\underline{Y} + z_B\underline{Z}$$

must be known and it is then possible to form an equation similar to (1.1) giving

$$\underline{C}_1 = X_1\underline{X} + Y_1\underline{Y} + Z_1\underline{Z}$$

where X_1, Y_1 and Z_1 are the new tristimulus values of

colour $\underline{C}_1$ in the ($\underline{XYZ}$) system.

1.2 Colour Matching Properties of the Human Visual System.

It is now important and necessary to consider the colour matching properties of the human visual system, and since some variations are bound to occur from one observer to another, even excluding defective observers, the average data of several experiments must be obtained.

In 1931 the C.I.E. defined the spectrum locus shown in Fig.1.1 to be representative of a standard observer's colour matching properties in terms of the three stimuli 700, 546.1 and 435.8 nanometers wavelength, with the units based on an equal-energy white, E, situated at the centroid of the $\underline{RGB}$ triangle. These data were based on separate experiments by Wright (1928-29) and Guild (1931) and transformed to the new primary stimuli from their own particular choice of stimuli.

Two main points are worthy of consideration in this diagram. Firstly, the locus falls on or outside the $\underline{RGB}$ triangle meaning that one of the chromaticity coordinates is zero or negative. The physical meaning of this is that a certain amount of one of the primaries must be added to the test field before a match can be achieved by the observer, and thus if $\underline{C}$ is the test colour which had to be desaturated by, say, $\underline{R}$ we get

$$\underline{C} + R'\underline{R} = R\underline{R} + G\underline{G} + B\underline{B}$$

The tristimulus values of $\underline{C}$ are R-R', G and B, where R-R' is a negative quantity, leading to a negative chromaticity coordinate.

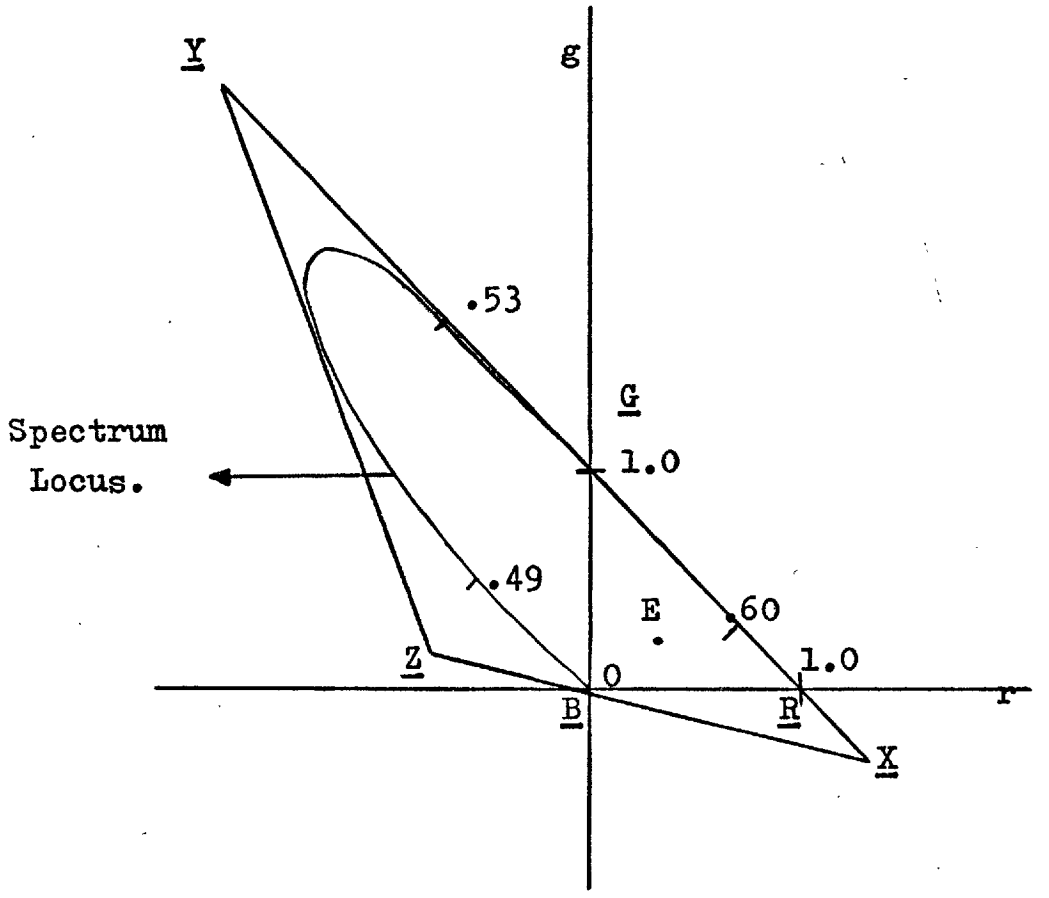


Fig. 1.1 Spectrum locus based on the three stimuli 700, 546.1 and 435.8 nm.

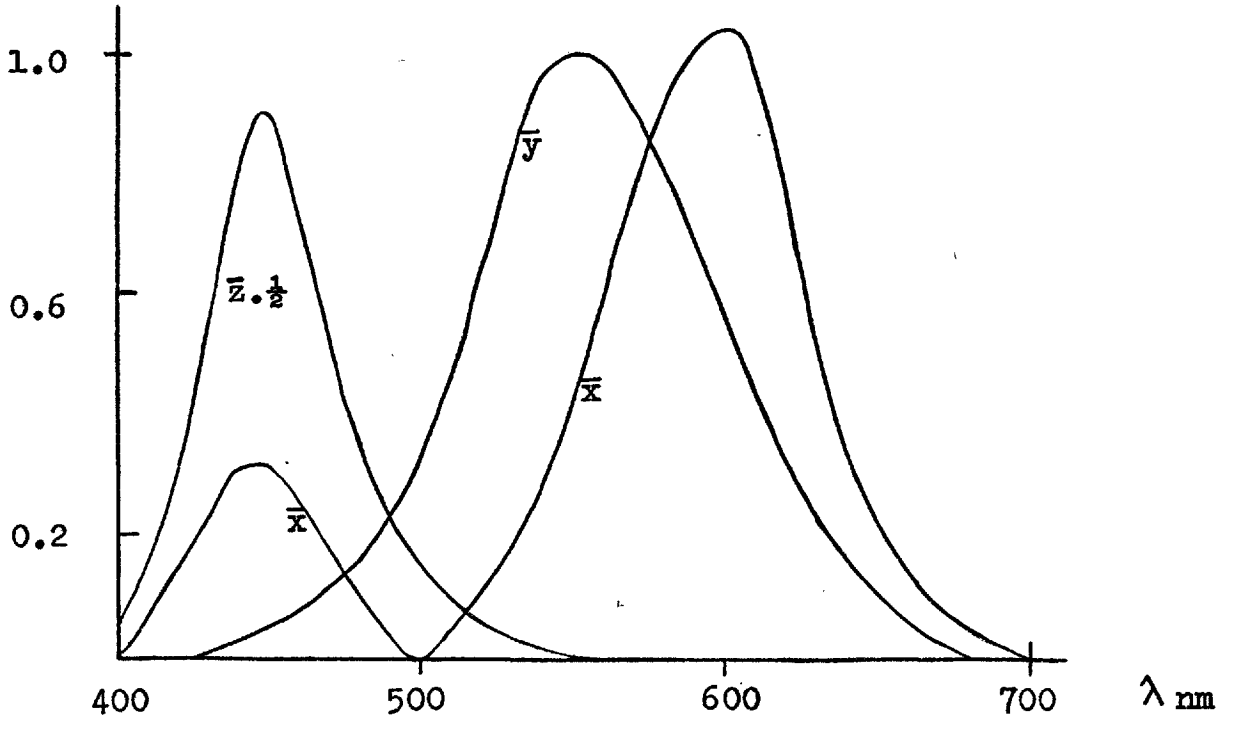


Fig. 1.2 C.I.E. (1931) distribution coefficients.

Secondly, since all real colours are a mixture of spectral colours, and the spectrum locus is everywhere concave, all real colours must lie inside the area bounded by this locus and the line joining its ends.

To aid computation and avoid the possible omission of negative signs it would be preferable to have a system in which the entire spectrum locus fell within the positive quadrant. For this reason stimuli X, Y and Z in Fig.1.1 were finally adopted by the C.I.E. on the recommendation of Judd, since considering the triangle X, Y, Z, the spectrum locus lies entirely on or within it. The final restriction placed upon points X, Y and Z to determine their exact positions were that X and Z primaries should have zero luminance and therefore that points X and Z should lie on the so called Alychne, a concept first introduced by Schrödinger (1925) and followed up by Judd in 1930. This system then has the great advantage that all luminance information is contained in the Y tristimulus value, calculation of which will directly give the luminance factor of a surface colour or the transmission factor of a filter.

The basic 1931 C.I.E. tables listing both the chromaticity coordinates x_λ, y_λ, and z_λ and the spectral tristimulus values $\bar{x}_\lambda$, $\bar{y}_\lambda$, and $\bar{z}_\lambda$ are extensively quoted in the literature, (see for example Wyszecki and Stiles (1967) or Wright (1969)) usually over a wavelength range of 380 nm to 780 nm. The spectral tristimulus values, also known as distribution coefficients or colour matching functions, are illustrated in Fig.1.2, and by plotting the

x_λ, y_λ values the spectrum locus is obtained in the x-y plane as in Fig.1.3.

1.3 The 1931 C.I.E. Chromaticity Diagram.

The important diagram obtained in Fig.1.3 -the 1931 C.I.E. chromaticity diagram - will be referred to continuously throughout the thesis and several points are worth some discussion at this stage. The coordinates of the standard illuminants S_A, S_B and S_C, corresponding to colour temperatures 2854, 4870 and 6740°K, are shown together with the equal-energy white, E, at the centroid of the triangle.

To define a colour C, the chromaticity coordinates (x,y) may be quoted, but perhaps a more immediately recognisable method would be to quote a second pair of coordinates, namely dominant wavelength and purity. If a straight line is drawn from the illuminant, say (x_c,y_c), through the colour C to meet the spectrum locus at a point (x_d,y_d), the wavelength on the locus at this point is referred to as the dominant wavelength, λ_d. The distance of the point C along the line $S_C\,\lambda_d$ is then taken as a measure of the purity of this particular colour and may be calculated from either

$$p_e = \frac{(x - x_c)}{(x_d - x_c)} \qquad \text{or} \qquad p_e = \frac{(y - y_c)}{(y_d - y_c)}$$

Strictly this is the excitation purity of the colour, another scale sometimes used being colorimetric purity, which is obtained by multiplying the above quantity with a factor (y_d/y), thus

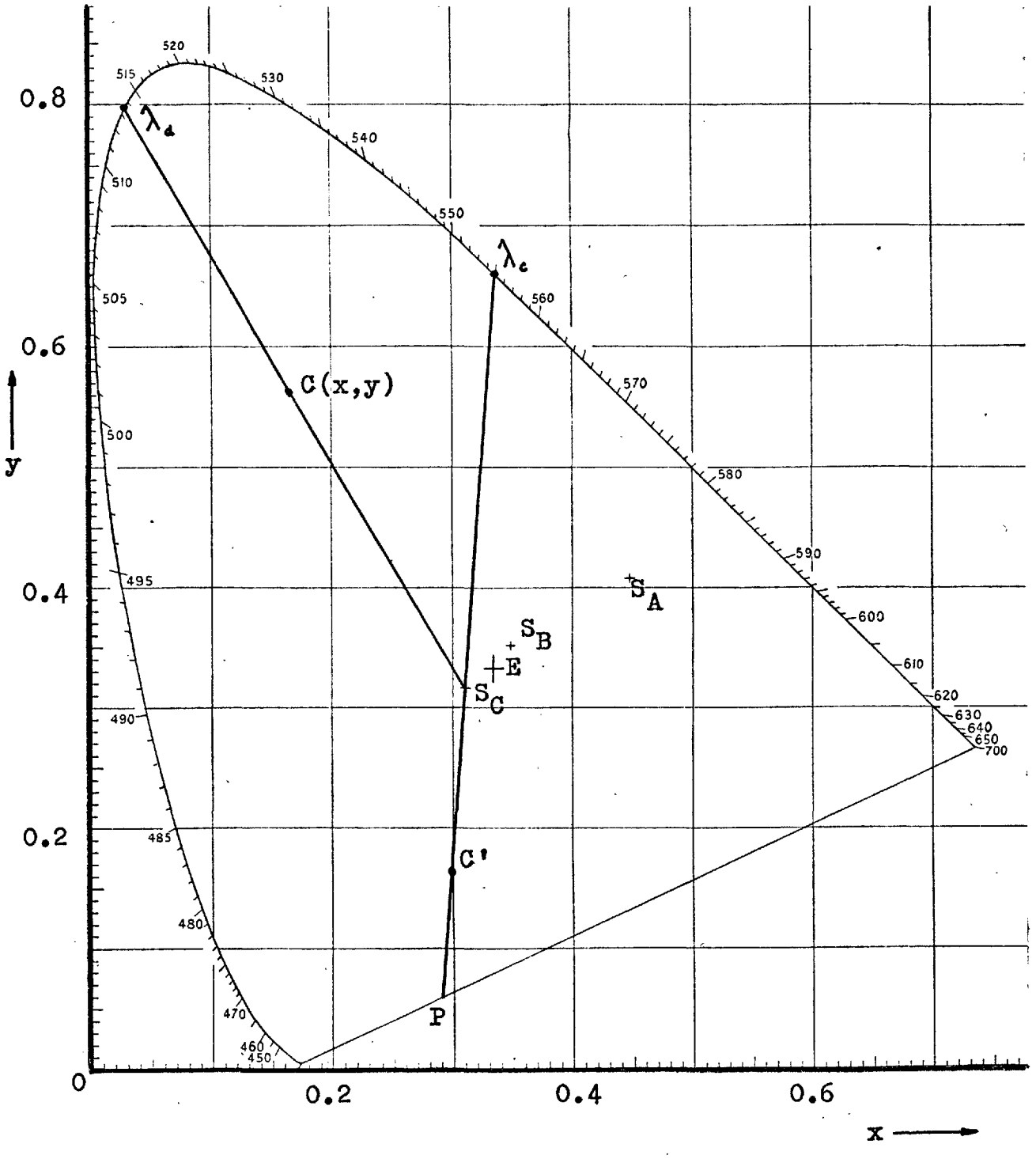


Fig. 1.3 C.I.E. (1931) Chromaticity Diagram.

$$p_c = \frac{y_d}{y} \cdot p_e$$

For the colours in the purple segment of the diagram the line must be continued back through the illuminant point giving a so called complementary wavelength at λ_c on the spectrum locus, although the purity is still the ratio of the distances $C'S_C$ and PS_C.

Similar data for larger fields than 2^o angular subtense have since been recommended (C.I.E.,1963) based on the work of Stiles (1955) (Stiles and Burch, 1959) and Speranskaya (1959).

1.4 Formulation of Object Colours.

In an attempt to specify exactly the colour of a surface, or of the light transmitted by a filter, on the chromaticity diagram, it is necessary to consider what happens when light strikes this surface.

The amount of energy reflected by an object over a wavelength range $d\lambda$ will be

$$P_\lambda \cdot \rho_\lambda \cdot d\lambda$$

where P_λ is the amount of energy striking the sample per unit wavelength interval and ρ_λ its reflection factor for that wavelength. The tristimulus values X, Y and Z of that reflected light will therefore be of the form

$$X = k\int P_\lambda \cdot \rho_\lambda \cdot \bar{x}_\lambda \cdot d\lambda \qquad \text{etc.....(1.4)}$$

replacing $\bar{x}_\lambda$ by $\bar{y}_\lambda$ and $\bar{z}_\lambda$ to give Y and Z. k is a constant whose value is unimportant since the eye will adapt to changes in the overall illumination level and we need only

therefore measure the tristimulus values relative to a perfect reflector under the same illumination. It can be shown that a summation rather than an integration is sufficiently accurate, so long as the wavelength interval is reasonably small, say less than 10 nm. Thus equation 1.4 may be replaced by

$$X = k\sum P_\lambda \cdot \rho_\lambda \cdot \bar{x}_\lambda \cdot \Delta\lambda$$
$$Y = k\sum P_\lambda \cdot \rho_\lambda \cdot \bar{y}_\lambda \cdot \Delta\lambda \quad \ldots\ldots\ldots(1.5)$$
$$Z = k\sum P_\lambda \cdot \rho_\lambda \cdot \bar{z}_\lambda \cdot \Delta\lambda$$

Since P_λ is a function of the illuminant, tables of $(k.P_\lambda .\bar{x}_\lambda .\Delta\lambda)$, $(k.P_\lambda .\bar{y}_\lambda .\Delta\lambda)$ and $(k.P_\lambda .\bar{z}_\lambda .\Delta\lambda)$ are available for several standard illuminants adopted by the C.I.E. in 1931, giving values of the three functions at wavelength intervals of 10nm or less throughout the visible spectrum. (O.S.A. 1953, Wyszecki and Stiles(1967) and Wright (1969)). The tables are usually scaled to give Y a value of 100 for a perfect reflector, whose value of ρ_λ will be unity at all wavelengths. The tristimulus values of a surface may then be obtained by measuring its value of ρ_λ at several points throughout the spectrum, and performing the necessary computations. The chromaticity coordinates (x,y,z) are then obtained by normalising the values of X,Y and Z. Asurface colour is usually specified by Y, x and y, since the former gives the luminance value and the latter pair of values its location in colour space.

It would seem possible therefore that two or more samples having different spectral reflection functions may, under certain illuminating spectral distrib-

utions, sum to give the same X, Y and Z values. Such samples do occur and are called metamers.

1.5 Recommendations for Colour Measurement.

The intensity of reflected light from a surface will in general vary with both angle of incidence and angle of collection, and it is therefore necessary when measuring a sample relative to a calibrated standard to measure both under identical angular conditions. Because of this variation the C.I.E. in 1931 specified certain measuring configurations and standards for accurate spectrophotometry, namely

i) 45° angle of incidence and normal collection to sample or vice versa, since this should relate closely to what is seen, due to the exclusion of any specular reflection,

and ii) the use of magnesium oxide as a standard, since it has a luminance factor approximately equal to 100 throughout the visible spectrum and is almost a perfect diffuser. A perfect diffuser obeys Lambert's Law, the intensity of reflected light being proportional to the cosine of the angle of collection, thus luminance is a constant.

Under this recommendation other luminance factors would be quoted relative to that of magnesium oxide. There have been many attempts to measure the absolute luminance factor of magnesium oxide samples, prepared by depositing the smoke from burning magnesium onto metal substrates. Quite large variations occur, it

being generally found that a value somewhat less than 100 is obtained and some slight wavelength dependence noted. Although some of the discrepancies may be put down to different preparation techniques several other notable points arise. The thickness of the deposited layer was found to be of importance by Tellex and Waldron (1955) and variations of up to 0.5% were found by Middleton and Sanders (1951) in samples prepared identically. Gibson and Keegan (1938) (Gibson, 1949) reported a decrease in luminance factor with time and explanations due to formation of $MgCO_3$ and absorption of water were put forward by Gordon-Smith (1952) and Blett-Talbot (1955) respectively. In 1959 therefore the C.I.E. recommended that magnesium oxide be used as a calibrated substandard and that all results be quoted with respect to a theoretical perfect diffuser. In 1967 (C.I.E., 1967) further recommendations were given concerning integrating sphere instruments and their geometry, together with acceptable angular discrimination of $45^\circ/0^\circ$ instruments.

The necessary component parts of a spectrophotometer for accurate colour measurement and specification without involving observer differences are now clear. The instrument must have a source of light containing all visible wavelengths followed by a dispersing system and some means of isolating monochromatic light throughout the spectrum. This beam must be incident on sample and standard in turn under identical angular conditions and a detecting system available, capable of accurately measuring the reflected or transmitted light from each specimen. The

required reflection factor at each wavelength may thus be obtained.

1.6 Goniophotometers.

Various characteristics of a surface determine the distribution of reflected light from that surface. In order to measure this distribution an instrument must have great flexibility in illuminating and viewing conditions over the complete hemisphere surrounding the surface. Perhaps the earliest attempt at building and using such an instrument was that by Bouguer in the 18th century for the investigation of matt surfaces. The goniophotometer has since been modified and improved by many succeeding workers, some being designed for special purposes, and attempts to reduce the number of polar luminance curves for particular problems have been put forward.

The necessary components of a goniophotometer are:

i) a source of illumination whose angle of incidence upon the sample may be varied continuously from grazing to normal incidence, on either side of the normal

ii) a detector whose angle of collection may similarly be varied, and whose receiver aperture restricted to definite dimensions

and iii) some means of reference to a calibrated standard under identical photometric conditions when required.

In addition a goniospectrophotometer must also include a dispersing system between source and detector to facilitate measurements under monochromatic

illumination throughout the visible spectrum.

The basic design of a goniophotometer is illustrated in Fig.1.4, showing a source S focussed on the entrance slit at A_1, a lens L_1 collimating the emergent beam onto the sample surface. The variable aperture at A_2, placed directly before the detector D, is at the focus of a second lens L_2 which collects the light scattered from the surface at this particular angle of viewing, r.

By comparing the reflected flux, measured at various angles of incidence and collection, with similar measurements from a calibrated standard it is possible to build up a family of polar reflection curves in different planes of incidence for a particular surface. Examples of such curves in one particular plane are shown in Fig.1.5 for three different surface types, the length of the radius vector in any one direction being proportional to the reflected intensity in that direction. It is possible to construct an instrument for absolute measurements, but more often relative reflection measurements are made by reference to a calibrated standard such as freshly smoked or pressed magnesium oxide.

1.7 Instrument Geometry.

Several geometric factors in the construction of a goniophotometer may influence the results obtained from that instrument. In particular the size of the illuminated patch on the sample, the angles of convergence of incident and collected beams, and receiver aperture size.

When there is any convergence or divergence

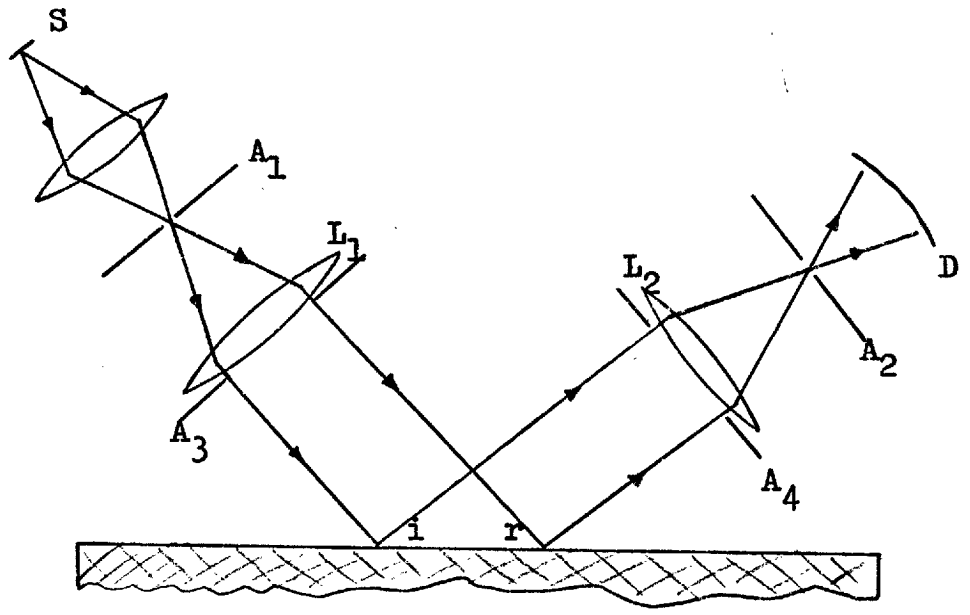


Fig. 1.4 A basic goniophotometer.

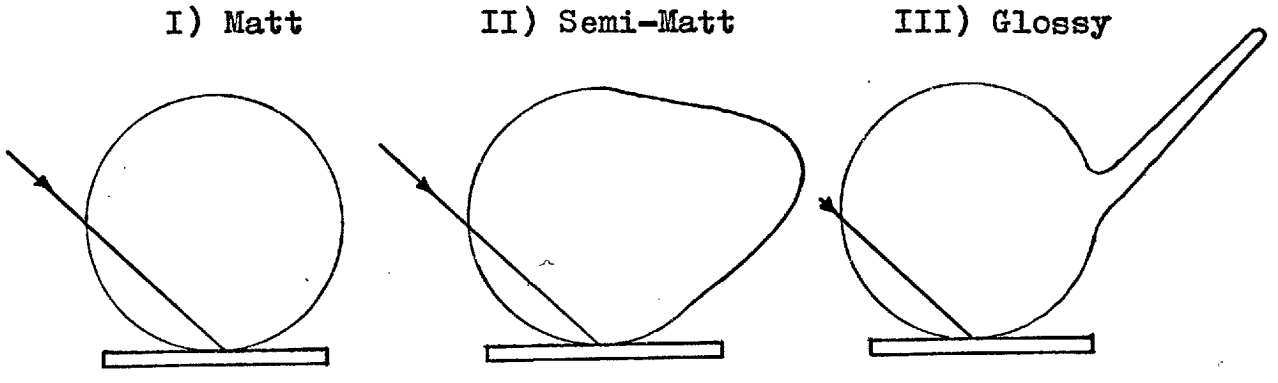


Fig. 1.5 Typical polar curves of reflected intensity for 45^{o} incidence.

of beams onto or from the sample this will inevitably lead to some spread in the angular values used throughout a polar curve, and only the mean angles will be specified. There is therefore an advantage in using collimated light at this point in the apparatus, although in the exceptional case of very small areas of illumination it is often necessary to use some convergence in the incident beam.

An increase in receiver aperture size has the effect of reducing the angular resolving power of the instrument, resulting in a flattening of any specular peaks in the polar luminance curve. To introduce some uniform method of measuring reflected light distributions several workers, notably Harrison (1950) and Nimeroff (1952), have suggested limiting dimensions to these quantities, although inevitably some recommendations apply to the measurement of specific materials.

The spectral content of the illuminating source has also been considered in some detail, but, since agreement between measured and visual observation depends to some extent on the colour of the sample as well as illuminant, no single source is completely adequate.

1.8 The Wright Spectrophotometer.

The instrument used for all spectrophotometric and goniospectrophotometric measurements was the Wright Spectrophotometer (Wright, 1954). A description follows and it can be seen that by suitable adjustment the instrument conforms to all the conditions normally specified for both precise spectrophotometry and precise goniophotometry. The

instrument has been modified for ease of operation and to improve the speed of data acquisition, so that this data may be processed directly by computer. The optical arrangement of the spectrophotometer is illustrated in Fig.1.6.

A tungsten ribbon filament lamp, run from a constant current supply, is imaged onto the entrance slit B by means of the achromatic condenser lens A. The slit is adjustable in both height and width, a field lens being placed directly in front of it to reduce vignetting in the system and ensure uniform illumination over the height of the spectrum. The two dispersing prisms C and D are separated from the entrance slit by several apertures at intervals, thus reducing the amount of scattered light in the instrument. Aperture Y restricts the cross-sectional area of the incident beam at the first prism face to 4.2cm * 5.0cm, and is placed directly after lens W of focal length 60cm. The dense flint prisms, each 10.5cm high and of 7.5cm and 8.75cm side respectively, disperse the light, forming a spectrum about 3cm in height and 25cm in length in the plane F at the focus of the lens E, focal length 115cm.

Here mirrors may be mounted on a long metal arm which pivots about a point beneath the first surface of the second prism. The lens E also turns with the arm, so that the mirror may run along the spectrum plane and select any desired waveband. A series of mirrors is available whose widths are 2mm, 5mm, 1, 2, 3, 4 and 5cm, so that any change of bandwidth on moving through the spectrum may be overcome if necessary, and the illumination level increased in, for example, the measurement of a very dense filter.

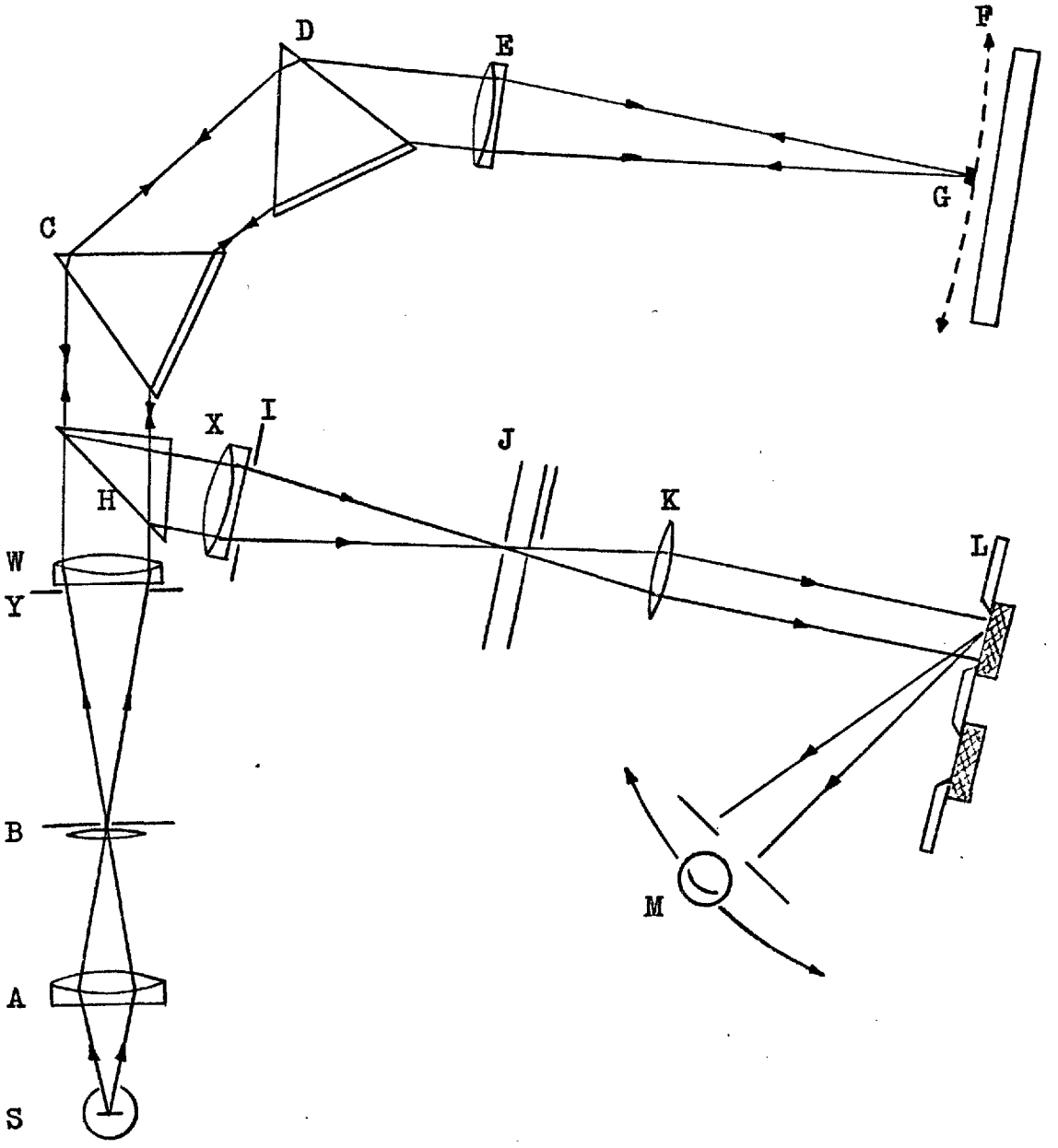


Fig. 1.6 The Wright Spectrophotometer.

All the mirrors are curved to the plane of the spectrum and thus have the same effect as a field lens in the plane of the spectrum. A continuous strip of mirror is also available so that, by methods described by Wright (1954), Boshoff (1957) etc., a template may be cut and the tristimulus values found directly by three measurements after suitable weightings for illuminant and sensitivity of the detector are taken into account. The rest of the spectrum is absorbed in two black plates mounted parallel, at 45° to the spectrum plane.

The waveband is reflected back from the mirror G, through the bottom half of the original prisms and finally reflected along the third branch of the instrument by means of a smaller prism H. This prism, which is only half the height of the original pair, may be rotated and tilted to bring the image of the entrance slit onto the exit slit. The instrument is thus a double monochromator. The aperture at I may be varied to alter the size of the final image, and again there are several fixed apertures between this and the exit slit J, as well as the objective X, identical to lens W. This exit slit is conjugate to the entrance slit and in construction they are identical, so that varying the size of the mirror in the spectrum plane only alters the final level of illumination, and bandwidth. Following this is a further lens K which collimates the beam as shown, a simple mechanical shutter being used to interupt it when necessary, for photomultiplier dark current readings etc..

The whole instrument is mounted on a rigid

cast iron base and covered by means of a blackened hard-board case, eliminating any back reflections through the instrument.

The samples are mounted on the table at L which can be moved in a plane at right angles to the monochromatic beam so that sample and standard may be alternated without any movement of the optics. This table may also rotate through 360° so that any angle of incidence on the sample may be obtained. An E.M.I. 9558A photomultiplier, selected for a good red response, has replaced the photocell as detector, and is mounted vertically at M with a 45° prism reflecting the light from the sample onto the photomultiplier cathode. The mounting M may also be rotated through 360° so that any angle of collection may be achieved and transmission measurements made.

In normal use the cross—sectional area of the beam incident on the sample is about 1.0cm * 0.8cm. This may be increased or decreased if necessary or, by use of a higher power lens at K, a reduced image of the exit slit J may be focussed on the sample. If the length of the exit slit is reduced, the illuminated area of the sample can be diminished to 1 sq mm or less, and this is the technique employed in several of the following measurements.

The H.T. supply to the photomultiplier dynode resistor chain was chosen for stability of output and the chain itself constructed from good quality resistors, housed in a separate metal box to minimise any fluctuations in the tube from heating, and complete the

earth shield. The photomultiplier anode current is measured by means of a digital voltmeter which monitors the voltage developed across a 1 megohm load resistor by this current. In order to reduce noise, mainly in the form of pick-up in cables and Shot noise in the photomultiplier tube, a capacitance of 10 microfarads is connected in parallel with the load resistor and may be switched in or out as required. This necessitates a certain 'rise time' of the order of a second between readings from zero. The voltage displayed on the digital voltmeter is passed to a serializer unit which trips the voltmeter at any required rate and converts the signal into a form suitable for a tape punch unit at its output. The values of voltage, or effectively anode current, are punched on five hole tape in Elliot Autocode and are then fed into an Elliot 803A computer for any necessary calculation.

CHAPTER TWO.

BACKGROUND AND AIMS OF THE PRESENT WORK.

Introduction.

When a beam of light strikes a surface many varied processes may take place, depending on its structure. If the surface is perfectly smooth the reflections, transmissions and absorbtions are straightforward obeying well known laws of optics. However, if the surface is optically rough scattering will take place, and any emergent reflected beam will be composed of scattered, diffracted, refracted and reflected elements.

It is possible to approach the problem of surface texture in many different ways. A rigorous mathematical approach may be used to obtain the reflected or transmitted light properties of certain materials or structures, but this is inevitably of only limited application. The mathematics involved become rapidly more complex for any but the simplest surfaces, and, unless successive approximations are employed, irregular or complicated structures are beyond the scope of such treatment.

Since the texture of a surface is essentially appreciated visually, with perhaps an exploratory touch with the fingers, the information concerning its structure must be obtained mainly from the reflected light viewed by the human eye. Invariably the best impression of texture is obtained by moving the head about so that effectively the viewing conditions are altered with respect to the

incident illumination, a condition which would suggest goniophotometry as an ideal method of investigation.

In the second part of the thesis a more mathematical approach to the problem of light interaction with a particular material is used in order to understand the reflection characteristics of the surface from which an observer would normally deduce the texture.

2.1 Surface Reflection Properties.

i) Smooth Surfaces.

The reflection properties of simple basic surfaces such as planes, spheres and thin film stacks are relatively easily formulated by the application of electromagnetic theory and their treatment is well documented. (see for example Born and Wolf, 'Principles of Optics' 1959). The particular case of thin film structures will be covered in more detail in the second part of this thesis.

It is possible to extend this approach to surfaces whose overall profile has a varying but regular shape such as a sinusoidal (corrugated) surface. If the mathematical equation of the profile and the width of the incident beam is known the specular reflected light intensity at any particular angle of reflection may be calculated, having first determined the reflection coefficient of the wave at various angles of incidence. In these circumstances the peak specularly reflected light may not in fact be single as in Fig.1.5, but consist of many peaks, in general at angles other than the specular angle of the mean surface.

In practice, however, such surfaces rarely

occur and are either microscopically or macroscopically rough.

ii) Rough Surfaces.

Much work has been published on this subject and many theories to the exact treatment of rough surfaces have evolved, however none are both general and rigorous.

It is important to have some quantitative measure of the transition point between a rough and a smooth surface, or the change from specular to diffuse reflection. Rayleigh suggested a method by which this may be done by reference to Fig.2.1, a surface of irregularities of height h, light incident upon the surface at an angle Θ. The path difference between the two rays a and b is

$$\Delta s = 2h.\sin\Theta$$

and the phase difference

$$\Delta\phi = \frac{2\pi}{\lambda}.\Delta s = \frac{4\pi h}{\lambda}.\sin\Theta$$

When this phase difference $\Delta\phi$ is zero or small the two rays will almost be in phase, as in the case of a smooth surface. However, if this difference is large the rays will interfere until at

$$\Delta\phi = \pi$$

they will cancel, and no energy flows in this direction. This is equivalent to a rough surface scattering light diffusely. By arbitrarily choosing the mid-value, a division of rough and smooth is obtained, namely the 'Rayleigh Criterion' that

$$\Delta\phi = \pi/2$$

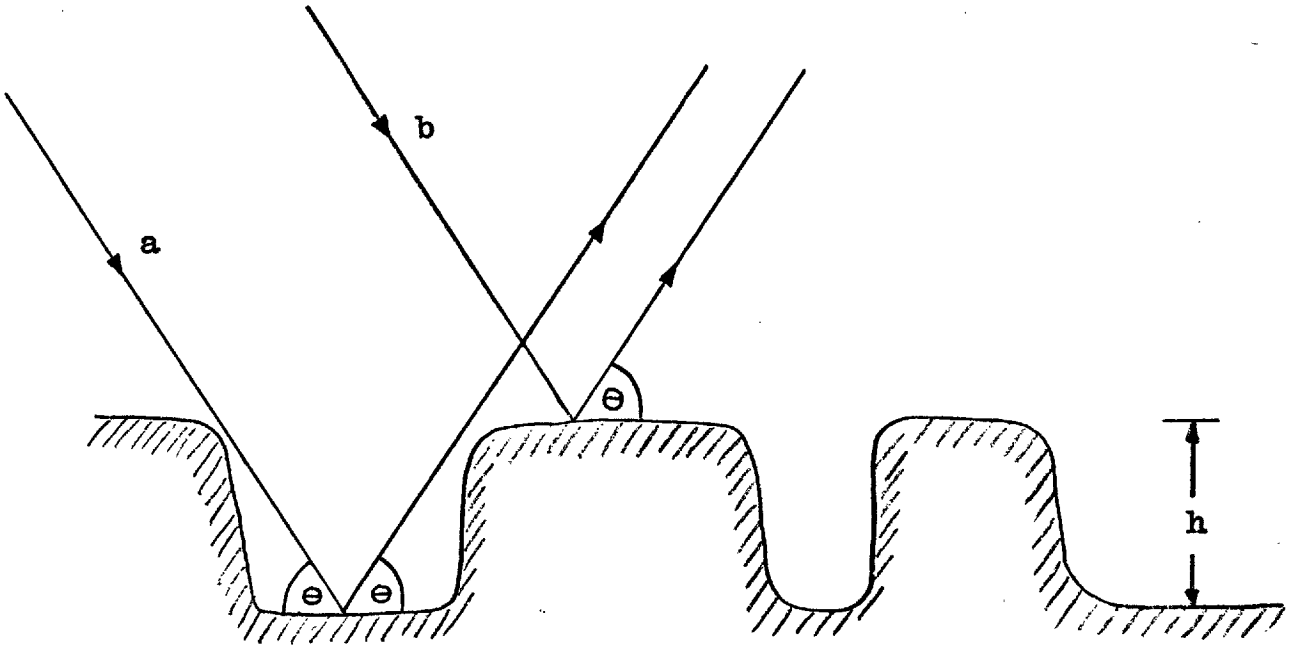


Fig. 2.1 Derivation of the Rayleigh Criterion.

Thus a surface may be considered smooth when

$$h < \lambda/8.\ \sin\theta$$

Other values of $\Delta\phi$, say $\pi/4$ or even $\pi/8$, have been proposed by other workers, but perhaps the best method is to express the factor $4\pi h.\sin\theta/\lambda$ as a measure of the surface roughness and state that a surface is effectively smooth when

$$h / \lambda \quad \text{or} \quad \theta \longrightarrow 0$$

In order to make calculations on scattering possible for rough surfaces, certain simplifications are necessary, the most obvious being to distinguish between defined periodic profiles and purely random profiles. The former are easier to handle but the latter are by far the more usual surfaces encountered. In either case most theories are based on the Kirchoff approximation of the boundary conditions required to evaluate the Helmholtz integral.

A comprehensive survey of this work is provided by Beckmann (1963) who also derives the general Kirchoff solution for the field scattered by perfectly conducting periodic surfaces of certain specified profiles. A sinusoidal surface, for example, is represented by the equation

$$f(x) = h.\cos Kx$$

where K, the phase constant of the surface, is equal to $2\pi/\Lambda$, Λ being its period or wavelength. By combining this with the general Kirchoff solution a relation is obtained for the reflectance from the surface as a function of incident and viewing angles, expressed in terms of a scattering coefficient, ρ. This coefficient is defined

as the ratio of the field reflected in a particular direction to that in a direction of specular reflection by a smooth perfectly conducting plane under the same conditions.

Fig.2.2 illustrates typical results obtained, showing the lobes of scattered light, for 45^{o} incident illumination, in four particular cases. The value Λ/λ remains constant at 10, but the value of kh reduces from i) to iv) as the surface becomes progressively smoother. This illustrates the slow transition from diffuse scattering to an almost pure specular reflection at 45^{o} viewing.

Other profiles such as sawtooth and rectangular are also considered with reasonable accuracy.

The second class of rough surfaces are those more commonly occuring samples whose roughness has a random profile. One possible mathematical approach to this problem is to assume some statistical distribution to the spread in angles of the reflecting facets to the mean level of the surface and from this calculate the statistical distribution of the scattered flux. (Beckmann and Spizzichino, 1963). By assuming a Gaussian distribution for the reflecting elements of an optically rough surface, Chinmayanandam (1919) derives an expression for the intensity of the reflected light from such a surface at an angle Θ of viewing to be

$$I(\Theta) = \exp \frac{(-8\pi^2 . \cos^2\Theta)}{(a\lambda^2)}$$

where a is a surface constant.

A comparison of theoretical and measured

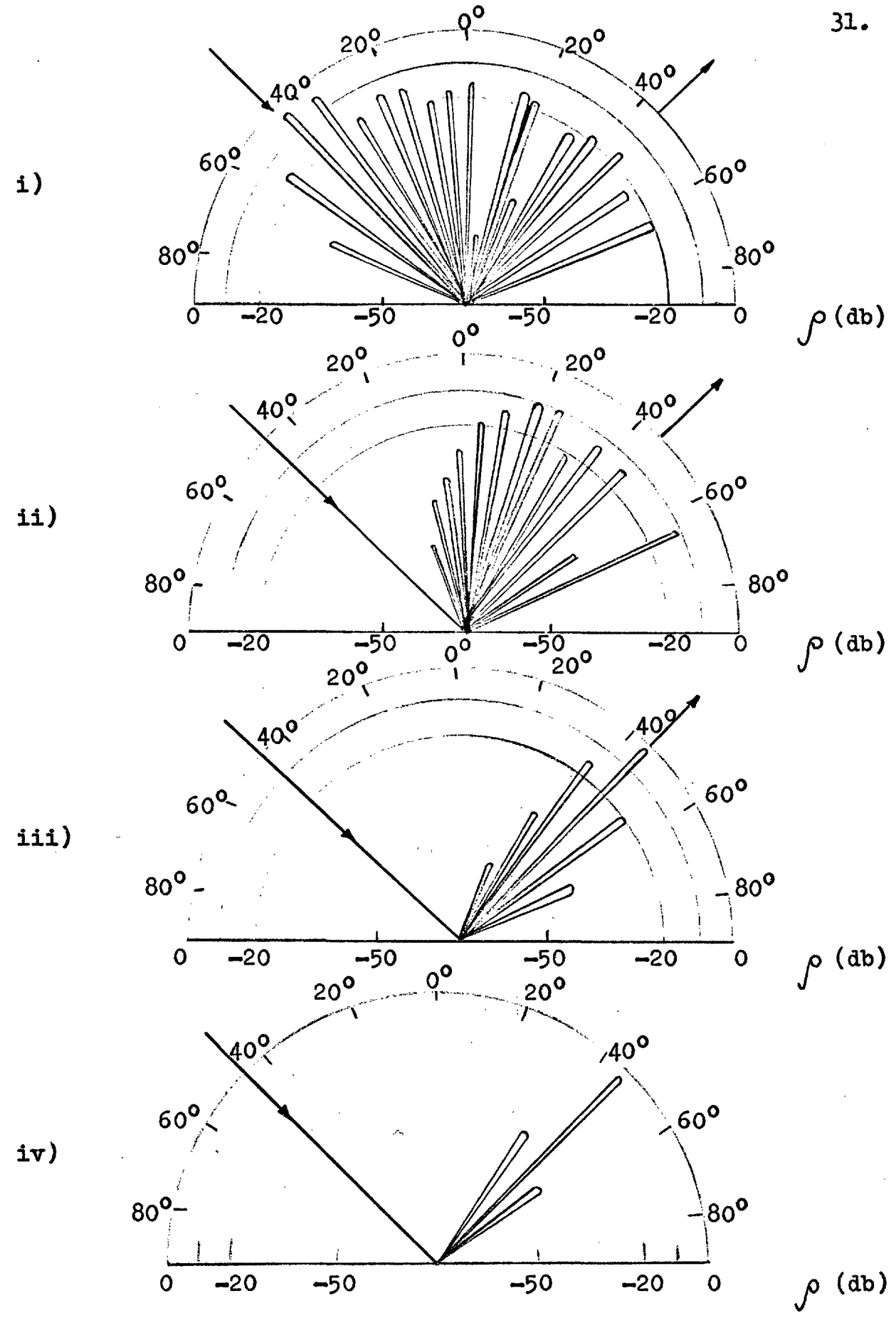


Fig. 2.2 Scattering by a sinusoidal surface. $\Lambda = 10\,\lambda$: $\theta = 45°$.

i) kh = 10 ii) kh = 3

iii) kh = 0.3 iv) kh = 0.03

(Beckmann and Spizzichino, 1963)

results shows that there is fairly good agreement up to angles of approximately 54°, but beyond this large discrepancies occur. Since one of the original assumptions is that the incident illumination should be uniform upon the sample surface, the author explains the theoretical failure at large angles in terms of a shadow effect of adjacent facets, and puts forward a complicated empirical relation which proves to be in better agreement at these extreme angles.

Several workers (Toporets, 1964: Polyanskii, 1966) have extended the general statistical microfacet treatment of surface roughness in order to obtain some correlation between the measured reflected flux and the mean heights of surface irregularities causing this roughness.

In particular Bennett and Porteus (1961) derived an equation for such reflectance in terms of the root mean square roughness σ, and the root mean square slope of the surface profile m, where, at normal incidence

$$R = R_o \exp\left[-(4\pi\sigma^2)/\lambda^2\right] + R_o \frac{2^5\pi^4}{m^2} \cdot (\sigma/\lambda)^4 \, (\Delta\theta)^2$$

R is the measured reflectance, R_o the specular reflectance of a perfectly smooth surface, $\Delta\theta$ the instrumental acceptance angle, and λ the particular wavelength used. The first term on the right hand side of the equation represents the specular component and the second term the diffuse component, so that if λ is sufficiently large only the specular component need be considered, from which the

value of σ may be calculated.

Verification of this formula was achieved by using incident illumination in the 2 - 22 μ infrared region, and good agreement was found in the measurement of known σ values.

Thus it is possible to express quantitatively the contribution of surface irregularities to the reflecting properties of a surface. In many cases however these irregularities are much longer than the wavelength of the incident light, and a more general method of analysing goniophotometric curves is necessary.

2.2 Analysis of Goniophotometric Information.

Apart from the purely mathematical treatment of the light reflection properties of various surface structures, which are inevitably limited in application, much work has been reported on relating measured photometric reflection quantities to the physical nature of various materials, and it is this approach which is of more direct significance to the present work.

Barkas (1939), by extending the ideas put forward by Bouguer, Pokrowski and others, published a method for the separation of reflected flux into its specular and diffuse components for surfaces of low gloss. A surface was assumed to contain many mirror like facets at various angles to the mean surface, and a formula was derived for the total emitted flux under given angular conditions in terms of the two component fluxes received from rough elements and mirror elements under these

conditions. This then does not rely on assumptions that the measured light reflected under say the $45^{\circ}/0^{\circ}$ configuration represents entirely the diffuse component, since observers may still receive information regarding the surface gloss at viewing angles other than specular. Therefore a comparison of specular reflection and diffuse reflection at just two viewing angles does not relate exactly to a visual estimate of gloss.

By using a goniophotometer it was possible to measure the angular reflected flux from both Bristol board and magnesium oxide surfaces and split them into both specular and diffuse components as in Figs. 2.3 and 2.4, for various incident angles. The diffuse component does not necessarily follow that predicted by Lambert's Law, since the diffusing facets need not all lie parallel to the mean surface, a fact allowed for in this treatment. However, in the case of magnesium oxide in Fig.2.4 the curves are fairly Lambertian in shape, showing that the rough facets are more uniformly distributed. The presence of a specular component for this material is assumed to be due to the observable presence of projecting larger smoke particles, giving rise to separate bright spots. Other attempts on similar lines have been put forward but are usually confined to studies on particular types of material.

The subject of gloss has received much attention from workers such as Hunter, Harrison and Judd because in surface specification it is sometimes of equal importance to such attributes as colour. In this connection

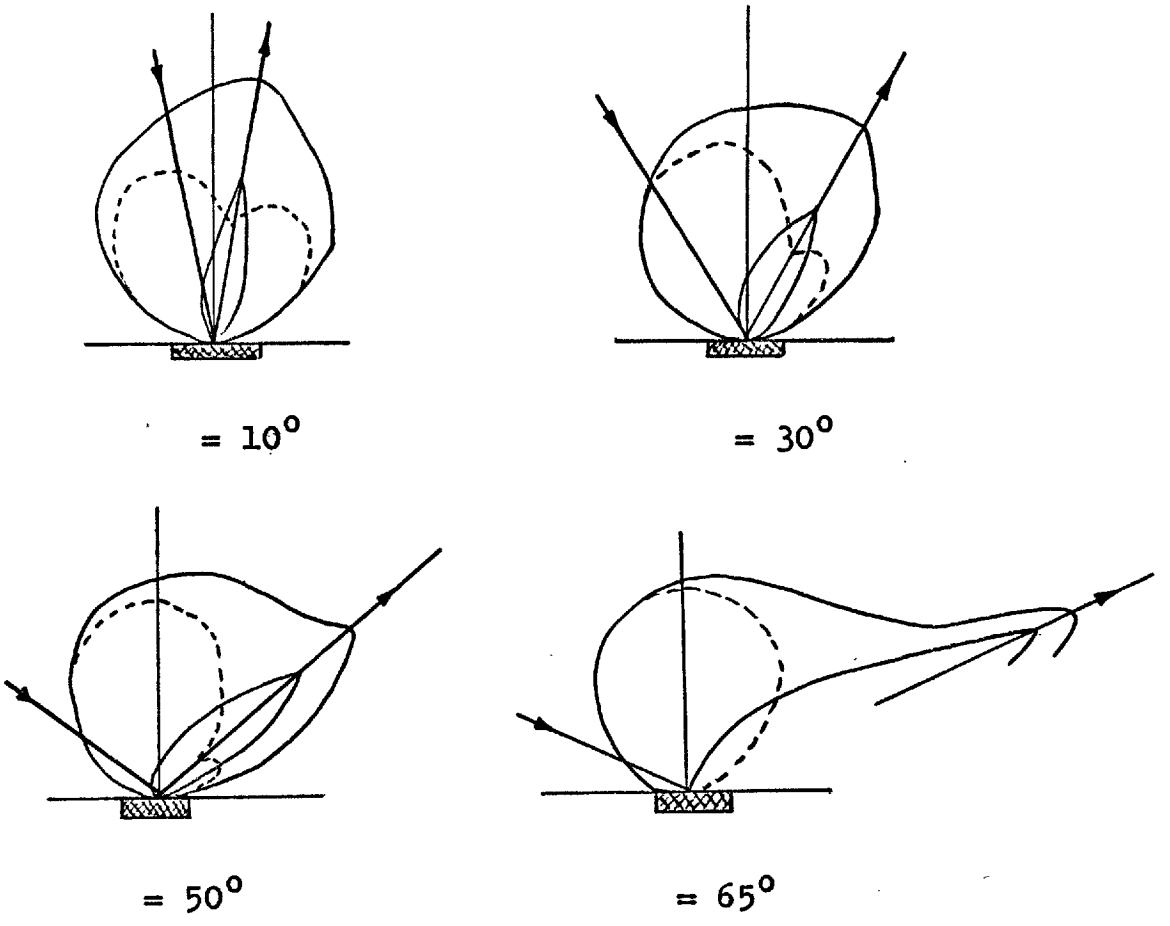


Fig. 2.3 Resolution of scattered flux into diffuse (- - - -) and specular (————) components for Bristol board. (Barkas, 1939).

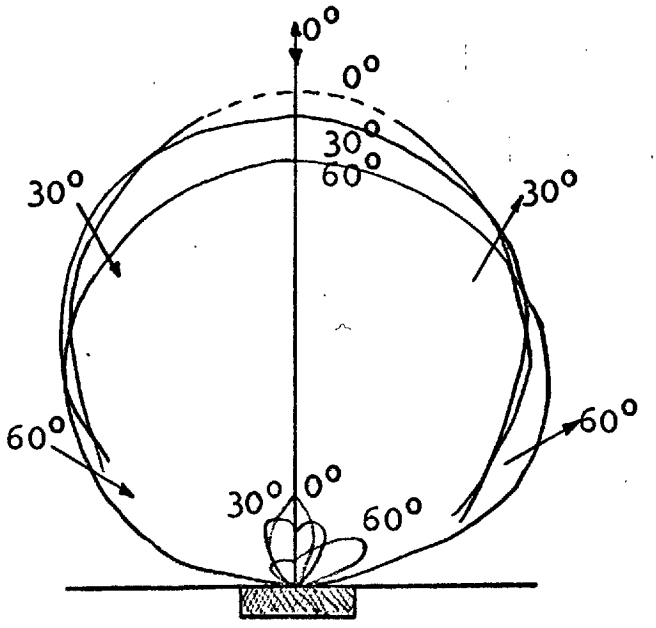


Fig. 2.4 Resolution of scattered flux into diffuse and specular components for magnesium oxide. (Barkas, 1939).

Nimeroff (1952) applied statistical analysis to goniophotometric curves and by reducing this data to particular properties of a curve, such as dispersion, skewness and kurtosis index, was able to relate subjective estimates of different types of gloss to just such definite properties.

Boshoff (1957) extended this approach in the gloss analysis of paint surfaces, much of the work being the determination of a so called just noticeable difference of gloss. In the course of this work a colorimetric method of analysing angular luminance curves was proposed, involving the use of the purity of light reflected at different angles from low gloss surfaces, an idea put forward by Judd. (see for example Judd and Wyszecki, 1963).

Under perfectly diffuse reflection conditions, where no specular component is included, the reflected light should be of the same colour as the body colour of the material under test. This is due to the selective scatterings, reflections and passages within the actual sample, emerging at this particular angle.

At the specular angle however the reflected light will be a mixture of top surface reflection, whose colour will be approximately that of the illuminant, and similar reflections to those mentioned above, which by chance emerge at the specular angle.

The exact ratio of the components in such a mixture will be determined by the type of surface under investigation, a glossier sample producing more top surface reflection.

At intermediate angles between diffuse and

specular conditions a series of chromaticity coordinates for a particular sample should lie systematically along a line between these two extreme colours, so that on increasing the angle of viewing up to the specular angle a series of coordinates as in Fig.2.5 is obtained, collapsing towards the illuminant point at roughly constant dominant wavelength. On passing the specular angle, in this particular case 45°, the points should move back towards the body colour progressively with increasing viewing angle.

It is therefore possible to estimate the ratio of specular to diffuse component at any angle by the position of the chromaticity coordinate at that angle relative to the two extreme cases. This ratio then allows the goniophotometric plot of the surface to be split into its two component parts as in Fig.2.6. The method will be further discussed later.

2.3 Surface Texture.

It has already been stated that the problem of surface texture is essentially a visual one, and that information used to differentiate between different samples must be contained in the reflected light.

Valyus (1966) suggests that some of the appreciation of texture must be as a direct result of the stereoscopic nature of the human visual system. This enables such effects as the characteristic lustre of metallic or glass surfaces to be perceived, as well as the more immediately recognisable stereoscopic effects of depth and perspective appreciation. Similarly the impression of relief

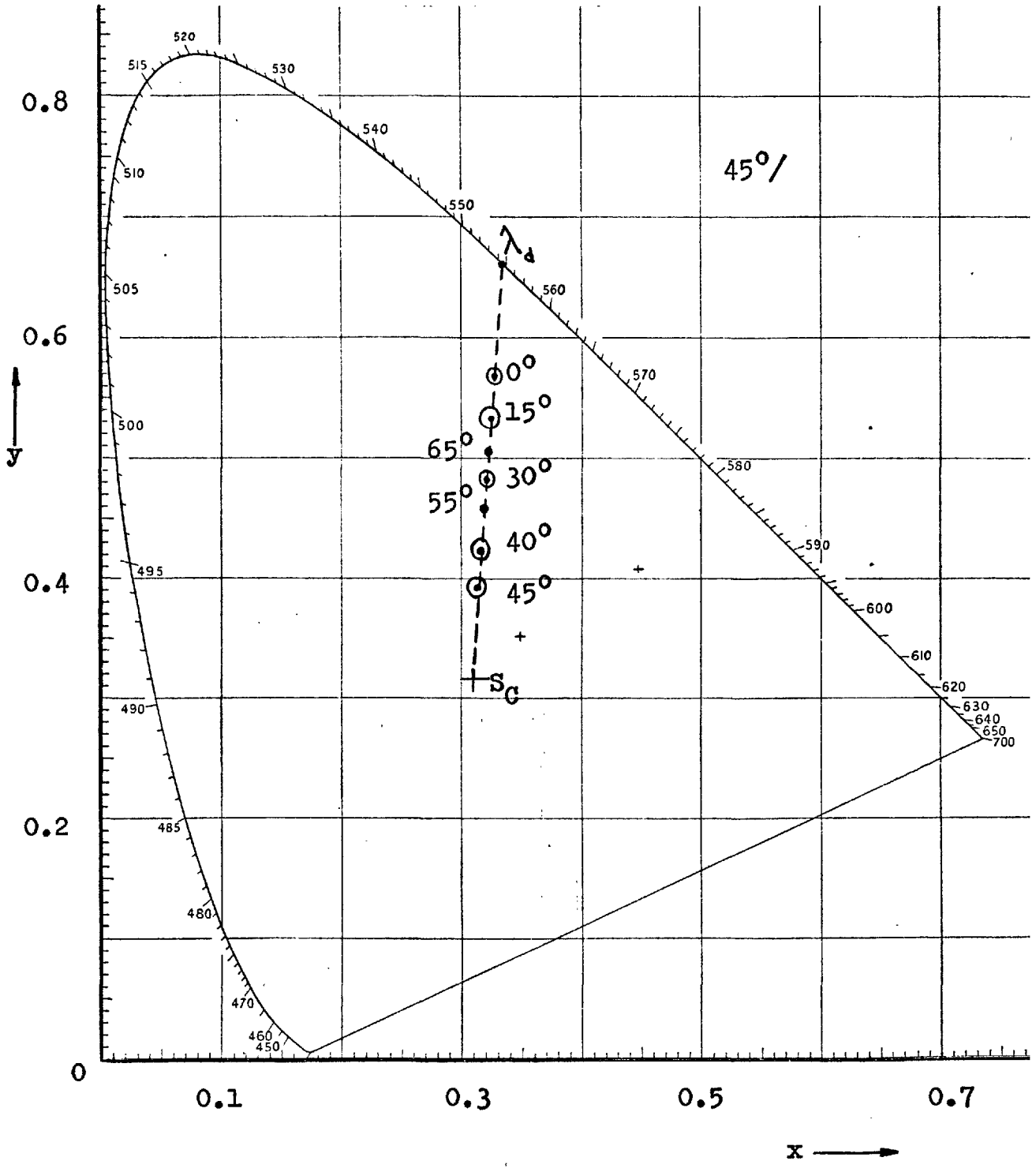


Fig. 2.5 1931 Chromaticity Diagram, showing typical angular variation in chromaticity coordinate for one surface.

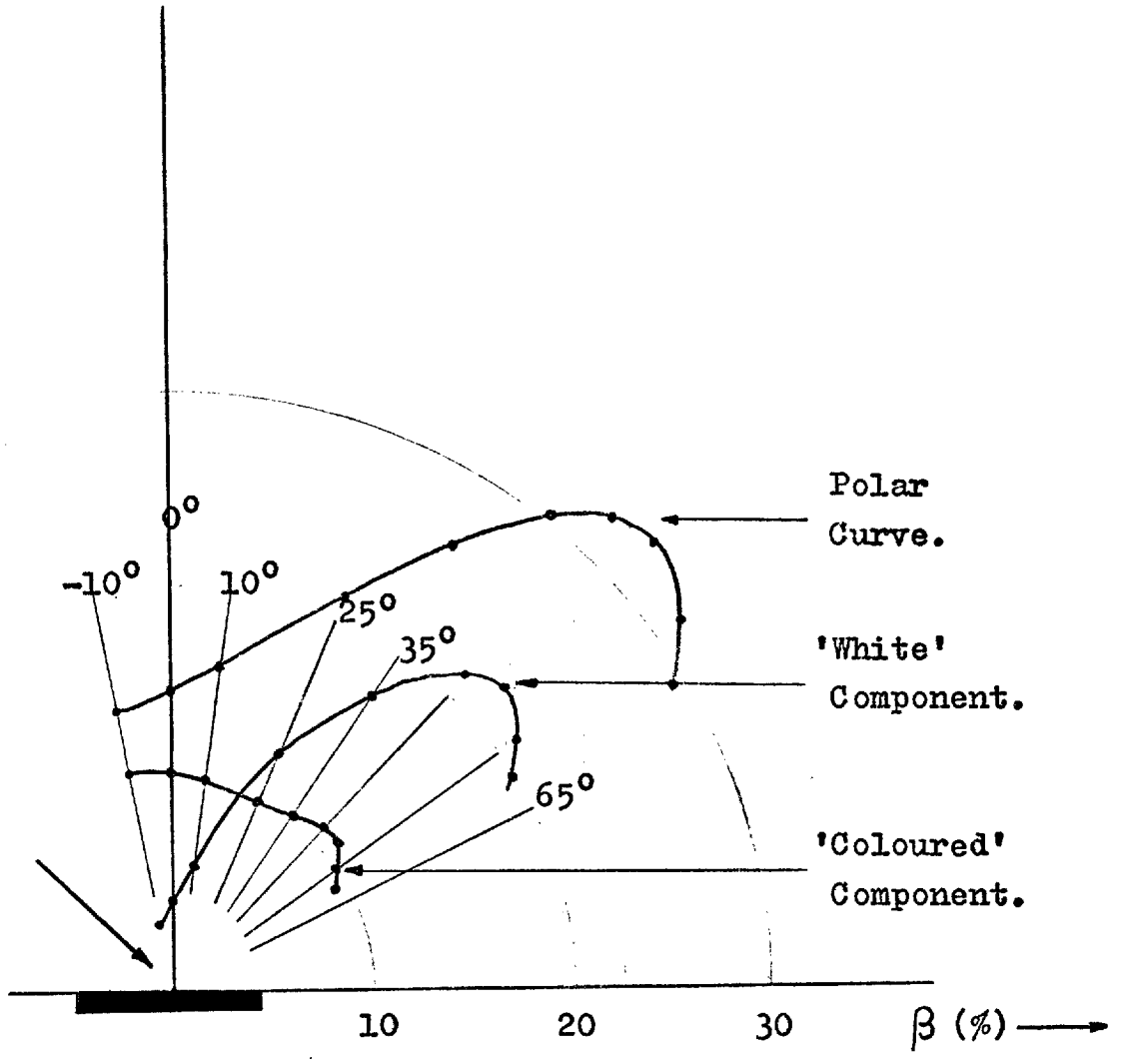


Fig. 2.6 Typical goniophotometric curve split into the two component parts of reflection. (Boshoff, 1957).

may be created by light and shade, contrast, and colour - desaturation giving an impression of perspective for instance - due to our stereo visual system. All these factors are said to give plasticity to our visual image, an important step in texture recognition.

In an attempt to define texture in a more definite way, Evans (1959) suggested the concept of a two dimensional variation. If surfaces vary continuously from rough to smooth, at the same time as their finish varies from perfectly matt to perfectly glossy, we should be able to classify every surface texture at some point. This is a very useful idea, but as will be seen later it requires more careful consideration of the exact quantities and scale involved, since for example a magnesium oxide surface microscopically would be considered rough, whereas on a macroscopic scale it must be considered smooth.

In an essay on surface texture Wright (1967) suggests that the visual impression of texture is due to many different effects which the incident light on a surface is subjected to. The penetration of such light into and through the material; the diffusion within its structure; the sheen of top surface reflection; the effects of light and shade and the many gradations of colour across the surface are some of the processes by which an interpretation of the reflected light distributions convey the information regarding the detailed structure of an object to the visual system.

The same author also discusses the application of these ideas, often in ignorance of any detailed theory,

by some of the great artists in the method of colour mixture and juxtaposition, and sometimes it is through their finished products that these concepts become more obvious.

2.4 Aims

The term surface texture is a very loosely defined property of a material. The word texture, originally applied to the weaving trade and cloth, is now used to describe the structure or substance of a material. The meaning which has been assumed here is really the appearance of a substance and the sensation of surface finish which is conveyed to an observer by the reflected light.

Two particular lines of investigation seem obvious, firstly the information the eye receives regarding the surface texture, from the reflected light, and secondly, the cause and root of this reflected light. Physically, the latter is important but due to the complexity involved for most materials, such analysis is applicable only to a specific sample. In more general terms the former approach is useful since this enables us to isolate the particular light reflecting properties the visual system associates with different types of texture.

In approaching surface texture from a colorimetric viewpoint it would appear that several features of a specimen are responsible for the correct overall appreciation of texture by the human visual system.

Small gradations of colour across the surface of samples, typical of their material, or perhaps due to

surface deformities as in the case of the folds in say velvet, are important in this respect, as also must be the correct interpretation of light and shade, caused by surface irregularities. It was therefore proposed to measure such gradations on several, preferably naturally occurring, samples of varying surface texture by scanning across such surfaces at several fixed points within an area.

The ability to alter the angular viewing conditions of a specimen when an observer is determining its texture cannot be overstressed. Measurements of typical angular chromaticity and luminance shifts for various structures should provide quantitative information of this type which would normally be used in evaluating the appearance of the sample. As Evans (1959) has indicated, the highlights of an object are extremely important to an observer since their removal from say a photograph may make the most glossy samples look matt, dull, shapeless objects. This is again the effect of the observer relating various angular views of the object, knowing the highlights to be specularly reflected light. Without such highlights there is no firm basis on which to build an impression of the surrounding contours and texture.

Similar measuring programmes on surfaces whose structure could, to some extent, be altered were envisaged, as also were measurements on a series of samples whose surface contours were periodic, but varying in profile from one to another. This was in an attempt to relate such angular luminance and chromaticity changes not only to the gloss content but also the actual physical structure of the material.

A natural consequence of such data would be to test how well such information was retained, or stored, by colour reproduction techniques which necessitated quantitative values to this information, and techniques for assessing this ability. The most immediately obvious media are colour photography, colour printing and colour television. These processes are effectively a two dimensional representation of an essentially three dimensional structure, and rely heavily therefore on correct reproduction of the visual attributes of texture. Such media must provide the fine variation of colour gradient, light and shade, and highlights present in the original, although relatively large errors may in many circumstances be acceptable in the absolute value of the colour at any one point (see for example Wright, 1948). It was felt that any programme of measurements as that outlined above would be incomplete without some discussion of the relevance of such results to the colour reproducing processes, and that some quantitative results would be useful in assessing the extent to which present materials are capable of handling such information.

To obtain anything like a complete picture of the entire reflection process from a particular material, it is essential to have a very detailed knowledge of its structure and construction. Without such information any theory may only be very general in application.

It was therefore proposed to study one of the specimens in some detail in an attempt to relate directly the small colour gradations and angular chromaticity and luminance shifts to the internal structure of, and the

interaction of light within, the material. In the latter part of the thesis, by discussing quantitatively such relationships together with knowledge of such variables as refractive index and colour pigmentation, it is found possible to explain some remarkable colour and texture effects.

CHAPTER THREE.

SOURCES OF ERROR AND THEIR TREATMENT.

Introduction.

An instrument as complex as a spectrophotometer is bound to be prone to errors from many possible sources. In any work involving the measurement of both small colour and small luminance variations it is important to isolate and minimise such errors if the results are to be meaningful.

Sources of error fall mainly into two categories - those inherent in the optical system of the instrument and those in the detecting system. Some however do not fall neatly into either category and must be treated as a function of the whole measuring process.

3.1 The Optical System.

i) Wavelength and Bandwidth Errors.

Their are two basic sources of error in the wavelength scale of an instrument. A systematic error due to a miscalibration and a random error introduced because of difficulty in setting to a predetermined point on the scale.

By regularly calibrating the Wright instrument against spectral wavelength lines obtained from a mercury - cadmium - zinc lamp, and checking this against the peak transmission wavelengths of a calibrated didymium filter, it is possible to minimise the effects of say vibrations,

causing a wavelength scale shift. The vernier used on the scale enables settings to 0.005cm to be accurately obtained. At the red end of the spectrum, where any random error would be greatest due to the prism dispersion, one nanometer wavelength interval is equivalent to some 0.025cm and thus sufficient accuracy is available.

The bandwidth of an instrument is determined mainly by the width of entrance and exit slits and, in the case of the Wright instrument, by the width of the mirror in the spectrum plane. Reduction of the entrance slit width both reduces the overall illumination level in the instrument and decreases the range of wavelengths present at any given point in the spectrum, thus increasing the spectrum purity. Owing to diffraction, a theoretical limit to this purity is reached with an infinitely narrow slit, but since a certain light output is necessary for the detector to function the slit must be opened to some extent. Correction formulae for finite slit widths have been put forward by such workers as Hardy and Young (1949), Eberhardt (1950) and Brodersen (1954), and it is also important to specify the shape of the transmitted waveband.

From work by Keegan, Schleter and Judd (1962) and Robertson (1965), who calculated chromaticity and luminance change with both wavelength error and finite bandwidth, it is possible to say that bandwidths up to 10nm may be used in the following work. In the Wright spectrophotometer this may be obtained throughout the spectrum by suitable choice of mirror size.

The above mentioned errors are particularly

important in the measurement of very saturated samples where the spectrophotometric curve is changing rapidly with wavelength, and in these cases it may be necessary to restrict even further the tolerances placed on such errors.

ii) Stray Light.

This may occur in a spectrophotometer for several reasons. Insufficient shielding from room lighting, back reflections from optical components, and multiple reflections of light reflected from the sample away from, and eventually reaching, the detector, are all possible causes. A less obvious, but perhaps more important one, is the incidence of light of other wavelengths onto the sample together with the monochromatic beam. This is often caused by imperfections in the optical components, but is normally removed by the second traverse of the dispersing system in the double monochromator type of instrument.

The Wright Spectrophotometer was tested by removing the spectrum mirror, and since no increase above the dark current was obtained, it was assumed to be free from stray light effects.

iii) The Light Source.

Drifting in such components as the light source may lead to significant errors, depending on the time course of such drifts. In the instrument used in this investigation readings at any one wavelength are comparative and taken within say 30 to 60 seconds, so that if any drift is sufficiently small over this time period it may be ignored.

Significant drifts were measured over periods of several tens of minutes despite carefully controlled supplies to both lamp and detector, and allowing a 'warm up' period of about an hour. However, their effect was so small over the time for the readings at one wavelength to be taken that no significant error is introduced from this source.

iv) Angular Errors.

Variations occur from one instrument to another on exact angles of incidence and collection used. Similarly, large variations in the width of the angular cone of light collected by the detecting system occur, and in an attempt to standardise these conditions the C.I.E. in 1967 recommended for $45^{\circ}/0^{\circ}$ geometry that:

The specimen is illuminated by one or more beams whose axes are at an angle of $45^{\circ} \pm 5^{\circ}$ from the normal to the specimen surface. The angle between the direction of viewing and the normal to the specimen should not exceed 10°. The angle between the axes and any ray of an illuminating beam should not exceed 5°. The same restrictions should be observed in the viewing beam.

Similar recommendations followed for $0^{\circ}/45^{\circ}$ instruments and integrating sphere instruments.

In general it is important to set as accurately as possible to the specified angle, but providing this central angle is correct, quite wide cones of reflected light are acceptable so long as the resolving power of the instrument is not excessively reduced. The

standard and sample must also be measured under identical angular conditions, and in general be mounted rigidly and accurately normal to the plane containing incident and collected beams.

It was found possible to comply with the recommendations at both standard and non standard configurations of measurement.

3.2 The Detecting System.

i) Response Linearity.

In operation the photomultiplier anode current must be such that it never exceeds a value 1/100th to 1/1000th of the current in the dynode resistor chain in order that the response of the detecting system will be linear over a wide range of incident illumination. This is important in any precise spectrophotometry since it is assumed that the measured anode current, or more correctly the voltage developed by this current, is proportional to the illumination at the photomultiplier cathode, and any loss of linearity would introduce significant errors into the measurements. The total illumination range is something less than 1000 to 1 in the following work - corresponding to a variation in the reflectance data of 100% to 0.1%. The linearity of response as a function of illumination in the system was checked by the following method.

Nine Johnson tiles from the grey series described by Robertson (1965), (Robertson and Wright, 1965) were used - tiles: Jet Black, 9843, 9837, 11616, 9855, 9849,

9846, 9862, 11612. This gave a range of reflectances from 0.4% to 80.7%. The tile 11572, a white tile, was accurately calibrated as a substandard and used throughout as a reference standard. A suitable wavelength, 600nm, was chosen, the reference tile having a reflectance of 86.6% at this point. The series of tiles were then calibrated at this wavelength giving the results in column 2 of table 3.1.

TABLE 3.1

	Column 1	Column 2	Column 3	Column 4
Tile	R%	R% at 600nm	R% at 600nm	R3/R2
Jet Black		0.395	0.392	0.9932
9843	0.46	0.515	0.511	0.9911
9837		1.570	1.568	0.9990
11616	4.6	4.602	4.604	1.0005
9855	29.51	29.340	29.346	1.0002
9849		32.538	32.508	0.9991
9846		38.168	38.164	0.9999
9862	60.8	60.511	60.485	0.9996
11612		80.707	80.767	1.0008

A neutral density filter was then placed at an aperture prior to the dispersing prisms and calibrated in situ. That the filter was not absolutely neutral was not important as only one wavelength was used throughout the experiment. The filter reduced the level of the illumination by approximately four times and thus extended the range of linearity to a factor of almost 800 to 1. This was approximately the range desired. The tiles were then

calibrated as before and the results, corrected for the effect of the neutral density filter, are given in column 3 of table 3.1. Finally a comparison of results is given in column 4 by taking the ratio of results 3 and results 2.

The assumption must be made that the tile calibrations by Robertson are accurate. This would be reasonable since his measurements were carefully made with a G.E.C. Universal Precision Photometer Unit and potentiometer arrangement which was shown to be linear over a range of 1000 to 1 (Robertson, 1965). It is then possible to make a plot of the present readings against their original calibration, those results in column 1 of table 3.1, a straight line AB resulting as in Fig.3.1. This confirms the linearity of the detector over this illumination range of approximately 200 to 1.

By choosing a neutral density filter which reduces the value of the highest reflectance tile, yet still keeps this point within the known linear range, it is possible to measure the points a second time and plot these values against the calibrated values corrected by the reducing factor of the neutral density filter. This produces a line, extending the line AB, through B. Three main possibilities may result:

i) a straight line (1), offset as shown in Fig.3.1 indicating some error in measurement of either tiles or neutral density filter,

ii) a continuing straight line (2) through the point B, indicating that the system was linear over the total range measured, and

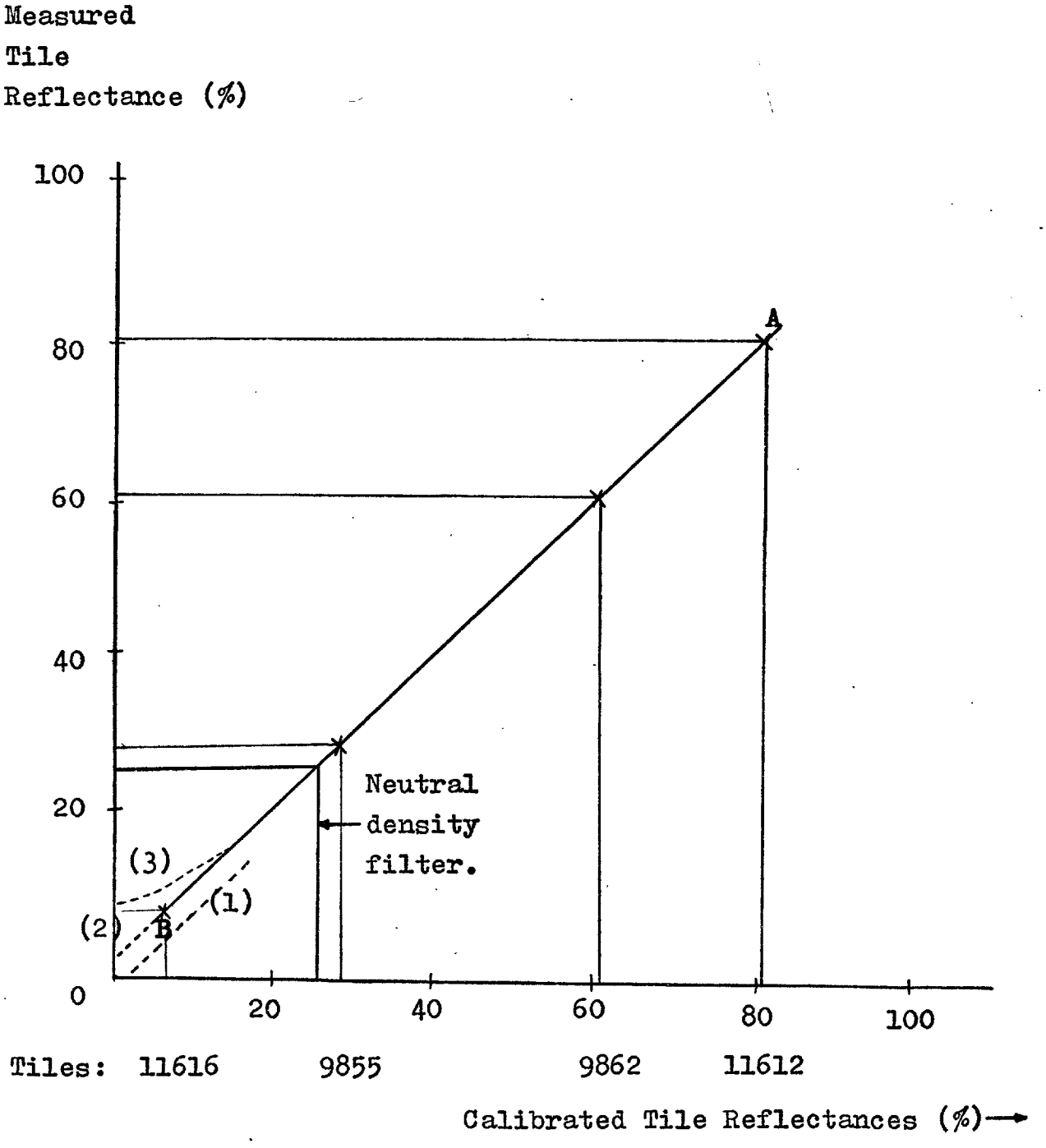


Fig. 3.1 Check on detector response linearity.

iii) a line curving away as shown in (3), as the linearity of the system disappears.

The results of the experiment did in fact follow the second course, and a convenient method of assessing error is to effectively slide the second results, along the line obtained, to their original values by correcting for the effect of the neutral density filter. The ratio of these results is then shown in column 4.

A larger error would be expected on the two lowest readings, due to errors inherent in measuring a reflectance of a fraction of a percent relative to a tile whose reflectance is some 87%. It is believed a fair assessment of the linearity would be obtained by taking the average of column 4, this giving a result of 0.9982 including the two lowest readings, and 0.9999 excluding them. It can therefore be seen that the linearity holds at this wavelength to better than 0.2% over a range of illumination of 800 to 1, a range considered to be quite adequate for the measurements to be made.

It is assumed that the measurements are representative of any other wavelengths within the range normally used. The method has the advantages that no accurately made apertures are necessary and the measuring system as a complete unit is tested.

ii) Uniformity of Cathode Sensitivity.

Some non-uniformity in sensitivity over the cathode area of the photomultiplier is inevitably present and although this will not effect a particular spectro-

photometric curve, any variation in angular conditions or comparison between sets of results taken at different angular settings will result in some error. Whenever any movement in the measuring system occurs, different parts of the cathode area will be used, thus changing the sensitivity of the detecting system.

It is possible to overcome this problem by using either a lens or opal diffusing glass directly before the detector, the latter being employed at times throughout the following work.

3.3 Other Types of Error.

i) Polarization Effects.

In an instrument such as the Wright Spectrophotometer much polarization is present in the incident beam upon the samples. This arises from the many glass faces which the beam meets at non-normal incident angles, each introducing some polarization.

Robertson (1965), by describing the state of polarization by the direction of the electric vector in relation to the plane containing incident and measured beams, measured, with respect to wavelength, both the polarization sensitivity of the detector (S) and the polarization present in the incident beam of the Wright Spectrophotometer (I).

The former quantity is defined as the ratio

$$\frac{\text{sensitivity to horizontally polarized light}}{\text{sensitivity to vertically polarized light}},$$

and the latter quantity, the ratio

$$\frac{\text{amount of incident light polarized horizontally}}{\text{amount of incident light polarized vertically}}$$

Since the photocell detector has been replaced by a photomultiplier the experiments were repeated, good agreement being achieved for the value of I, and a figure of unity obtained for S, thus

$$S = 1.00$$

$I = 3.80$ @ 400nm $I = 3.58$ @ 500nm

$I = 3.52$ @ 600nm $I = 3.51$ @ 700nm

By placing a piece of polaroid immediately prior to the sample and a second piece before the detector it is then possible to measure the luminance factors under the four main polarised conditions of incident and collected beams. Measurements which were made were in general in good agreement with those of Robertson, indicating a marked dependence on the state of polarization of the two beams, and on the type of surface structure under investigation. In general, differences will be greatest for glossy samples reducing in the case of matt surfaces due to the diffusing and scattering processes an incident beam will be subjected to.

This then is a very important source of error in such an instrument, unless suitable precautions are taken. By using the normal incidence and 45^{o} collection configuration for measurements it is possible to reduce any polarization errors and obtain consistent results, since at normal incidence the top surface reflection from even glossy samples is reasonably constant for any degree of polarization.

Complete removal of any polarization in the instrument would be a better solution, and to some extent this may be done by coating the surfaces of all optical components in the system. An easier method in this particular case would be to vary rapidly with time, space or wavelength the state of polarization in the beam, so that light will appear effectively depolarized, by placing some device at the exit slit of the spectrophotometer.

Many methods are available, the chosen one being a 6mm thick retardation plate of calcite inserted after the exit slit, with its optic axis at 45^{o} to the horizontal, and a sheet of polaroid positioned so that only 'horizontally' polarized light reaches the calcite. The state of polarization of the emergent beam in such a system varies rapidly with wavelength according to

$$\delta = \frac{J.t}{\lambda}$$

where δ is the retardation in cycles, J the birefringence of the material and t its thickness. Thus if t and J are large, within the waveband used there will be many cycles. (Buc and Stearns, 1945). This may be checked by rotating a piece of polaroid in front of the detector, whereupon little or no variation in output signal should be obtained. This indeed was confirmed to be so.

Such a device is not suitable for the receiving arm of the instrument since its transmission will be dependent upon the state of polarization of the incident light, however the diffusing glass used to reduce the effects of non-uniformity in the photomultiplier cathode should

prove adequate in also reducing polarization errors at this point.

ii) Reference Standards.

Reflectance measurements in a spectrophotometer are normally made with reference to an accurately calibrated standard. The most widely used standard at present is magnesium oxide in either a smoked or pressed form, and any deviations from the accepted calibration will inevitably lead to error in the final result.

Whichever method of preparation is chosen, the oxide must be freshly made for each series of measurements, and even variations between identically prepared samples have been reported. For this reason a ceramic white tile, (Johnsons no. 11572) reported by Robertson (1965), (Robertson and Wright, 1965), has been used in the following work where possible, but, since it has a glossy surface, this is only possible when measuring under such configurations as $0^{\circ}/45^{\circ}$. Ideally, the same author recommends the use of the complete white to black series of tiles (see previous section on linearity) so that the difference between sample and standard may be kept to a minimum.

Several studies on the departure of magnesium oxide from a perfect diffuser have also been reported, for example Preston (1929-30), Barkas (1939), Boshoff (1957) and Robertson (1965). Variations from a perfect Lambertian surface have been found and Boshoff reports a shift in the chromaticity coordinates of oxide surfaces at increasing viewing angles. The results quoted

in Chapter 4 tend to reflect these imperfections for pressed magnesium oxide surfaces also.

Other errors occur in automatic recording instruments which are not found in an essentially manual instrument such as the Wright Spectrophotometer. Pen inertia and the effects of automatic slit width variation are some of these particular errors, which, since they do not affect the work of this thesis, will not be considered in any more detail here.

Despite all the precautions mentioned above some error is bound to be present in the process of measurement and it is important to have some idea of its magnitude, if results are to be expressed with any meaning.

Results of spectral luminance factor β_λ, or spectral transmission value τ_λ, are invariably difficult to measure at either extreme of the visible spectrum in a spectrophotometer. At the blue end, say below 400nm, lack of light in a tungsten source, and the transmission of prisms in the system tends to reduce the output signal from the detector to very small quantities, whereas at the red end, say above 700nm, the sensitivity of the photomultiplier is beginning to drop rapidly.

In the Wright Spectrophotometer the problem below 400nm is resolved by using a broader mirror in the spectrum plane since the bandspread in the blue is very wide, and no significant increase in bandwidth is therefore

introduced. Above 700nm the photomultiplier, having been chosen for a good red response, remains reliable up to approximately 780nm, and since in any case the colour mixture functions $\bar{x}_\lambda$, $\bar{y}_\lambda$, $\bar{z}_\lambda$ are small in these extreme regions it is believed that the results are accurate throughout the spectrum from 380nm to 770nm.

The summations

$$X = k\sum P_\lambda \cdot \beta_\lambda \cdot \bar{x}_\lambda \cdot \Delta\lambda \qquad \text{etc.}$$

over 10nm intervals are bound to introduce some error over the ideally integrated quantities, however, de Kerf (1958) has shown that the method is accurate to within 0.2 N.B.S. units for all samples except those with very rapidly varying β_λ functions.

Uncertainties in spectrophotometric data however are still bound to occur from random fluctuations in the photometric scale readings of the instrument. It is important at this stage to consider the effect these uncertainties have on computed tristimulus values and chromaticity coordinates, a problem dealt with by both Nimeroff (1953) and MacAdam (1953, 1954).

It has already been shown that the chromaticity coordinates (x,y) of a colour, whose spectral reflectance function is ρ_λ , are given by

$$x = \frac{X}{X+Y+Z} = \frac{\sum_\lambda (\rho_\lambda . P_\lambda \cdot \bar{x}_\lambda . \Delta\lambda)}{\sum_\lambda \left[\rho_\lambda (P_\lambda \bar{x}_\lambda + P_\lambda \bar{y}_\lambda + P_\lambda \bar{z}_\lambda)\Delta\lambda\right]}$$

and

$$y = \frac{Y}{X+Y+Z} = \frac{\sum_{\lambda}(\rho_{\lambda} \cdot P_{\lambda} \cdot \bar{y}_{\lambda} \cdot \Delta\lambda)}{\sum_{\lambda}\left[\rho_{\lambda}(P_{\lambda}\bar{x}_{\lambda} + P_{\lambda}\bar{y}_{\lambda} + P_{\lambda}\bar{z}_{\lambda})\Delta\lambda\right]}$$

Since the functions $P_{\lambda}.\bar{x}_{\lambda}$, $P_{\lambda}.\bar{y}_{\lambda}$ and $P_{\lambda}.\bar{z}_{\lambda}$ have internationally agreed values it may therefore be assumed that any errors in the chromaticity coordinates must arise solely from uncertainties in the ρ_{λ} values. The variance of ρ_{λ} is assumed to be given by

$$\text{Var}\ (\rho_{\lambda}) = \sum_{i=1}^{n} \frac{(\rho_{i\lambda} - \rho_{m\lambda})^2}{n-1}$$

where $\rho_{i\lambda}$ is the ith individual measurement of the spectral reflectance at wavelength λ, and $\rho_{m\lambda}$ is the mean value of n measurements.

Nimeroff defines the following quantities in terms of this variance, thus

$$\text{Var}\ (x) = \frac{\sum_{\lambda}(SP_{\lambda}\bar{x}_{\lambda} - XT_{\lambda})^2\ \text{Var}(\rho_{\lambda})\Delta\lambda}{S^4}$$

$$\text{Var}\ (y) = \frac{\sum_{\lambda}(SP_{\lambda}\bar{y}_{\lambda} - YT_{\lambda})^2\ \text{Var}(\rho_{\lambda})\Delta\lambda}{S^4}$$

$$\text{and the Cov}\ (x,y) = \frac{\sum_{\lambda}(SP_{\lambda}\bar{x}_{\lambda} - XT_{\lambda})(SP_{\lambda}\bar{y}_{\lambda} - YT_{\lambda})\ \text{Var}(\rho_{\lambda})\Delta\lambda}{S^4}$$

where $S = X + Y + Z$ and $T = P_{\lambda}\bar{x}_{\lambda} + P_{\lambda}\bar{y}_{\lambda} + P_{\lambda}\bar{z}_{\lambda}$.

The chromaticity coordinates x_i, y_i, obtained from the ith set of individual measurements of ρ_{λ}, are assumed to have a joint normal distribution about their mean values x_m, y_m.

It can be shown that the ellipse expected to

contain 95% of all chromaticity points computed from the n spectral reflectance functions will be given by

$$(x_i-x_m)^2 Var(y) + (y_i-y_m)^2 Var(x) + 2(x_i-x_m)(y_i-y_m)Cov(xy) = 5.99 \left\{ Var(x).Var(y) - \left[Cov(xy)\right]^2 \right\}$$

By comparing this equation with the general equation of an ellipse

$$(x_i-x_m)^2 \left[\frac{1}{a^2}\cos^2\theta + \frac{1}{b^2}\sin^2\theta\right] + (y_i-y_m)^2 \left[\frac{1}{a^2}\sin^2\theta + \frac{1}{b^2}\cos^2\theta\right]$$

$$+ 2(x_i-x_m)(y_i-y_m)\cos\theta\sin\theta\left[\frac{1}{a^2} + \frac{1}{b^2}\right] = 1$$

(where a and b are the lengths of the semi-axes and θ is the angle between the x axis and the semi-axis a.) it is possible to plot the ellipse around any given point in the chromaticity diagram.

A typical example, calculated from a series of results taken on the Wright instrument, is shown in the enlarged portion of the chromaticity diagram in Fig.3.2, centred on the point (0.3644, 0.3284). Although the exact size may vary somewhat from point to point, this illustrates the typical uncertainty in any measurement on the instrument from purely random fluctuations, and therefore differences in colour of this magnitude, or less, cannot be specified with any certainty.

The tendency for such results to be orientated along a yellow-blue axis is well known, since Nimeroff (1953) showed that a purely random error in ρ_λ will produce

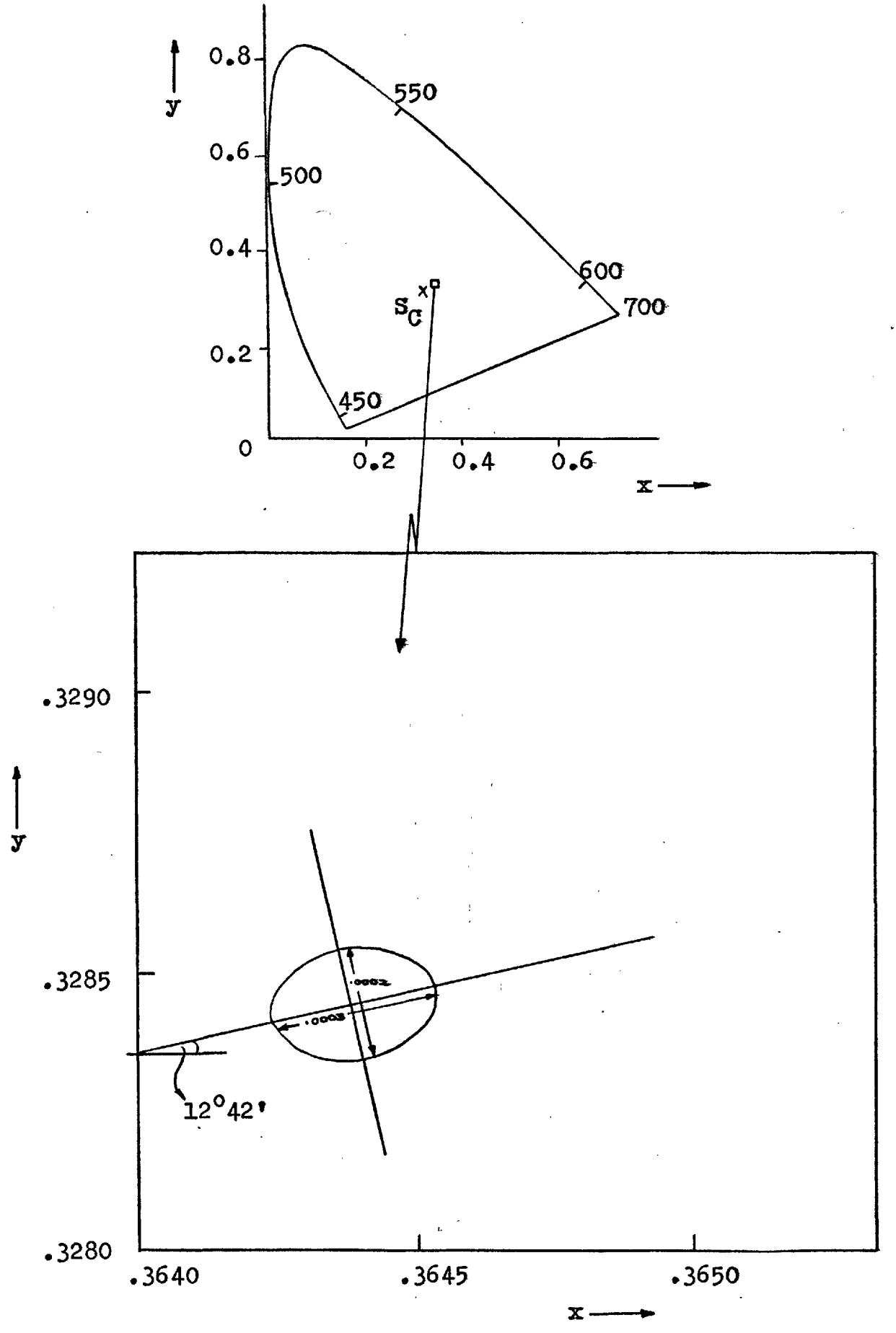


Fig. 3.2 Error ellipse in enlarged chromaticity diagram for random spectrophotometric fluctuations.

chromaticities distributed in an ellipse orientated in this direction, and so this variation may well be a property of the C.I.E. coordinate system itself.

Conclusions.

The major causes of error in an essentially manual spectrophotometer upon measuring spectral reflection or transmission functions of a sample are outlined above. Each possible error has been minimised where it would affect the desired accuracy of the measurement of small variations in both chromaticity and luminance with change in location or angle on the sample.

Random fluctuations in the final output of the instrument are inevitable, and the typical magnitude of uncertainty in measured chromaticity coordinate values is given above, and it is perhaps important to consider the significance of this error here.

The most widely accepted criterion in the judgement of spectrophotometric accuracy is that the magnitude of any error in colour measurement should be less than that detectable by the normal human eye. The criterion is particularly applicable in this work since colour differences less than this so called just noticeable difference, or variations in luminance less than that detected by the human eye, should not convey any information regarding the visual appearance of texture, and it is this which is of the main consideration here.

In an attempt to produce a chromaticity diagram whose colour spacing was more uniform than that of

the 1931 diagram, the C.I.E. in 1959 recommended the use of the C.I.E. - U.C.S. diagram. The chromaticity coordinates of this system are given by

$$u = \frac{4x}{-2x + 12y + 3}$$

$$\text{and } v = \frac{6y}{-2x + 12y + 3}$$

in terms of the 1931 coordinates. The diagram produces a variation of approximately four times in the size of a 'j.n.d.' over the entire range of colours, and it is therefore possible to give some sort of estimate to the typical average colour discrimination of the human eye in terms of u and v. In the most favourable conditions a value

$$\Delta c = 0.0004$$

has been suggested by several workers (Shipley and Walker, 1956; Wright, 1957 and 1959; Perry, 1958) for this limit by a trained observer, where

$$\Delta c = \left\{ (\Delta u)^2 + (\Delta v)^2 \right\}^{\frac{1}{2}}$$

Similarly a figure of 1% is suggested for the smallest detectable luminance change.

On this basis it is possible to calculate a value of Δc for the uncertainty in chromaticity coordinates, due to the random fluctuations in the system, for the extreme points of Fig.3.2. A figure of 0.0002 is obtained for the quoted results, which lies well within the limits of the above criterion and would therefore be acceptable for the present work.

CHAPTER FOUR.

THE EFFECT OF SURFACE ROUGHNESS ON GONIOSPECTROPHOTOMETRIC DATA.

Introduction.

It has already been indicated in Chapter 2 that the overriding physical factor in any discussion of surface texture must be the actual structure at the surface. Since very few objects in practice have perfectly smooth surfaces, microscopically we must consider nearly all samples to be in some measure rough, and to vary generally in a random, rather than a periodic, fashion.

The effect such a roughness has on the light reflection properties of a material varies widely depending on the exact structure involved, however the surface will tend to scatter and diffuse more of the incident light than a similar, perfectly flat one. Owing to the enormous complexity of the large number of such inter-reflections which are thereby created it is only possible to generalise by saying that the diffusely reflected component must increase in magnitude for a randomly rough surface, and to an observer this would generally create the appearance of a more matt surface. This is the principle employed in paint manufacture in producing both matt and glossy paints by varying the binder to pigment particle ratio.

It is important however to now consider the scale of the roughness involved because both rough, glossy specimens and smooth, matt ones are well known. The former

surfaces, for example the hard backs of certain large beetles, tend to be only macroscopically rough so that in detail they are in fact fairly smooth, the roughness being on such a scale that it has little optical effect on the light reflecting characteristics of the material over small areas. Smooth matt surfaces on the other hand, although appearing to the unaided eye to be smooth, on a microscopic scale invariably have a rough structure which creates the necessary scatterings and so on, typical of a matt surface. An outstanding example of this is the surface of a pressed magnesium oxide tablet which appears both smooth and matt. Should too much pressure be applied in the press, especially in a rotary movement, the top particles of oxide are ground into an almost microscopically smooth structure, creating glossy specular highlights at these points.

It would appear from the preceding introduction that only the microscopic structure is of any relevance to the reflection properties of a material which of course is just not so. It seems likely that the visual system absorbs this information almost subconsciously, noting the extent to which a material is matt or glossy and relating this to the type of microstructure which must cause it. Superimposed on this impression however is the information the eye is capable of discriminating, such as surface structure and undulation, causing light and shade, highlights and gradations of colour. It is just such information which is of great importance in the reproduction of texture in a flat two dimensional representation, since it is necessary to copy such variations in reflected light

faithfully if a convincing copy of the structure is to be achieved.

Since the approach of this work is photometric and colorimetric it was decided to investigate the effect of surface macrostructure on just such variables.

Two convenient approaches were readily available in the investigation. Firstly a material whose surface could be deformed at will, and secondly one which had been manufactured in several different surface finishes, although of the same basic material. It had also to be borne in mind that random and periodic variations may produce widely differing results.

4.1 Randomly Rough Surfaces.

i) Samples and Method of Measurement.

In selecting a material for such an experiment a powder surface, which could be pressed into a fairly smooth structure, measured, randomly deformed, and finally remeasured, was considered to be suitable. Since the properties of magnesium oxide powder are well known to colorists and equipment is readily available for handling pressed samples of the material it was decided to use the oxide for these further experiments.

Extremely high quality magnesium oxide powder was formed into tablets some 25mm in diameter using a Zeiss ELREPHO Press. In this process the oxide surface is pressed against a glass plate, thus producing a matching replica of the glass profile, and therefore by using a very

smooth piece of glass the resulting oxide profile should have few deviations from a macroscopically flat, smooth finish. The sample was then rigidly mounted on the kinematic slide mount in the Wright Spectrophotometer and the instrument adapted to the following specifications.

The final monochromatic beam in the instrument was restricted in cross-sectional area to some 0.15 cm square by methods outlined in Chapter 1, and four patches, each approximately 0.15 cm square, were arbitrarily chosen along a horizontal line across the oxide surface. The position of the slide adjusting lever in each of these four locations was carefully noted so the points could be relocated at will, and the fifth position, that of the reflectance standard in the incident beam, similarly noted.

Previous to the experiment it was found that relocating each point on the sample and standard in turn at each wavelength was more accurate than measuring the sample and standard throughout the wavelength range one location at a time since drifting in the electronics was appreciable, whereas the error in position relocation was very small.

The reference standard used was smoked magnesium oxide, freshly smoked from pure magnesium ribbon onto a metal substrate to the recommended depth, because the material in general has been found to have better reflectance and diffusing properties than its powdered counterpart.

The spectral reflectance of the four points was then measured from 380nm in the violet through to 770nm

in the red at several angles of collection from normal to 65° to the normal at a constant incident angle of 45°. All measurements were made with respect to the reference standard, measured under identical conditions.

Without removing the sample from its mount within the instrument, the oxide surface was arbitrarily disturbed over approximately three-quarters of its area, until visually it appeared quite rough. The remainder of the area was left as undisturbed as possible to act as a control point in the experiment. The first three points, located in the rough area, and the fourth point, in the remaining smooth area, were then remeasured as before under similar conditions.

It is a well established fact that over a period of a few days magnesium oxide samples deteriorate (Gibson and Keegan, 1938), a fact most readily noticed by the yellowing process which takes place. In order to minimise such effects all the necessary results were taken over a period of about two days and as usual all samples and standards were made immediately prior to measuring.

ii) Results.

Each spectral curve for a given angular arrangement, position on the sample, and either rough or smooth was then reduced to its chromaticity coordinates and luminance value by means of a computer programme run on an Elliot 803A computer, calculating these values for the C.I.E. recommended illuminants A, B, C and D_{6500}. For ease of comparison illuminant C will be used throughout the

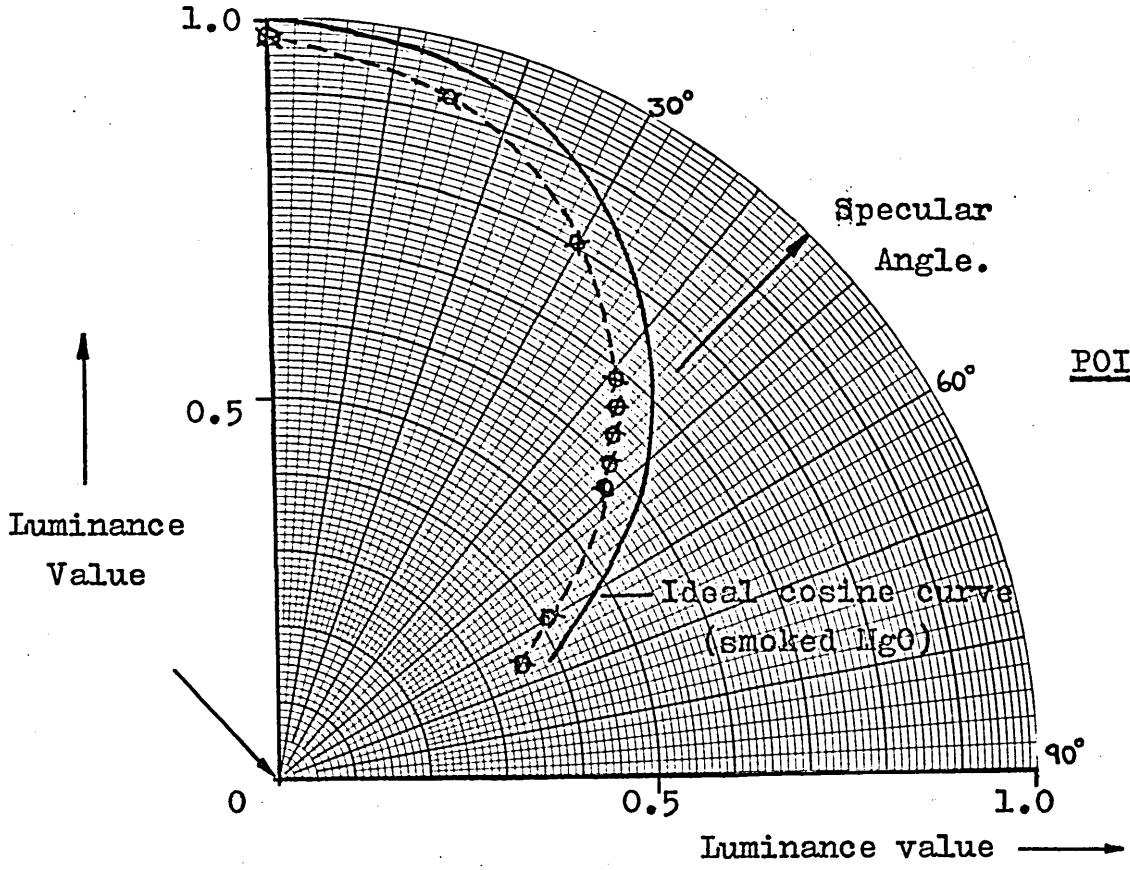


Fig. 4.1 Polar Luminance Curve. (× Smooth : ⊙ Rough points)

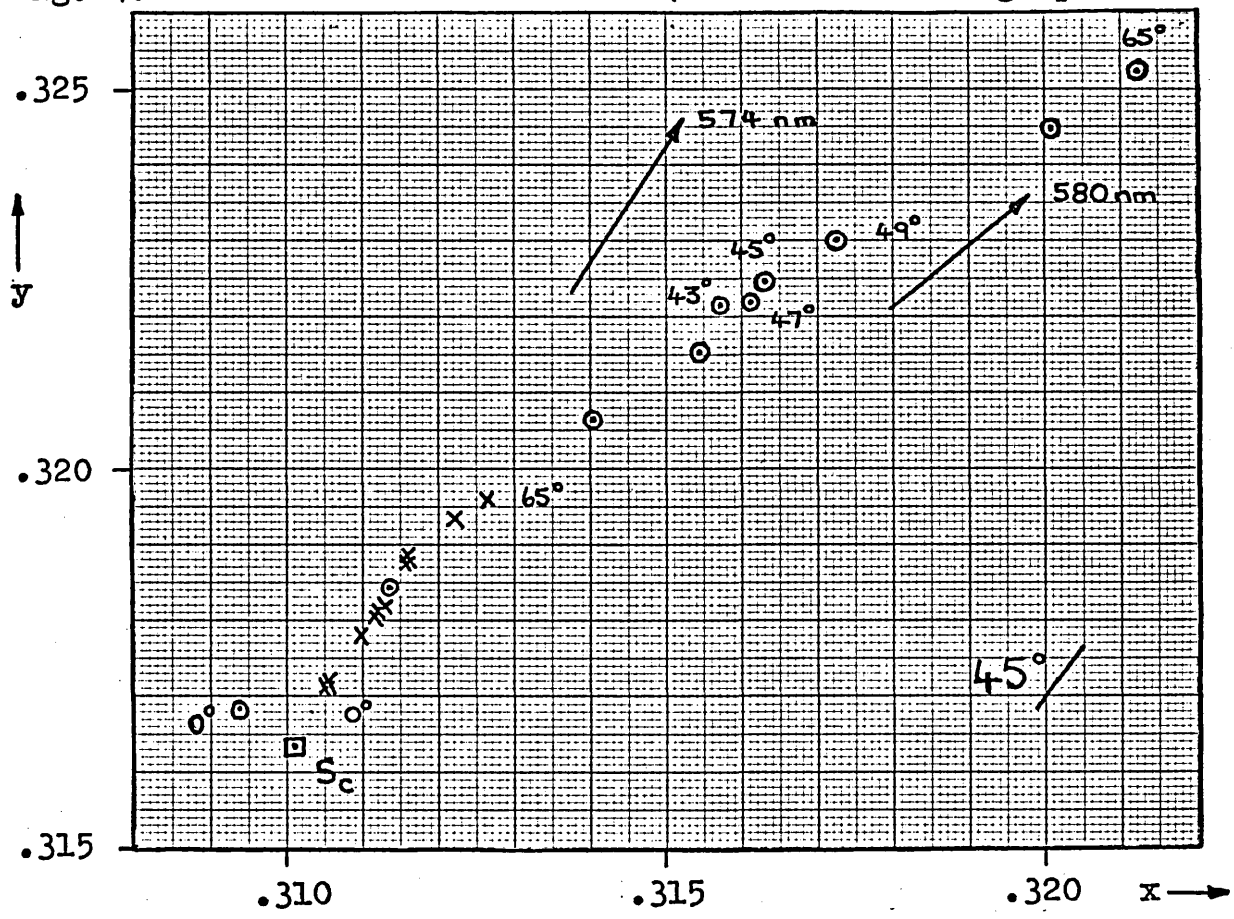


Fig. 4.2 Chromaticity Coordinates (Viewing angles as in Fig 4.1)

Viewing angles increase progressively except where marked.

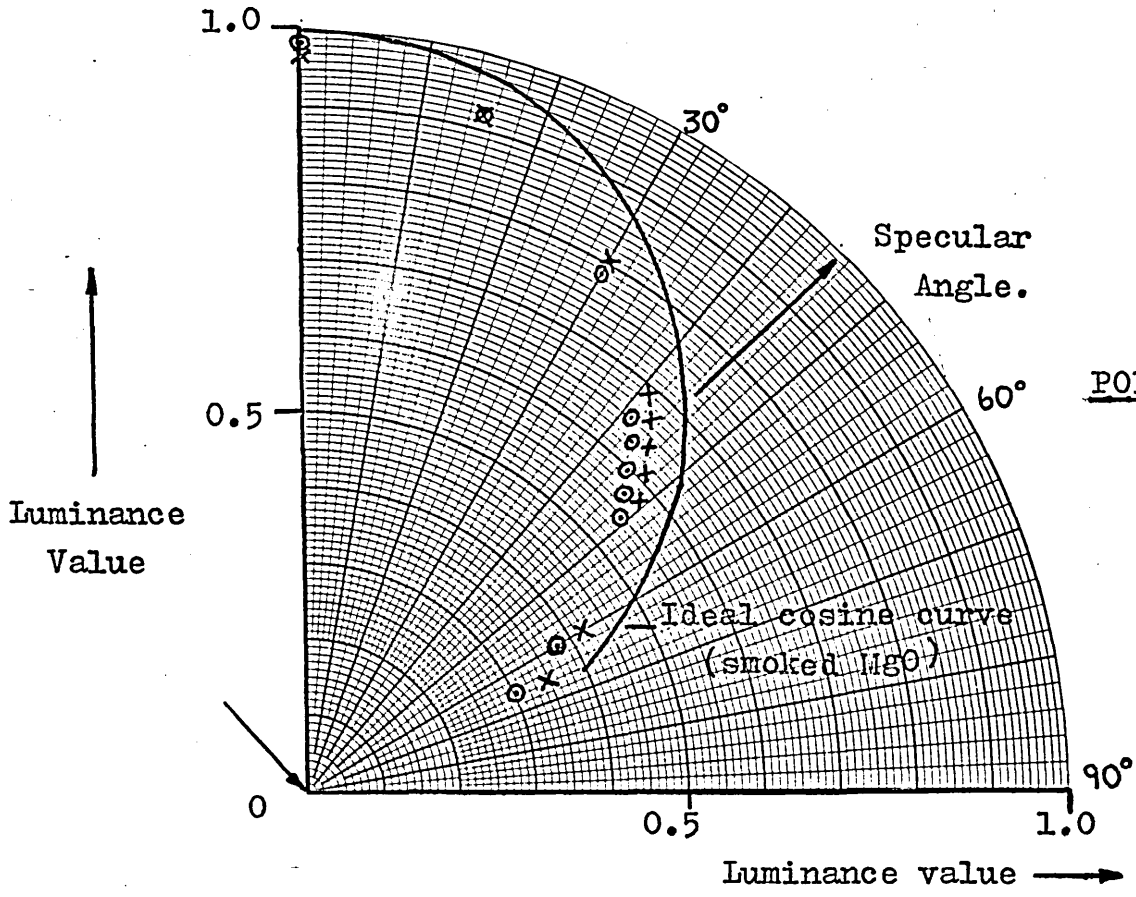


Fig 4.3 Polar Luminance Curve. (× Smooth : ⊙ Rough points)

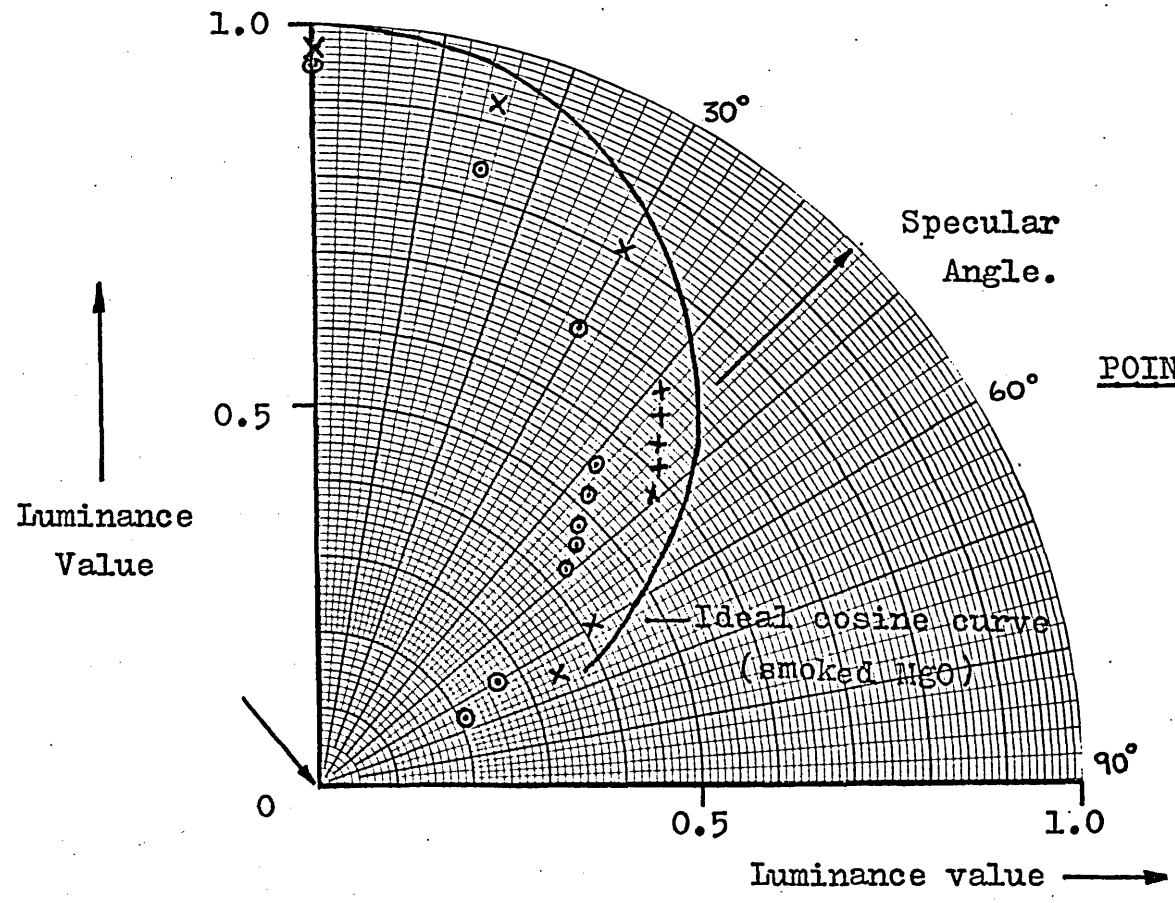


Fig 4.4 Polar Luminance Curve. (Smooth × : Rough points ⊙)

POINT 2

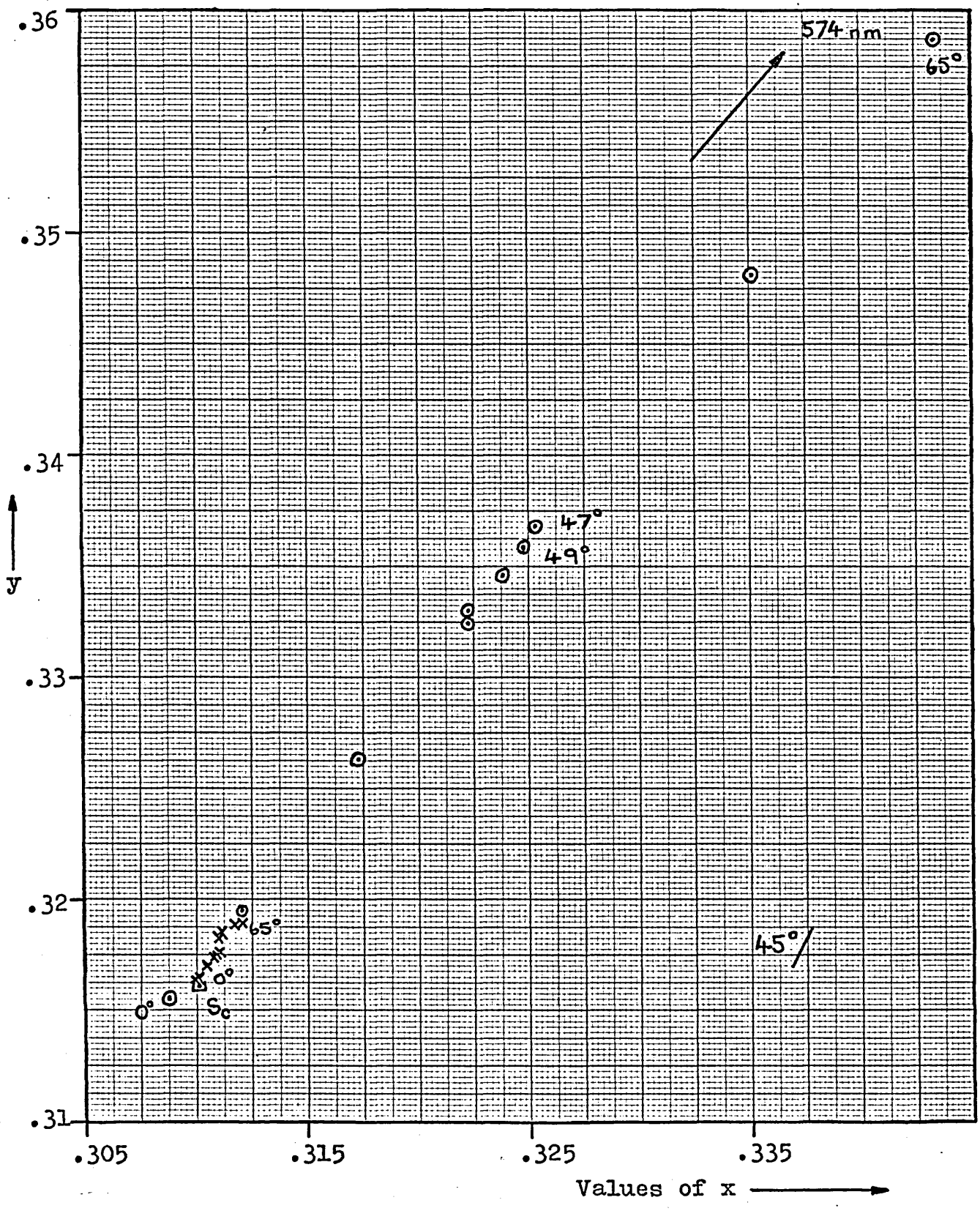


Fig. 4.5 Chromaticity Coordinates. (Viewing angles as in Fig.4.3) Viewing angles increase progressively except where marked.

POINT 3

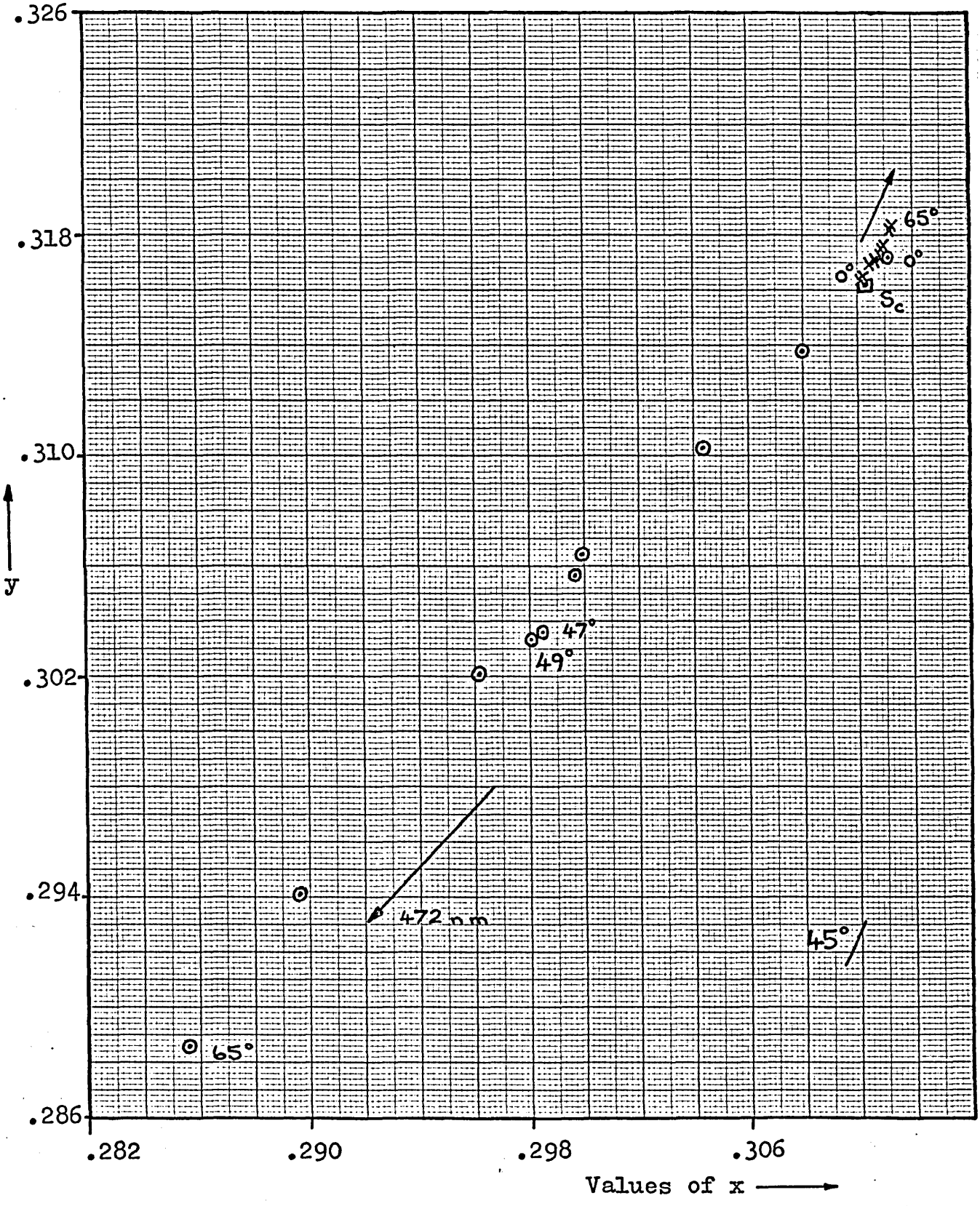


Fig. 4.6 Chromaticity Coordinates. (Viewing angles as in Fig.4.4) Viewing angles increase progressively except where marked.

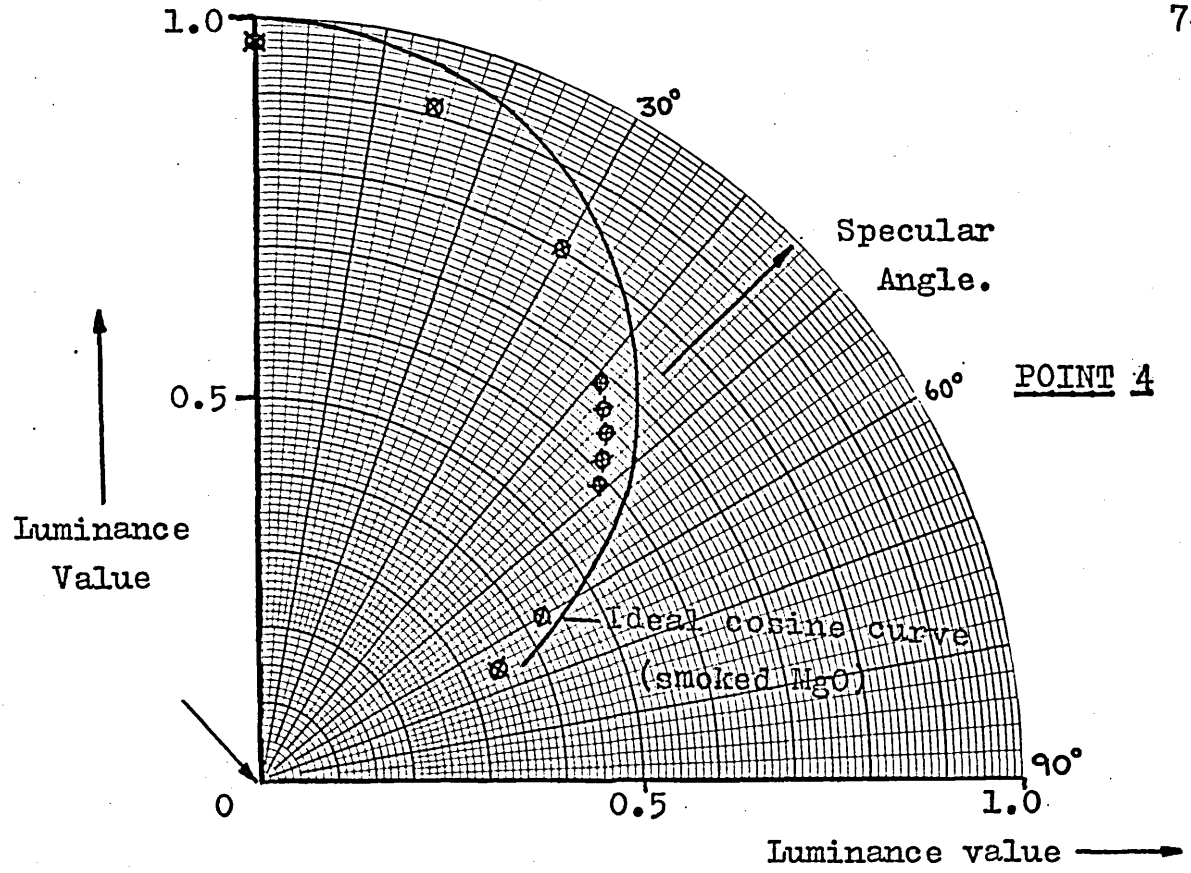


Fig. 4.7 Polar Luminance Curve. (× Smooth : ⊙ Rough points)

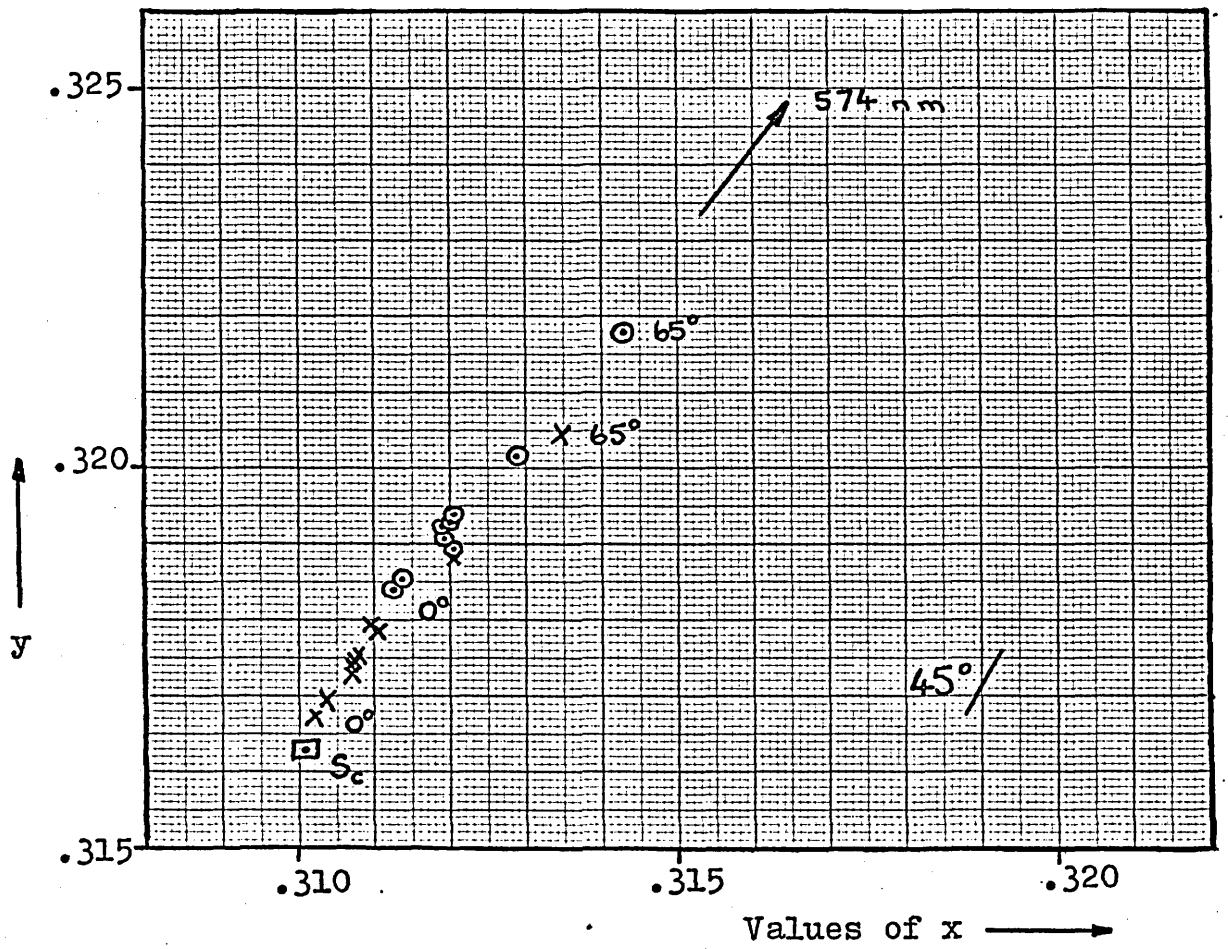


Fig. 4.8 Chromaticity Coordinates. (Viewing angles as in Fig.4.7). Viewing angles increase progressively except where marked.

following results.

Figures 4.1, 4.3, 4.4 and 4.7 show the polar luminance plots of the specimen under test. The continuous line represents the perfect Lambertian diffuser, which the smoked oxide surface is here assumed to be. Departures from the cosine distribution do occur, (Billmeyer et al, 1971) especially at large angles of incidence to the surface normal, but at incident angles used here, are assumed to be negligable. The crossed and ringed points represent the angular luminance plots for the smooth original, and the final roughened, oxide surfaces respectively up to an angle of 65° to the normal.

It can be seen that at all four points the pressed magnesium oxide curve follows the smoked oxide curve well with an overall reduction of about 5% in luminance value. However the curves for the roughened surfaces are far less predictable, in general being lower in value than the corresponding curves for the smooth surface by anything up to about 15%, but at times being fractionally greater.

Positions 1 and 4 show little difference in luminance value whether the surface was rough or smooth. However it should be noted that position 4 was the control point, remaining untouched throughout the experiment. Position 3 reduces considerably in luminance at all angles when roughened, but position 2 is somewhat higher when rough at angles of viewing less than 15°, beyond which it also reduces progressively below that of the smooth oxide surface.

The pressed oxide samples appear to be good diffusers, showing little or no specular reflection and following the perfect Lambertian surface closely. The presence of any specular peaks would tend to be under-emphasised if anything since the reference smoked magnesium oxide surface was assumed to be Lambertian in character, however the error would be small at this angle of incidence, and the above results must be accurate. The rough surface similarly is a good diffuser, and the roughening process in no way appears to affect this property, the only photometric effects being to alter the percentage reflectance value in a somewhat unpredictable fashion, depending on the exact surface contours involved.

It is the colorimetric properties which are of perhaps more direct relevance here and the chromaticity coordinates corresponding to the spectral reflectance curves measured as above are plotted in Figures 4.2, 4.5, 4.6 and 4.8, on an enlarged section of the 1931 C.I.E. chromaticity diagram. The points were obtained with 45^{o} incident light at collection angles from normal to 65^{o} to the normal, the crossed points representing the original smooth surface and the ringed points, the final roughened surface. Each graph represents one particular position on the surface, Figure 4.8 being the unroughened control point.

In the case of measurements taken on the smooth surface, in all four cases the chromaticity shifts progressively away from the illuminant point with increasing collecting angle. This shift is almost identical at each

measuring position on the sample surface, the coordinates increasing in purity at an almost constant dominant wavelength of approximately 574nm up to, and including, the 65° point.

The corresponding results for the same positions when rough however show a somewhat different trend. Again the tendency for the coordinates to move away from the illuminant towards the spectrum locus at constant dominant wavelength is observed, but the increase in purity is much larger as the angle of collection increases. In fact the purity of the $45^{\circ}/65^{\circ}$ point on the smooth surface is obtained at a collecting angle of between 15° and 30° on the rough surface.

Position 1 approaches approximately the same dominant wavelength as its smooth counterpart and position 2 a slightly longer dominant wavelength. Position 3 however reverses its direction completely and moves towards the blue section of the chromaticity diagram. The control position 4 shows little difference between the two sets of results as would be expected, and will be discussed further in the following section.

A table of comparative purity and dominant wavelength values at three angles for both rough and smooth surfaces follows.

The variation in dominant wavelength, in Table 4.1, is only to be expected since chromaticity coordinates so close to the illuminant point require only a small movement on the chromaticity diagram to produce large shifts in dominant wavelength. The variations in

dominant wavelength therefore belie the close proximity of the coordinates at a given angle for the smooth surface.

TABLE 4.1.

		0°		45°		65°	
Posn	Struct	p_e%	$\lambda_d$nm	p_e%	$\lambda_d$nm	p_e%	$\lambda_d$nm
1	Smooth	0.38	569.8	0.84	571.6	1.58	574.3
	Rough	0.60	494.5	3.34	577.6	5.40	580.5
2	Smooth	0.08	568.7	0.54	569.5	1.26	573.5
	Rough	0.59	483.7	8.56	573.6	20.22	574.3
3	Smooth	0.13	572.2	0.40	572.2	1.05	574.1
	Rough	0.48	577.6	5.87	476.1	12.13	475.3
4	Smooth	0.19	566.1	0.49	571.6	1.98	574.6
	Rough	1.55	585.3	1.32	571.6	2.61	574.0

iii) Discussion of Results.

The physical properties of smoked magnesium oxide and the powder used to press samples do seem somewhat different. Electron microscope photographs (Heidenreich, 1942) have shown the particles of magnesium oxide smoke to be regularly cubic, some 0.2 μ in width, this coincidentally being the optimum size for the scattering processes of light. This is further aided by the high refractive index, leading to a large index difference between the oxide and air.

The powder used however, when viewed under a good quality microscope, appeared very irregular, the particles possessing both straight and highly curved outlines. The large variation in size was assumed to be due to aggregates of several particles, these being 20 μ , and more, in diameter. The smallest found were approximately 5 μ to 10 μ in diameter although it was difficult to ascertain if these were truely single ones. This should still lead to a good diffuser, since diffraction and scattering does begin to occur with particles of this size, and light is not necessarily reflected and refracted according to the Fresnel equations. The diffusing properties would not be expected to be as efficient as those for the smoked material however.

Thus the flat pressed oxide surface may be assumed to be flat to this sort of precision, a fact verified microscopically, the rough surfaces above on the other hand exhibited undulations of the order of 0.1mm to 0.5mm varying widely with location.

The above results are of main interest in two particular respects. Firstly, the use of magnesium oxide in a pressed form as a reference standard and secondly, the colorimetric effect obtained on roughening a powdered surface.

When used as reference standard it is normally assumed that a magnesium oxide sample remains a constant colour or at a constant chromaticity coordinate, namely that of the illuminant, under all usual modes of measurement. Any deviations which occur will introduce some

error into a particular set of measurements unless specifically taken into account when calculating the tristimulus values of the sample under test. Very little attention seems to have been paid to this problem, perhaps the first being Boshoff (1957) who published figures regarding measured shifts in smoked magnesium oxide samples. The variations reported above in Figures 4.2, 4.5, 4.6 and 4.8 for the smooth oxide surface show a gradual movement of the colour towards the yellow part of the C.I.E. diagram as the collecting angle is increased, but no attempt has been made to determine whether this is a true shift of the pressed oxide surface or whether the effect was created by some movement in the chromaticity coordinates of the smoked reference surface, which was assumed to be ideal.

It is true that the results of Boshoff do indicate a tendency for a smoked magnesium oxide surface to move in a direction roughly opposite to that shift reported here, in fact towards the blue segment of the chromaticity diagram, as the collecting angle increases, however this movement is not sufficiently large or sufficiently well defined to accommodate the above data. It must therefore be noted that certainly some error would be introduced when using pressed magnesium oxide as a reference standard at large viewing angles in terms of chromaticity coordinate, although even in precise spectrophotometry any such error would be small.

If the surface of a pressed oxide standard were not perfectly smooth however, reference to Figures 4.2, 4.5 and 4.6 show errors due to angular instability of colour

significant enough to introduce errors which are not really tolerable in any type of spectrophotometry. Although it has been shown earlier that the diffusing properties of a rough surface are still fairly acceptable, the colorimetric properties appear to be both unpredictable and poor, in fact beyond collecting angles of about 20^{o} very large errors may be introduced, depending on the particular surface contours of such a sample.

Turning to the colorimetric aspect of the results, there appears to be a very marked connection between the surface structure and the angular variation in chromaticity. As would be expected the results of point 4 on the surface, the control point, remain reasonably alike for both conditions of measurement. The small variations present are assumed to be partly due to spectrophotometric errors, but in the main the effect of contamination of small oxide particles from the other roughened areas of the sample.

On this basis then, the other, large chromaticity shifts must be a direct result of the change in surface structure of the other three positions. These positions showed an increase in excitation purity of anything up to 20% at a collecting angle of 65^{o} over that value at normal viewing, whereas for the same positions when smooth the equivalent increase was only about 1%. In general all movements were towards the yellow part of the chromaticity diagram except for the point 3 when rough which was remarkable in that it moved in a direction almost

opposite, towards the blue portion.

Visually, positions 2 and 3 were rougher, or surface undulations deeper, than position 1 and it may be noted that the increase in purity of results associated with position 1 is much less than that associated with either of the other two. Similarly the position 3 appeared overall to be at an angle nearer normal to the incident light, effectively making the angles of collection greater with respect to the average orientation of the surface than the values quoted. This would explain to some extent the reduction in luminance curve for the roughened surface in position 3, a fact further explained by the possibility of shadowing effects due to rough facets adjacent to this area.

The reason for the observed chromaticity shifts are not obvious when considered as a direct result of macroscopical disturbances of the physical surface. Since there is no marked increase in the specularly reflected component on roughening, it is fair to assume that the diffusely reflected light from such a material results from scatterings, diffusions and inter-reflections within the oxide itself, emerging randomly at various angles to the surface normal, and that any top surface specular reflection is very small indeed. Reference to Figure 4.9 indicates a progressively large selective wavelength absorption to be taking place as the viewing angle is increased, in this case for point 2, at the blue end of the spectrum. However, if the equivalent reflection curves for point 3 were substituted the reduction in reflectance would occur nearer the red end,

POINT 2

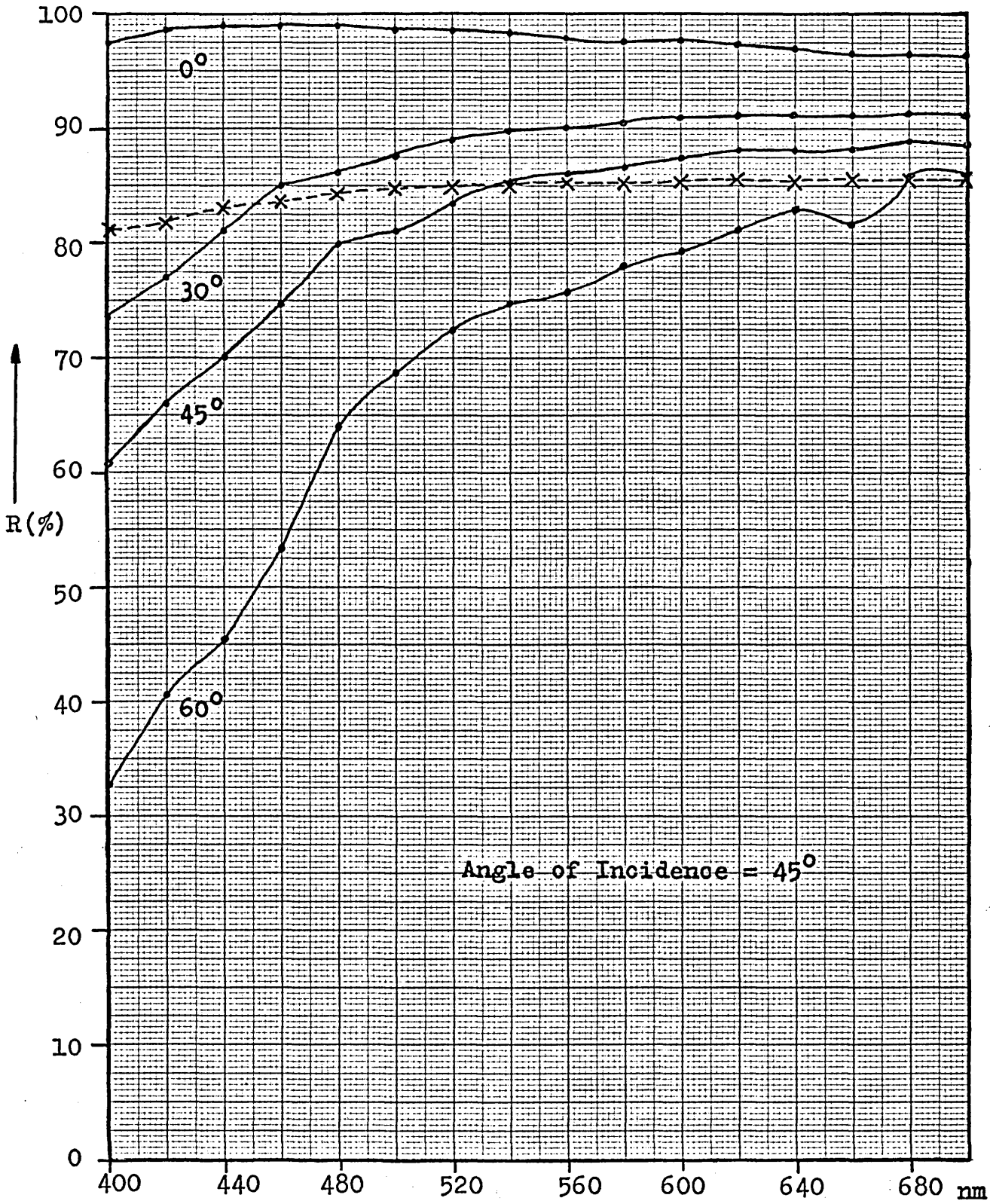


Fig. 4.9 Wavelength Reflectance curve at point 2 (Rough)
Angles of collection 0°, 30°, 45°, 65°.
Extreme curve (45°/65°) for smooth surface represented by dotted curve (x) as comparison.

since the chromaticity shifts towards the blue portion of the C.I.E. diagram. In a sense this would not be expected since such wavelength distribution changes would normally be associated with structural changes on a microscopic level rather than on this much larger scale.

The results show a marked trend for the angular increase in purity to be larger at points where the surface was rougher in the previously explained meaning of the word. Obviously however, some limit must be reached where this will no longer be true. In general the macroscopical roughness of a surface does tend to increase the body colour of that material compared with the same material crushed flat where the top surface 'white' reflection 'dilutes' the colour, however the chromaticity shifts in this case were not always in a constant direction.

The results are relevant to only one powdered material and it is important not to generalise in detail to other types of arbitrarily rough surface without first considering their own particular light reflecting processes.

4.2 Rough Surfaces With a Periodic Profile.

i) Samples and Method of Measurement.

In order to have sample surfaces whose profile was as periodically accurate as possible it was necessary to turn to manufactured materials. The four chosen samples were different finishes of an I.C.I. Perspex, Grade Opal 040. The first was the normal polished perspex gloss finish and the second had a matt surface, termed

'satin' by the manufacturer. Both specimens were flat. The third and fourth samples were glossy but each possessed a definite surface structure - the third termed 'diamond' and the fourth 'pyramid'. Each specimen was some 3 mm thick and no backing layer was attached during the measurements. Reference to Plate 4.1 illustrates the particular structures involved, the lighting being placed to emphasise this detail.

Using an incident angle of 45° the reflectance of each sample was measured in turn at eight different viewing angles from the surface normal to 65° to the normal, throughout the spectral range from 380nm in the violet to 770nm in the red. The reference used was freshly prepared magnesium oxide, pressed, since by careful weighing of the oxide powder it was possible to obtain good reproducibility on each daily prepared specimen. Sample and standard were mounted as usual on the kinematic slide in the Wright Spectrophotometer and the photomultiplier aperture restricted to some 5 mm in width to obtain good angular resolution. Readings on the first glossy sample were more closely spaced to the specular angle in an attempt to define more satisfactorily the expected enormous increase in angular luminance curve in this region, although the complete range of angular measurements was identical in all four sets.

The final exit beam from the monochromator of the instrument was increased in cross-sectional area to a little over 1 cm square at its point of incidence on the specimens. It was felt that this reproduced the more normal observing conditions of the eye since within this

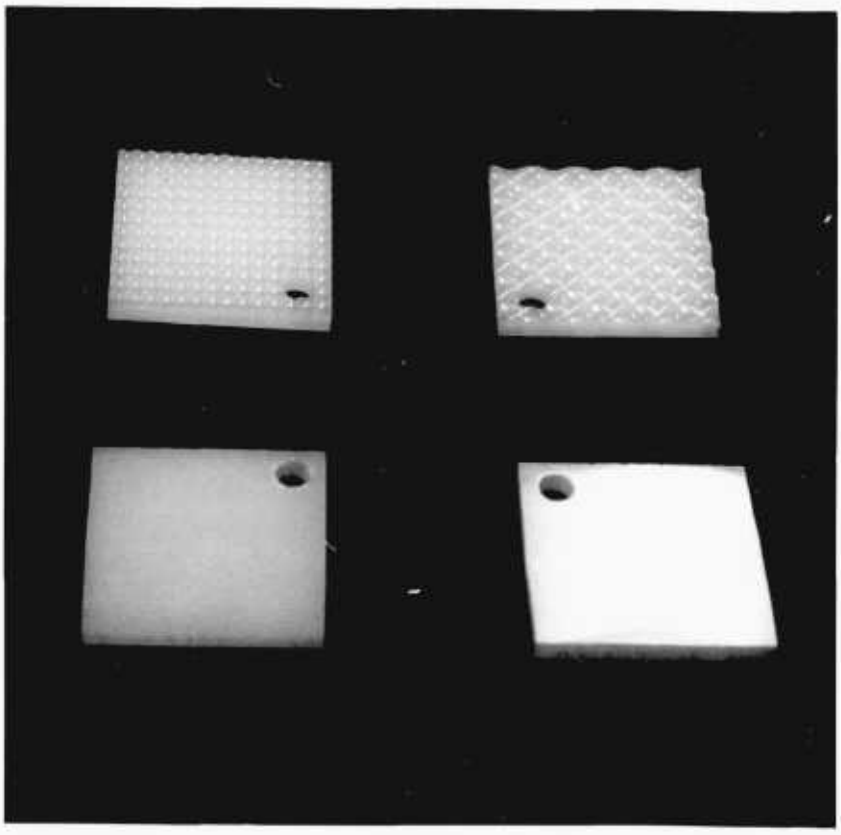


Plate 4.1 The four perspex samples, Grade Opal 040, illuminated to emphasise the structure.

Pyramid	Diamond
Satin	Glossy

area several periods of the structure occurred. As before exact relocation of the measured area on returning from the standard reference surface was most important if the consistency of results was to be maintained, and to this end several preliminary repeat measurements were made as a check. Such relocation was again found to be excellent and introducing negligable error into the final result.

Having ascertained these preliminary results the experiment was conducted and the data reduced as previously described to tristimulus values and chromaticity coordinates by the usual methods.

ii) Results.

The data quoted in this section will all be with respect to standard illuminant C for ease of comparison.

The polar luminance distributions of each of the four samples (1 to 4) are illustrated in Figures 4.10, 4.12, 4.14 and 4.16 for an incident light angle of 45^{o}. Figure 4.10 shows the sharp, specularly reflected peak intensity associated with a flat glossy sample, while Figure 4.12 clearly demonstrates the expected polar luminance curve for an almost matt sample, having a much reduced peak under 45^{o} viewing conditions. Figures 4.14 and 4.16 however are, in many respects, similar to the polar curve obtained for the matt specimen despite the fact that their actual surface finishes were almost identical to sample 1 whose luminance curve showed the large specular peak. This is clearly a direct result of the surface structure differences occurring in the two later figures. It is

SAMPLE 1

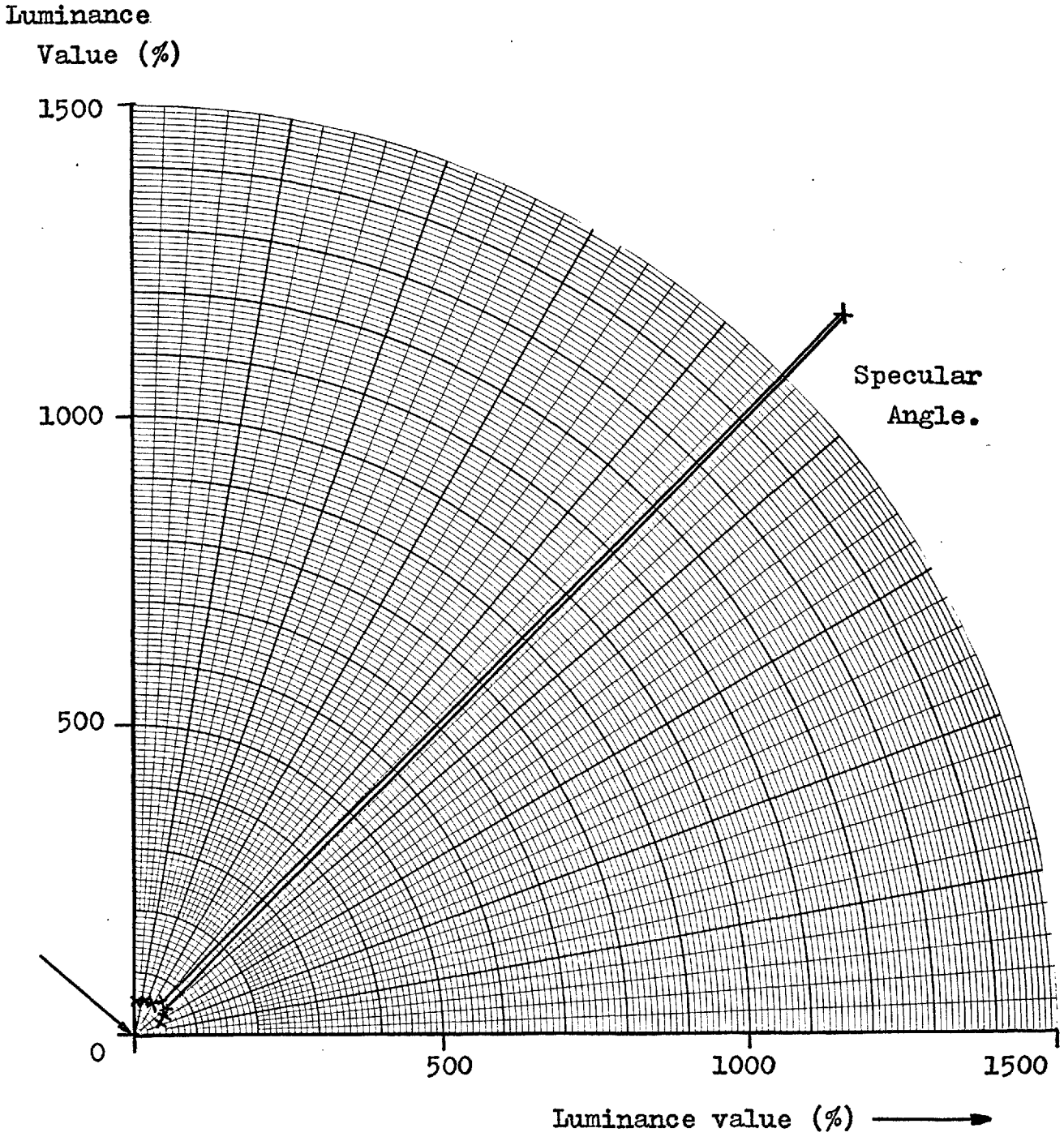


Fig. 4.10 Polar Luminance Curve - Sample 1.

SAMPLE 1

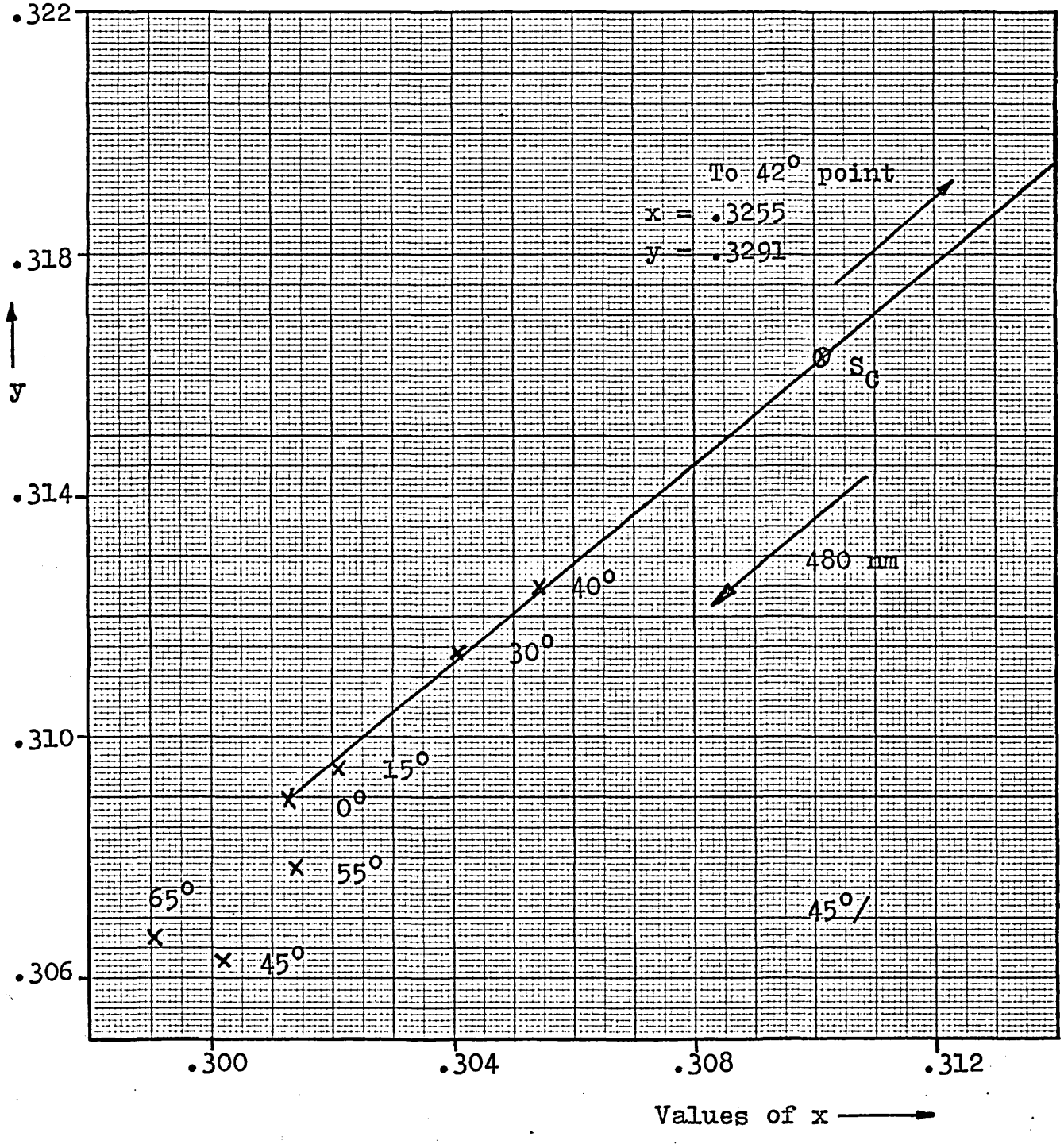


Fig. 4.11 Chromaticity Coordinates - Viewing angles as shown.

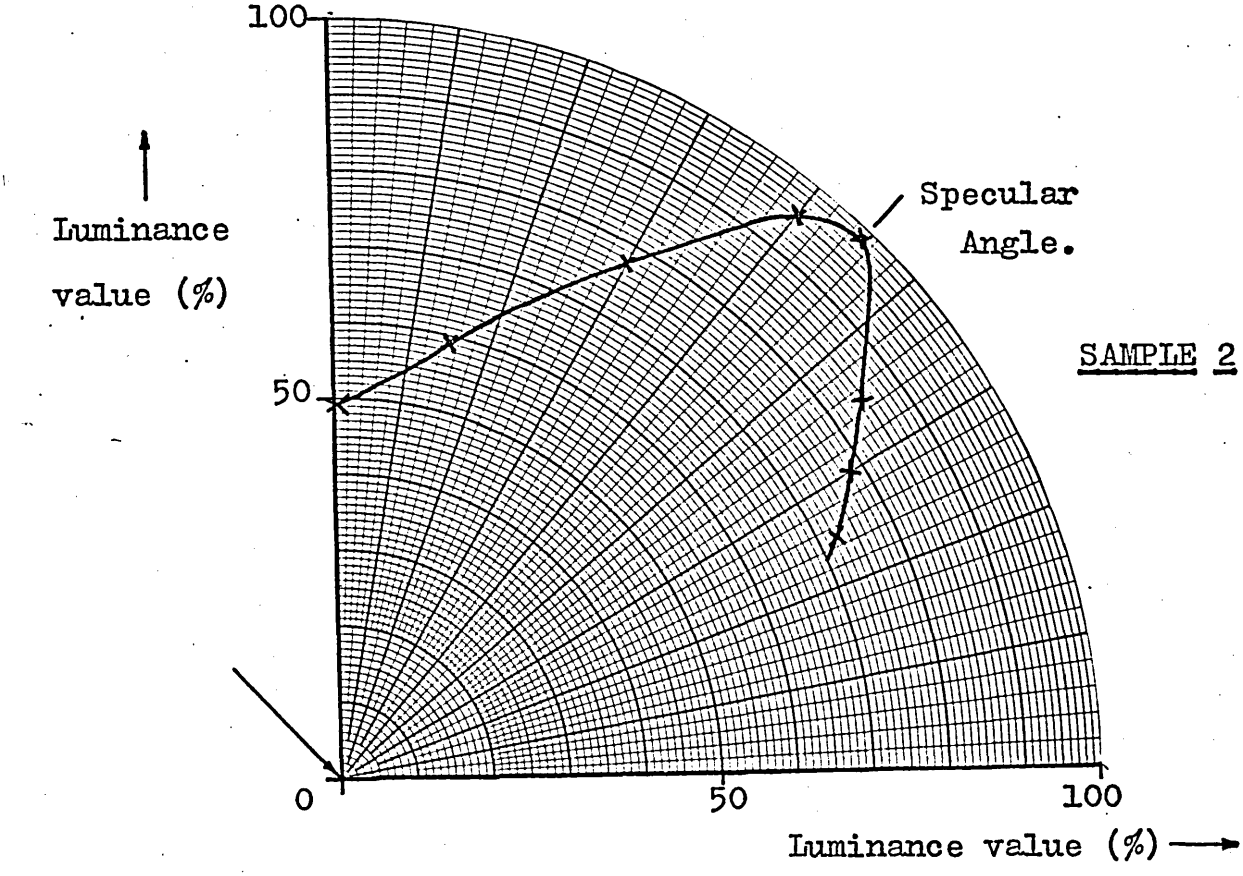


Fig. 4.12 Polar Luminance Curve - Sample 2.

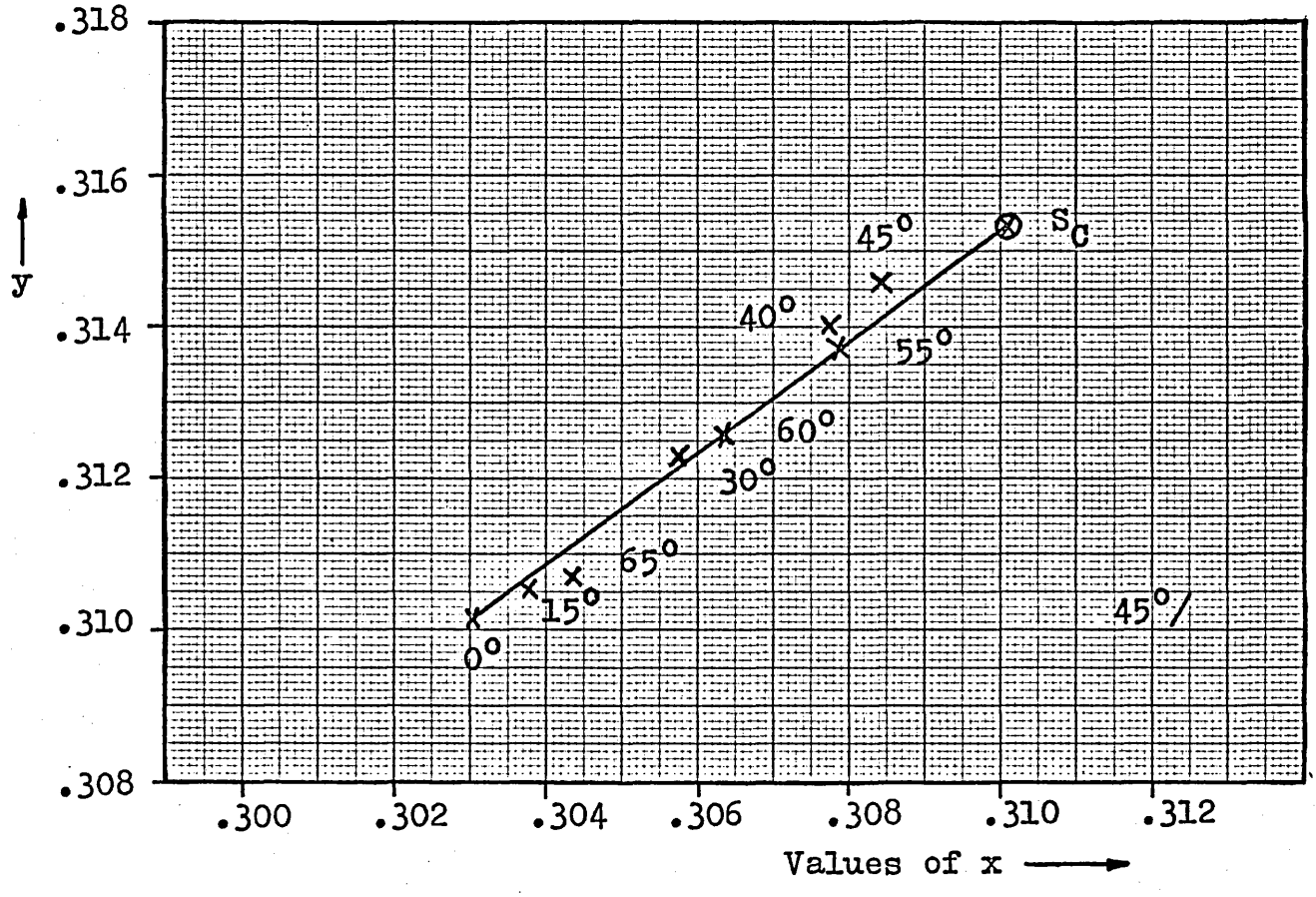


Fig. 4.13 Chromaticity Coordinates. Viewing angles as shown.

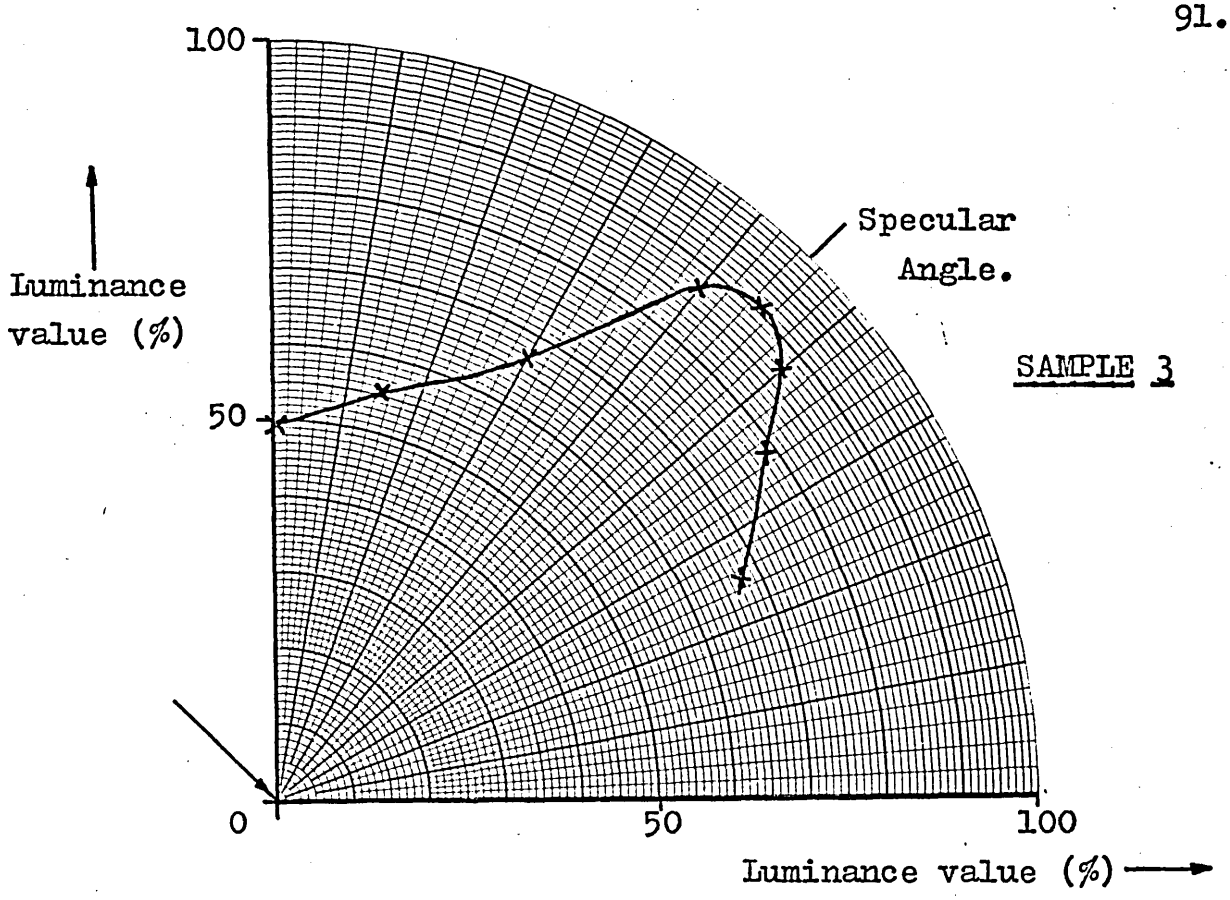


Fig. 4.14 Polar Luminance Curve - Sample 3.

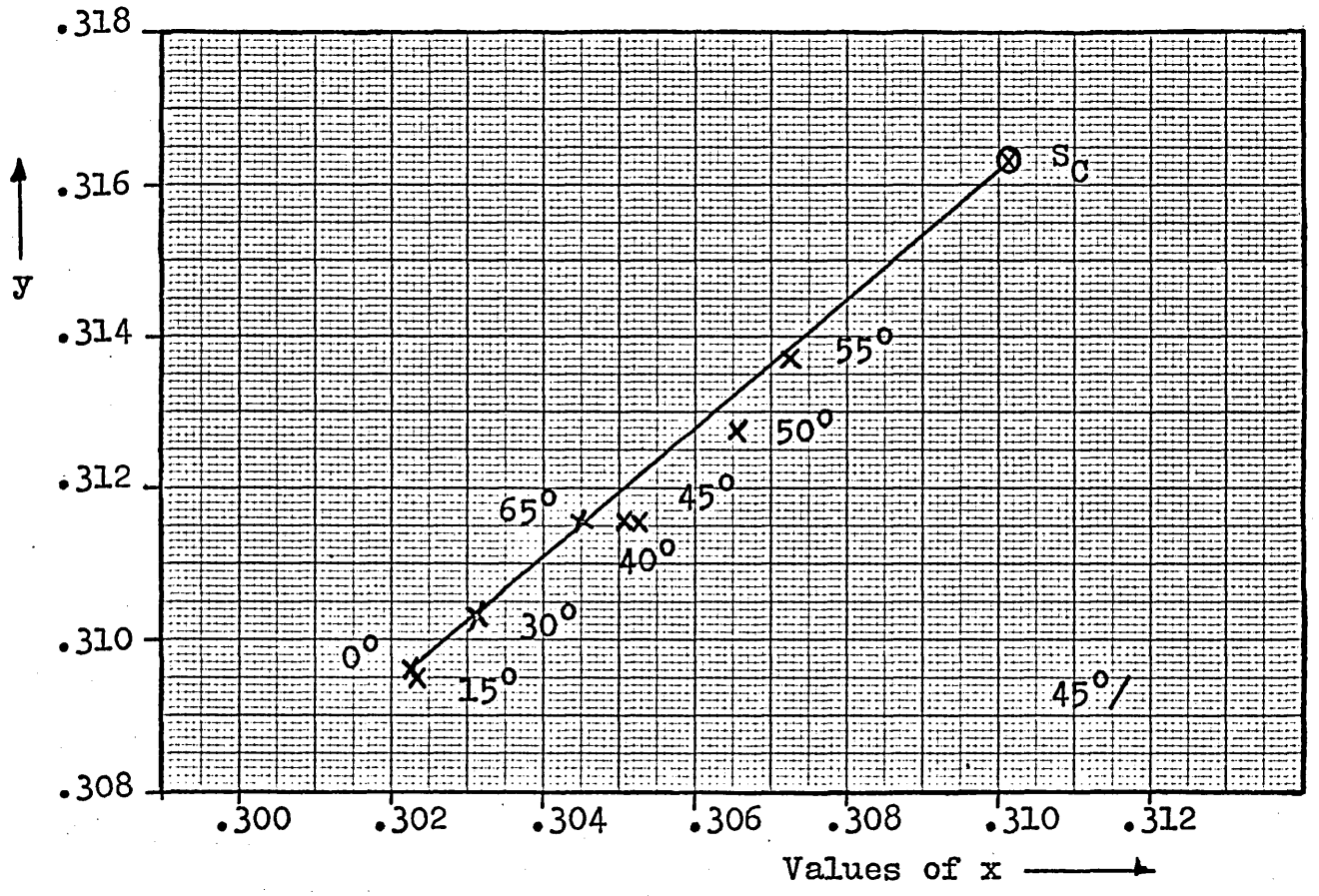


Fig. 4.15 Chromaticity Coordinates. Viewing angles as shown.

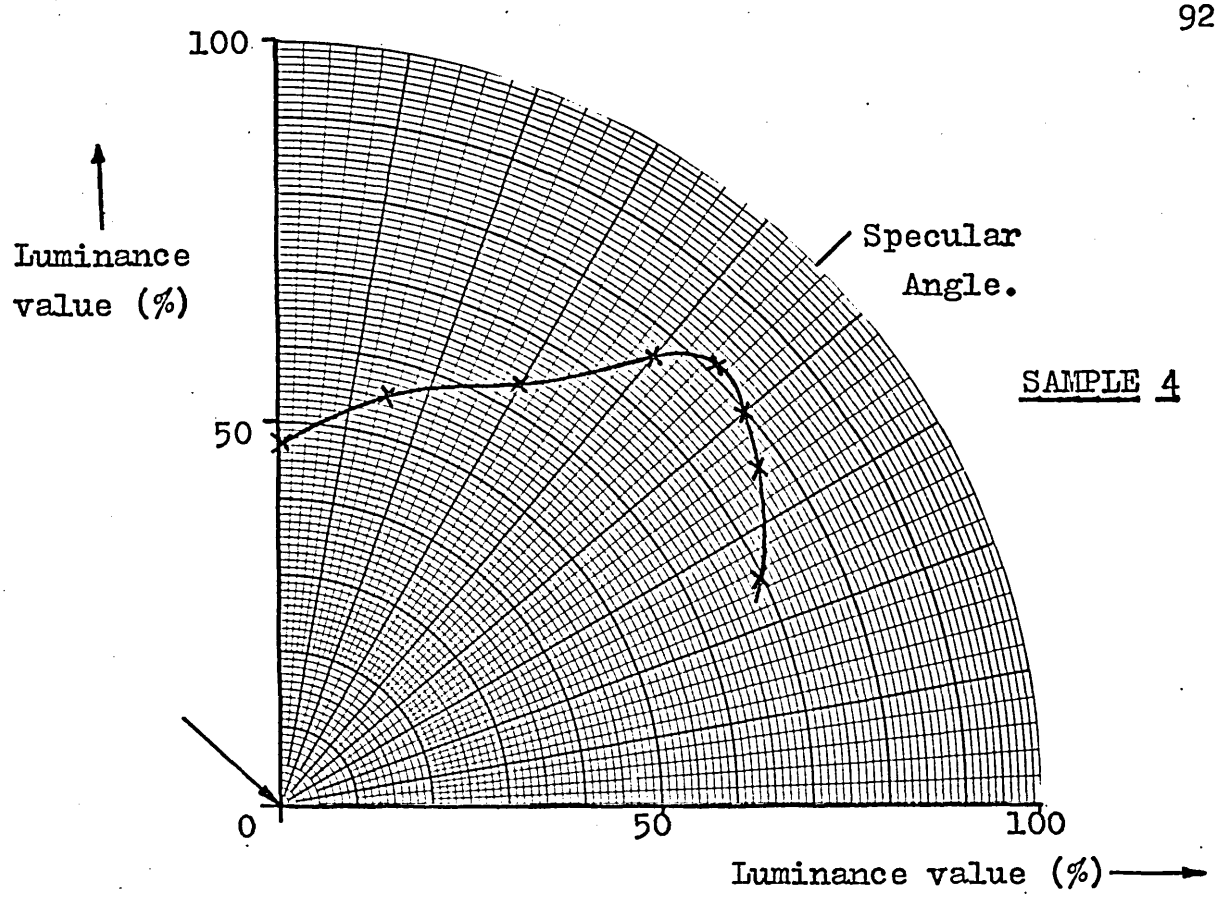


Fig. 4.16 Polar Luminance Curve - Sample 4.

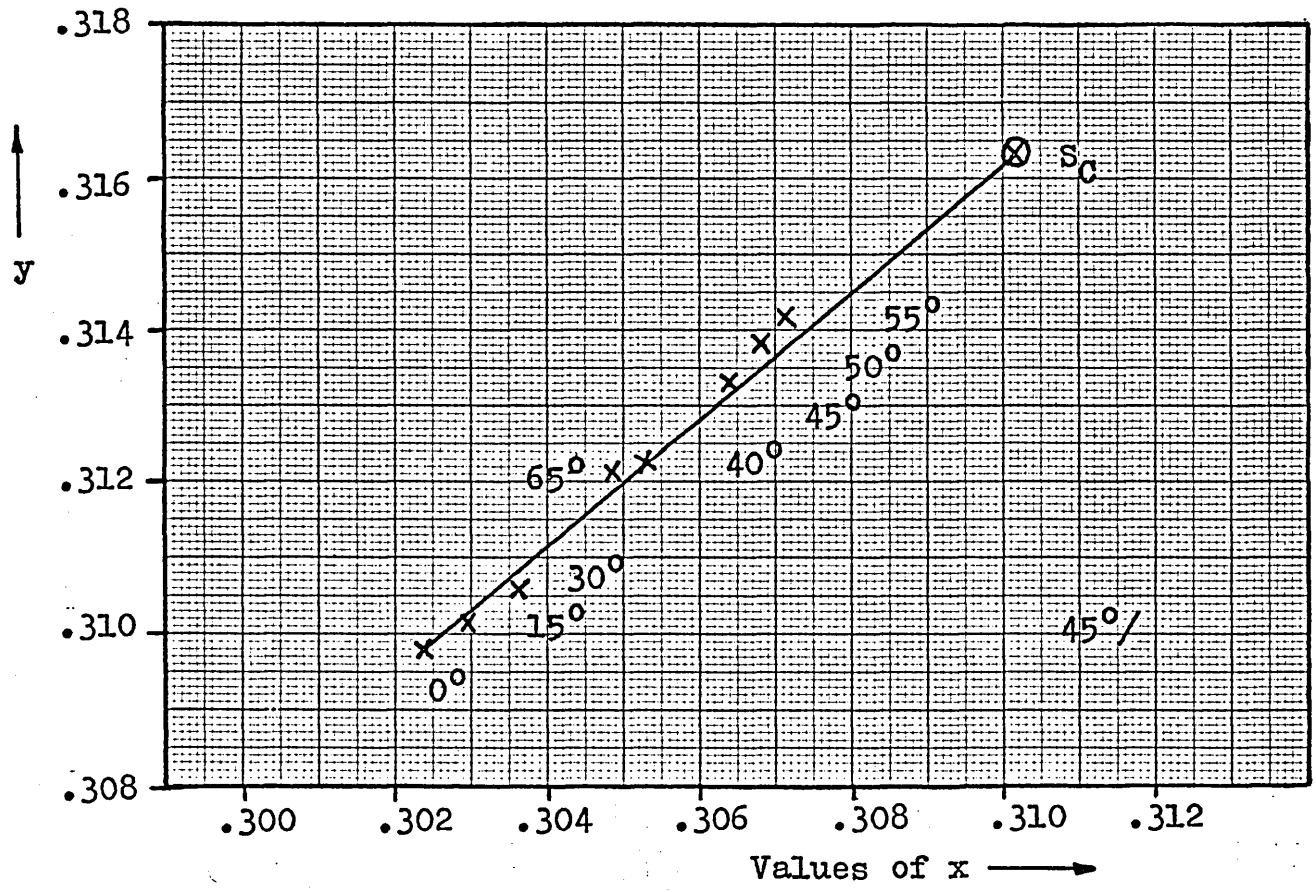


Fig. 4.17 Chromaticity Coordinates. Viewing angles as shown.

possible to generalise in saying that sample 4 appears a more matt surface overall from its polar distribution curve than sample 3, despite the fact that both surfaces were apparently equal in gloss to sample 1. Other than near the specular angle the curves show similar absolute values, differing for example at the $45^{\circ}/0^{\circ}$ position by less than 5% for all samples.

The equivalent colorimetric properties are illustrated in Figures 4.11, 4.13, 4.15 and 4.17 by plotting the chromaticity coordinates for the samples 1 to 4 respectively as a function of measuring conditions on a portion of the 1931 C.I.E. chromaticity diagram, with respect to standard illuminant C. The colour of each sample, described as bluish white by observers, occupied the section of the diagram shown, only slight variations in the chromaticity occurring under measuring conditions of $45^{\circ}/0^{\circ}$ for all four samples. This was as expected since the four had been chosen for their similarity in colour.

In the case of sample 1 in Figure 4.11, as the angle of collection approaches specular, so the chromaticity coordinates approach the source point along an almost straight line between S_C and the $45^{\circ}/0^{\circ}$ point. This would be expected as progressively more specularly reflected light is collected, after which the points move out, the purity of the colour increasing as more 'body' reflected light is collected. Two points will however be discussed later since they do not fit into this normally acceptable pattern. The coordinates of

the measured colour at 42° collecting angle are on the opposite side of the illuminant point at a good distance from it, and the specular point itself shows properties not normally associated with it.

The matt surface 2 shows a similar, but more ordered, movement of chromaticity coordinate with changing angle of view, a minimum of purity occurring at the specular angle. The overall movement is somewhat smaller than the corresponding one for a glossy surface finish but illustrates the presence of a good deal of top surface reflected light even in a fairly matt sample.

The interesting data however are those contained in Figures 4.15 and 4.17 for samples 3 and 4 respectively. Once again the effect of the chromaticity coordinates collapsing towards the illuminant point at almost constant dominant wavelength as the specular angle is approached clearly appears, but in these cases the movement continues well beyond the 45° viewing position until an angle of approximately 55° is reached. On reaching this minimum purity the points again reverse in direction with increasing collecting angle as the 'body' colour is restored.

A listing of the angular variation in excitation purity is given in Table 4.2 for all four samples in order to give a rapid comparison of the effects obtained from the different structures.

TABLE 4.2

Sample:-	1	2	3	4
Angle of View	p_e%	p_e%	p_e%	p_e%
0°	4.03	3.11	3.61	3.56
15°	3.76	2.87	3.57	3.34
30°	2.67	1.80	3.23	3.12
40°	2.07	0.78	2.58	2.19
45°	5.02	0.42	2.53	1.64
50°	—	—	1.94	1.37
55°	4.28	0.96	1.40	1.21
60°	—	1.68	—	—
65°	5.28	2.75	2.63	2.30
Approx. $\lambda_d$nm	480.0	481.4	479.9	480.1

iii) Discussion.

A very important point arises from the preceding polar luminance curves. The results obtained from samples 1 and 2 are well known curves, indicating the obvious difference between the high gloss surface and its fairly matt counterpart. Such curves may be analysed by well established methods, for example those of Nimeroff (1952), to obtain an accurate measure of the surface gloss. One particular method is to determine the kurtosis index, α_4, for the actual goniophotometric curve, a method shown to correlate well with the distinctness-of-image gloss. The

application of this approach to curves similar to samples 3 and 4 is obviously misleading. Although the figure obtained, which would be of the order of that obtained in case 2, does indicate what in practice is obtained, that is little or no image formation at the specular angle, observers under any other conditions rank the surface gloss of samples 3 and 4 highly.

It is difficult on observing such rough samples to determine whether by careful choice of measuring conditions one would obtain a truer representation by a goniophotometric curve of the real appearance of such material. As a test of this, several other configurations were measured and a selection of results of polar luminance distribution appear in tables 4.3 and 4.4.

Table 4.3 illustrates the effects of rotating the sample about an axis in the plane of measurement and normal to the sample surface, readings being given at each 20° step. The material was symmetrical in each 90° quadrant, therefore only angles of rotation between 0° and 90° are considered. Intermediate angles were checked during a continuous rotation of the specimen for irregularities at angles other than those measured in detail. For an angle of incidence of 45° the results for an arbitrary 0° angular position have been normalised to unity at each collecting angle, and data at the other angular steps given as a fraction of this result.

The similarity in results for each setting within a few percent, and the constancy of each column, indicates that only slight variations in the polar luminance

curves occur as a function of angular rotation of such a sample.

TABLE 4.3

	Angle of Incidence = 45°				
Angle of	Angular rotation of sample.				
Collection	0°	20°	40°	60°	80°
-5°	1.00	0.99	0.95	0.94	0.93
10°	1.00	0.97	0.95	0.93	0.96
25°	1.00	0.95	0.92	0.93	0.98
35°	1.00	0.99	0.97	0.98	0.97
37°	1.00	1.00	0.99	0.97	0.96
39°	1.00	1.02	0.97	0.97	0.94
40°	1.00	1.02	0.99	0.99	0.93
41°	1.00	1.01	0.98	0.98	0.92
43°	1.00	1.00	1.01	0.98	0.94
45°	1.00	1.04	1.01	1.01	0.97
50°	1.00	1.02	1.00	0.99	0.97
55°	1.00	1.04	1.04	1.01	0.97
60°	1.00	1.03	0.97	0.96	0.97

Table 4.4 outlines similar results obtained when the angle of incidence of light striking the sample surface is varied. The luminance data are given for angles on either side of, and in the immediate vicinity of, the specular angle, and the figures already quoted in the

preceding section for 45° incident light have again been made unity. An easy comparison may be made with these further data by again quoting them as fractions of the first column.

TABLE 4.4

	Angle of rotation = 80°		
Angle of collection	Angle of Incidence.		
about specular.	45°	30°	15°
-10°	1.00	0.85	0.70
-5°	1.00	0.88	0.74
-3°	1.00	0.87	0.72
-1°	1.00	0.85	0.72
Specular	1.00	0.85	0.72
1°	1.00	0.86	0.71
3°	1.00	0.84	0.72
5°	1.00	0.85	0.72
10°	1.00	0.88	0.75

Again the constancy of each column indicates little or no deviation from the polar curves already quoted, the only difference being that as the incident angle is reduced so the corresponding luminance curve will also reduce in value in the region of specular reflection.

Similar, although not such exhaustive, tests on sample 4 suggest the same conclusions applicable on

this surface.

One method of analysing the true surface gloss which immediately seems obvious is to decrease the measuring spot to dimensions very small compared with those of the structure under investigation. In the above data the area of cross-section of the incident light beam effectively integrated the effect of many 'cycles' of roughness, a process the human visual system does not necessarily duplicate. In practice on attempting to employ such a method by reducing the spot size to some 0.5 mm square compared with a structure 'cycle' of some 4 to 5 mm it was found to be fairly ineffective. The results did tend to give somewhat more peaked curves than those already quoted but their variation was large, dependent mainly on location as might be expected, and no true absolute value for the material could really be quoted. Since a spot considerably smaller would be necessary in practice, effectively to reduce the surface at any given point to a smooth one, the method was not really suitable using the present instrument. Multiple reflections and shadowing from adjacent peaks also tended to affect such measurements to the extent that no reliable information was received.

An important point is raised here however, since the measurement of texture must reflect the visual assessment of a surface. It therefore follows that the information concerning the gloss content of a sample such as the present one must be made with a patch area whose dimensions are more closely related to the area from which the eye gathers its knowledge of gloss content, in this case

obviously less than 0.5mm square. In regular, periodic structures this may be assisted by, visually, considering areas at identical points on the structure period - a difficult instrumental operation. Thus we have two basic visual assessment processes - a macroscopic investigation of surface contour, together with a spatially, very precise, investigation of, say, gloss content - often beyond the capabilities of the instrument, and thus defining the limits at which an instrument may measure gloss information directly related to the texture of a surface.

Finally it is important to consider the scale of roughness involved. It is not possible simply to extend such results as the above ones to materials whose roughness is on a smaller scale since the reflection and collection process is far too complex. However, on a macroscopic level it appears much of the preceding is generally true. Sample 4 for example, whose structural period was much smaller than that of sample 3, was measured to have an even more matt polar distribution curve than sample 3, although their respective material surface finishes were identical and only the structure different.

Turning to the colorimetric aspect of the results, Figures 4.11 and 4.13 are in accordance with previous statements as to the mixing of 'surface' and 'body' reflected light, with the exception of the points at 42° and 45° collection for sample 1. It is felt that the explanation of such points, which when remeasured remained

at these coordinates, is probably due to some optical phenomenon since the critical angle for total internal reflection in perspex is approximately 42°.

However the corresponding plots for the two surfaces 3 and 4, Figures 4.15 and 4.17 respectively, illustrate a somewhat different property of the material when structured. The reduction in purity, at almost constant dominant wavelength, with increase in viewing angle is again present, but continues up to an angle of approximately 55° when the trend reverses direction. Despite the fact that the polar luminance curve maximises at the specular angle, 45°, the spectral distribution of reflected light continues to approach more closely that of the illuminant up to angles of ten or more degrees beyond.

If one simplifies the problem by assuming such reflected light to be a mixture of top surface reflected light, whose colour is that or approximately that of the illuminant, and internally reflected and diffused body reflected light, whose colour would be approximately that measured under 45°/0° conditions, it would appear that the ratio of these quantities continues to increase for samples 3 and 4 despite the fact that apparently top surface reflection maximises at 45°.

Due to the complexity of the reflection processes involved in such a rough structure a simplified approach is not necessarily correct. Shadowing and multiple reflections from adjacent facets may have the effect, for instance, of reducing the overall level of reflected light at certain angles without affecting its spectral content.

The manifestation of these processes would be in results as those found above.

The apparent similarity of results from sample 3 and 4 is somewhat incorrect since on more detailed angular measurement it was found that the point of minimum purity for sample 3 was at 62° viewing angle, and that for sample 4 at 64°. The sudden increase in purity at 65° viewing conditions tends to support such ideas as those outlined above in that at some point the effect returns to one almost identical to a smooth surface. Measuring under angular conditions of 45°/65° would then give results similar to those of samples 1 or 2, a result found to occur in Figures 4.15 and 4.17.

A consquence of such results may be particularly important when measuring rough surfaced materials in spectrophotometers, for instance industrially. In the above cases there is a point at approximately 55° viewing angle which is almost as high in luminance as the specular angle reading, and whose distribution is more nearly that of the illuminant than that at the specular angle. Therefore large errors may occur in measurements on say integrating sphere instruments where the specular angle is purposely excluded. Work by Billmeyer and Marcus (1969) has shown the dependence of results on measuring conditions to vary as the surface texture of the sample varies. The changes however were relatively small since only samples having a texture which had non- directional characteristics were used.

4.3 Conclusions.

On using pressed magnesium oxide samples as reference standards allowance must be made for the variation in chromaticity with angular viewing conditions. Such variations would appear to increase in size if disturbances in the perfectly flat surface are present and introduce extremely large errors at viewing angles greater than 20°. The diffusing characteristics of flat magnesium oxide surfaces appear to be good at an incident angle of 45°, and extremely constant over large areas, however the presence of any surface roughness, although not significantly impairing the diffusing properties of the material, will tend to alter the absolute reflectance value in a somewhat unpredictable fashion.

Measuring techniques for perfectly flat surfaces are well documented, however when employed on structured materials they effectively integrate the reflection effects from large areas and as a result the final data are not necessarily in agreement with visual observation. Measuring configurations which overcome these difficulties appear generally to be difficult or impossible to achieve and analysis of goniophotometric curves in order to obtain a gloss scale should not be attempted without knowledge of the surface structural characteristics, otherwise large differences will occur between visual and measured rankings. A periodically structured surface may also give rise to angular chromaticity shifts not normally associated with its smooth counterpart, and shadowing effects within the surface may also lead to distortions in polar luminance

distribution.

The foregoing discussion illustrates a most important point regarding any analysis of surface texture; in any specification of texture a simple gloss-matt scale is insufficient. The minimum specification would need to be a two dimensional one with a rough-smooth scale as the second variable. On a microscopic level this secondary scale is adequately covered by usual goniophotometric curves, since the eye cannot resolve individual contributions from the various facets, a situation duplicated by the detector in the measuring instrument. The curves may be analysed by techniques discussed earlier in Chapter 2, in particular those resulting from the microfacet theory (Toporets, 1964). Such theories result in equations relating the specular component (S) to the diffuse component (D) thus

$$\frac{S}{D + S} = \exp\left\{-kh^2 (\cos^2 i)/\lambda^2\right\}$$

where h is the microfacet height, k a constant, and λ the wavelength of the incident light. Obviously therefore a measure of the irregularities (h) may be obtained from goniophotometric data, a fact illustrated by Billmeyer (1971) who took as a measure of the quantities S and D, the areas under the respective parts of their polar luminance plot.

However for macroscopic variations in roughness the integration is not performed by the human visual system in many cases and the usual polar distribution curves must then be further aided by the addition of data from

either goniospectrophotometric scans across the material with a spot, very small in comparison to the typical size of the surface undulations, or physical traces of the surface from such an instrument as a profileometer. The former may in certain circumstances prove difficult since few instruments are capable of such measurements and in many cases the data itself has, as mentioned above, been found difficult to interpret. This is due in part to the complexity of the optical reflections involved, and partly the lack of generality in any treatment of such surfaces.

CHAPTER FIVE.

COLORIMETRIC ASPECTS OF SURFACE TEXTURE.

The results of the previous chapter indicate a definite link between the physical structure of a surface and its angular colorimetric properties. Further, the particular material also affects these properties and both lead to definite chromaticity changes, with location, across any sample. Such chromaticity variation must naturally be enhanced by the presence of actual colour differences within the material itself, and all contribute in part to the total colour effects observed upon viewing under every-day conditions.

The very essence of texture appreciation would appear to depend on the ability to perceive such variations in colour down to the smallest limits. The presence of smooth, glossy or greasy surfaces for example is normally noticed by the specular reflections or highlights - effectively a desaturation of the object colour, and similarly a rough, irregular, matt surface by the variations in light and shade, and therefore colour, caused by the small protruding facets.

This type of data tends to add a certain 'plasticity' to the final visual image, without which materials tend to look flat and featureless, possessing an overall matt finish. Since such information is fundamental therefore in the visual appreciation of texture, and consequently, in its successful reproduction in any colour

medium, an investigation into the extent of such variations in different samples was felt to be extremely important.

5.1 Choice of Samples.

The possible range of materials for such an experiment is extremely wide and in order to make the data obtained reasonably compact for any following analysis and discussion, yet at the same time to cover as wide a range of variables as possible, it was necessary to choose the samples to be measured with care.

Firstly it was decided to concentrate on naturally occurring samples rather than man-made materials, in contrast to the preceding chapter, since such materials are of particular interest in the reproduction field, usually occurring more often and invariably presenting the greatest problem. This mainly arises from the greater complexity and nonuniformity of reflection characteristics from such materials, this in turn being due to the very complicated nature of construction involved. Many samples in this category, however, were not suitable since the measuring programme on each was such that reasonable stability of their properties over periods of several days was necessary to obtain self consistent results.

Three samples were then chosen which fulfilled such conditions and gave a range of surface textures typical of those found in normal circumstances.

Sample a), the inner surface of a piece of tree bark, whose surface was fairly rough, showing a definite structure, had an extremely matt finish. The colour variation in general

appeared to be very small indeed.

Sample b), the inner surface of a scallop shell, was extremely glossy, possessing a smooth, but curved, surface, the curvature varying somewhat from point to point. There was a reasonable colour variation already present in the sample, depending on the exact location under test.

Sample c), an iris leaf, was the least permanent of the specimens and special care had to be taken that the necessary measurements were made before any appreciable deterioration in its condition had taken place. The sample again appeared to possess only very small colour variation across its surface and its structure was almost flat, showing no marked deviations or undulations. The finish would be classified as matt.

5.2 The Measuring Programme.

The particular sample under test was mounted rigidly on the kinematic slide mount in the Wright Spectrophotometer and the cross-sectional area of the incident beam reduced to some 1mm square. Points were then arbitrarily chosen along a horizontal line across the sample surface at spacings of approximately 4mm and the position of the slide adjusting lever carefully noted in order that accurate relocation be possible.

The reference standard, freshly pressed magnesium oxide powder, was similarly mounted and used under identical conditions to those of the test sample. Corrections were applied to the results in the light of the results of Chapter 4.

The spectral reflectance of each point was then measured throughout the visible spectrum, from 380nm to 770nm at 10nm intervals, at several viewing angles between normal and 65° to the surface normal. The angle of incidence used for the investigation of samples a) and b) was 30° to the surface normal and that for sample c), 45°. To avoid possible systematic errors, and therefore any systematic variation in chromaticity coordinates, measuring techniques were varied somewhat arbitrarily so that at times each location was measured under various angular conditions and similarly at other times all points on the specimen were measured at each angle in turn. No obvious systematic movement of chromaticity results however was detected due to the method of measuring.

It was felt that in essence such data were a reasonable duplication of the typical information received by an observer, via the visual system, regarding the reflection properties of an object. It must therefore contain many of the necessary 'clues' used in assessing the particular surface texture. Also a clear estimate of spatial chromaticity variations would be obtained, both under normal measuring conditions and varying angular conditions.

Specified angles, although accurate with respect to the instrument slide mount, must be treated as approximate since no sample was perfectly flat, and therefore some spread must be present from point to point on the sample.

5.3 Results.

The resulant spectral reflection curves were reduced further to their respective chromaticity coordinates and luminance values, and will all be quoted with respect to illuminant S_C in this chapter.

The data are given in three distinct sections depending on the sample.

Figures 5.1 to 5.10 inclusive show, alternately, the polar luminance distribution and the angular chromaticity coordinates at each of five points, 1mm square, separated by some 3mm, on the sample a) - the results from the sixth point being somewhat unreliable due to the slide mount partially obscuring the reflected light towards the detector. Figures 5.11 to 5.24 inclusive and Figures 5.26 to 5.37 inclusive show corresponding data for seven points on sample b) and six points on sample c) respectively. The first chromaticity diagram of each set shows an insert of the enlarged area in relation to the whole chromaticity diagram. Figure 5.25 illustrates the spectral reflectance curves for position 2 on sample b) at seven different angles of collection in order to illustrate the detailed changes responsible for chromaticity shifts observed in Figure 5.14.

Finally, figure 5.38 compares the result obtained at a viewing angle normal to the surface for each location on a particular sample, the result which would be quoted in any routine measurement of a surface colour.

5.4 Discussion of the Results.

It is possible to draw certain conclusions

Sample a)
(Inner Surface
of Tree Bark)

POINT 1

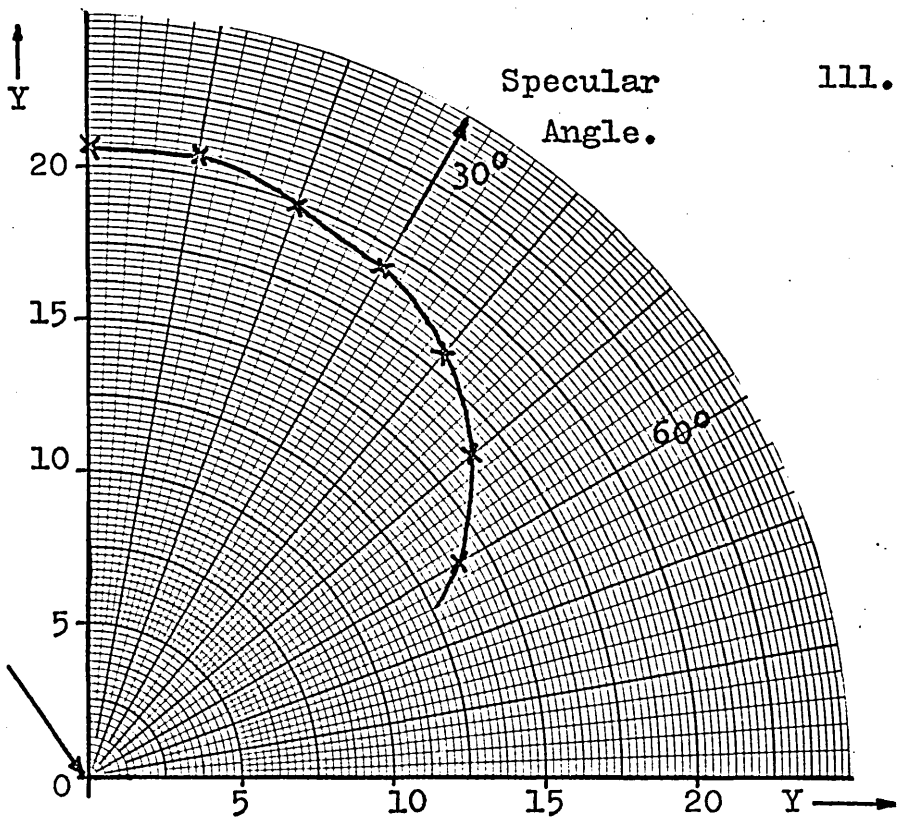


Fig. 5.1 Polar Luminance Distribution for 30° Incidence.

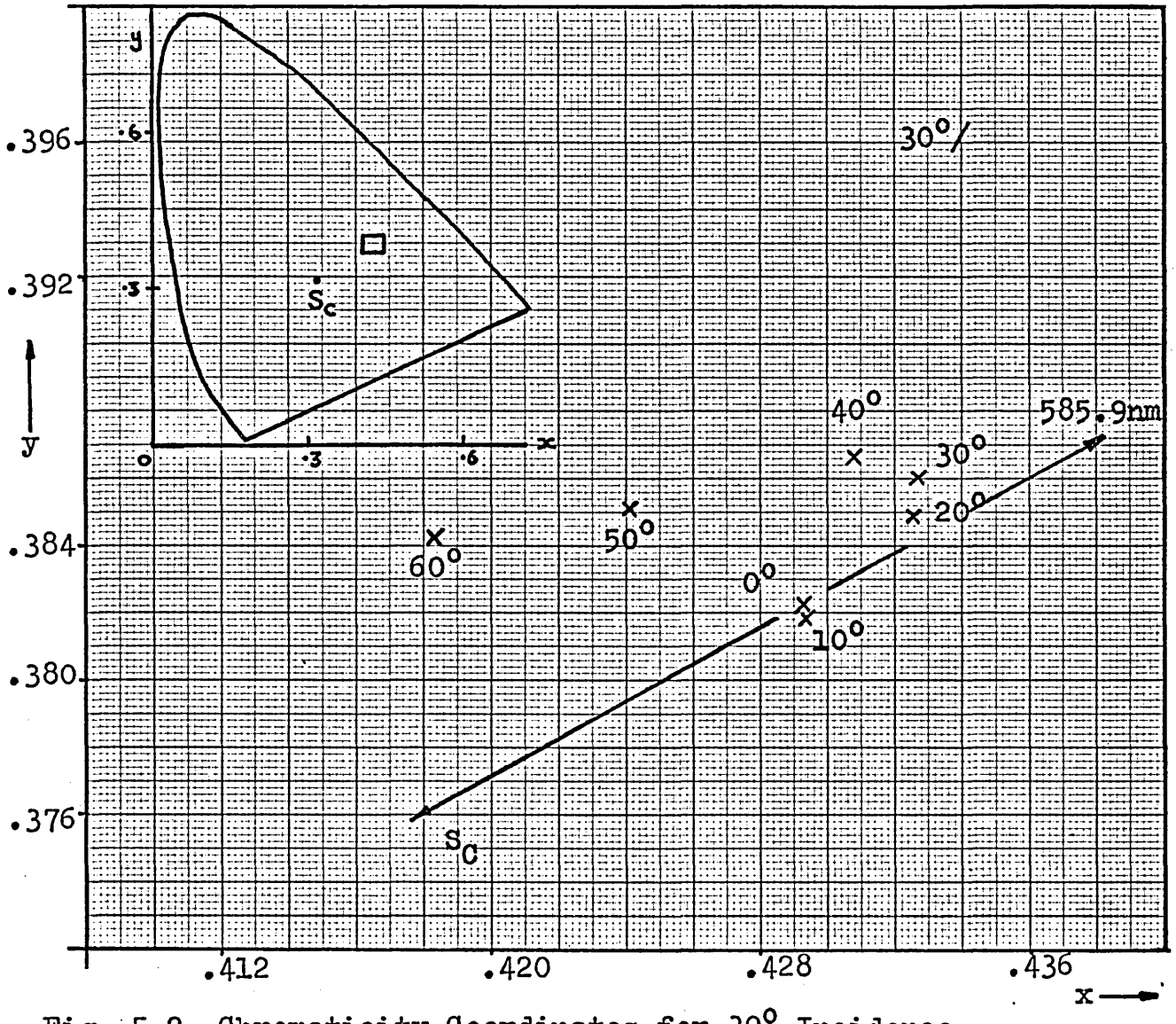


Fig. 5.2 Chromaticity Coordinates for 30° Incidence.

Sample a)
(Inner Surface
of Tree Bark)

POINT 2

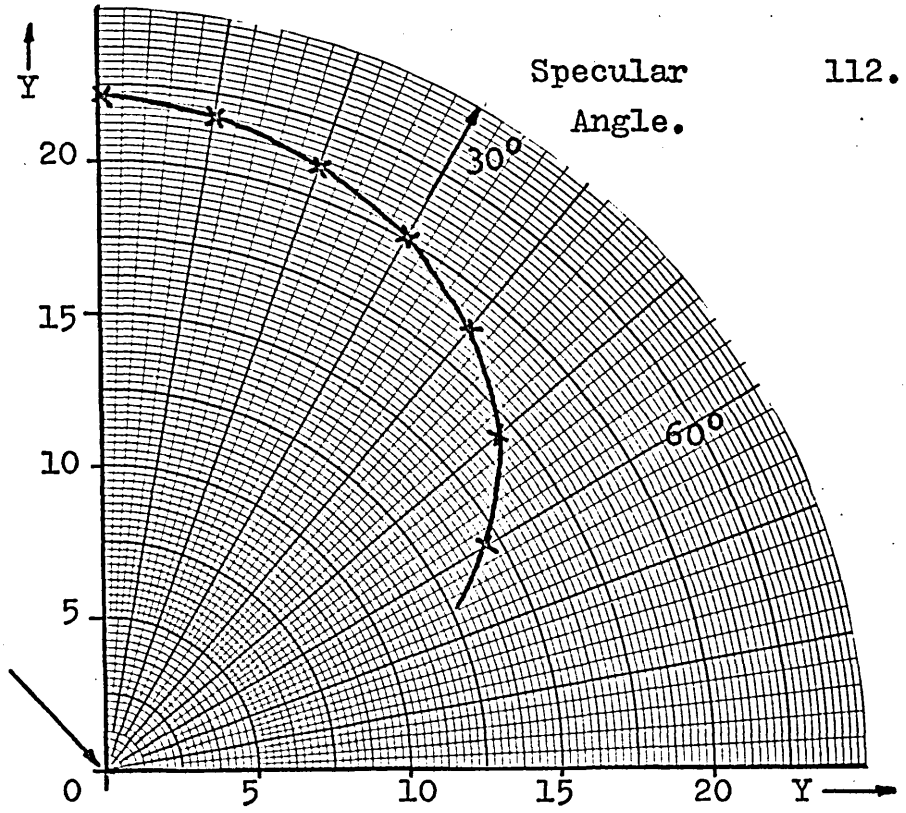


Fig. 5.3 Polar Luminance Distribution for 30° Incidence.

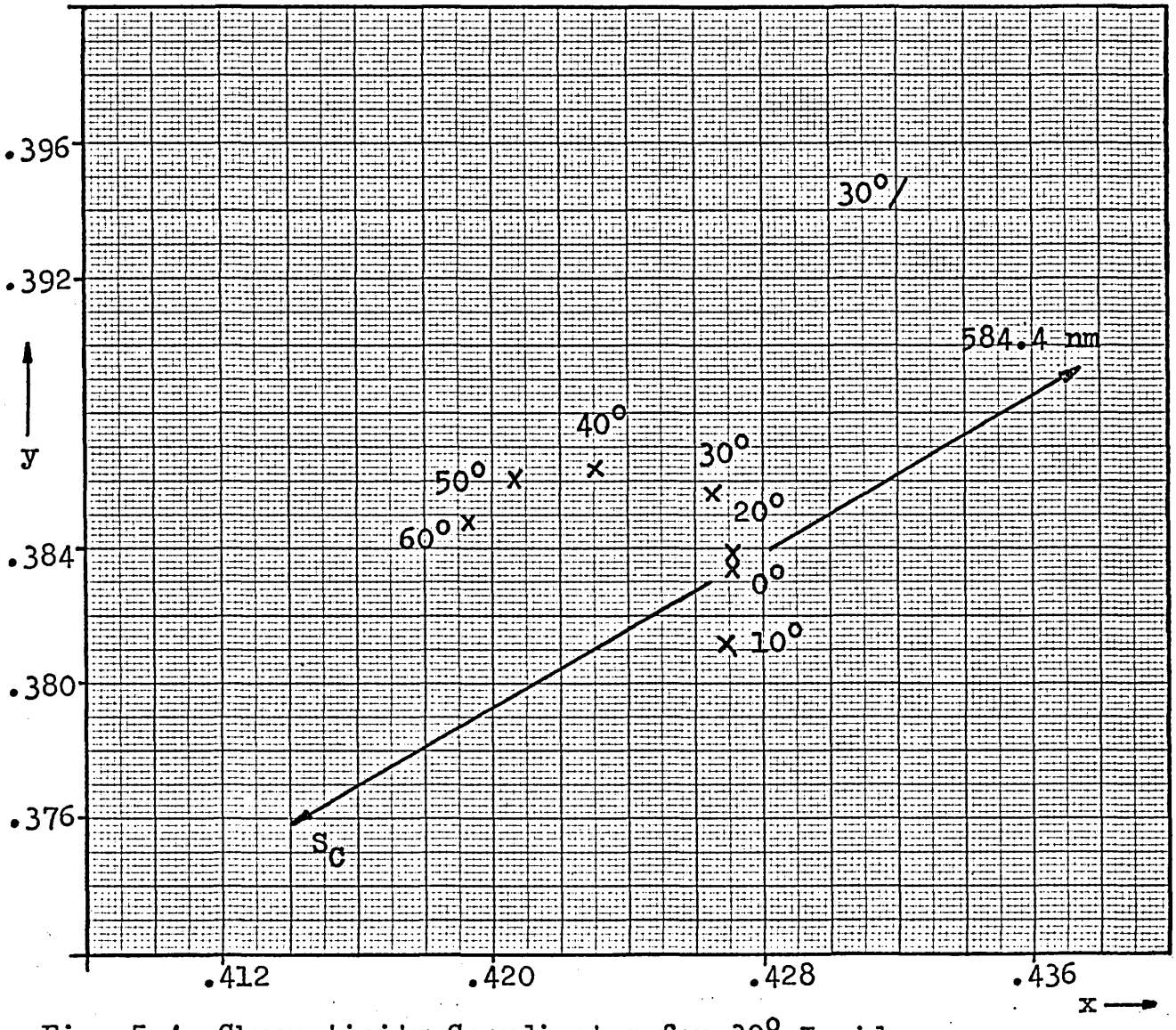


Fig. 5.4 Chromaticity Coordinates for 30° Incidence.

Sample a)
(Inner Surface
of Tree Bark)

POINT 3

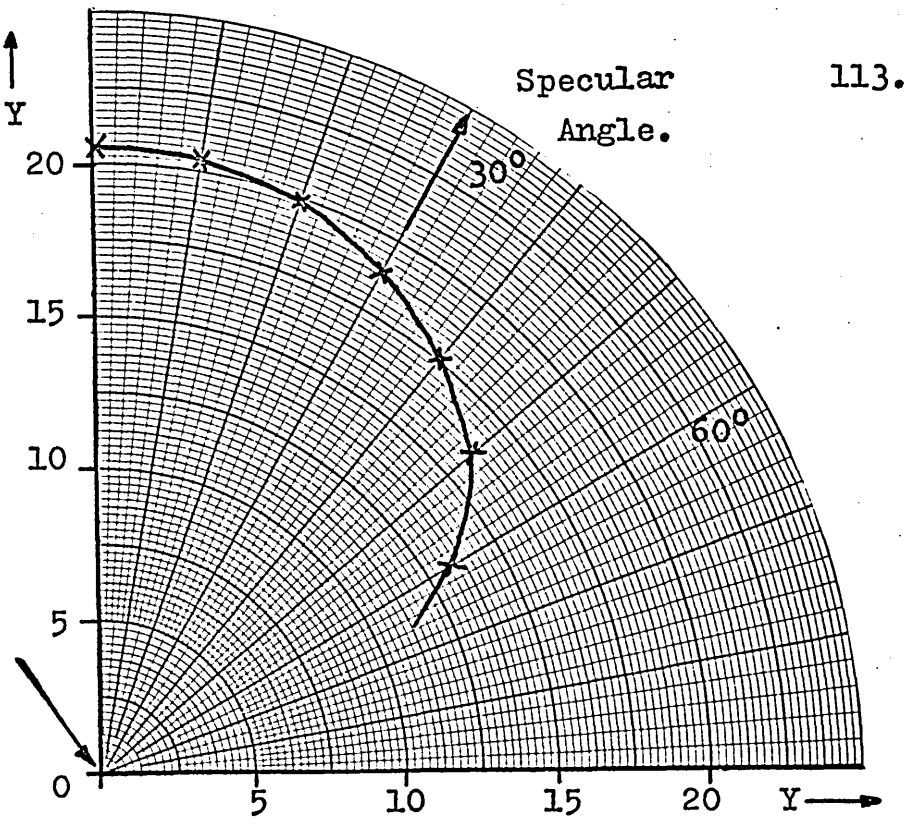


Fig. 5.5 Polar Luminance Distribution for 30° Incidence.

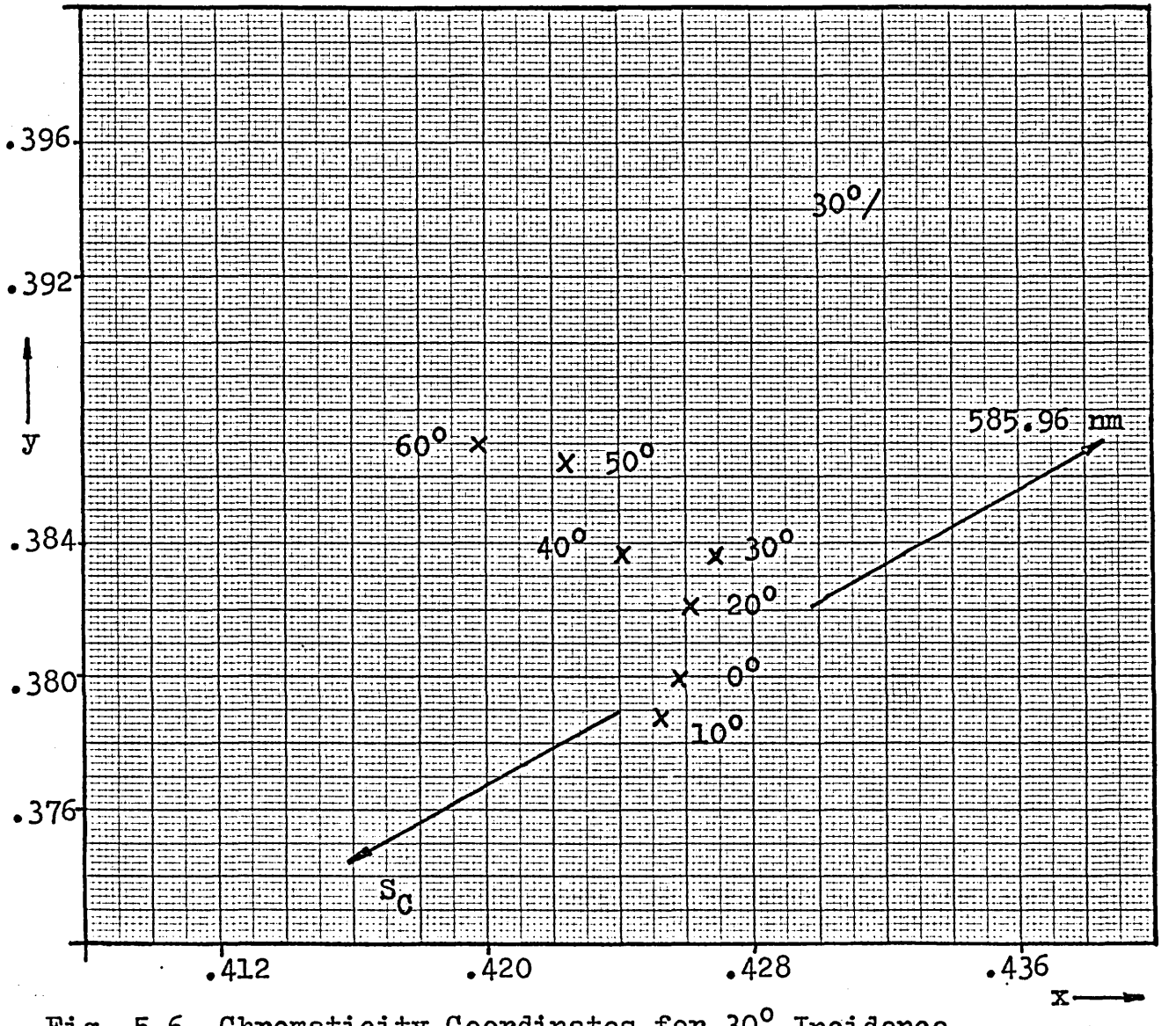


Fig. 5.6 Chromaticity Coordinates for 30° Incidence.

Sample a)
(Inner Surface
of Tree Bark)

POINT 4

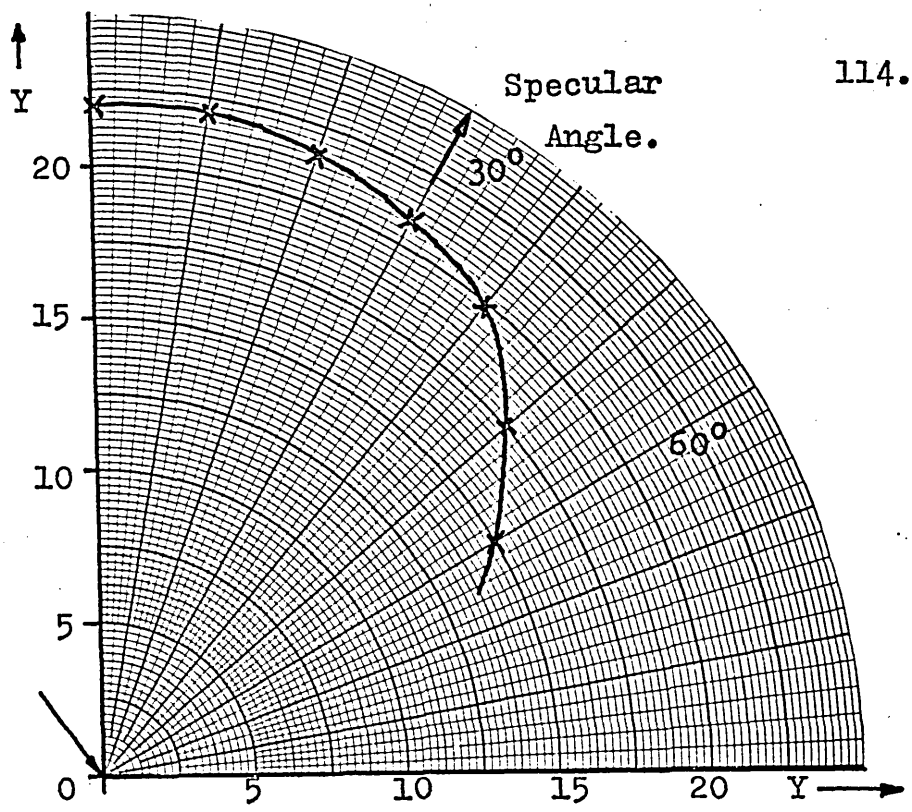


Fig. 5.7 Polar Luminance Distribution for 30° Incidence.

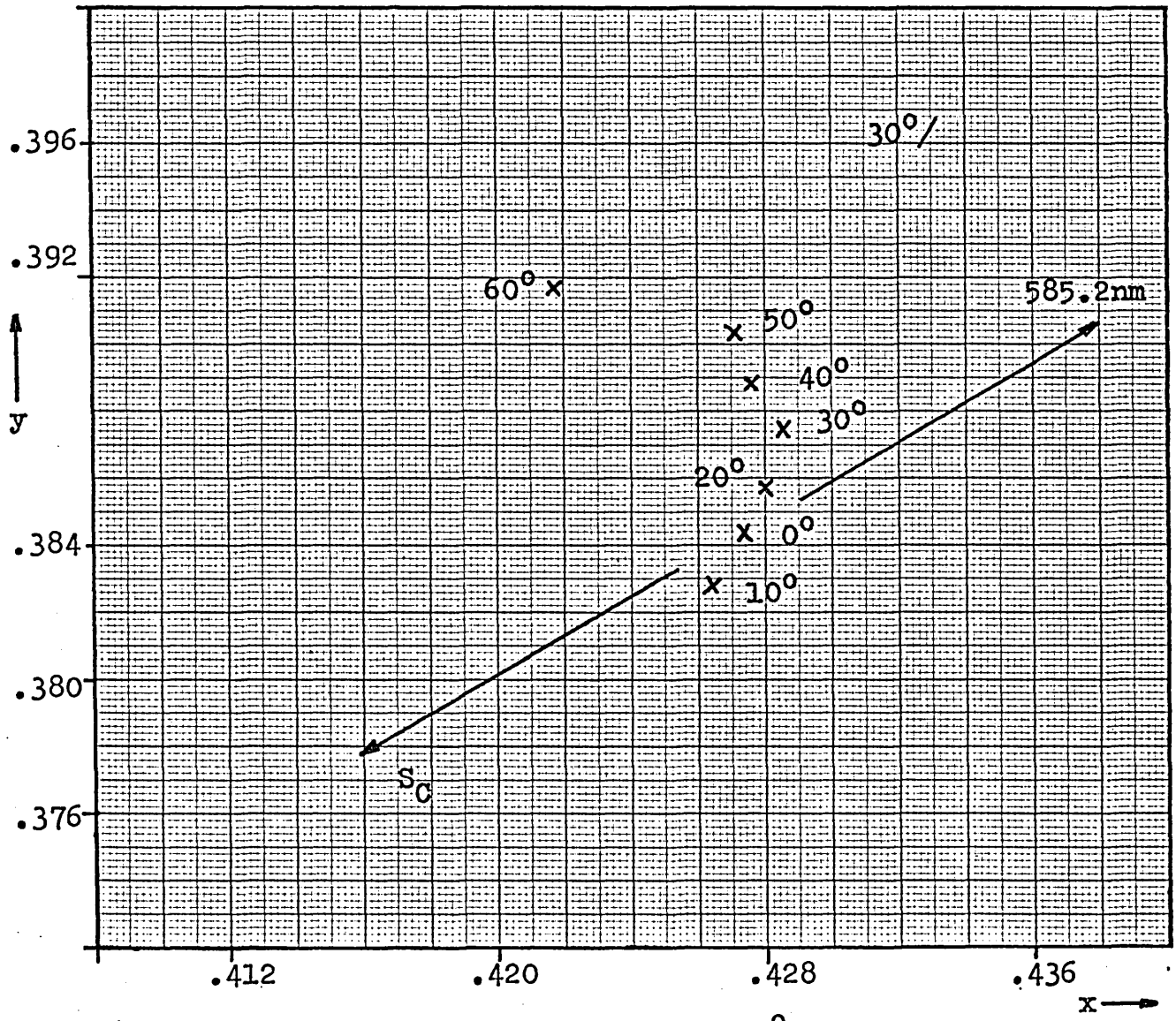


Fig. 5.8 Chromaticity Coordinates for 30° Incidence.

Sample a)
(Inner Surface
of Tree Bark)

POINT 5

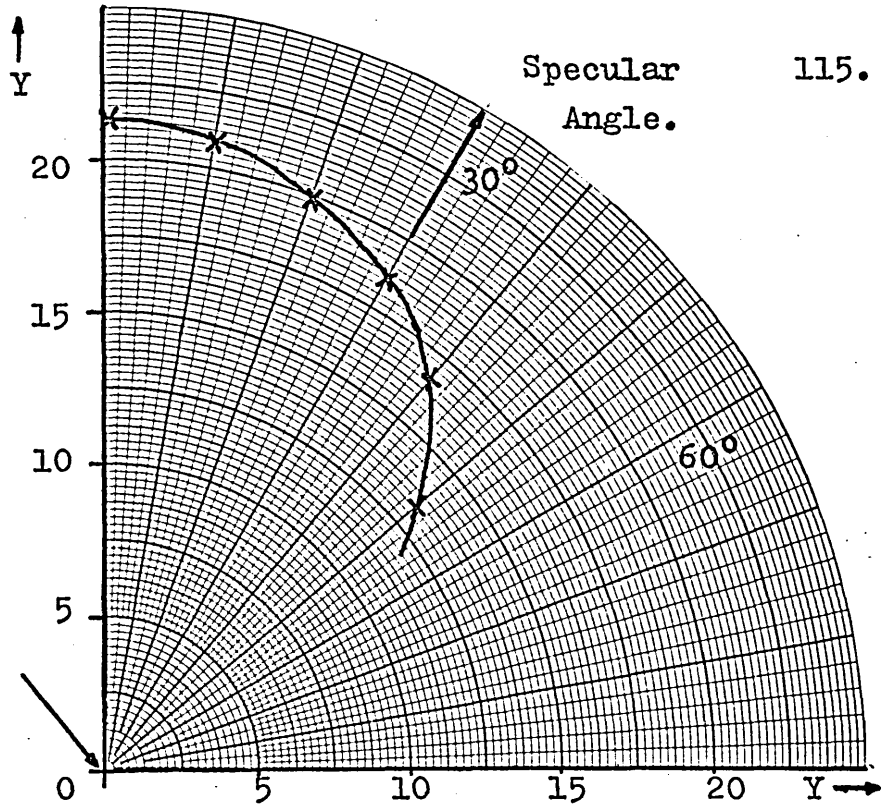


Fig. 5.9 Polar Luminance Distribution for 30° Incidence.

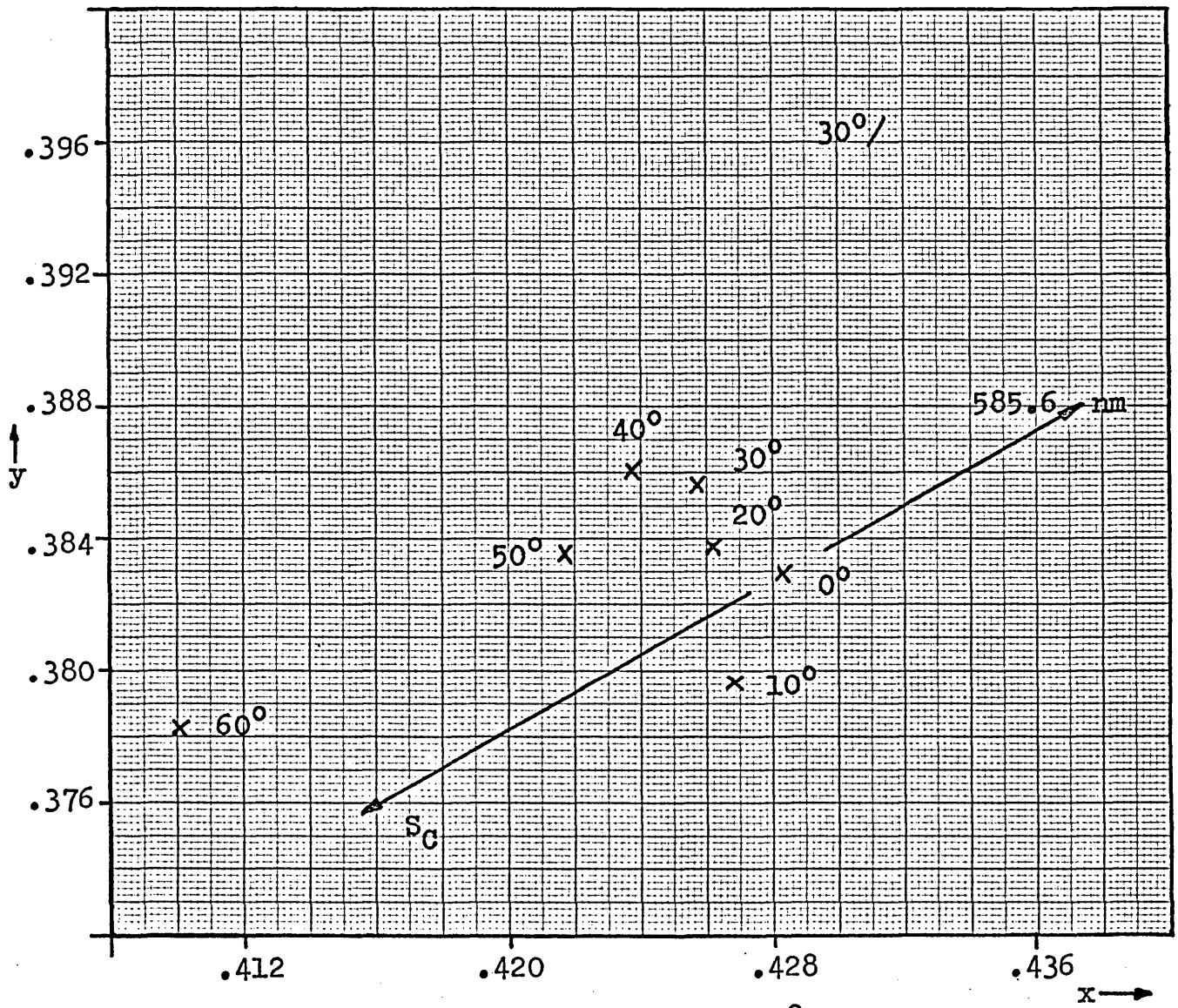


Fig. 5.10 Chromaticity Coordinates for 30° Incidence.

Sample b)
(Inner
Surface of
Scallop Shell)

POINT 1

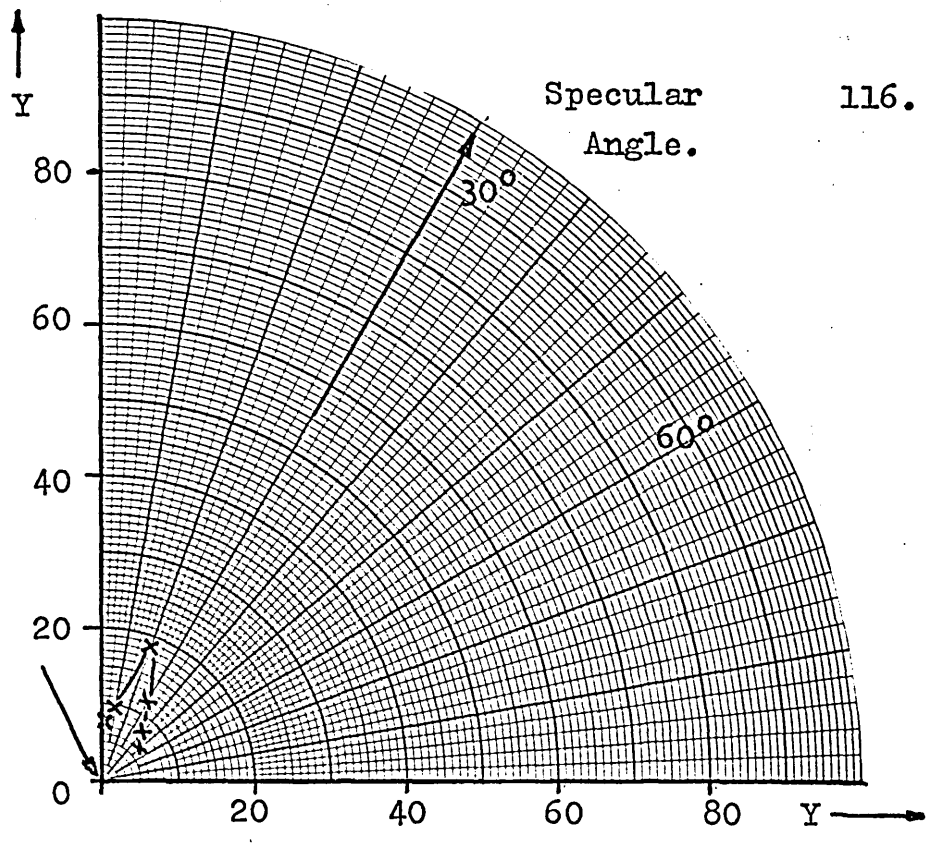


Fig. 5.11 Polar Luminance Distribution for 30° Incidence.

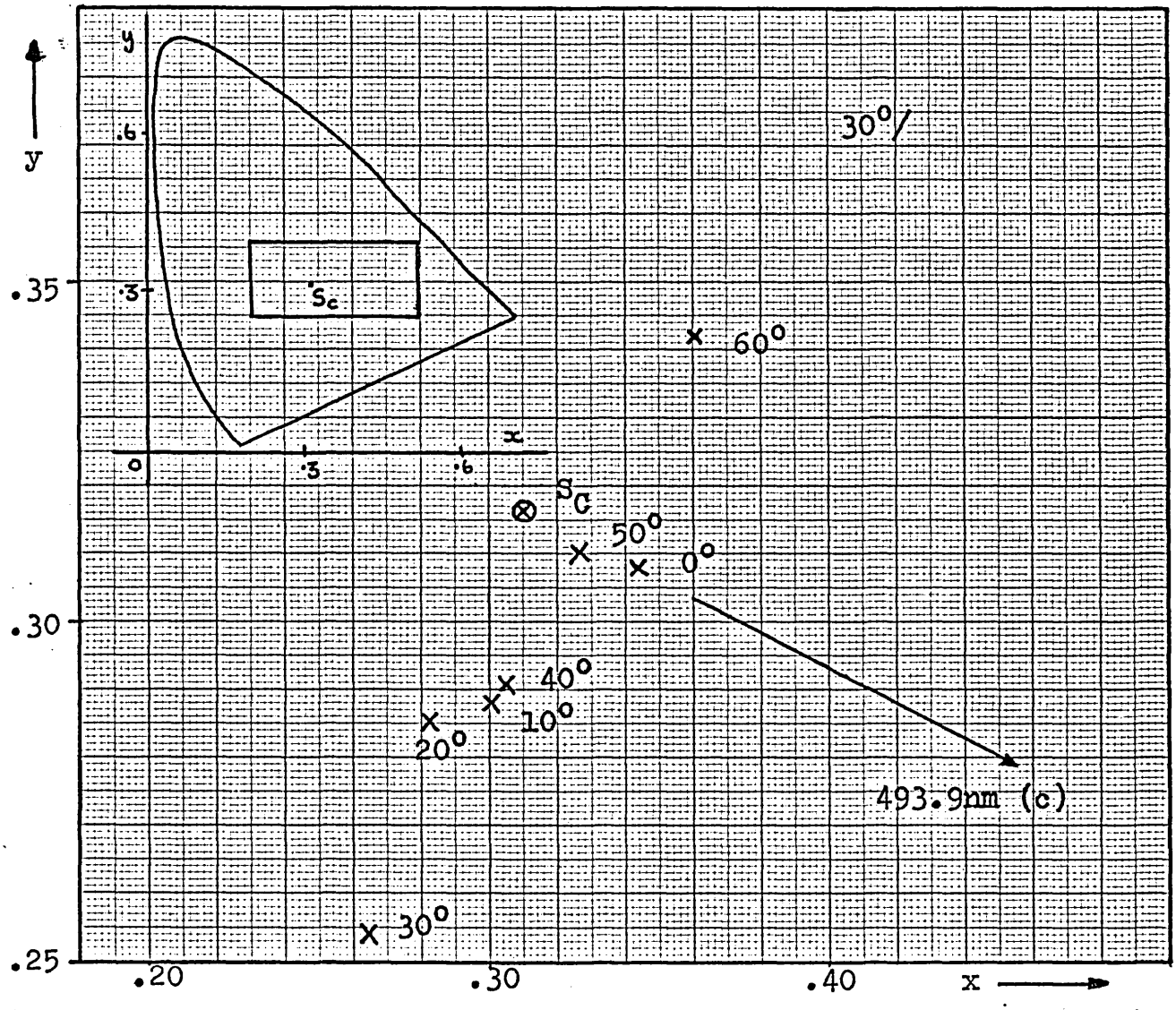


Fig. 5.12 Chromaticity Coordinates for 30° Incidence.

Sample b)
(Inner
Surface of
Scallop Shell)

POINT 2

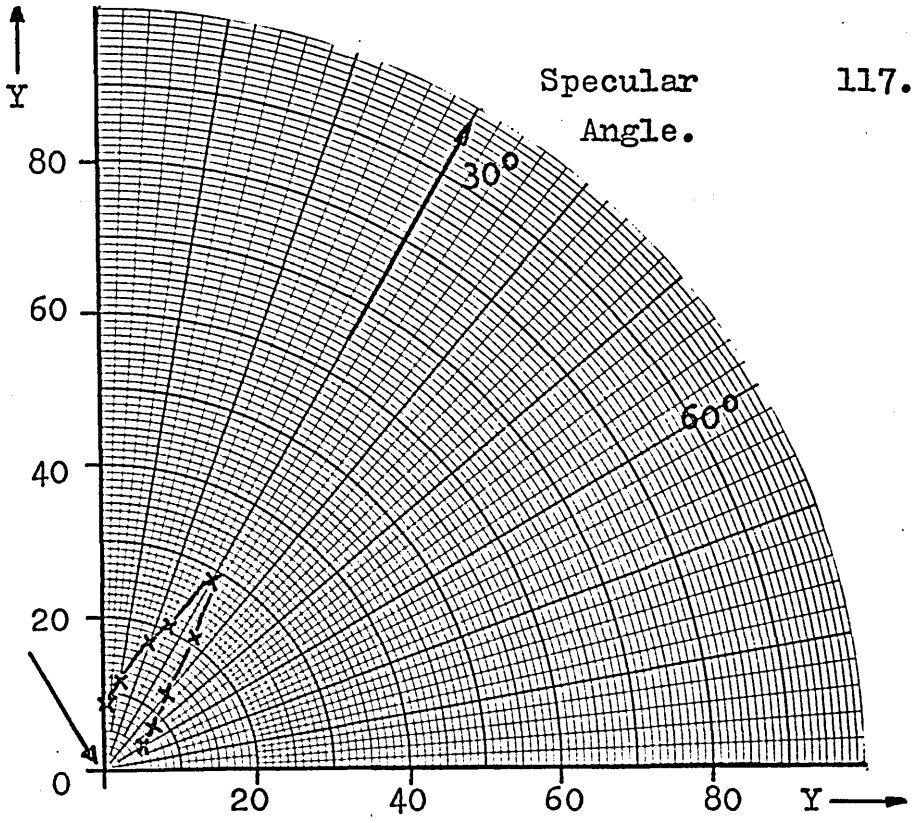


Fig. 5.13 Polar Luminance Distribution for 30° Incidence.

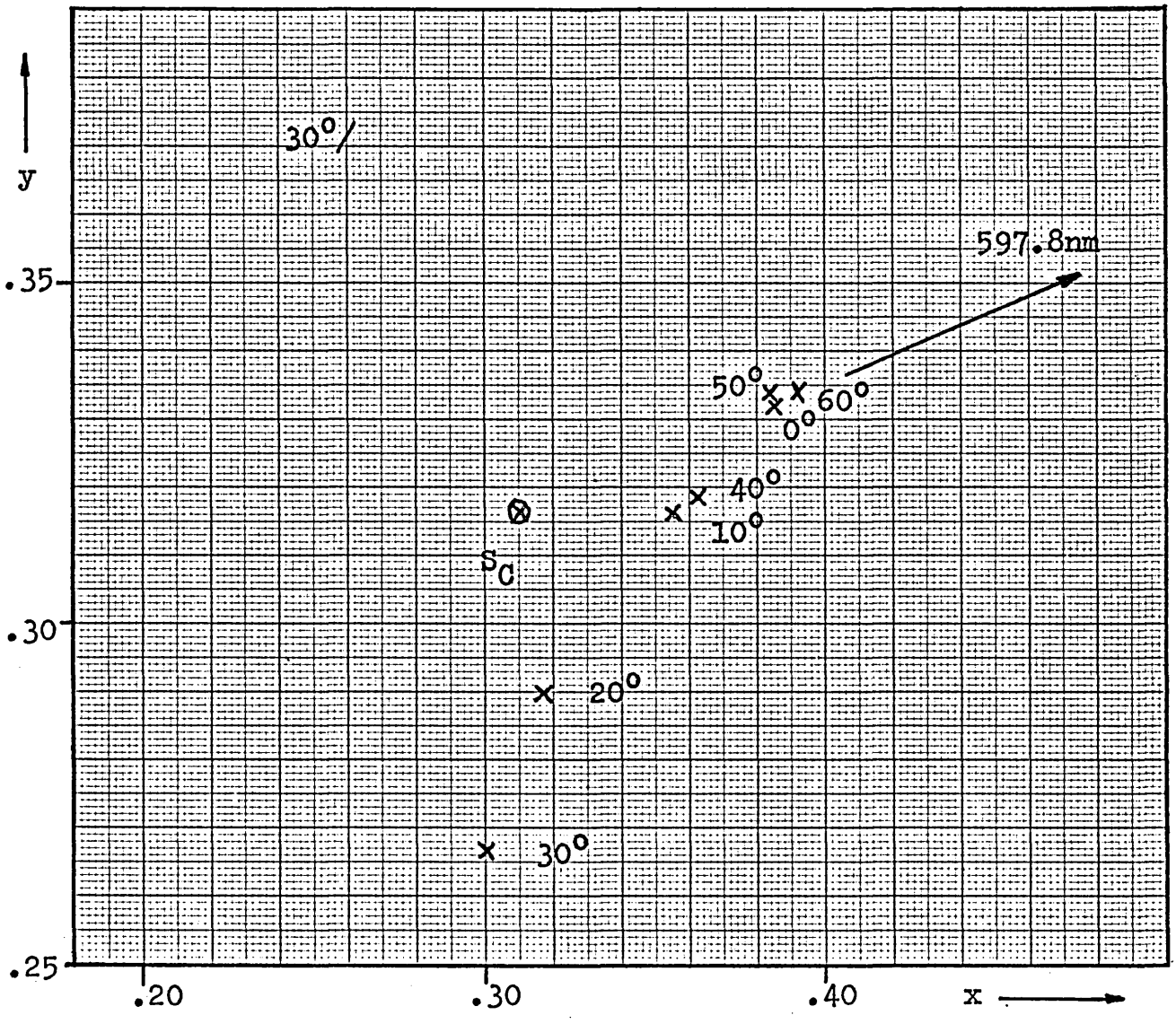


Fig. 5.14 Chromaticity Coordinates for 30° Incidence.

Sample b)
(Inner
Surface of
Scallop Shell)

POINT 3

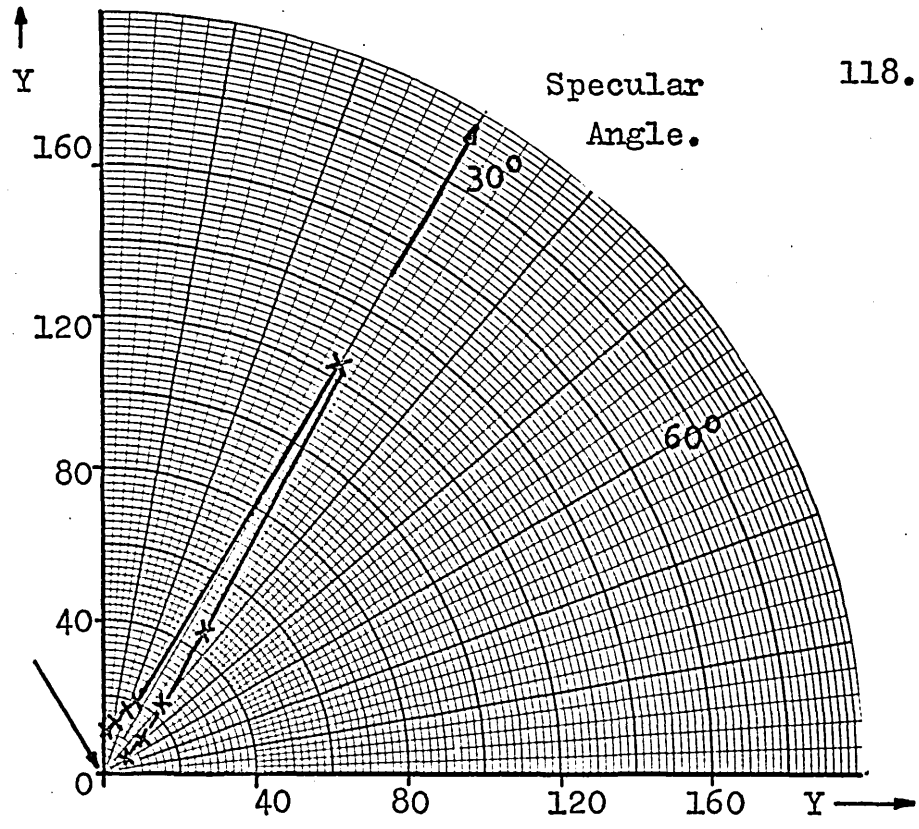


Fig. 5.15 Polar Luminance Distribution for 30° Incidence.

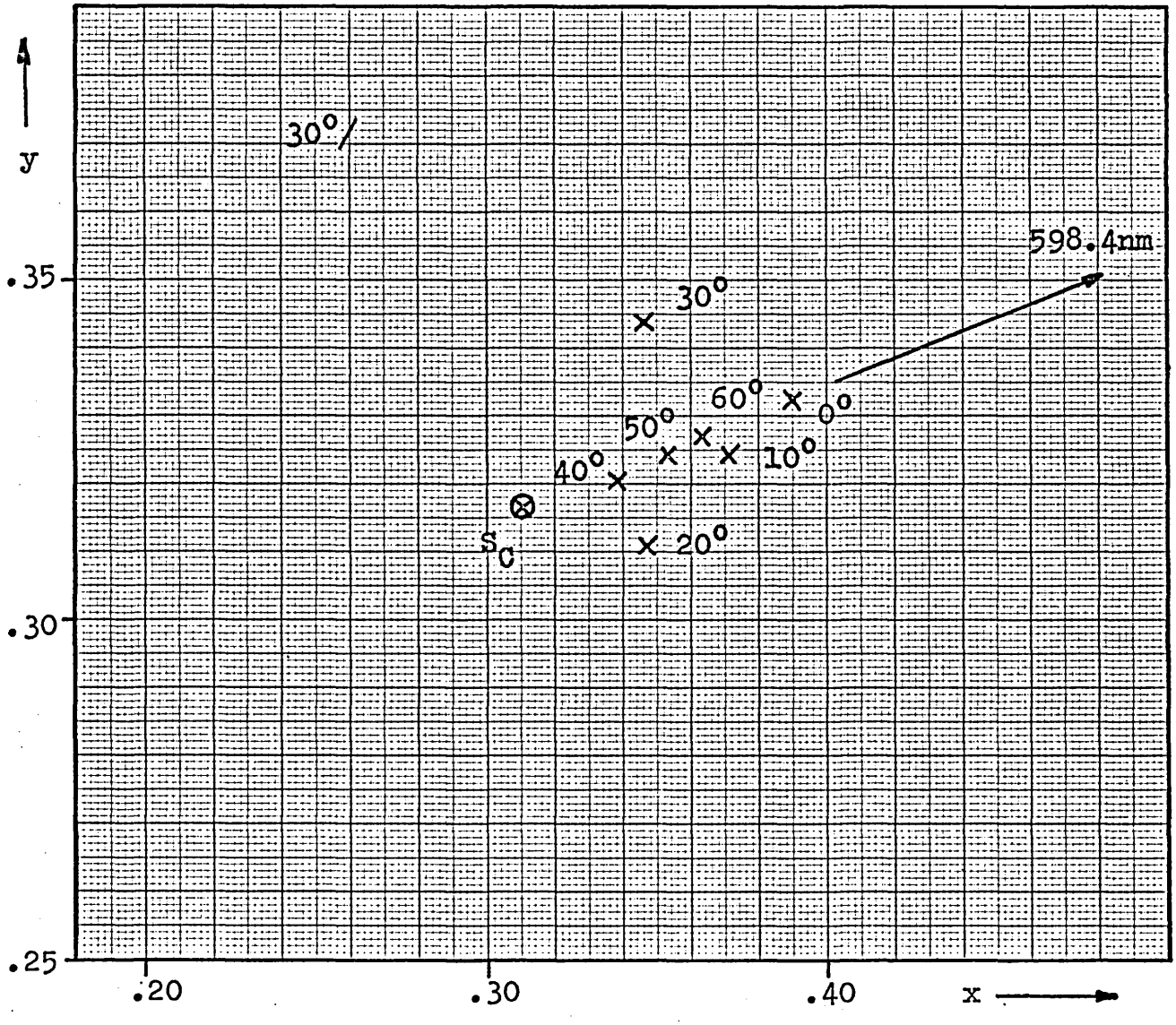


Fig. 5.16 Chromaticity Coordinates for 30° Incidence.

Sample b)
(Inner
Surface of
Scallop Shell)

POINT 4

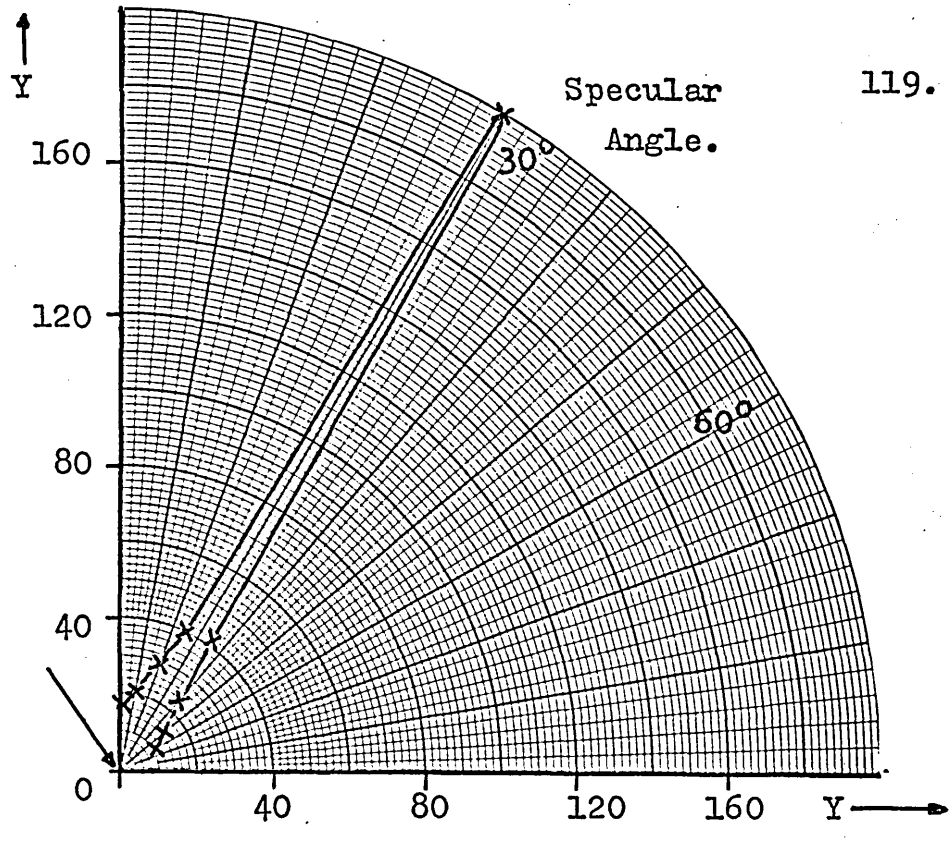


Fig. 5.17 Polar Luminance Distribution for 30° Incidence.

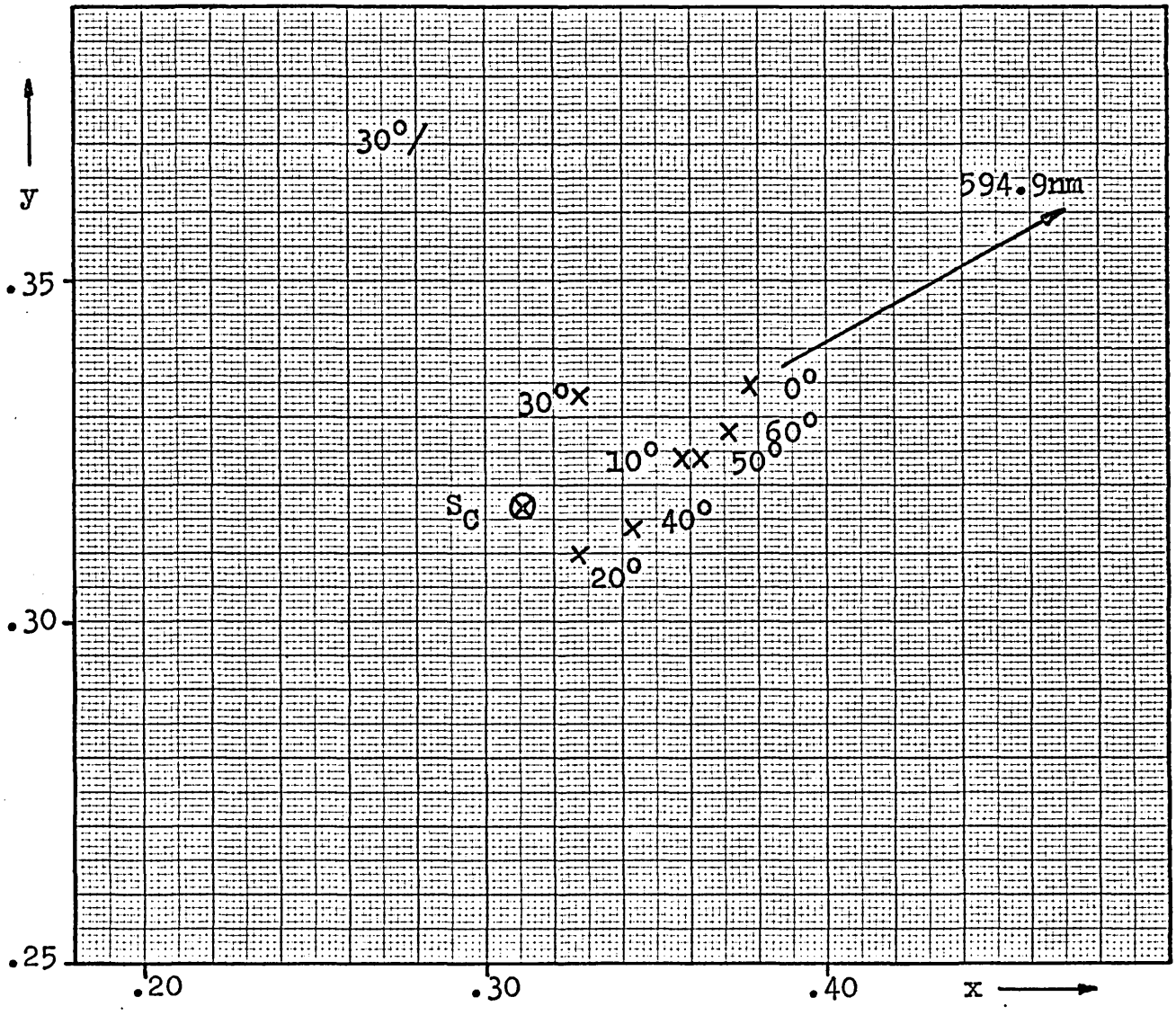


Fig. 5.18 Chromaticity Coordinates for 30° Incidence.

Sample b)
(Inner
Surface of
Scallop Shell)

POINT 5

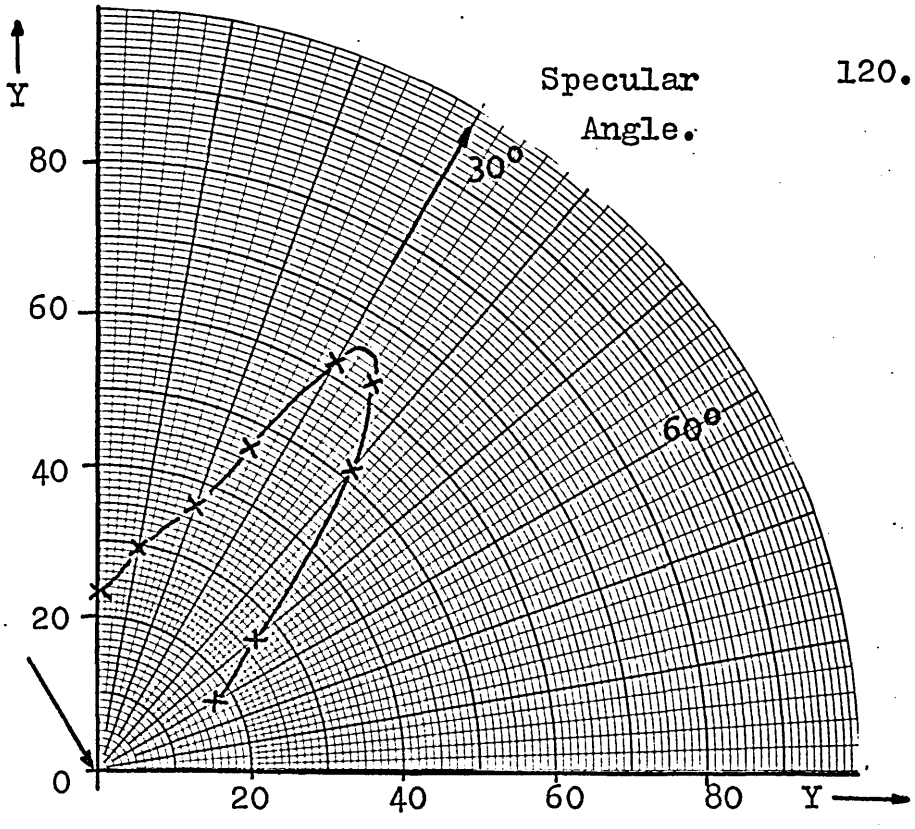


Fig. 5.19 Polar Luminance Distribution for 30° Incidence.

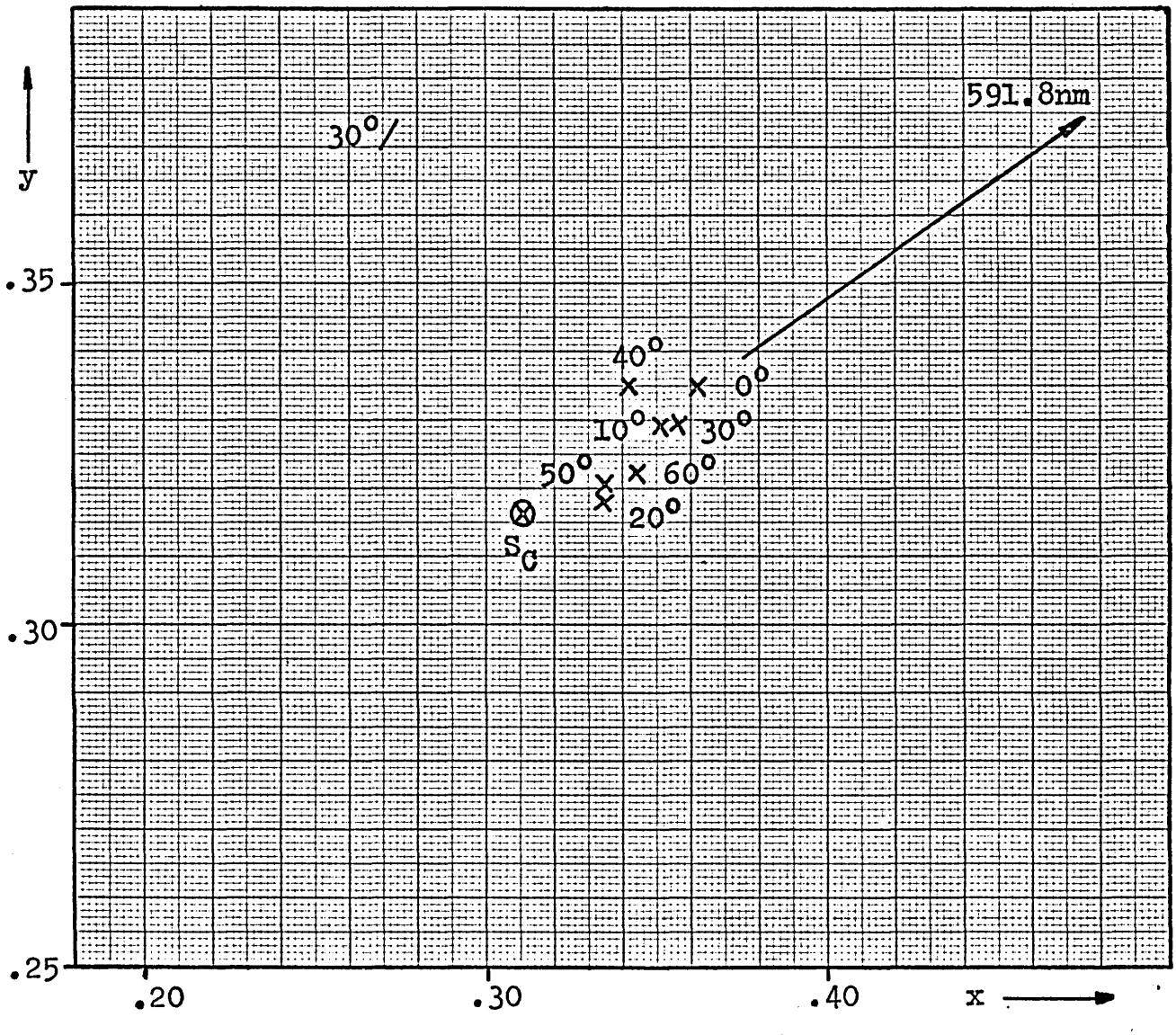


Fig. 5.20 Chromaticity Coordinates for 30° Incidence.

Sample b)
(Inner
Surface of
Scallop Shell)

POINT 6

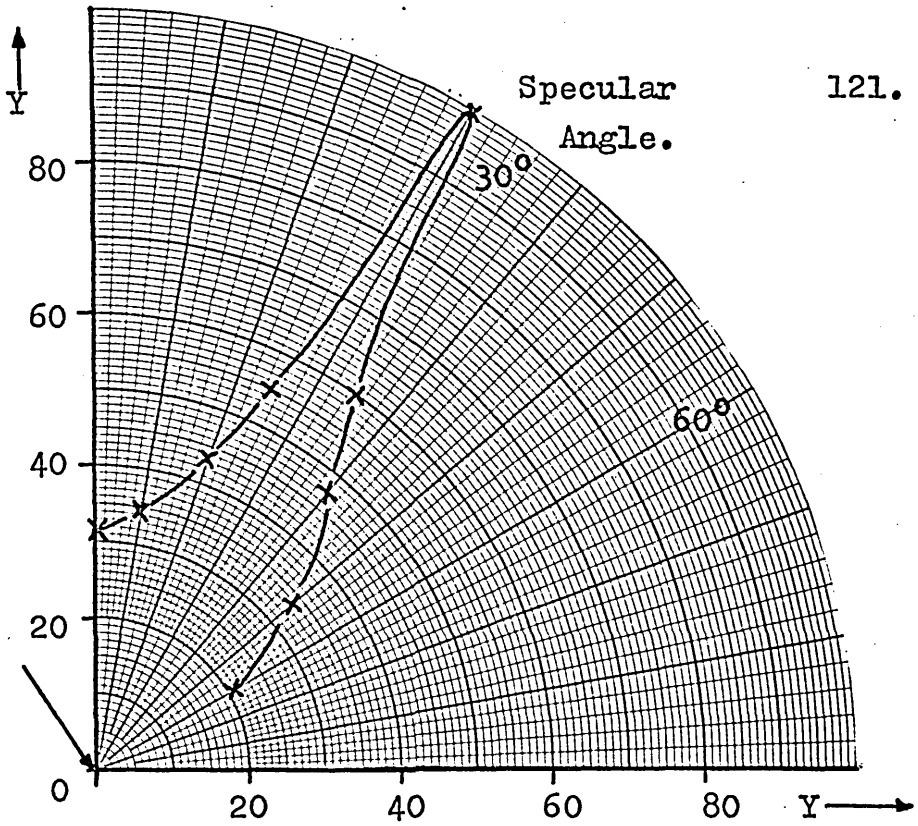


Fig. 5.21 Polar Luminance Distribution for 30° Incidence.

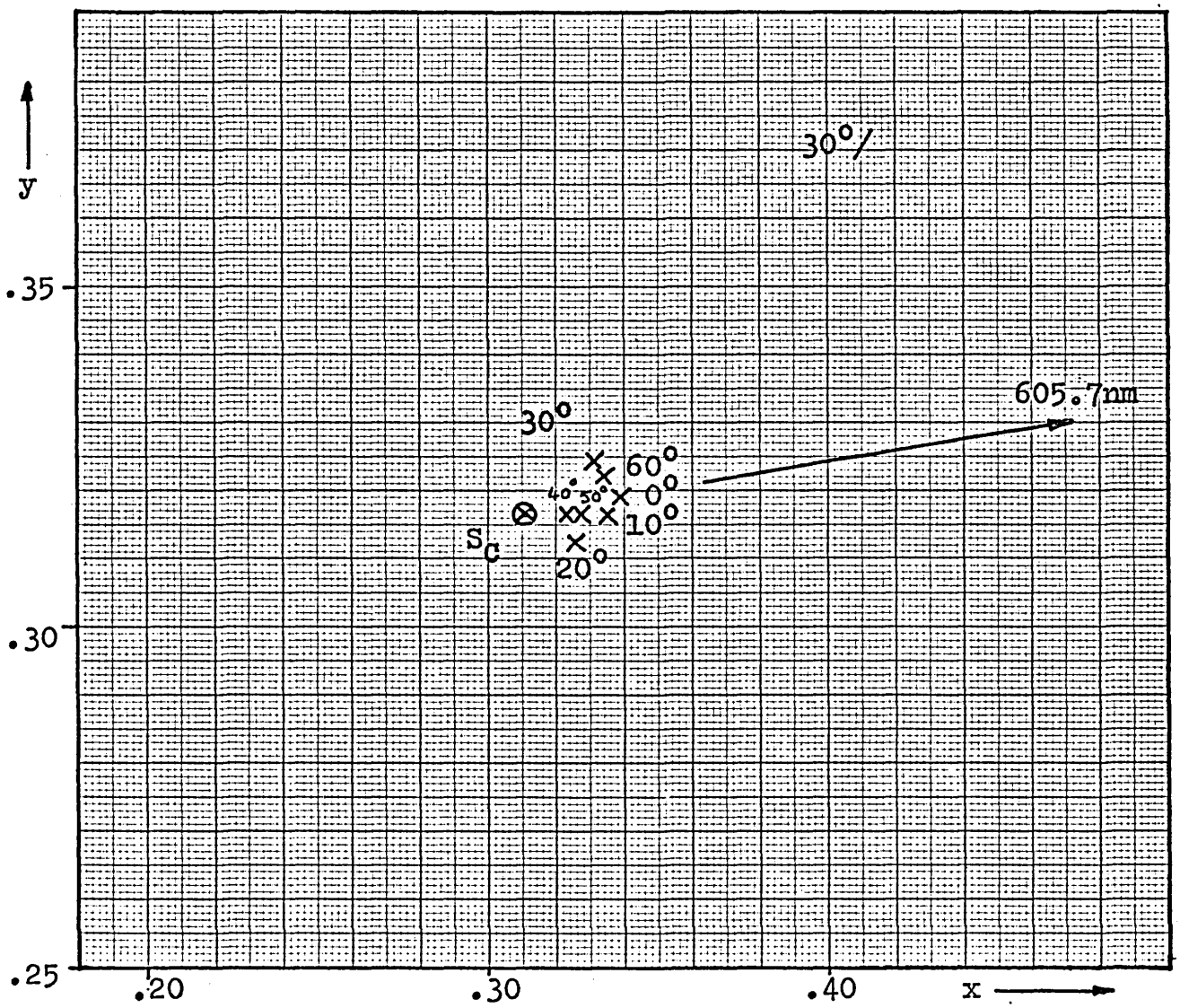


Fig. 5.22 Chromaticity Coordinates for 30° Incidence.

Sample b)
(Inner
Surface of
Scallop Shell)

POINT 7

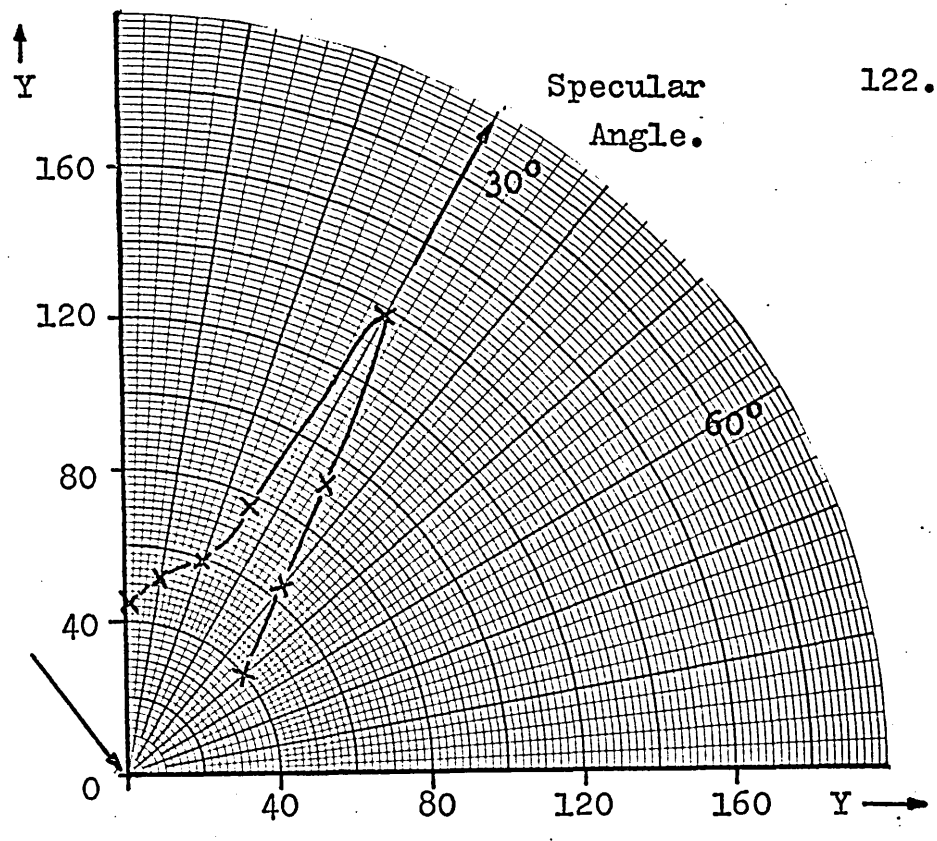


Fig. 5.23 Polar Luminance Distribution for 30° Incidence.

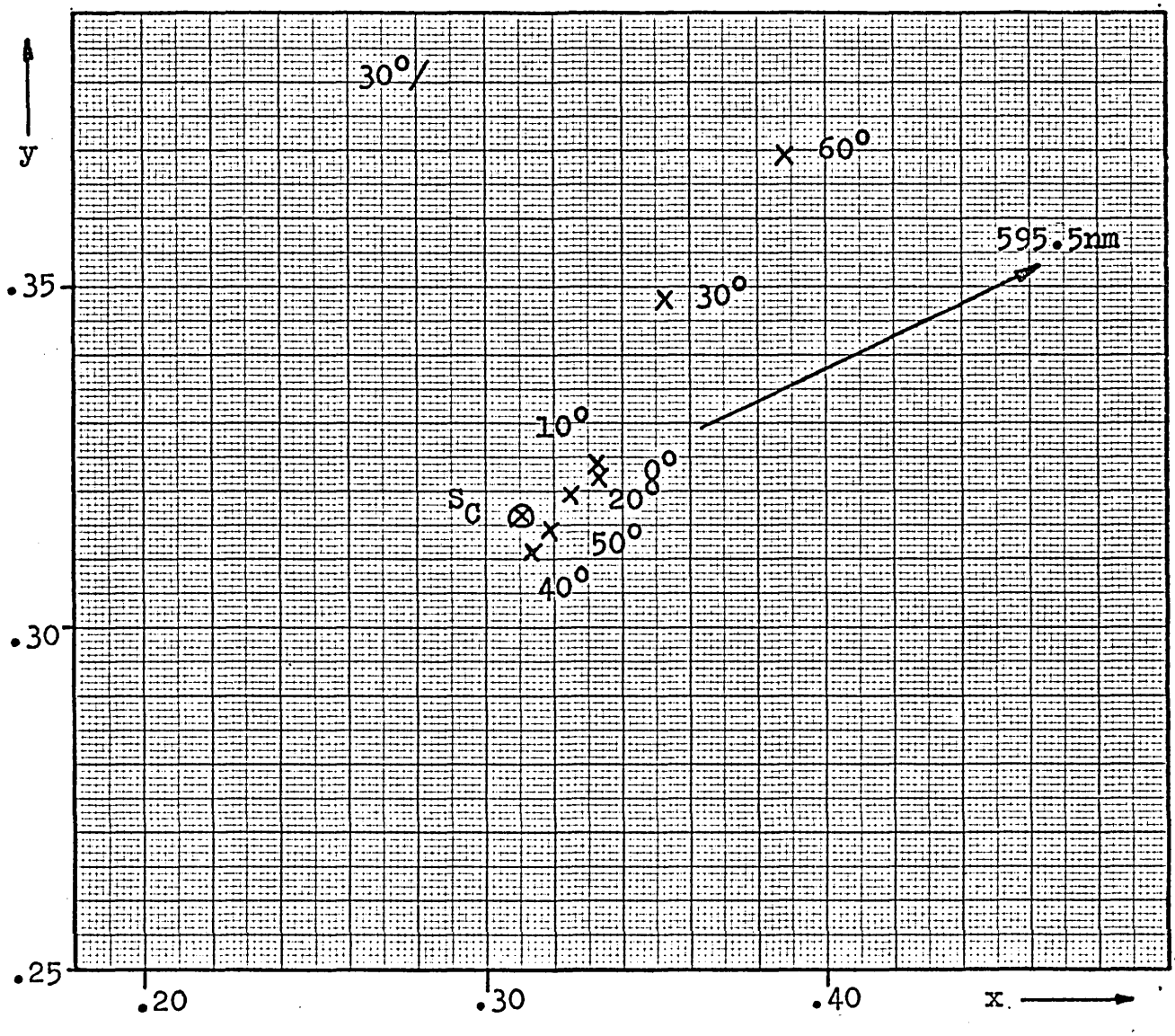


Fig. 5.24 Chromaticity Coordinates for 30° Incidence.

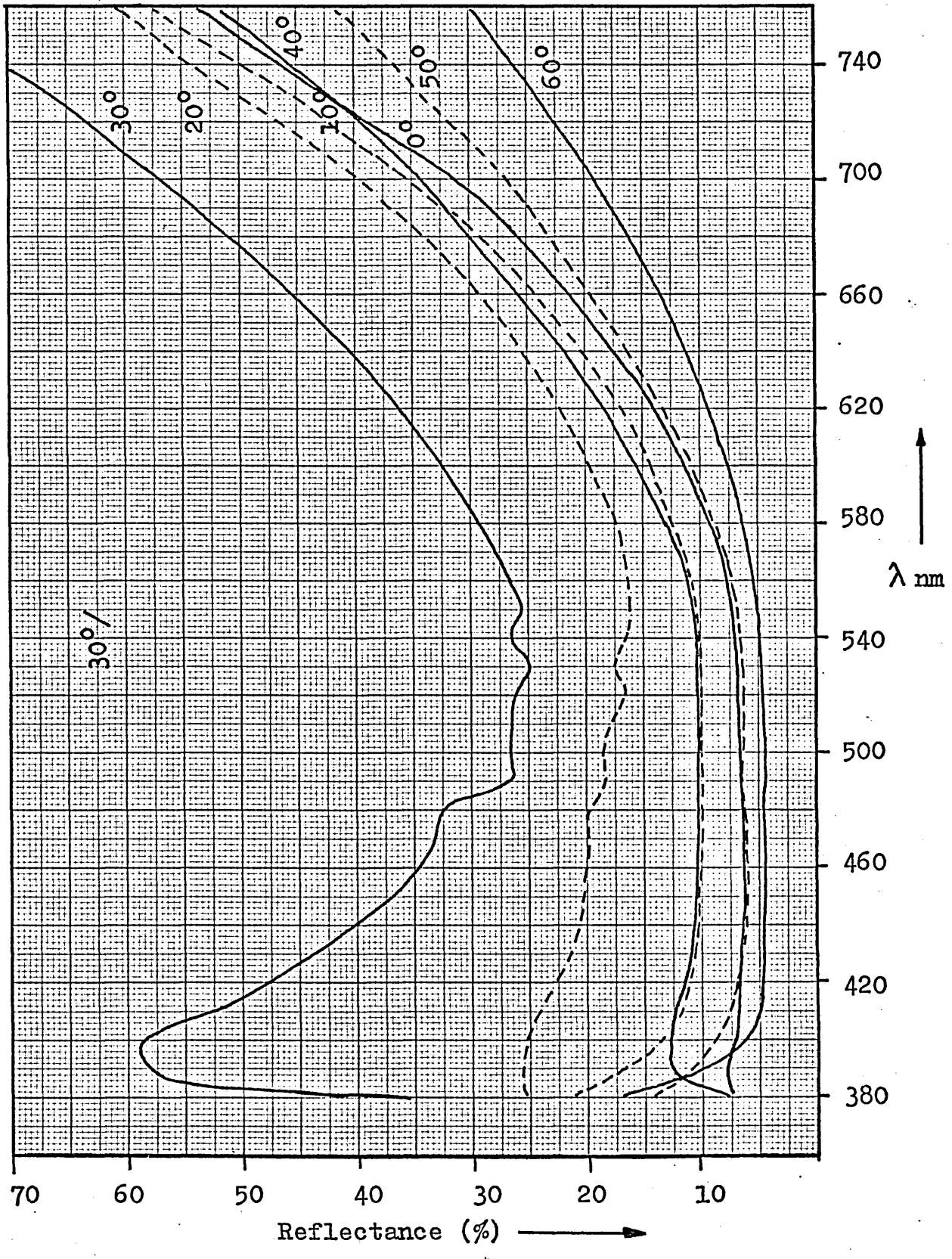


Fig. 5.25 Spectral Reflectance Curves for Sample b) (Scallop Shell) at Position 2. Angle of Incidence 30°, Viewing 0°, 10°, 20°, 30°, 40°, 50° and 60°.

Sample c)

(Iris Leaf)

POINT 1

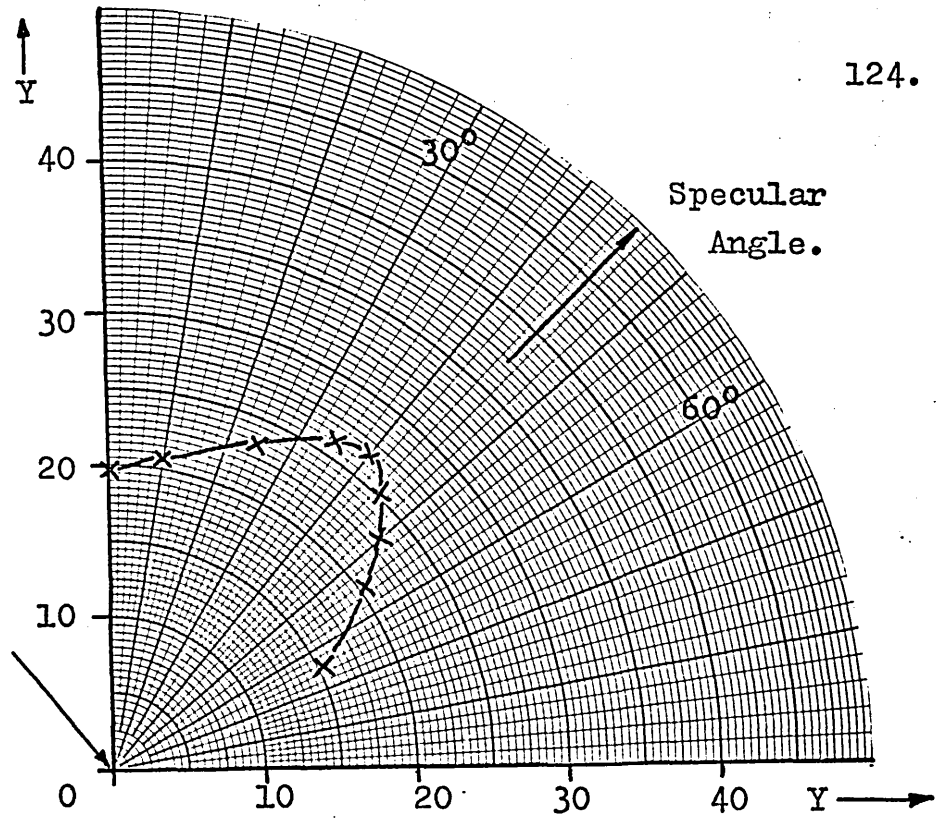


Fig. 5.26 Polar Luminance Distribution for 45° Incidence.

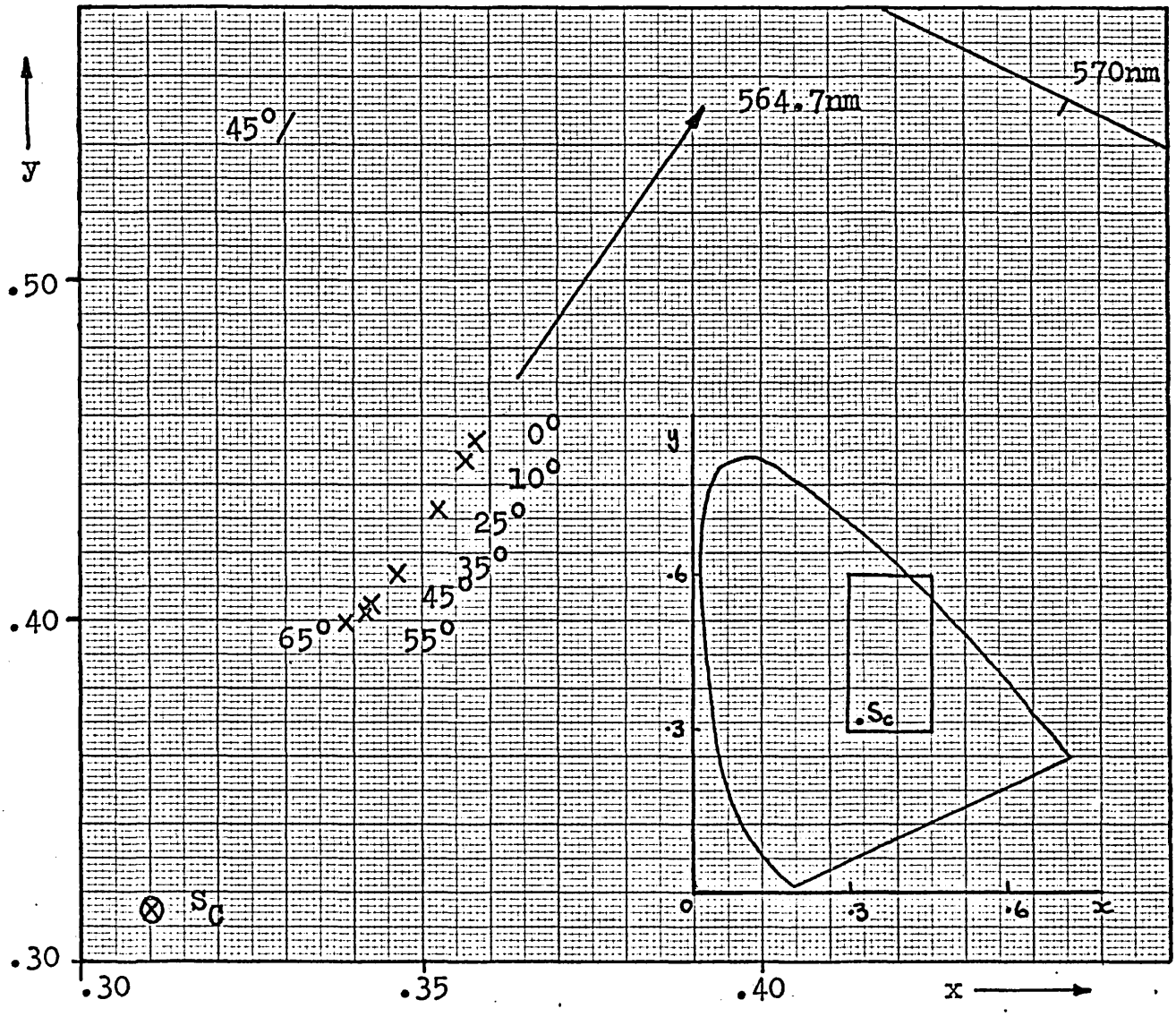


Fig. 5.27 Chromaticity Coordinates for 45° Incidence.

Sample c)

(Iris Leaf)

POINT 2

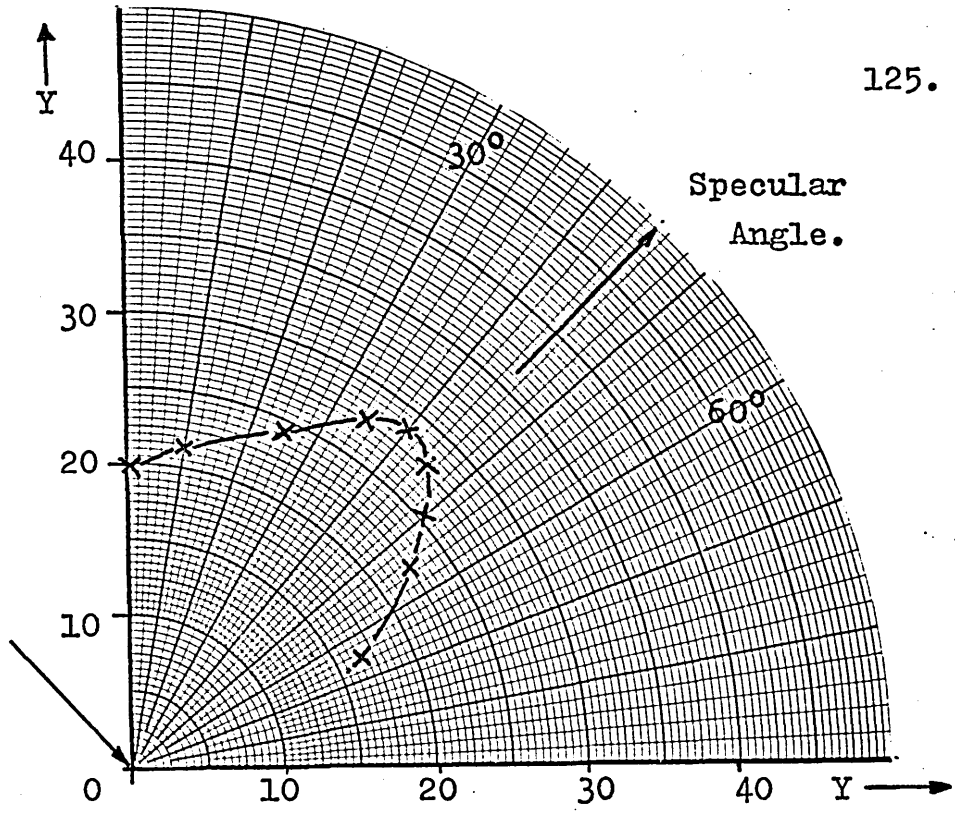


Fig. 5.28 Polar Luminance Distribution for 45° Incidence.

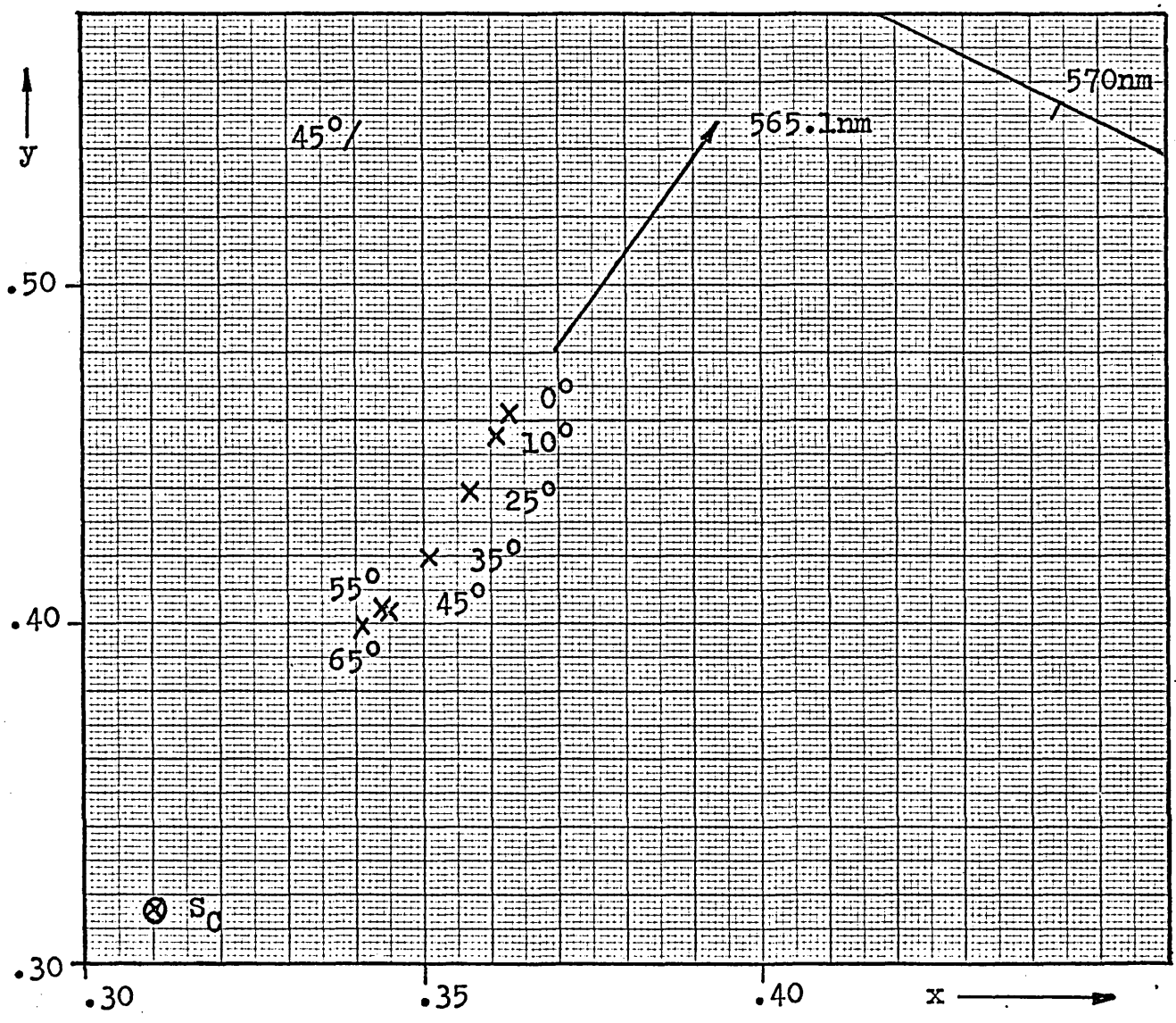


Fig. 5.29 Chromaticity Coordinates for 45o Incidence.

Sample c)

(Iris Leaf)

POINT 3

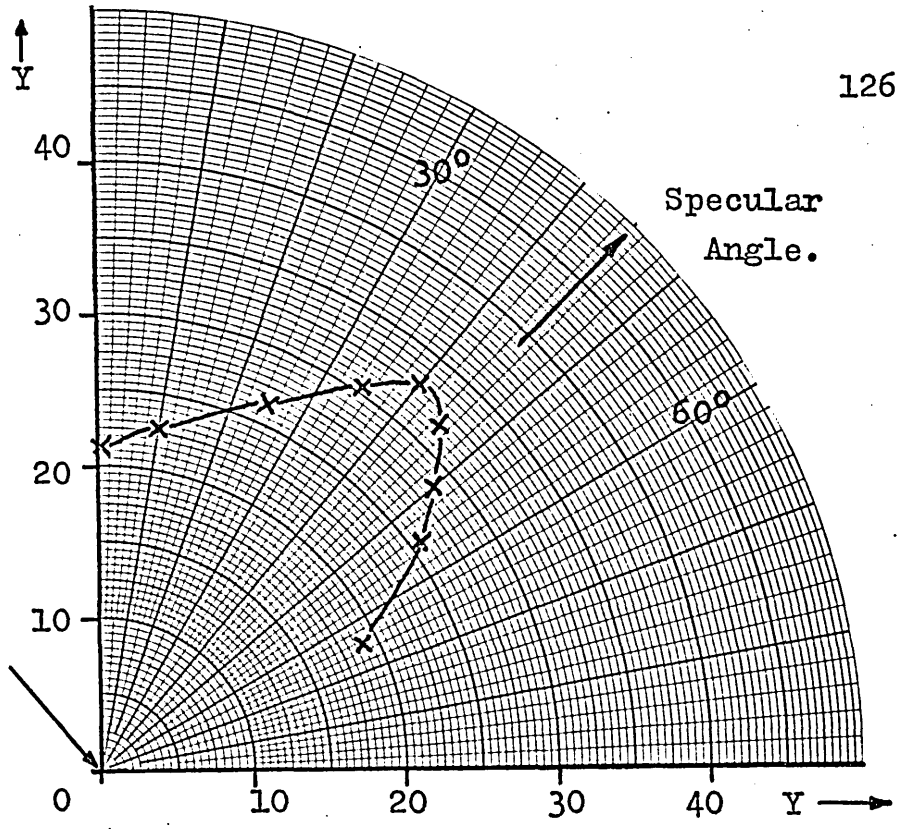


Fig. 5.30 Polar Luminance Distribution for 45° Incidence.

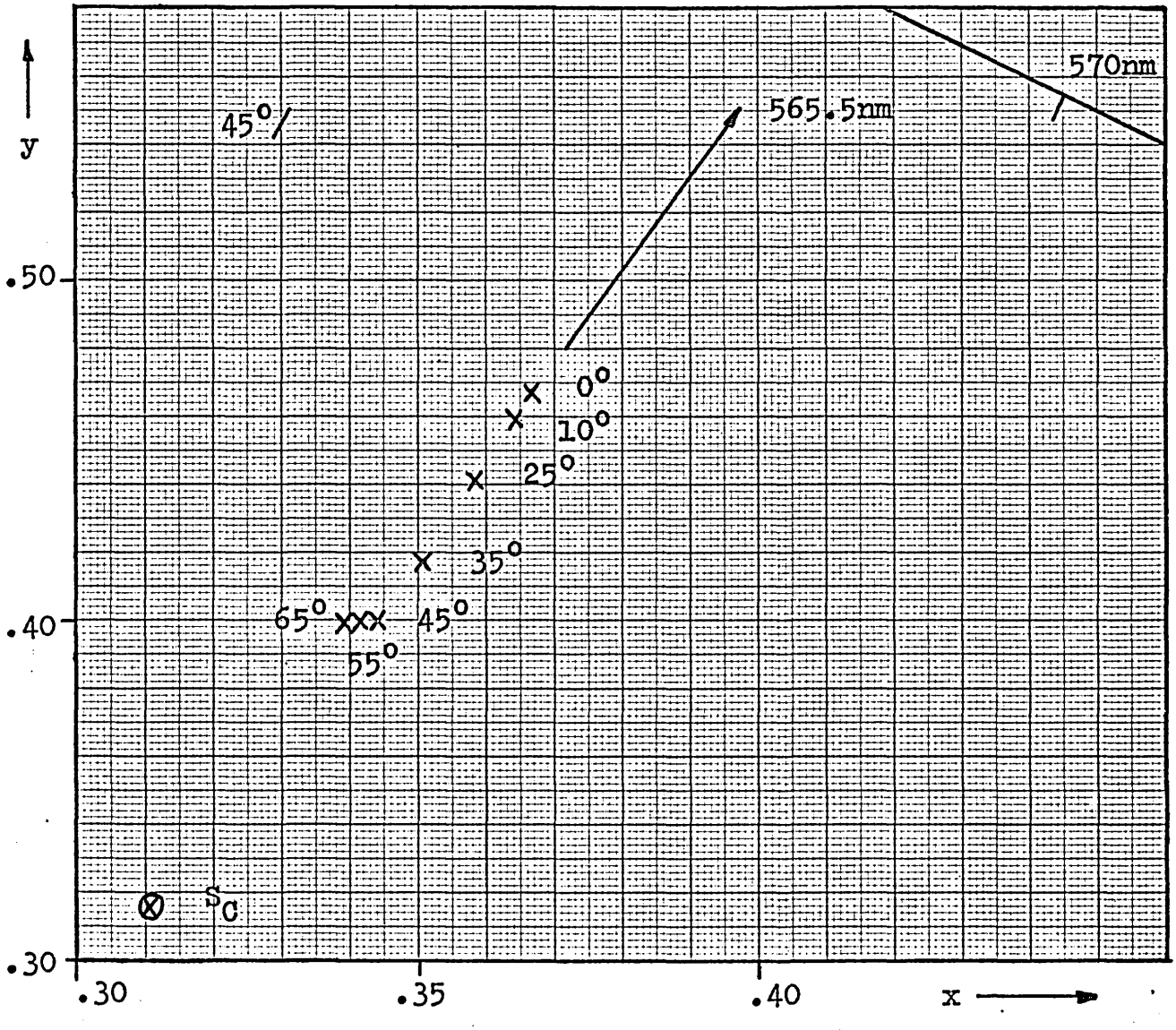


Fig. 5.31 Chromaticity Coordinates for 45° Incidence.

Sample c)

(Iris Leaf)

POINT 4

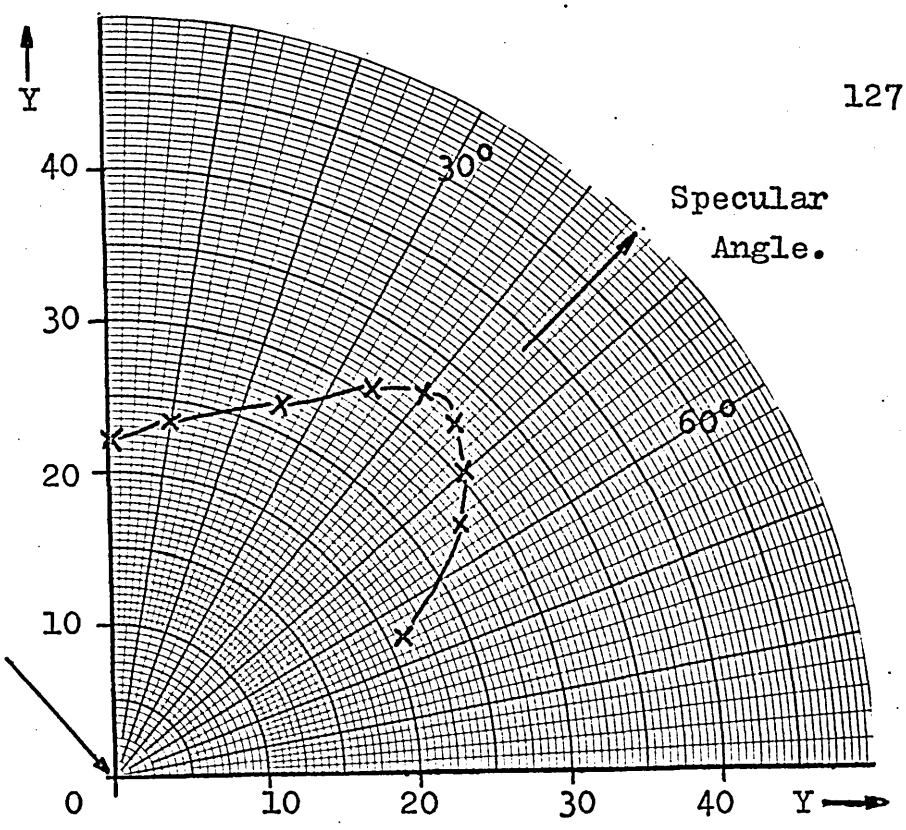


Fig. 5.32 Polar Luminance Distribution for 45° Incidence.

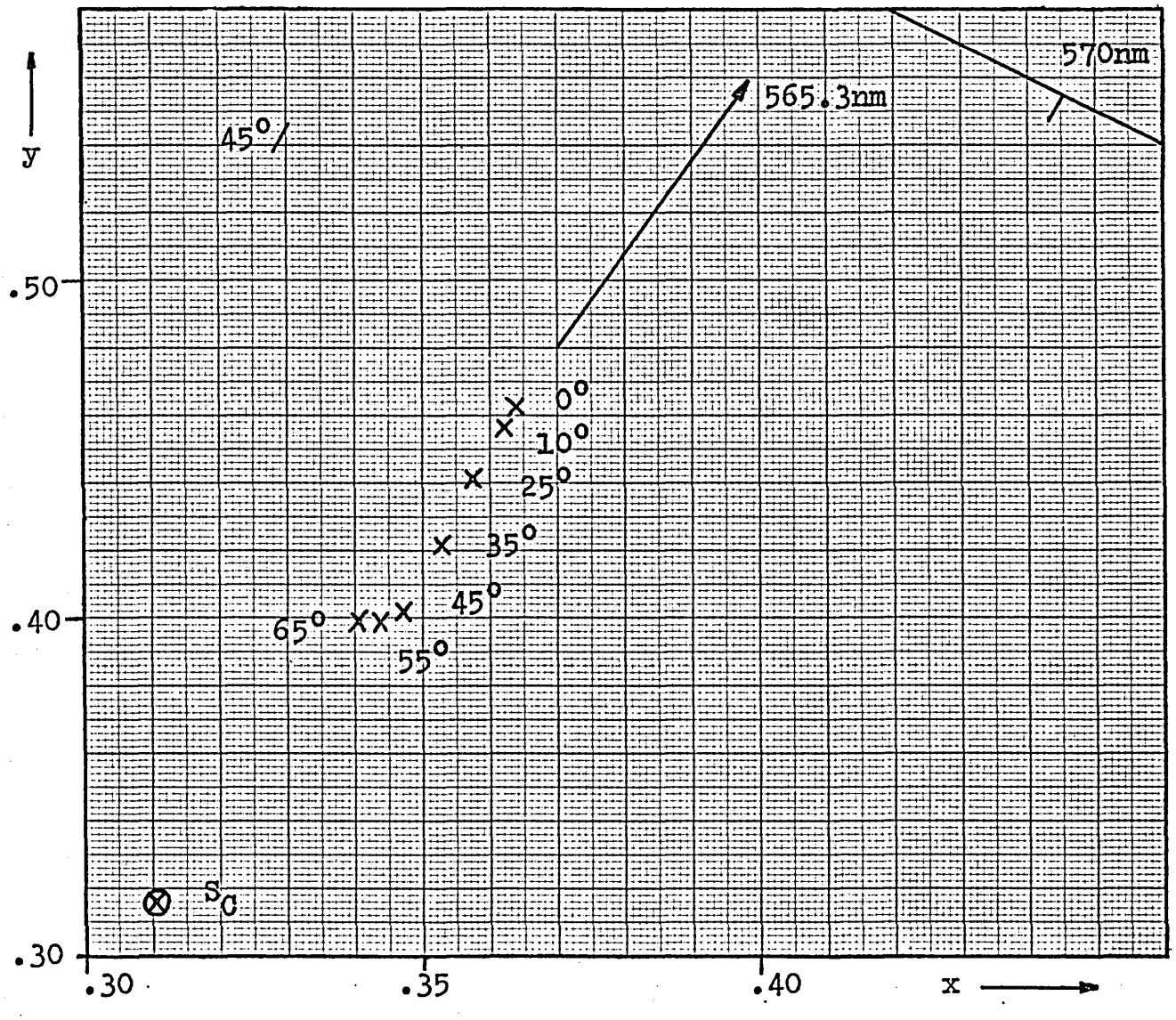


Fig. 5.33 Chromaticity Coordinates for 45° Incidence.

Sample c)

(Iris Leaf)

POINT 5

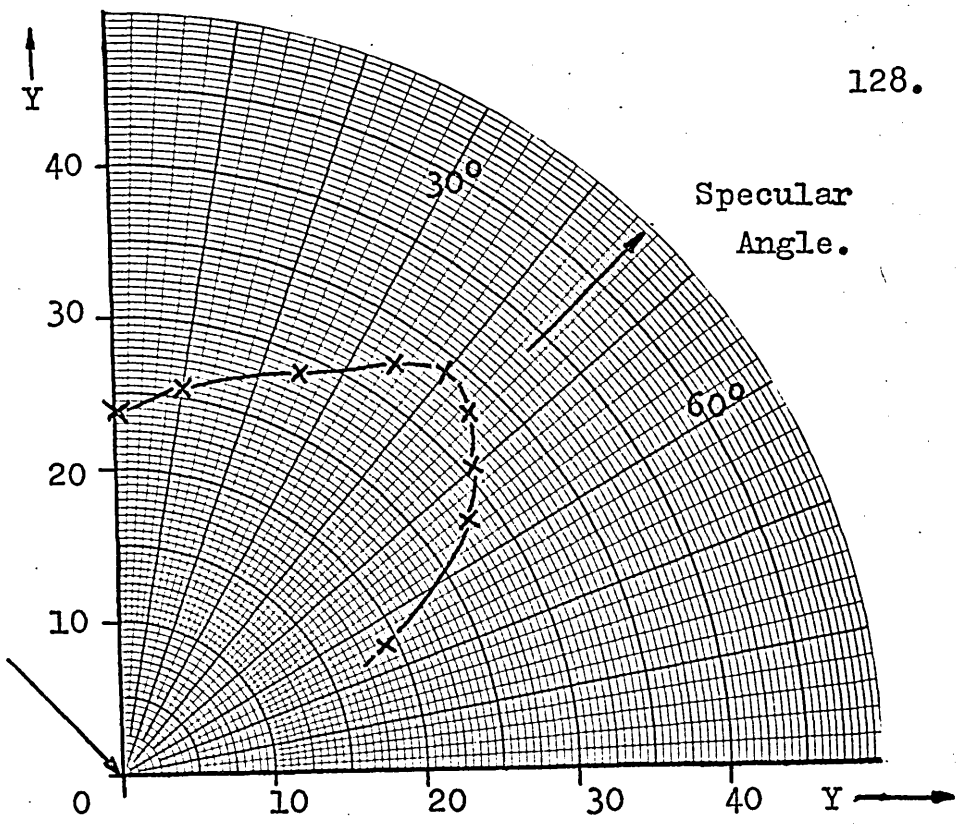


Fig. 5.34 Polar Luminance Distribution for 45° Incidence.

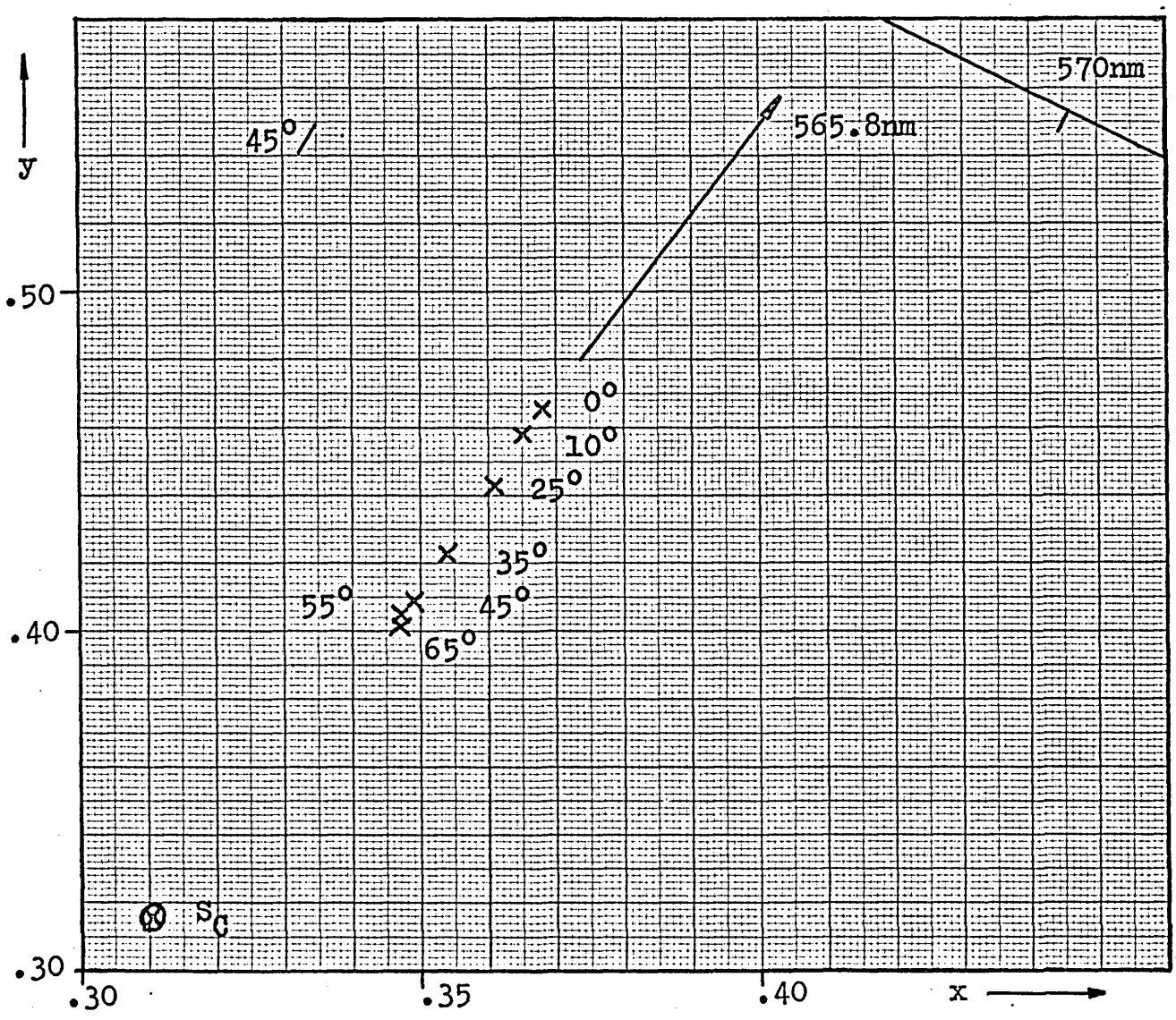


Fig. 5.35 Chromaticity Coordinates for 45° Incidence.

Sample c)

(Iris Leaf)

POINT 6

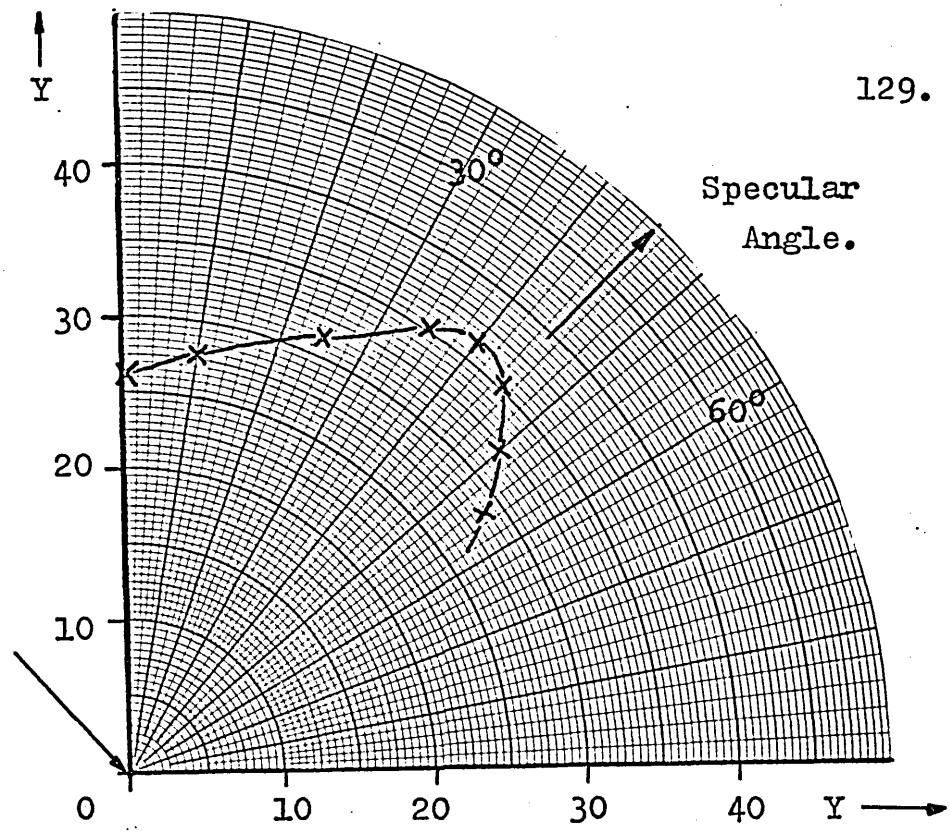


Fig. 5.36 Polar Luminance Distribution for 45° Incidence.

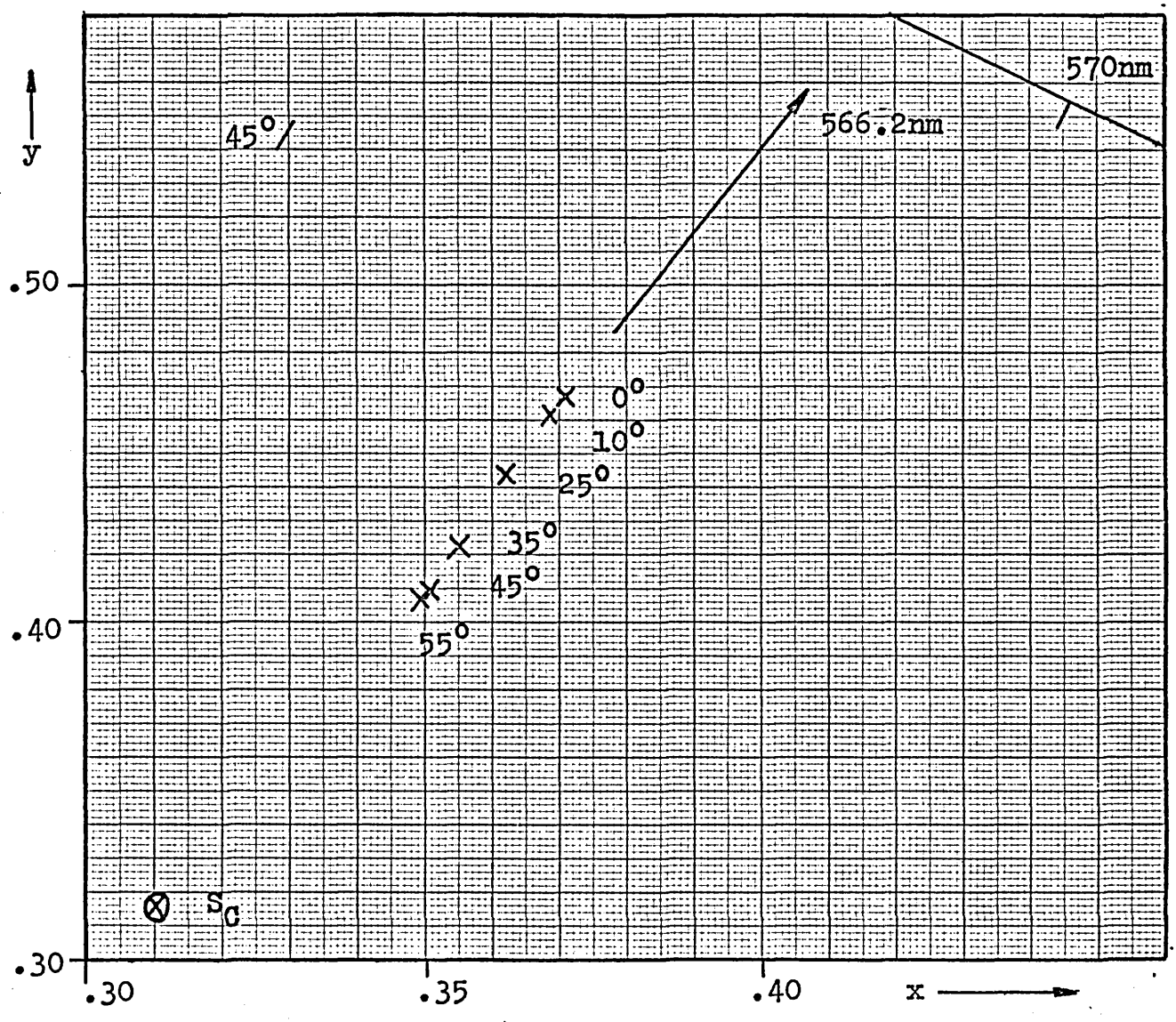


Fig. 5.37 Chromaticity Coordinates for 45° Incidence.

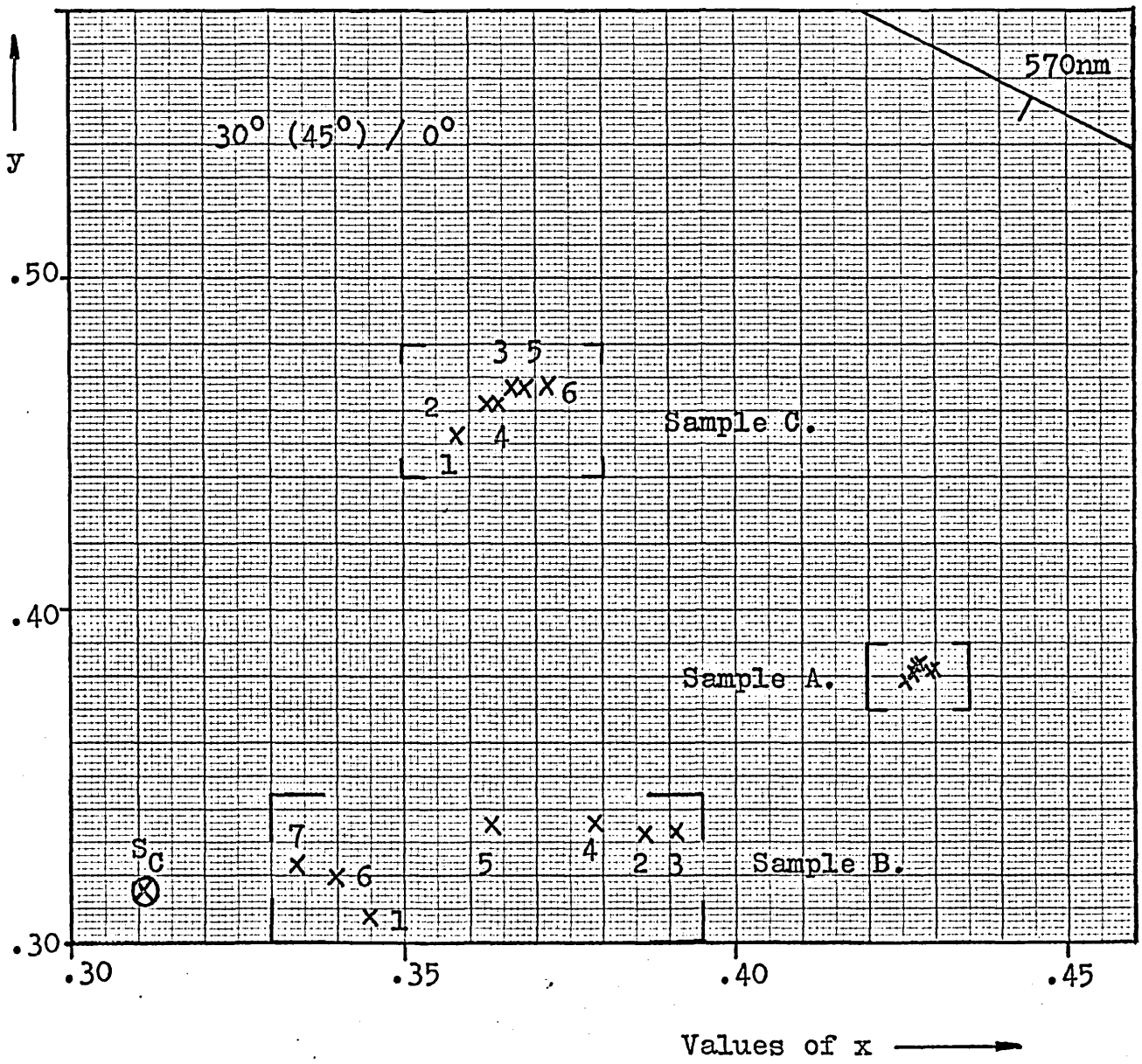


Fig. 5.38 Chromaticity Coordinates at 0° Viewing Angle for All Positions on Samples a), b), c), with Respect To Illuminant S_C and Spectrum Locus.

from these data which are borne out by further measurements on similar surface types.

1) The three sets of angular luminance curves are in the main as expected, showing the transition from the extremely matt surface a), via the matt sample c), to the very glossy example b). The first five polar curves illustrate how matt the surface a) is in fact, since no specular peak at all is present, unlike those for sample c) where, although the surface would be classified as matt by visual observation, a distinct specular peak is discernable on the polar plot. The odd numbered Figures from 5.11 to 5.23 inclusive however confirm the extreme glossiness of sample b).

It is now possible, however, to consider the spatial variation of luminance factor across such specimens. In the case of the extremely matt, almost Lambertian, surface of the tree bark, a variation of only about 2% in a value of approximately 20% is recorded between the six points measured, over the entire angular range considered. This 10% variation in result becomes a 30% one when considering sample c), this too being virtually constant over the entire angular range. The seven points considered on sample b) illustrate an enormous spatial variation in luminance, a variation which does not remain constant with angle, despite an almost perfectly smooth surface. The effect of surface curvature is most readily noticed in this latter specimen since the specular angle varies over 15° or more in terms of instrumental angle, however this should not affect such conclusions in any great manner.

It must be noted therefore that such spatial variations in luminance value, as a fraction of the total luminance value, occur to a much greater extent and less predictably in the glossier specimens of this type, a fact supported by measurements on the glossy samples in the latter part of this thesis and other widespread data on matt objects such as vegetation and earth. This may well be visually translated as a sharpening up of highlights, emphasising a glossy surface relative to a spatially flat even matt one. Certainly in the limiting case of a perfect diffuser there would be no such differences from point to point.

2) Colorimetrically several points are worthy of consideration. Certainly there would appear to be a systematic angular chromaticity movement dependent on the type of surface under consideration and almost independent of position on that surface. The largest deviations from this rule are found in sample b) and are thought to be due in a large measure to two distinct errors. Firstly, the varying curvature of the surface makes angular comparisons difficult, despite accuracy in the instrumental angles, and secondly, errors in reflectance measurements near the specular angle on high gloss surfaces are bound to be larger due to the large disparity between sample and standard readings,

In no case is there good agreement between the measured angular chromaticities and the suggestions of Judd (1963) and Boshoff (1957) with regard to 'top surface'

and 'body' reflected light. Thus, although such ideas can be seen to hold for perfectly flat, man-made specimens, as those illustrated in Figure 5.39, their quantitative application is not possible in relation to surfaces of more complex texture.

In detail the chromaticity coordinates of sample a) for any one location appear to be little influenced by any specular component and remain fairly independent of the illuminant point, as one might expect. As the even numbered Figures from 5.2 to 5.10 inclusive show, there is a definite movement up to 10° viewing angles, whereupon the trend reverses and the points move in a regularly increasing arc in the opposite direction. Thus the specular angle has little meaning colorimetrically as well as photometrically here, and what angular movement is present within the coordinates is extremely small indeed.

Sample b) however, in Figures 5.12, 5.14, 5.16, 5.18, 5.20, 5.22, and 5.24, illustrate a movement closer to that of the ideal surface mentioned in Chapter 2, showing a movement away from the 0° point, increasing up to the specular angle after which it slowly reverts back to the original. The movement here however is not directly towards the illuminant point but towards the blue-purple section of the chromaticity diagram. A further complication introduced probably by optical effects from the multilayered shell structure, producing a distinct blue component at 30° as shown in the spectral reflection curves of Figure 5.25. Despite this the specimen does show that a glossy surface will produce this type of movement, returning to the original

0^{o} viewing point by angles of approximately 60^{o}.

Finally sample c), illustrated in odd numbered Figures from 5.27 to 5.37 inclusive, shows the almost ideal angular chromaticity movement up to the specular angle, collapsing towards the illuminant point at almost constant dominant wavelength. Beyond this point however, the trend continues, albeit at a very much reduced rate, and thus despite a maximum luminance factor at the specular angle the colour reaches a minimum saturation beyond this angle.

The exact solution to such colorimetric shifts requires an extremely detailed knowledge of the surface construction and also an equally detailed treatment of the light interaction with this material, as in Chapters 7 and 8. However it is possible to draw general colorimetric conclusions with respect to the photometric properties of different materials.

It would appear from all the available goniospectrophotometric data that three very basic types of surface are of colorimetric importance. Namely:-

i) a glossy surface

ii) an almost matt surface possessing only small specular increase in reflected light

and iii) extremely matt surfaces, tending almost to Lambertian in characteristics and whose specular angle is of no photometric significance.

Their importance stems from the fact that three distinct types of angular chromaticity movement appear to be discernable.

i) The regular collapse of coordinates towards

the illuminant point on approaching the specular angle and then the movement back to the 0^{o} viewing point at angles of approximately 20^{o} to 30^{o} beyond, dependent somewhat on the angle of incidence employed. Such results are often difficult to obtain for reasons outlined above.

ii) The regular angular movement of chromaticity coordinates towards the illuminant point up to, and including, the specular angle. There would then appear to be a whole range of possibilities for points at greater angles, at one extreme returning systematically towards the 0^{o} point but even at large viewing angles reaching only a small distance towards it, and at the other extreme continuing collapsing towards the illuminant, although at a much reduced rate. The movement, however, remains systematic with angle and the range tends to reflect an increasingly matt surface as one approaches the latter case. From the point of view of texture discrimination therefore, such measurements tend to be important in the range of viewing angles from specular to say 20^{o} beyond.

iii) No definite trend is apparent in results obtained from extremely matt surfaces, since the illuminant point has little or no influence on the angular chromatic variations, this presumably being due to lack of light directly reflected from the top surface. No definite pattern emerges in this category, the exact distribution of points being very dependent upon the material under investigation.

This final pattern, although unpredictable, is quite distinguishable from the earlier class i) and ii) types, and certainly, as would be expected, sample a), the

tree bark, falls into this category with a regular, small but illuminant independent movement of chromaticity coordinates. The magnesium oxide surface of the previous chapter also exhibits these properties, but is influenced to some extent by the illuminant point due to its almost perfect 'whiteness' at normal viewing angle.

The difference between class i) and class ii) surfaces is well shown by the results contained in Figure 5.39. They represent measurements taken on either side of a colour chip similar to those of the Colour Harmony Manual (Granville and Jacobson, 1944). The chips are produced from a cellulose-acetate base to which a pigment layer has been applied - thus one side is extremely glossy, points marked X in Figure 5.39, and the other side fairly matt. It can be seen that, although both sides have an almost identical dominant wavelength, the angular purity variation of the matt side is much smaller, especially when considering angles beyond the specular one. Thus the glossier surface would definitely fall in class i) whereas the more matt finish is beginning to show many of the characteristics of class ii), as its angular luminance plot would predict.

In the latter half of Chapter 4 it was found that a rough finish on a glossy surface considerably reduced the specular luminance peak under that of a flat specimen. This reduction should be enough to remove such a material from the so-called class i) to class ii), and to some extent it is now understandable why the chromaticity coordinates continue towards the illuminant point beyond the specular angle, since they must also be exhibiting the

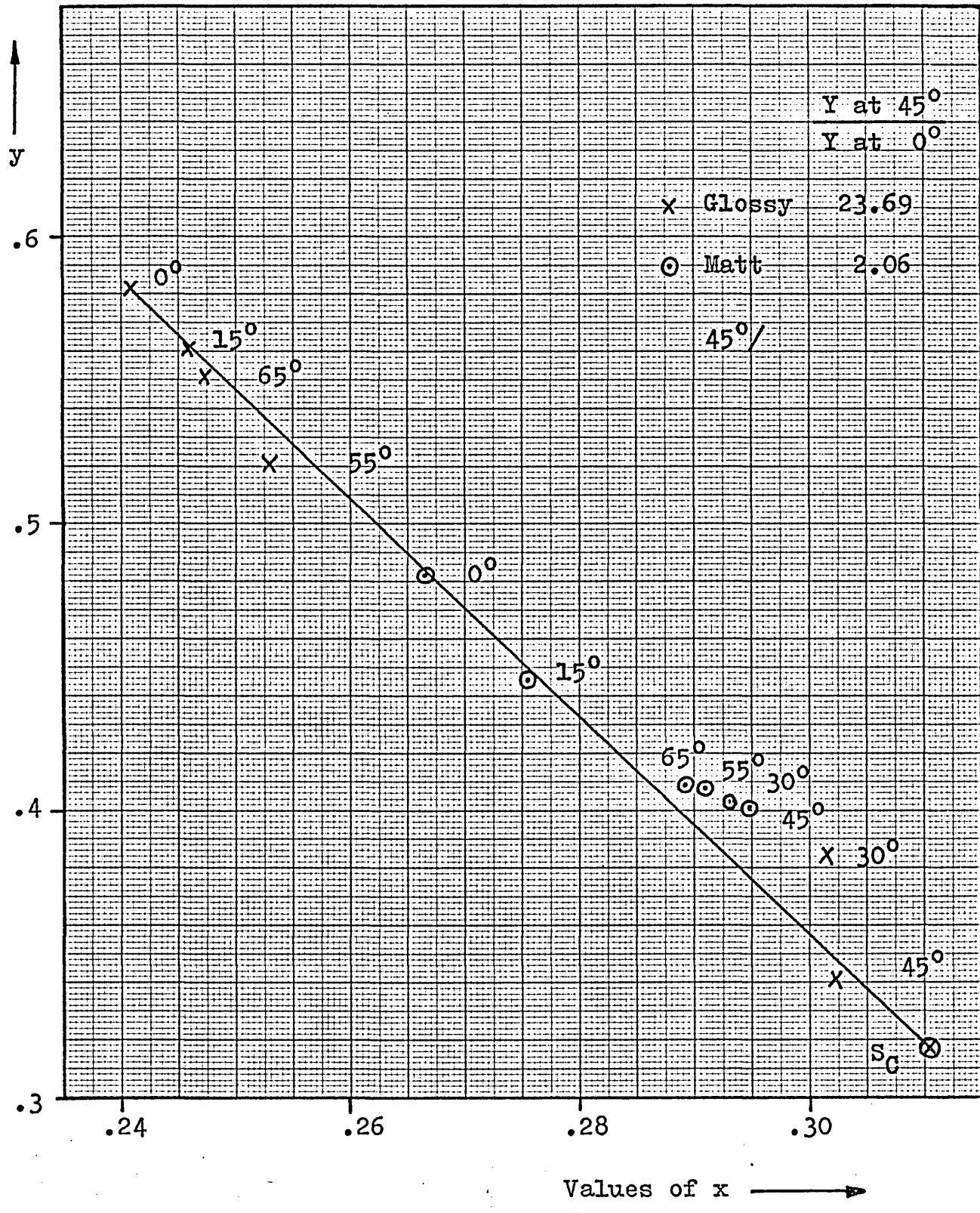


Fig. 5.39 Chromaticity Coordinates for Glossy (X) and Matt (⊙) Sample at an Angle of Incidence of 45° and a Viewing Angle from 0° to 65° as illustrated.

colorimetric properties of class ii) surfaces also.

3) Finally there remains the important information on the size of typical chromaticity movements, associated with either spatial or angular changes in measuring conditions.

In the case of the angular variation in viewing conditions it is not really possible to put any definite figure on typical colour differences which is meaningful. This arises since not only is the magnitude of such differences of interest, but perhaps more important is the order of spread in the coordinates from a given number of sample locations. Equally, although one could resolve this by defining an area by means of two dominant wavelengths - one maximum and one minimum - and in addition two corresponding purity values, this may be grossly misleading when some points are very near the illuminant and others far away, as here. This arises since a small movement in a point of very low purity may well cause an enormous variation in dominant wavelength.

However, by observing the angular chromaticity plots presented earlier it is possible to make a general comment. Such a spread in chromaticity coordinates upon changing the viewing conditions is very small for the matt surface a), while that for sample c), a less matt surface, is a factor of about 6 or 7 times as large in values of y, while remaining approximately the same in values of x. Both sets of points being roughly in the same area of the chromaticity diagram. Sample b) - the very glossy sample -

is not constant from location to location across the surface, leading to values greater and smaller in spread than either sample a) or c). From other measurements on glossy materials it would appear that such movements are normally much larger than those from a) or c), especially in the vicinity of the specular angle, but the complications which arise from the type of surface sample b) possesses, and which have been discussed earlier, tend to mask this in certain locations.

The more interesting case however from the point of view of texture reproduction is that of spatial chromaticity coordinate movement at a viewing angle of 0^{o}. Table 5.1 sets out the measured values for x and y at the various locations on the three samples, and their corresponding dominant wavelengths and excitation purities. The following Table 5.2 gives the spread in these latter two quantities for each sample.

This is felt to be a useful and valid method of expression in this case since the spread is relatively small, and the arguements put forward earlier apply only partially in the case of sample b) and not really at all in the others. Furthermore the data are of importance in the following chapter.

The spreads obtained increase progressively with the gloss content, but it is felt that much of this is due to actual surface colouration rather than the type of surface, especially in the case of sample b). The figures do indicate that the variation for these particular materials is often of the order of the colour discrimination

of the normal human eye, sometimes smaller, often a good deal larger, despite the apparent visual constancy over the surface of say sample a). The results are thus extremely important in any attempted texture reproduction of such a surface.

TABLE 5.1

Location	1	2	3	4	5	6	7
Sample							
A							
x	.4293	.4271	.4259	.4273	.4283	.4266	
y	.3823	.3832	.3799	.3844	.3830	.3809	
λ_d	585.85	585.41	585.96	585.18	585.59	585.83	
p_e	49.66	45.20	43.98	45.58	45.41	44.43	
B							
x	.3443	.3862	.3907	.3785	.3629	.3394	.3337
y	.3077	.3328	.3328	.3352	.3350	.3191	.3225
λ_d	c493.97	597.78	598.43	594.90	591.81	605.68	595.51
p_e	10.54	24.82	26.03	23.40	19.17	8.60	7.99
C							
x	.3582	.3633	.3669	.3641	.3683	.3712	
y	.4533	.4624	.4665	.4621	.4654	.4675	
λ_d	564.72	565.09	565.48	565.27	565.82	566.19	
p_e	49.79	53.58	55.96	53.68	55.69	57.05	

TABLE 5.2

Sample	$\Delta\lambda_d$(nm)	Δp_e(%)
A (matt)	0.78	5.68
B (glossy)	> 100	18.04
C (semi-matt)	1.47	7.26

5.5 Conclusions.

Only a very limited number of surface types have been investigated in detail, due to the enormous complexity and number of other possible surfaces. Such effects as 'negative gloss' - the effect in pronounced spiked surface structure, for the peak of directional reflectance to be along the angle of incidence - have been omitted, since they often occur in materials unsuitable for measurement - the above example, in forests viewed from the air. The enormous variation in surfaces is often better specified by such classifications of gloss as those of Hunter (1937) and Hunter and Judd (1939).

However from the colorimetric point of view, certain points are of interest from the above results.

1) The spatial variation in luminance value from point to point on a surface appears to increase as the gloss content of that surface increases, and becomes somewhat unpredictable in high gloss samples.

2) Systematic angular chromaticity movements do occur and are dependent on the surface type. Extremely matt

surfaces show little or no distinct trend, the movement apparently being almost entirely governed by the surface characteristics. The intermediate range between matt and glossy shows a whole series of variations - the important coordinate movement being that of points measured at viewing angles just beyond the specular angle, since those up to the specular are usually well behaved. Glossy samples are fairly predictable up to and beyond the specular angle. In general, for a given starting chromaticity the movement is greater for a glossy sample than that for a matt one.

3) Three distinct chromaticity movements are obvious, corresponding to three degrees of gloss content, and measurements under 45^{o} illumination at 0^{o}, 45^{o} and 65^{o} viewing angles would be sufficient to identify a sample as such.

4) Theories involving the division of reflected light into 'top' and 'body' reflected light can only be successful, and then only qualitatively, in a relatively small number of cases, since very little evidence was found in the measured, naturally occurring samples of any such distinct divisions.

5) Sizes of typical spatial variation in chromaticity are given in Table 5.1 for different surface finishes. In such samples differences of less than 1nm and 1% are common in the values of dominant wavelength and excitation purity respectively.

CHAPTER SIX.

THE COLOUR REPRODUCTION OF SURFACE TEXTURE.

It is apparent from the foregoing chapters that the spatial variation in chromaticity of a material and the surface texture of that material are closely connected. Few surfaces exist which, even on a macroscopic scale, are perfectly smooth and perfectly flat. Therefore, although a sample may be of only one colour over its entire area, the variation from point to point will still exist in almost every case. The particular surface texture and structure governs the magnitude of this effect markedly, as has been shown, and conversely, much information concerning these properties is available from such chromatic changes.

This is obviously extremely important in colour reproduction where one is essentially trying to represent the effects of a three-dimensional structure - the texture - upon a two-dimensional print or screen, which in turn will have its own surface finish. In such cases the ability to reproduce small colour differences and also the dark, shadowy colours, and light, desaturated colours of the highlights becomes an overriding factor in the assessment of the medium's abilities.

6.1 Factors Influencing Texture Reproduction.

The quantitative measurement of how good a reproduction of an original may be has received much attention and involves several complicating factors. At

first sight, a simple check on the tristimulus values of the two elements - the original and reproduction - appear to be all that is necessary, the error being proportional to the discrepancy between these. It has been shown, (MacAdam, 1951; Bartleson, 1959, 1962) that for many observers exact tristimulus value reproduction of many well known object colours, such as flesh and grass-green, is not the most desirable one, and therefore the simple approach may well be in error.

The quantitative estimation of the discrepancy between tristimulus values is also difficult. Were it done simply by taking the distance between coordinate points in the 1931 C.I.E. diagram, the values obtained would be confusing since equal distances do not represent equal visual steps (Wright, 1941). Similar attempts in more nearly uniform systems such as the $U^*V^*W^*$ system also give problems since the relative weightings of chromaticity and luminance errors are difficult to determine (Hunt, 1967). Changes in overall adaption between the original and reproduced scene lead to further problems (Hunt, 1965).

However, in the present investigation only one aspect of this comparison is important, namely the ability of a medium to reproduce small colour variations. If it is possible to assume a reasonably good colour reproduction, what then becomes important is the relative copying of colours at various locations which may vary slightly, for example in their purity value.

The emphasis must definitely be placed on the purity variation at almost constant dominant wavelength,

since the evidence of the previous chapters indicates that angular viewing changes lead basically to a movement of chromaticity coordinates along, or closely around, a line of constant dominant wavelength. Invariably, therefore, the problem reduces to one of varying colorimetric purity together with light and shade variation from protruding facets, in a material of only one basic colour.

Wright (1948) puts forward the suggestion of a 'purity gamma' for colour photographic processes, similar to the characteristic curve of a black and white photographic process, which relates the logarithm of the exposure to the density of the developed emulsion. Here the relationship between the purity of the reproduction and the purity of the original would be of some definite form for a particular hue. Therefore, just as the accuracy of light and shade reproduction depends on the exposures of the scene being within the linear region of the density gamma curve and the slope of this region, so the reproduction of small purity variations would depend heavily on the form of this 'purity gamma'. This in turn would appear to lead to good or bad texture reproduction.

6.2 Investigation of the Reproducing Ability of Photographic Materials.

Since we are only interested in the relative reproduction of colours and not their absolute reproduction, it is possible to have some measure by obtaining the tristimulus values of the original and the copy. Natural objects are difficult to use since point to point relocation

is not easy when transferred to the photograph, and the required range of purity may not be available. Suitable colour chips were therefore required which would equate to these varying, angular colorimetric properties.

The official German Standard Colour Chart, or DIN system (Richter, 1955), is based upon a method of arranging colours according to hue (T), saturation (S) and darkness degree (D). The terms hue and saturation are translational terms and are not strictly accurate. Reference to Figure 6.1 indicates the position of all the theoretical colours in such a system for one value of D, their chromaticity coordinates being given by the intersection of the saturation contours and the radial hue contours. Obviously all such colours are not realisable in a simple reflection atlas.

However, a given series, at constant T and D values, does give a good set of samples varying basically only in purity value, for a given dominant wavelength.

This therefore meets the necessary requirements in an attempt to illustrate angular chromaticity variations with permanent samples.

To supplement these rather widely spaced samples, some chips prepared by Crawford (1971) were used. The method of preparing these samples was to mix varying quantities of two different, coloured paints and run the mixture over a glass slide, finally masking the back of the paint surface with tape. This provides a very closely spaced range between the two extreme colours, and the results, measured on a 'Colormaster Model V' colorimeter are given

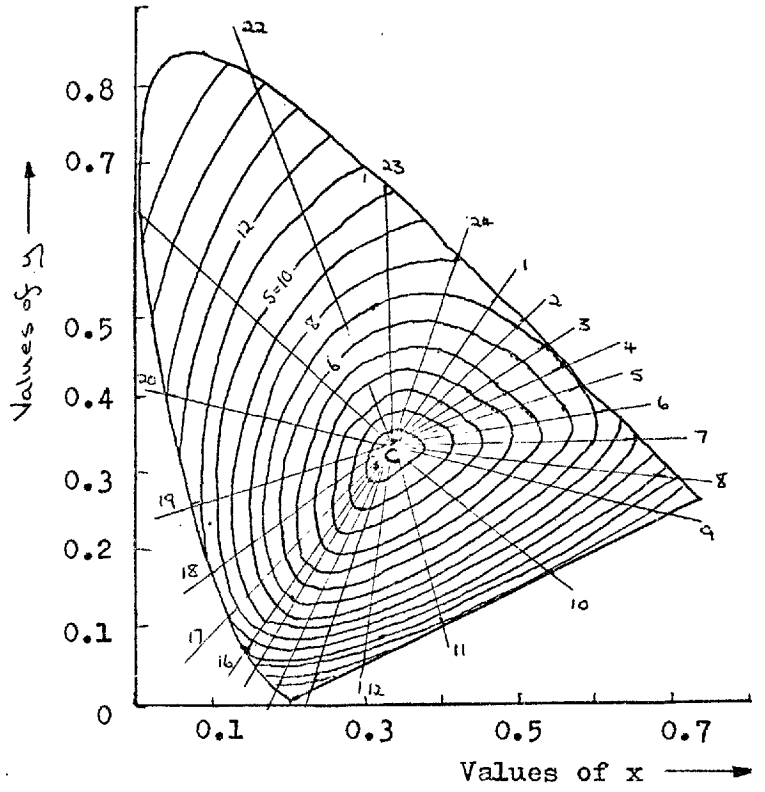


Fig. 6.1. C.I.E. chromaticity diagram showing radial contours of constant hue and contours of constant saturation used in the DIN system.

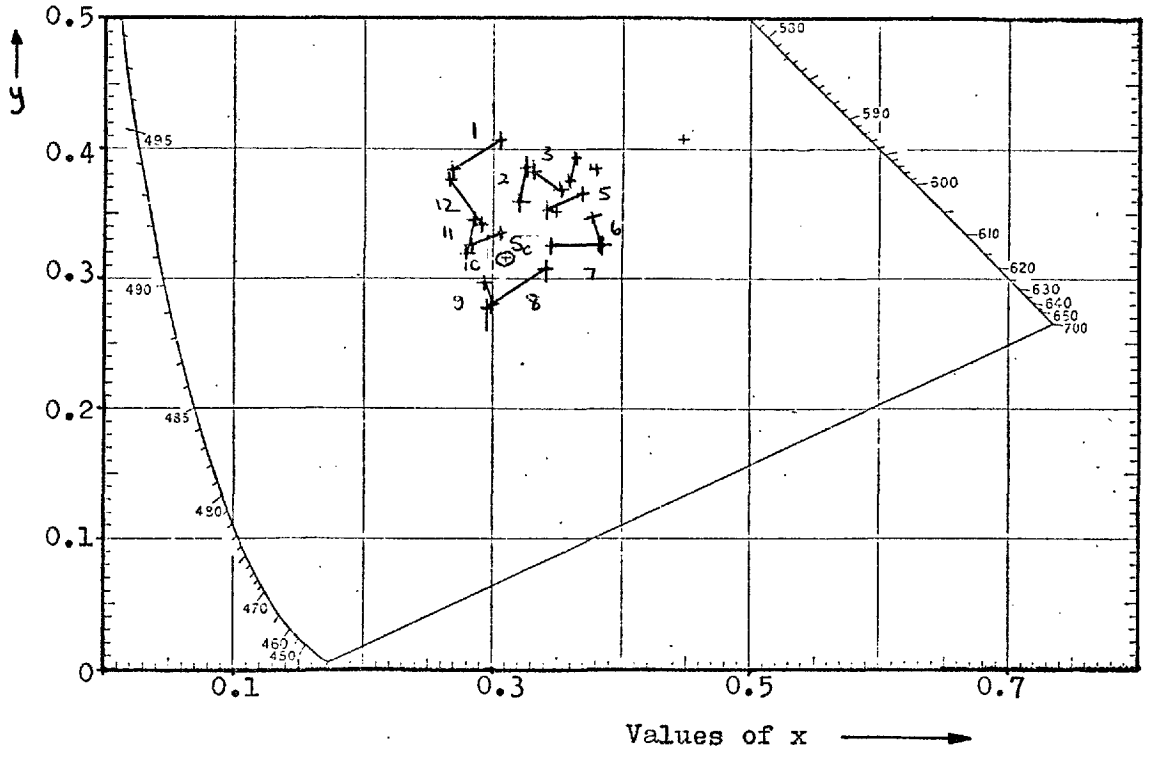


Fig. 6.2. Chromaticity coordinates of series of chips produced by Crawford under illuminant S_C.

1	AG – NG	5	B – DG	9	L – PB
2	MG – DG	6	DP – B	10	PB – DG
3	MG – B	7	DP – DG	11	PB – HG
4	PP – P	8	L – DP	12	AG – LBG

in Figure 6.2. The differences in colour for most series were such that most observers could arrange them in order, in good viewing conditions, with only one or two mistakes at the most.

Not all series were suitable, since small differences in purity were desired at a reasonably constant dominant wavelength, and as can be seen, not all series collapse towards the illuminant point - source S_C.

It was not possible to control any medium to be tested, and therefore it was decided to choose colour photography as the most easily available. Since no control on processing was possible, conditions similar to everyday ones applied, in that the exposed material was returned to the manufacturer direct, for processing normally, and the resulting frames measured.

The conditions under which the photographs were taken, however, were carefully chosen and maintained. All photographs were taken in a G.E.C. Illumination Booth, with extra diffusers to maintain even illumination over the whole field of view. The illuminant was chosen to be C.I.E. source S_C and checked by means of a 'Megatron' colour temperature meter. This illumination was incident normally on the sample series, mounted on a black 'velvet pile' paper, to prevent light scattering, and surrounded by a series of identical neutral grey chips just within the viewing field. These were to act as a guide to uneven illumination and general errors in colour reproduction.

A single lens reflex camera, with a well corrected lens, was placed to photograph this field at an

angle of 45° to the surface normal. Each series of chips was photographed complete on one frame, so that point to point variations on the film were kept to a minimum and the exposure was identical within the series. Exposures were then made over the whole range from f1.8 to f16 at various shutter speeds, and the entire operation repeated for different positioning of the chips within one frame.

The series chosen for investigation were

DIN T = 23, D = 2 (or 23: :2) - a red series

DIN T = 7, D = 2 (or 7: :2) - a green series

and to supplement these

series 7 or DP - DG

series 12 or AG - LBG

respectively of the Crawford chips.

The films were

I) Kodacolor X - a colour negative film,

II) Kodachrome X - a colour reversal film, and

III) Agfacolor CT18 - a colour reversal film.

After processing, the results were viewed by several observers and the best reproduction of each film chosen under illumination approximately that of source S_C. These were then measured at the centre of each sample together with the surrounding grey samples. The prints from film I) under $0^{\circ}/45^{\circ}$ configuration, by reflection, and films II) and III) by straightforward transmission. Other reproductions were also measured at exposures about this ' best ' result.

Finally, all the chips used were carefully

calibrated under $0^{o}/45^{o}$ conditions on the Wright Spectrophotometer using an area, sufficiently magnified, and location which duplicated those measured on the photographs, to avoid any influence of sample surface variation.

6.3 Results and Discussion.

Figures 6.3, 6.4, 6.5 and 6.6 illustrate the chromaticity coordinates of the four test series DIN 23: :2, DIN 7: :2, series 7, and series 12 respectively together with their best reproductions by the three chosen types of film.

It is immediately obvious that no copy is perfect, although as explained above this is not surprising. Apart from colorimetric errors inherent in such experiments, exact chromaticity reproduction is rare. However, the first important point that emerges is that, if an observer were asked to specify which reproduction applied to which chip in a series from the chromaticity coordinates alone, in nearly every series this would be possible since the ordering in terms of purity value, or saturation, of the reproductions is the same as their equivalent originals.

The DIN series are both reproduced with a good variation in purity value, apparently almost that of the originals for the reversal material. In the case of the negative material, some collapsing of the chromaticity coordinates towards more desaturated colours is obvious, accompanied therefore by poor absolute colour reproduction and also an apparently poor 'location' of the illuminant point. However, even these badly reproduced sets are still

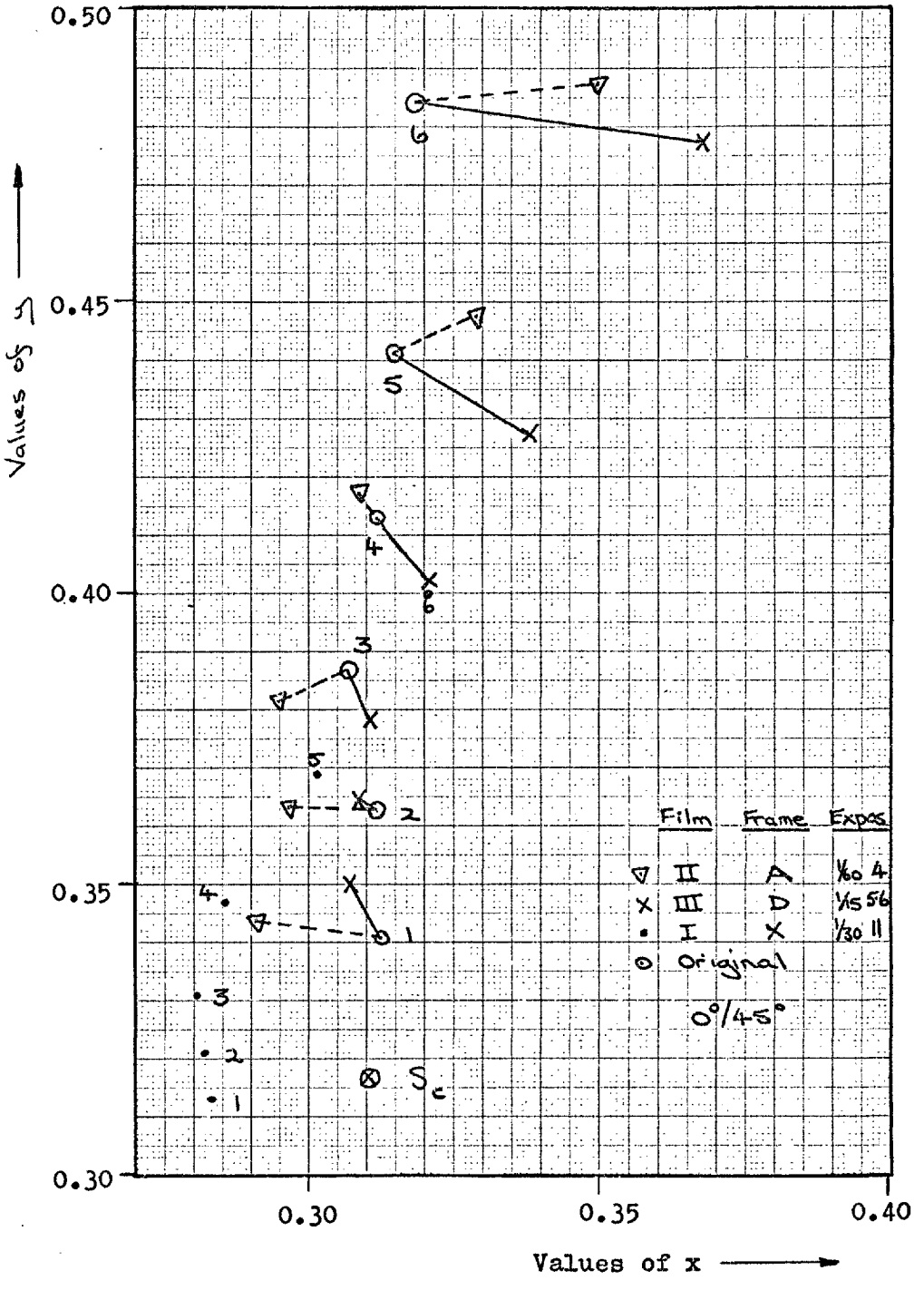


Fig. 6.3. Chromaticity coordinates of series (23: :2) for original and reproductions under conditions $0°/45°$ and illuminant S_C.

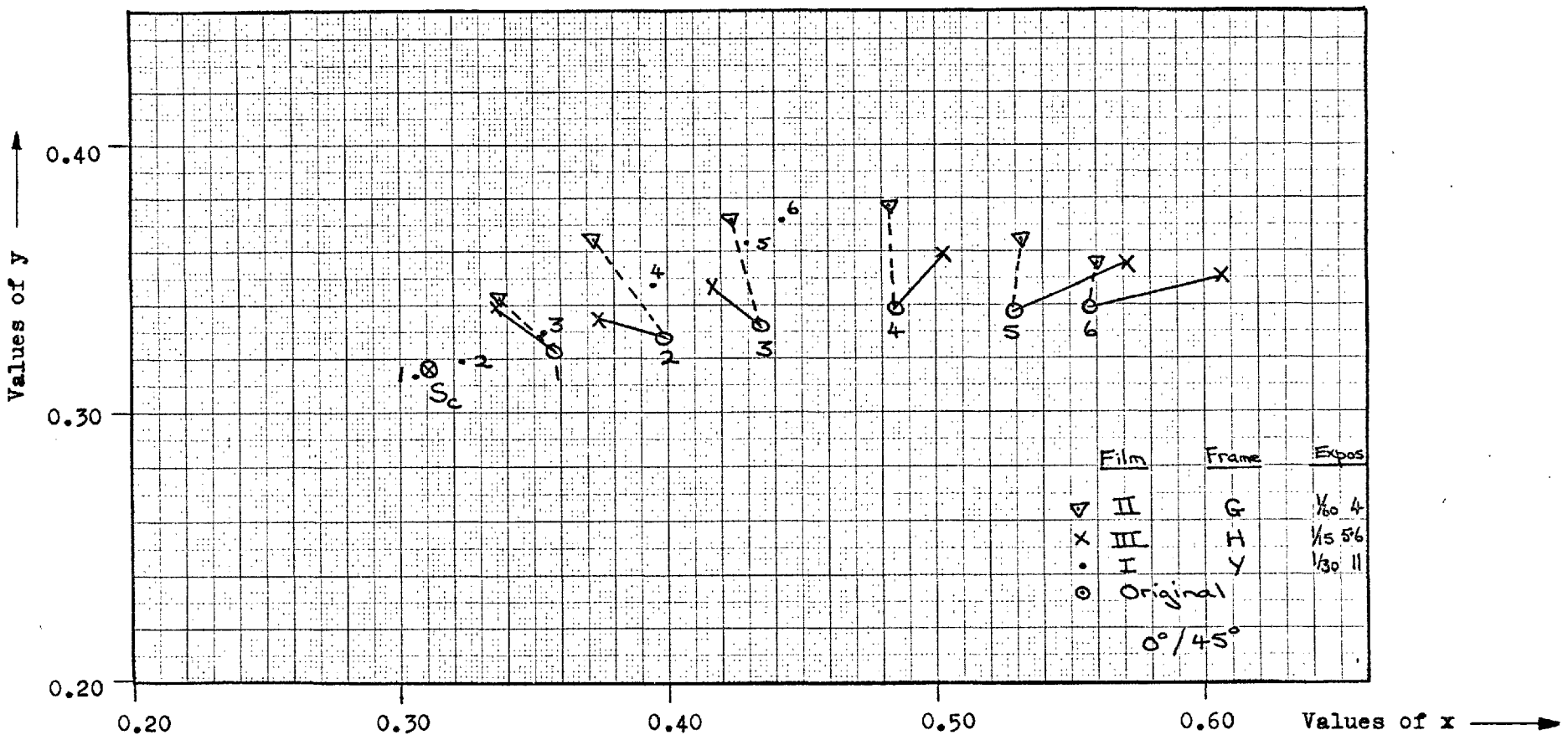


Fig. 6.4. Chromaticity coordinates of series (7: :2) for original and reproductions under conditions $0^{o}/45^{o}$ and illuminant S_C.

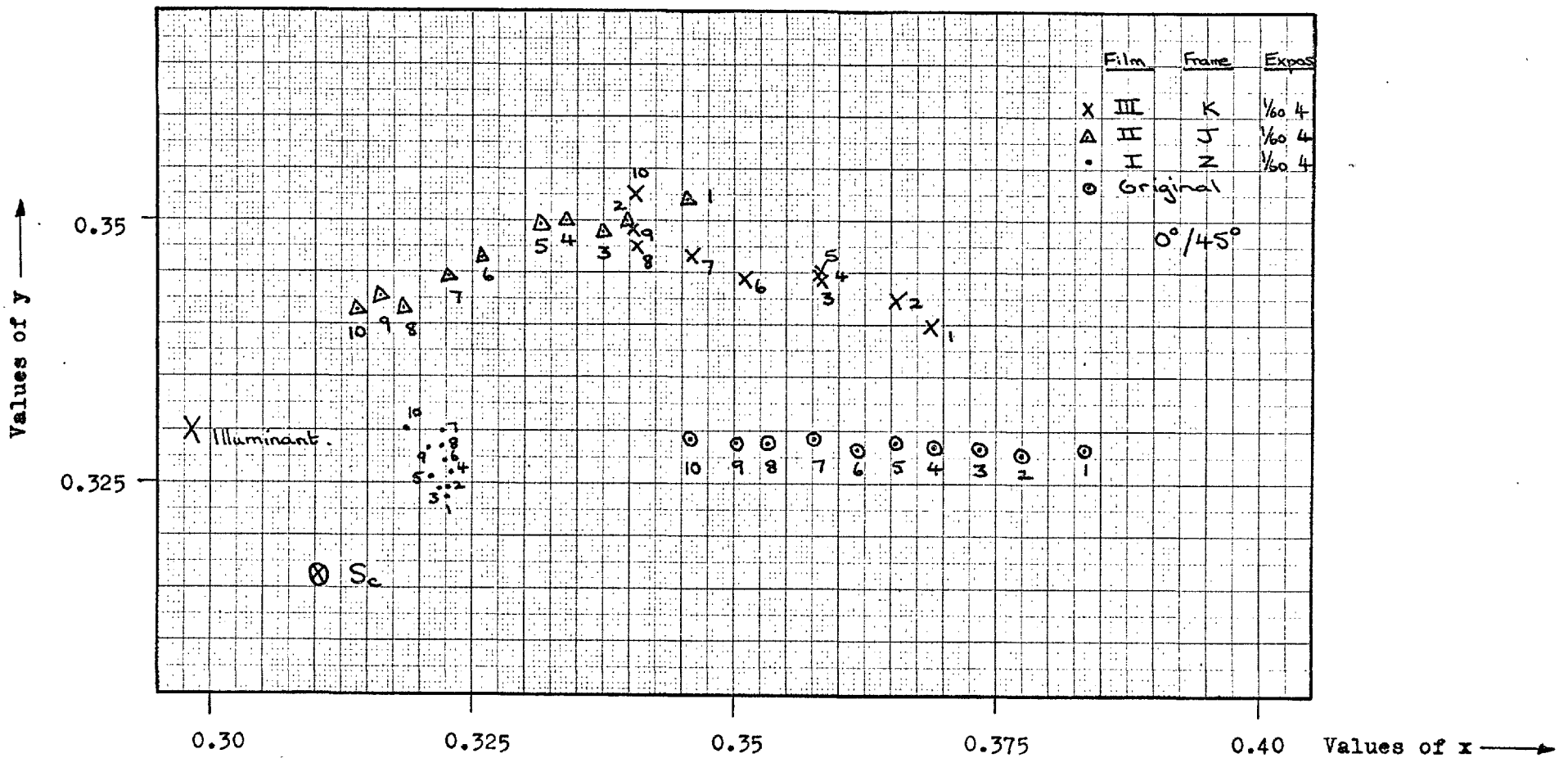


Fig. 6.5. Chromaticity coordinates of series (DP-DG) for original and reproductions under conditions $0^{\circ}/45^{\circ}$ and illuminant S_C.

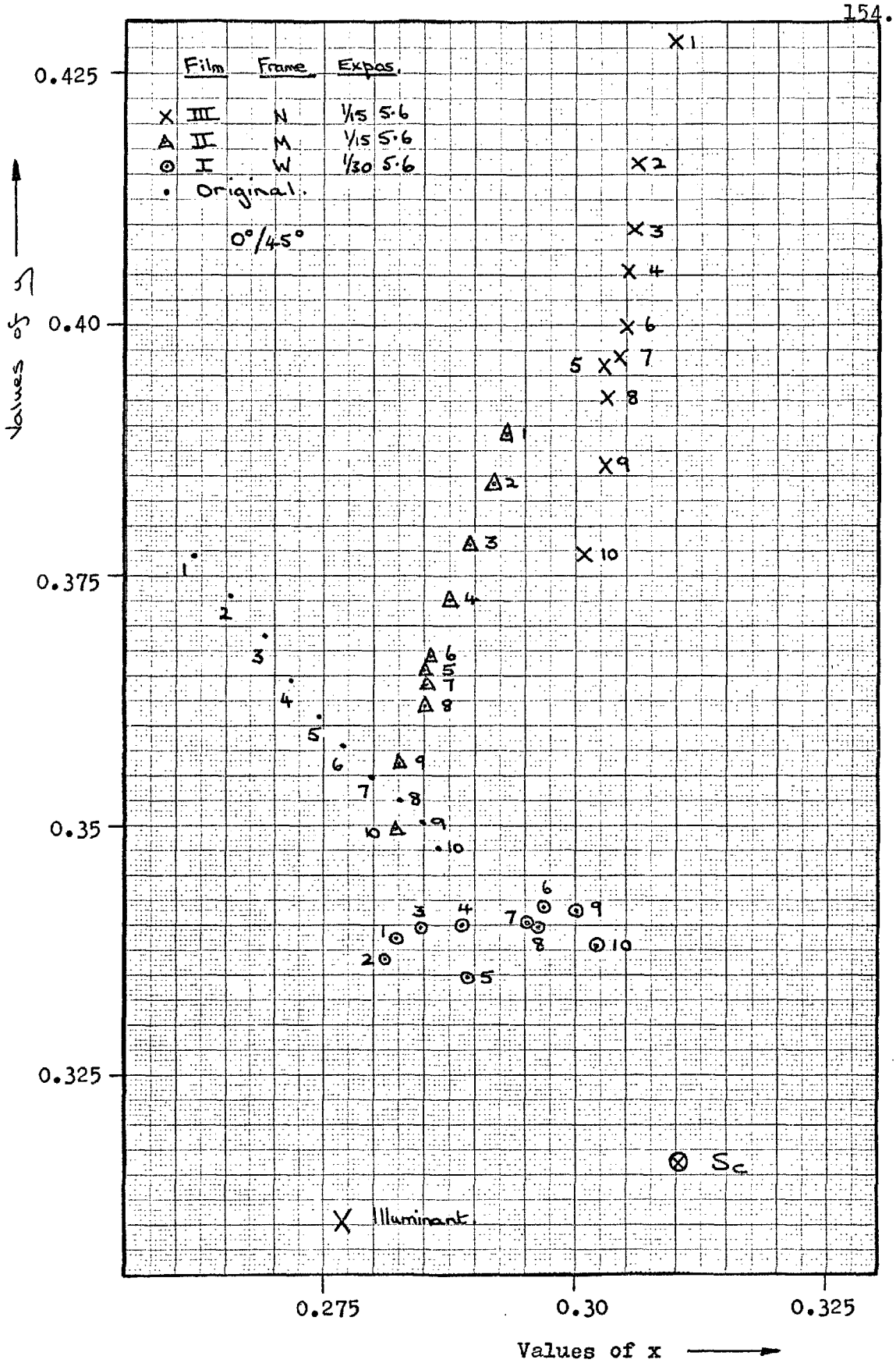


Fig. 6.6. Chromaticity coordinates of series (AG–LBG) for original and reproductions under conditions $0°/45°$ and illuminant S_C.

well ordered in terms of saturation, showing the correct arrangement of sample points and direction of their location in colour space.

The more closely spaced series are at first sight reproduced less well, the reversal materials both showing the colorimetric purity changes to be recorded well overall, with certain clearly observable errors at some midpoints. Again the absolute colour reproduction is in some error.

The negative material, on the other hand, leads to very confusing results. Little definite pattern is discernable, and it is true to say that without the labelling, the points would be almost impossible to identify.

Both types of material will now be covered in somewhat more detail.

6.3.1 Negative Material.

The immediate conclusion one might draw from such data is that the medium could represent large point to point gradations but would fall down over the smaller ones, represented by the latter two series, typical of angular variations found in the more matt type of texture. It would qualitatively appear therefore that the two distinct types of test - the widely spaced chips of the first two series and the more closely spaced ones of the latter series - represent the cases on either side of the point of breakdown for the medium, as far as good purity reproduction is concerned. This is verified, since, although Figures 6.5 and 6.6 show a confusing array of points, the

extreme values at points 1 and 10 are clearly defined and show the boundaries of what may only be called a general movement between them.

Since this is of the order of, or slightly larger than, one step in the more widely spaced series, breakdown is shown to occur somewhere between the two types of spacing.

The criticism is valid however, only within the confines of the experiment and certain points are therefore important.

Firstly, apart from errors inherent in this type of experiment, namely incorrect illuminant, uneveness of illumination, chromatic aberrations of lenses etc., the photographic process of 'integrating to grey' may also introduce large errors. The arrangement, first suggested by Evans (1946), is a method by which the constituent primaries of the process are balanced automatically to give a grey upon spatial integration over the photograph. This is a quick, automatic method of handling such material in bulk. Obviously in a frame of the type described above some colorimetric error will be introduced since the photograph is mainly of one hue, surrounded by black and grey.

Secondly, the position of the illuminant point may not be that specified, due to erroneous calibrating within the illuminating booth. This is not quite so critical, however, since some measure of the error may be obtained by measuring the surrounding greys in the reproduction and comparing these with their original positions, close to the illuminant point at S_C.

Thirdly, the illumination may not be constant over the entire frame introducing colorimetric distortions, but this again may be checked by measuring the almost constant greys from point to point.

The last two points will be dealt with in more detail in the next section, but since the first is of such overriding importance, little more may be deduced from the results on this type of material.

6.3.2 Reversal Material.

Here one has a much more favourable looking situation. The chromaticity coordinates, although not exact copies of the original, do present a systematic ordering of purity value, and, with certain exceptions, do so even in the more closely spaced series.

a) In the case of the two DIN series, both types of reversal film seem to make an adequate job of reproducing the purity movement with more absolutely accurate coordinates than in the previous section. This success may be more accurately judged with reference to Figure 6.8. Since the length of exposure may affect such results, the equivalent measurements taken on series (23: :2) for exposures either side of the 'best' one for film II) are given, together with this 'best' frame and the similarly chosen one for film III), in Figure 6.7.

If the average dominant wavelength for the series - approximately 553nm - is used to determine the values of colorimetric purity for various reproduced points

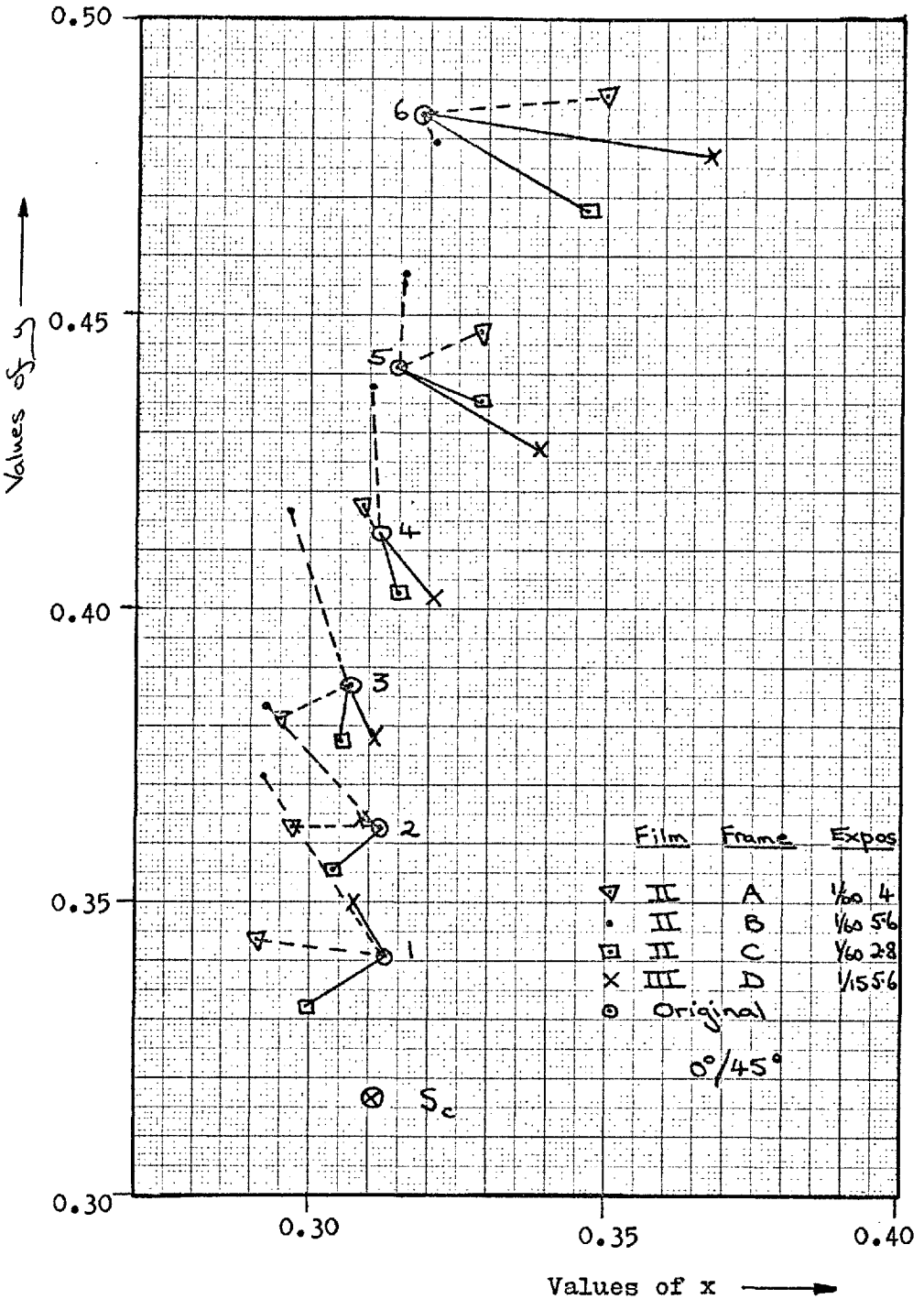


Fig. 6.7. Chromaticity coordinates of series (23: :2) for original and reproductions at several different exposures under conditions $0°/45°$ and illuminant S_C.

at different exposures it is then possible to plot the original purity values against those of the various reproductions. This is done in Figure 6.8.

The ideal locus of such points would obviously be a straight line at 45° to the axes, drawn in over Figure 6.8, thus giving an exact purity reproduction throughout. This certainly cannot be so with extremely saturated colours, almost upon the spectrum locus, and one would doubt that this would be maintained in the vicinity of the illuminant point.

Over the range considered (approximately 7% to 48% in terms of excitation purity, or 4% to 66% in terms of colorimetric purity), the results given by frame (A) of film II) are excellent, falling almost exactly upon the line. With the exception of the most saturated point in the case of frame (B), the other exposures on this film also show a similar 45° trend, although displaced either side of the frame (A). This is not critical since only relative, rather than absolute, agreement, within limits, is required from the point of view of texture reproduction. The only stray point, at highest levels of saturation on frame (B), may in fact be extremely significant, since this would require a purity in reproduction of some 55% to preserve the linearity of the plot for frame (B) instead of the 46% indicated. This may well be the first indication of the upper limit of the linear portion for this particular hue. Further, more saturated, samples were not available to check this point however.

On this basis the results of film III) appear

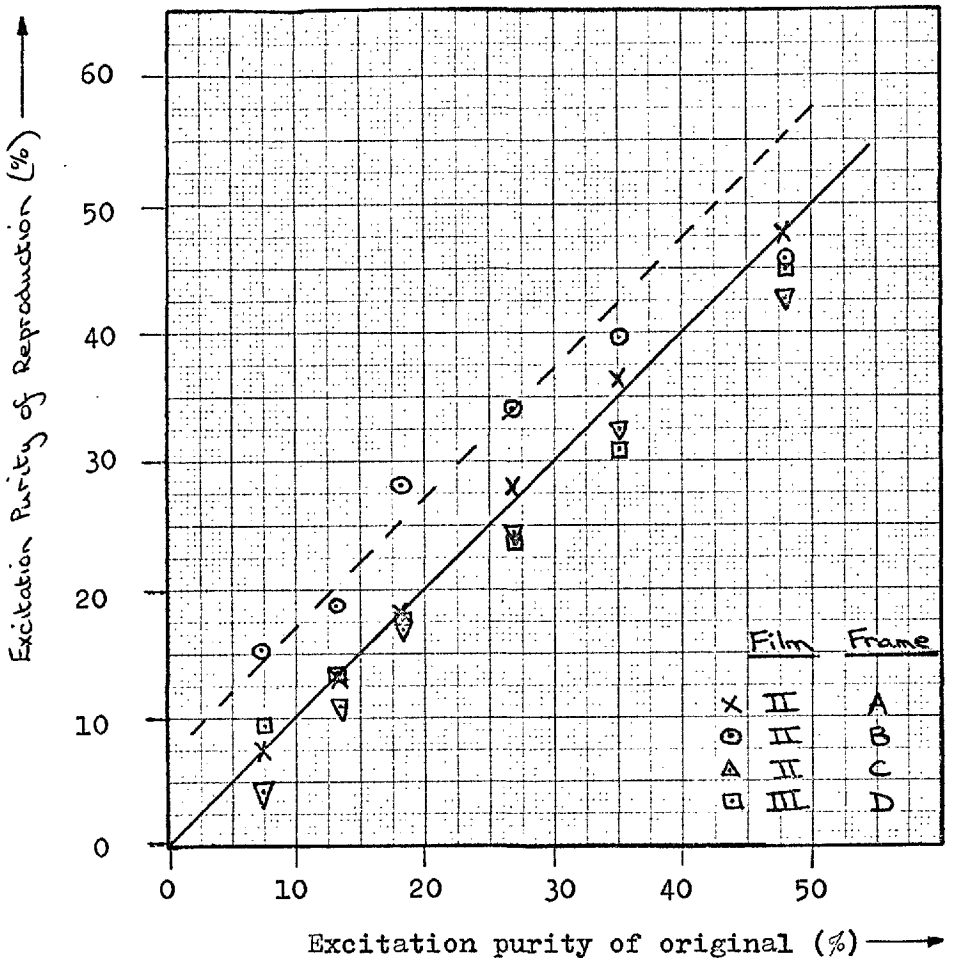


Fig. 6.8. Plot of excitation purity of original versus that for several reproductions at various exposures for series (23: :2) using an average dominant wavelength.

to be good, but not quite as accurate as those of film II). Exposure appears to be important, within limits, only in obtaining the correct absolute purity values but not the relative ordering. The exposure however, will determine other factors which in turn may to some extent affect the reproduction of texture, for example the light - shade content of the photograph.

In assessing the values of purity for any particular set of chromaticity coordinates an important point arises. Above, the value of dominant wavelength has been taken as the average value for the actual series under test. This has given results which do indicate the most accurately reproduced purity scale to be also that chosen as the 'best' reproduction. However, certain chromatic differences are obvious between the original series and the various reproductions, leading to appreciable variations in the value of dominant wavelength from point to point. The excitation purities of frames (A) and (D) for films II) and III) respectively were then recalculated, for both DIN series reproductions, by the usual methods outlined in Chapter 1 and also Wyzsecki and Stiles (1967). The values were then plotted against the originals in Figures 6.9 and 6.10 for series (23: :2) and (7: :2) respectively.

The curves obtained here deviate by fairly large amounts from the ideal 45° line. They in fact possess a shape remarkably similar to that proposed by Wright (1948) in his sketch, showing a reduction in the reproduced purity value compared to that of the original, up to values about

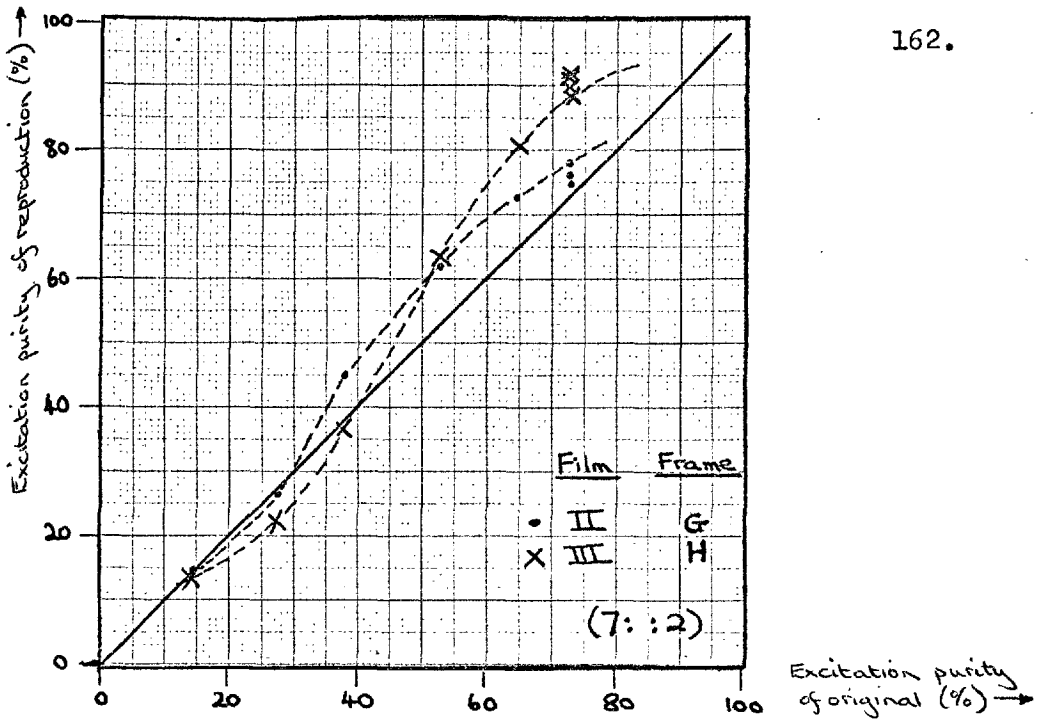


Fig. 6.10. Purity 'gamma' curves for series (7: :2) using real dominant wavelengths for both films.

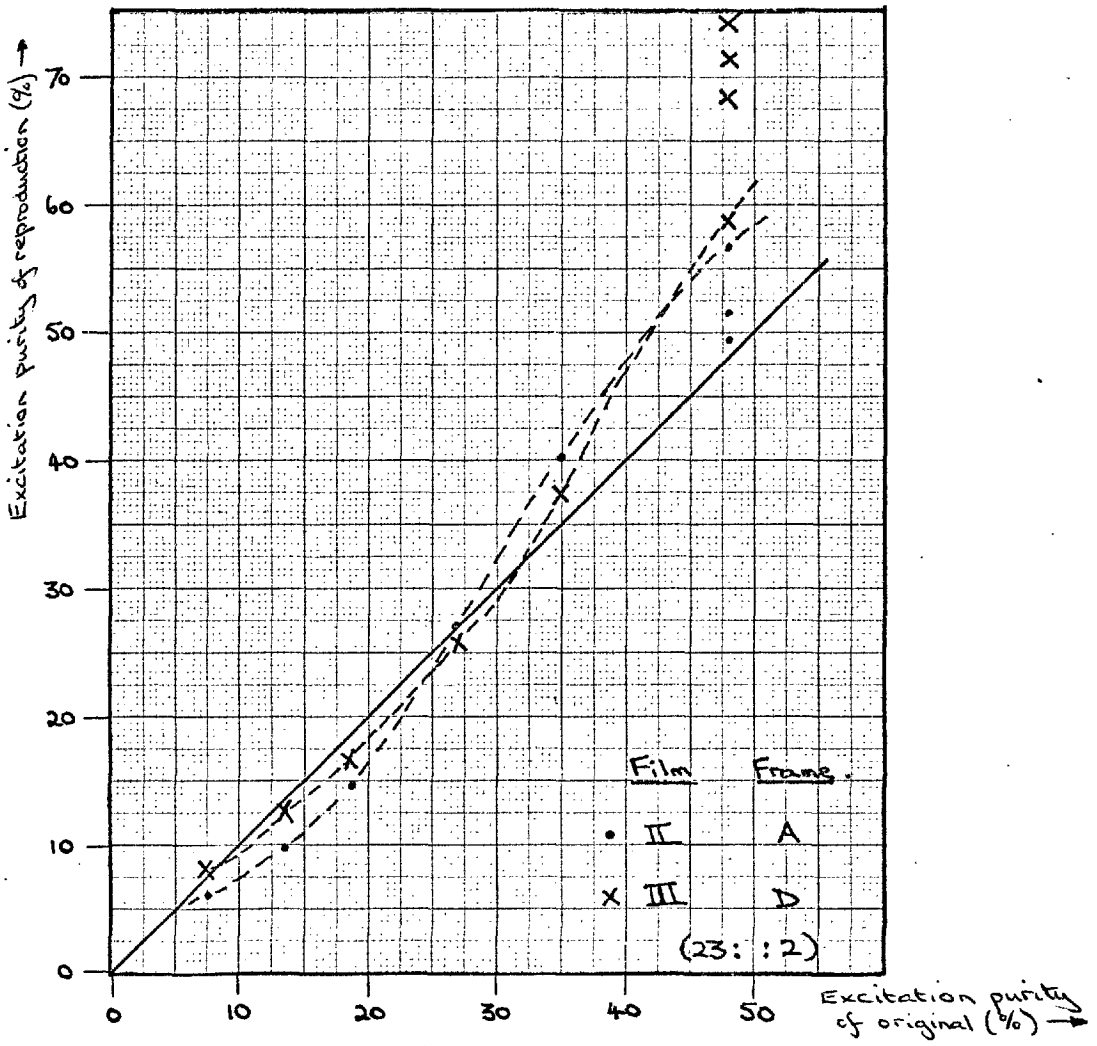


Fig. 6.9. Purity 'gamma' curves for series (23: :2) using real dominant wavelengths for both films.

30%, thereafter a marked increase in this value over the original. The curves also give the impression of flattening off at either end somewhat. This might be expected, in that 100% purity of original, or spectral colour, will always, of necessity, be reproduced as something less than this value, and a perfect white may also be distorted slightly from the illuminant point.

The cross over points for each film are fairly consistent for the different hues, in that film II) gives a value between 25% and 30% and film III) a value between 30% and 40%.

The graphs indicate a 'gamma' value, or gradient, somewhat greater than unity - approximately 1.6. This should not inhibit the satisfactory reproduction of texture, if anything it effectively magnifies it, except at the extreme ends of the purity range. Most of the samples dealt with earlier should therefore be reproduced well as far as the texture is concerned. However, extremely white samples, such as the magnesium oxide specimens, or objects of extremely saturated coloration may represent some problems, if they fell within say the first or last 5% of the excitation purity scale. This may therefore distort the highlights, or specular points, of highly glossy specimens, although a distortion of the highlights would probably be insignificant, with respect to the fact that a highlight of some description occurred, in terms of texture appreciation.

It must be stressed that the graphs are obtained from measurements on the frame whose exposure was judged to be best by observers. The most saturated point for

each series was measured on several reproductions of varying exposures and some of these are indicated by further points on Figures 6.9 and 6.10. For both series, exposures on either side of the earlier one gave smaller purity values for film II), yet still above that of the original. Film III) could only be measured at exposures shorter than the chosen one and these all gave larger purity values in reproduction than even the 'best' frame.

Therefore even exposures which are slightly different to the most acceptable one still give a more saturated colour than the original at saturation levels above the 'cross over point' of the purity curve.

b) Turning to the two more closely spaced series - series 7 and 12 - certain points require further discussion.

i) Taking the results of series 7, Figure 6.5, again there are obvious colorimetric errors in the reproduced chromaticity coordinates. Two particular types are obvious. Firstly a shift of the entire range, suggestive of an illuminant coordinate movement in the reproduction to a higher value of y and a lower value of x, and secondly, systematic distortions of chromaticity coordinates within one series - that of film III).

In Figure 6.11 the chromaticity coordinates of four of the grey samples used as surround are given. They fall close to the illuminant point, S_C, and have very little spread in their values. Samples 1 and 3 occupied positions respectively left and right of the frame, and samples 2 and 5 similarly above and below. The coordinates

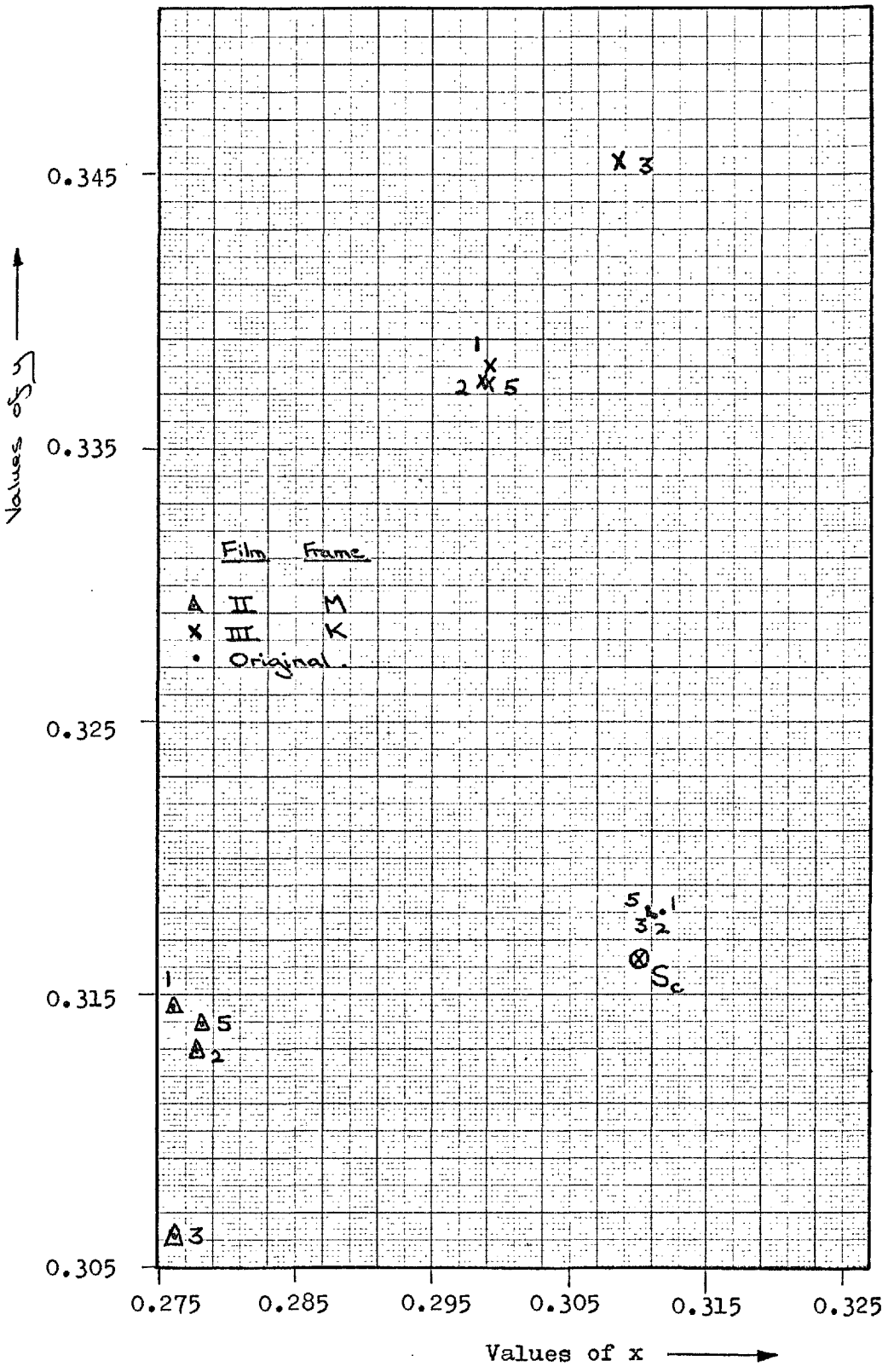


Fig. 6.11. Chromaticity coordinates of greys used as surround, both original and reproductions, under conditions $0°/45°$ and illuminant S_C.

of the four greys when reproduced in frame (K) of film III) are also given in this figure together with the corresponding results on frame (M) of film II). The former surrounded the series 7 (DP-DG) and the latter series 12 (AG-LBG).

It is now possible to attempt a somewhat better estimate of where the illuminant point is, during the time of the exposure, from the position of these neutral colours, and this has been approximately indicated in Figure 6.5 for the results of film III). The series now shows a much closer colorimetric copy of the original by allowing for the discrepancy in illuminant points. It is not possible, however, to transform back to the original illuminant S_C with accuracy, mainly due to lack of linearity within such a figure.

The coordinates of the grey samples raise a further point in that the coordinates of the point 3 show a marked movement away from the others, towards the yellow part of the spectrum locus. This suggests an uneveness in illumination, or lack of consistency over the photographic frame. It also explains the systematic distortion of the coordinates of points 4 and 5, 9 and 10 on film III) because it is also in this direction, assuming the original series to present a set of progressively decreasing purities. Since chips 4,5,9 and 10 were all in the same area of the frame as grey 3 it appears to be conclusive.

ii) Moving to the results of Figure 6.6 one again finds evidence of a distortion in illuminate coordinate

position. The approximate coordinates of the photograph illuminant for film II) have been derived from Figure 6.11 as before, except this time from the third set of grey points, and is indicated in Figure 6.6 also.

Again it can be seen that the chromaticity coordinates collapse to this point and this partly explains colorimetric errors.

Obvious systematic frame errors are again present between reproductions of chips 6 and 10 - the bottom row, for both films. In fact they overlap. Referring to the greys in Figure 6.6, it appears probable from the position of sample 3 - the right hand side - that the effect is due partly to a distortion of the illuminant at this side towards the blue, since the chips in each series were laid out systematically left to right, 1 to 5 in the top row and 6 to 10 in the bottom, in these two frames. This may again be due to uneven illumination or distortion within the photographic frame.

To distinguish between the two causes is difficult, especially since the cause of the overall illuminant shift may well be due to a third possibility - namely the processing of the film itself. Such illumination variations within the cabinet are possible since the chromaticity movements are extremely small and could certainly change to this extent between exposures. The effect, however, is present in both films for the samples in Figure 6.6 but for only one film in Figure 6.5. Unless both films suffered from almost identical distortions on frame II)(M) and III)(N) it seems more likely to be an

illumination variation. For the present investigation, it is not necessary to explain the exact cause of the error, only to note its presence in explaining the apparently erroneous coordinates of certain reproduced colours.

It appears therefore that the errors present may almost all be explained by illuminant shifts and that in all likelihood without these, the medium would reproduce the small purity changes well as indicated by all the other points which have not received any detailed mention above.

Attempts to quantify these results, as for the previous ones in Figures 6.8, 6.9 and 6.10, would be wrong, since the errors outlined above are virtually impossible to correct mathematically without introducing equally significantly large errors.

Qualitatively one may say that purity variations of less than 1% are well recorded allowing for errors above and beyond the actual photographic medium. (Series (DP-DG) ranges in excitation purity from 13.0% to 22.8% and series (AG-LBG), similarly 7.3% to 15.9%, and therefore both are if anything well down in the 'toe' of the purity curve, setting an even more exacting problem for the medium.) Certainly the resulting chromaticity coordinates of the reproductions could then be well ordered without the labels in Figures 6.5 and 6.6.

6.4 Colour Difference Reproduction Over a Saturation Range.

Since texture appreciation depends not only on the angular chromaticity variation, basically changes in purity, but also spatial chromaticity variation over the

surface of a material, a further important criterion for good reproduction is obtained - that is good colour difference reproduction. This is shown in the above data by good ordering of the test chips in colour space in reproduction, however it is possible to obtain a more quantitative estimate of this ability by comparing the magnitudes of actual colour differences.

The reproduced colours and original colours are, in general, in close proximity on the chromaticity diagram. For this reason it is valid to compare the reproduction of such colours and their colour differences in terms of the simple geometric magnitude of their differences in colour space.

By expressing the colour difference

$$\Delta E = \sqrt{(x_1 - x_2)^2 + (y_1 - y_2)^2}$$

where x and y are the chromaticity coordinates of two samples (1 and 2), it is possible to compare the colour difference (ΔE) between two original chips and their reproduced colour difference ($\Delta E'$) on the photograph. Ideally the ratio of the two quantities ($\Delta E'/\Delta E$) should be close to unity over a large range of saturation and hue. Such a comparison, especially in a coordinate system as visually non-linear as the x-y space, is only valid in an application such as the present one where the comparison of colour difference is made within a small area of colour space.

The ratio of original and reproduced colour differences ($\Delta E'/\Delta E$) has been derived for the above data

and is shown plotted against the average purity of each reproduced colour step for DIN series 23: :2 and 7: :2 in Figures 6.12 and 6.13 respectively, for the three films. The ideal line of unity has also been dotted in.

Similar data for the more closely spaced series are difficult to obtain due to the overriding effects of non-uniform frame illumination and errors in the chromaticity of the illuminant. However the colour difference ratio has been derived for series (AG-LBG) and each film to illustrate typical values, but is plotted against the purity of the original chips in Figure 6.14, since the dominant wavelength of the reproduced colours varies widely, and therefore the purity of the reproduction has little meaning. Data for differences between samples 5 and 6 have been omitted due to large illumination error at this point.

For the two reversal films Figures 6.12 and 6.13 show that the colour differences are reproduced well for the two main hues chosen, over a fairly large range of saturation. The ratio of colour differences remain close to, or above, unity at points above about 20% in reproduced purity, although it was impossible to continue the saturation range beyond these limits, where it would be expected that the agreement in colour difference ratio would tend to become worse.

The results for the colour negative material indicate a poor and confusing reproduction in the main for the reasons previously outlined.

Figure 6.14 indicates that for small colour differences the reproduction is less accurate for all materials,

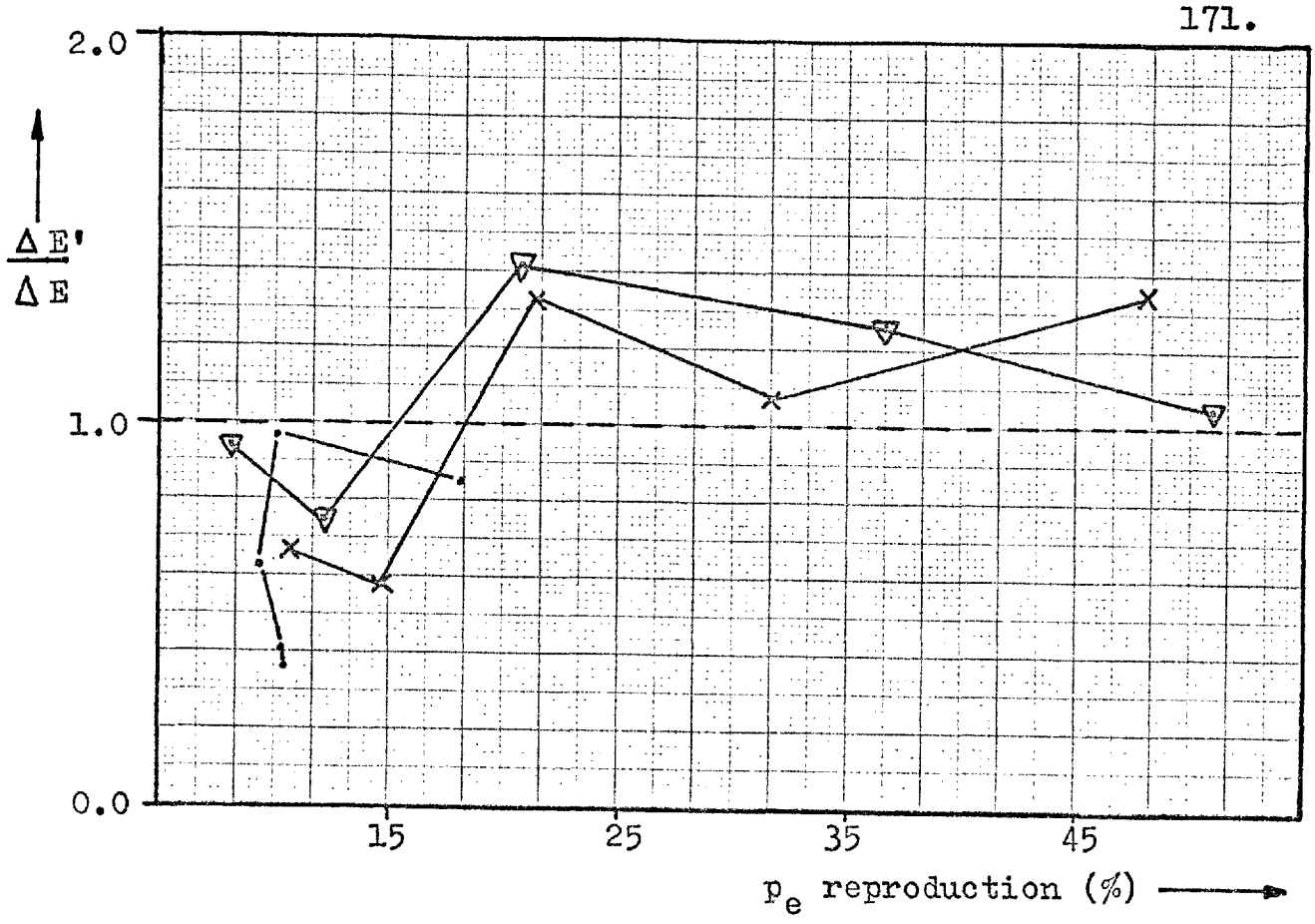


Fig. 6.12 The ratio of reproduced to original colour difference for the series (23: :2) and the three films.

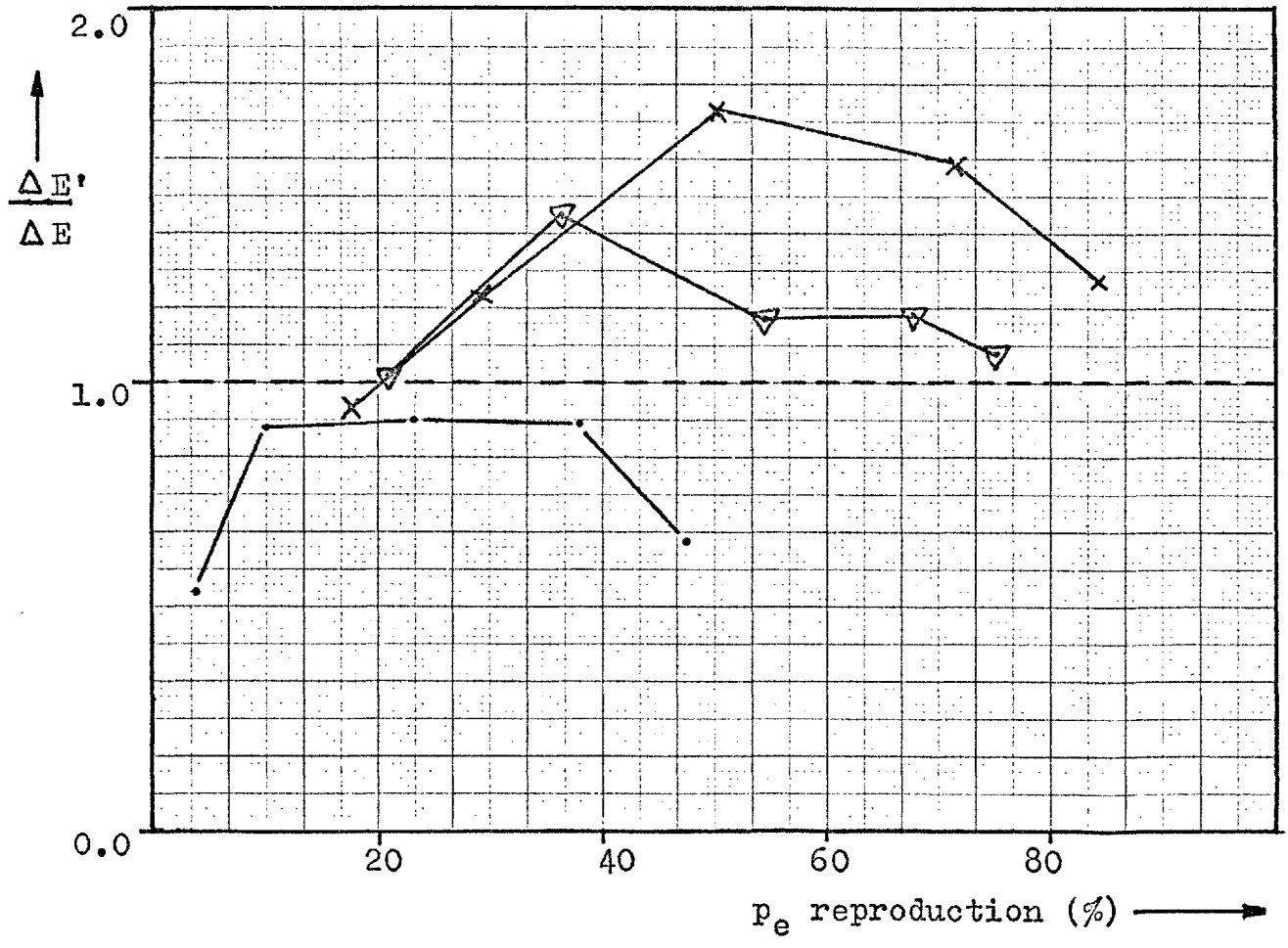


Fig. 6.13 The ratio of reproduced to original colour difference for the series (7: :2) and the three films.

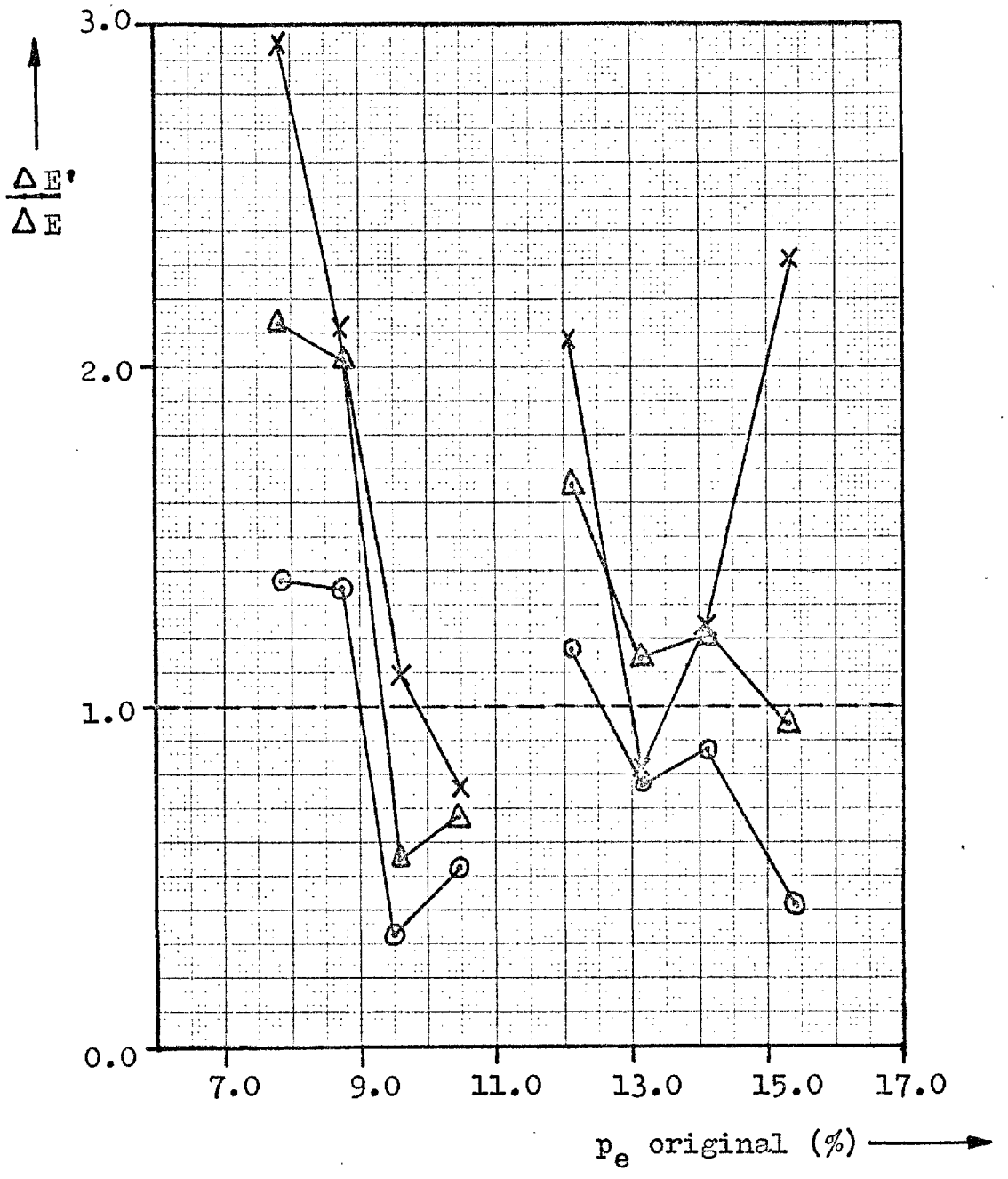


Fig. 6.14 The ratio of reproduced to original colour difference for the series (AG-LBG) and the three films.

due mainly as before to the larger effect of illumination variations.

6.5 Further Factors.

Luminance values are also important in differentiating between various textures. Again it is obvious from earlier chapters that it is the variation with angle which is important, not necessarily the absolute values.

In photographic terms however the relationships between the original and reproduction in this direction would tend to be complex, depending upon the photographic medium. The discussion of this will therefore be restricted to its influence on the colorimetric approach already dealt with.

If the luminance values of the reproduction at least follow those of the original, with wide limits on their absolute values, then the results earlier will remain unchanged. Typical luminance comparison curves follow in Figure 6.15 for measurements on series (7: :2) for both films. It is clear that both reproduce these well, if at different levels, levels which would be very exposure dependent, and therefore the earlier discussion remains valid.

It is felt that further discussion is of little help since the whole effect is extremely dependent on just such factors as exposure, material and processing, some of which are beyond experimental control.

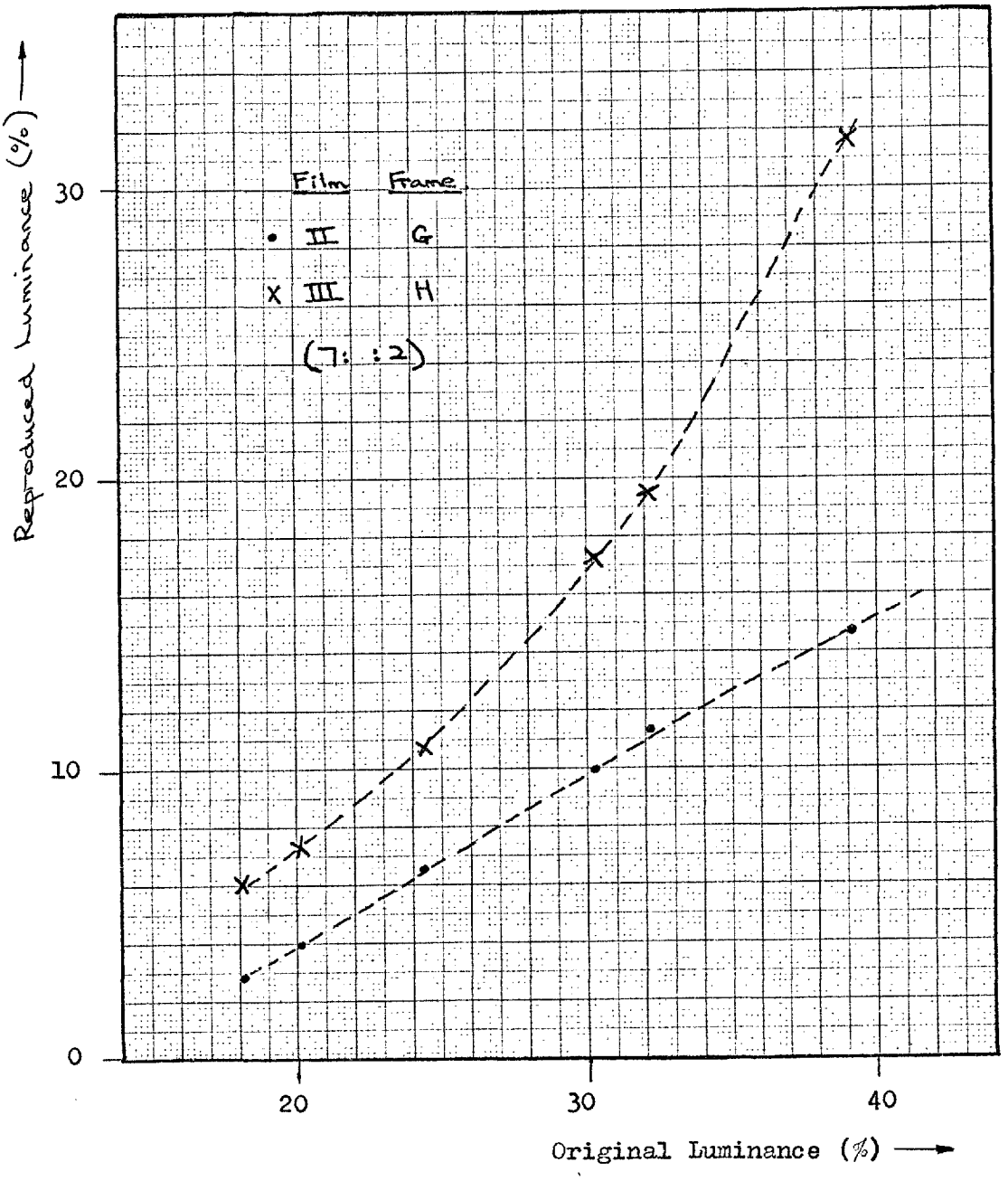


Fig. 6.15. Plot of original luminance versus reproduced luminance for series (7: :2) on both reversal films under conditions $0^{\circ}/45^{\circ}$ and illuminant S_C.

6.6 Conclusions.

In earlier chapters it has been shown that different types of colorimetric change do occur at various angles for surfaces of differing texture. Since these are almost always at nearly constant dominant wavelength, the important variation is that of purity. If colorimetrically we are therefore to define the important parameters with respect to texture reproduction it must certainly be that of correct reproduction of purity variations.

This has been tested in the cases of colour photographic materials, and even with no control over the processing very good results have been obtained with reversal material, down to limits of purity typically found to exist in earlier chapters. Negative materials were good except at the lower purity increments where they appeared to break down, although it is likely that this is due in part to the method of processing rather than the material itself.

Errors, where they existed, in the reproductions have been shown to be mainly due to the illumination difficulties.

A method of determining the quality of purity, and therefore texture, reproduction is outlined and the 'purity gamma' curves have been derived for the reversal materials both for an average dominant wavelength, and the more realistic condition of a varying dominant wavelength.

In the former case the results indicate an extremely close, exact purity relationship at the correct

exposure, whereas the second case indicates a slope of reproduction versus original of approximately 1.6, and the first evidence of the flattening of this curve at the extreme ends of the purity scale, thus leading to poor reproduction at these points.

Good agreement was obtained on these points for two different hue conditions - one in the green, the other in the red.

Given control over the processing of such photographic material it should be possible to obtain results more colorimetrically accurate than those above. The above established criteria for good texture reproduction may then be employed to check to a finer degree these properties. Unfortunately the necessary control was not available in other media to enable such a programme to be undertaken, however the criteria for good reproduction remain the same whatever the process.

6.7 The Role of Luminance Reproduction in Texture Appreciation.

Although the colorimetric features of surface texture have been stressed in the earlier chapters, it is apparent that the luminance variation of a surface also conveys a great deal of information about this property. The field of goniophotometry and gloss measurement is primarily based on this fact, and the exclusion of such data in the assessments of this chapter was in no way intended to reduce this importance.

The acceptance of photography and television for many years in black and white form is indicative of the success such systems have achieved in conveying more than a simple flat monochrome image of the scene and its component parts. The fact that such a system also records, and passes on, information regarding the surface quality of objects by means of accurate luminance reproduction from point to point is in a very large measure responsible for this acceptance.

Therefore, despite the extra dimension of colour being unavailable, it is still possible to give a satisfactory reproduction of surface finish and structure in terms of luminance gradations to such an extent that, for example, manufacturers are often content to advertise their products in this manner.

With the addition of colour to a reproduction process, the further information given above on the colorimetric aspects of surface texture is necessary to assess the ability of the process to reproduce texture satisfactorily.

It is perhaps significant in this respect to consider the relative importance of both luminance and colour

reproduction in relation to the fine detail of the picture. An indication of this is supplied by consideration of colour television broadcasting where, despite the large increase in potential information of a subject, the signal carrying luminance information still retains some four times the bandwidth of the colour difference signals (Hunt, 1967). This arises from the knowledge that luminance differences are of much greater importance than colour variations in detail appreciation by the human eye. The high definition luminance signal therefore retains a very great deal of importance even where a system has expanded to include colour information.

6.8 The Practical Effects of Viewing Colour Transparencies in Dark Surround Conditions.

At several points in the preceding chapter a purity 'gamma' of 1.0 has been considered ideal; however this statement requires some qualification.

Since reversal materials have been the main centre of discussion above with regard to this quantity, certain other factors which will have marked effects on the colours when viewing transparencies in practical conditions must be considered.

The measurements which are illustrated earlier have been made in the ideal circumstances of specular transmission, with virtually zero stray light present. Such a result indicates the ideal transmission colour, which in practice is not obtained on projection due to the presence of stray light or flare. Such flare originates either at the

projector, multiple reflections between screen and objects in the room, or from secondary sources within the room, all affecting screen image. The presence of this flare is such that the overall gamma value of the process is lowered and inevitably the colour saturation is decreased (Hunt, 1969).

Transparencies are invariably viewed by projection in a darkened room, thus the reproduction is edged by a dark surround whose effect has been shown to make the image appear lighter than in the case when a higher luminance surround is employed, for instance in reflection prints. This influence varies over the picture area, being greater towards the edges and occurs to a greater extent in the dark areas of the reproduction (Breneman, 1962). It is then possible to determine the magnitude of the effect this has on lowering the overall gamma value of the process (Bartleson and Breneman, 1967). A figure of 1.5 has been given for the gamma value required to compensate for this effect when viewing in dark surround conditions, and 1.2 in dim conditions, in order that the tone reproduction be apparently correct. These values are further increased to offset the presence of flare. Reflection prints, which are viewed in average levels of ambient surround illumination do not require the former correction.

On increasing gamma values for the above reasons it follows that the colour saturation will also increase, thus increasing the saturation for reversal materials above that of print materials. However it is possible partially to compensate for this by viewing prints at high illumination levels (Hunt, 1952).

A further complicating factor exists in that it has been shown that a dark surround tends to decrease the apparent saturation of a picture (Hunt, 1950).

It is most important at this stage to avoid confusing the subjective concept of saturation with the more objective measurement of excitation purity; however, some correlation does exist and although it is difficult to be definite about the ideal form of a purity 'gamma' relationship, it is now evident, from the factors outlined above, that a 'gamma' greater than unity would tend to compensate some of these effects.

CHAPTER SEVEN.

THE COLORIMETRIC AND PHYSICAL PROPERTIES OF A PARTICULAR SURFACE TEXTURE AND STRUCTURE - THE MORPHO BUTTERFLY WING.

In a sense, such a study of surface texture must inevitably treat the enormous number of differing surface types in a somewhat general manner. Effectively the samples already discussed represent distinct types of surfaces, from which general conclusions may be drawn as to the effects such structured finishes will have on both photometric and colorimetric reflecting properties.

To attempt a more complete analysis of the light reflecting properties of any particular sample requires a more exact knowledge of the material involved and it was felt that some outstanding type of surface reflection should undergo such an investigation. Certainly, some of the most remarkable types of material to be found in nature are those whose reflected light is composed of various, differing iridescent colours. The effect is to produce a shimmering object whose surface depth is difficult to gauge, yet at the same time possesses a lustre reminiscent of a metallic finish, and whose slightest angular movement is readily discernable due to the immediate variation in reflected light.

Such specimens are far from rare and are extremely interesting since the combined effect of colour and texture is almost impossible to achieve in man-made materials, yet were it so would create a completely new

approach to colour finishing.

7.1 Structural Colours.

Fox (1953) defines the chief physical events which take place when light is incident on a material, those being reflection, refraction, scattering, diffraction, interference and absorption. In fact any, or all, of these may create some colouration in the object and such colours will be pigmentary or structural, or perhaps even a combination of both.

The pigmentary colours are of little interest in this particular section, and it is therefore important to differentiate between these and the structural colours.

Structural colours arise basically from the following causes:

1) The total reflection of white light from simple top surface reflections, or small disturbances and spaces within the material. The latter lead to either matt, chalky whites from such random disturbances, or glossy, pearly whites from regular arrangements.

2) The presence of 'Tyndall blues' due to scattering by small particles suspended in a fluid. The exact colour and intensity will depend on the particle size and relative refractive indices of the particles and the fluid. No angular change in colour is obtained on viewing, such colours being distinct therefore from the following types.

3) Iridescent colours from the interference by successive thin layers, these usually being thin plates or laminae separated by a medium of a different refractive

index. Such colours are dependent on viewing angle, the hue being determined by the relative thicknesses, while the degree of saturation and the lustre depend upon the number and uniformity of the constituent laminae.

4) Diffraction by fine striations, ridges or pits giving brilliant spectral flashes and colouration.

Finally the presence of a pigmentary colour and a differing structural colour would together form a new colour of a completely different hue.

To differentiate between such colours is relatively easy since chemical, pigmentary colours are little affected by physical investigations such as pressure, swelling or distortion, whereas structural colours, depending heavily as they do on minute exact dimensions, are altered enormously by this type of treatment. Pigmentary colours however are often affected by chemical solvents and bleaches, and usually may be so extracted. Visually, however, structural colours are easily distinguishable by their change of hue on varying angles of incidence and viewing, unlike their pigmentary counterparts.

Many examples of structural colours have been reported, in some cases quantitative work has been undertaken to support the proposed optical phenomena involved in the observed reflected light. Some of the earliest discussions on structural colours were those of Rayleigh (1919) and Rayleigh (1923), who argued that the cause of such colours be from optical phenomena and not from metallic like pigments. This was later quantitatively confirmed by Merritt (1925).

Sanders (1964), working on electron microscope photographs of precious opal, showed the colours to be produced by diffraction from a regular, three - dimensional structure of spherical particles of silica some 1500 to 4000 Å in diameter. It was shown that the longest diffracted wavelength possible was given by

$$\lambda_{max} = 2.37\ d$$

where d was the diameter of the spheres, and the corresponding shortest wavelength

$$\lambda_{min} = \lambda_{max} \sqrt{1 - 1/\mu^2} = 0.72\ \lambda_{max}$$

where μ is the refractive index of silica.

The effect of multilayer interference has been shown to be responsible for the striking reflection properties of certain beetles - Chrysochroa fulminans and Heterorrhina elegans - (Wright, 1967) where the colours range from a gold to a deep green, although the detailed physical structure of the material remains in doubt. Similar effects are extremely important in the blue-green colours in the 'eye' of the peacocks wing feathers and these too have been studied by the same author (Wright, 1964).

Some spectrophotometric measurements of such materials may only be done on a microscopic level, however, as in the case of Greenewalt et al (1960) in their work on hummingbird feathers. Here it was shown that the observed reflectance spectra of iridescent feather surfaces may be interpreted as interference spectra in reflection from platelets stacked seven to fifteen deep in the

barbules of the feathers and identifiable under an electron microscope.

The presence of such multilayer structures has also been reported in the tapetum lucidium of cats eyes and in certain species of butterflies (Miller et al, 1968), one explanation being that their role is to selectively reflect back to the receptors wavelengths pertinent to the animals behaviour and surroundings.

In the present work it was proposed to concentrate on one particular example - that of the South American Morpho butterfly.

7.2 The Morpho Butterfly.

Depending somewhat on the particular species of Morpho under test, the upper wing surfaces of the specimen, particularly the species menelaus, didius and cypris, exhibit a brilliant series of iridescent colours, from violet through blues to green, for various angles of viewing. This gives a marked lustre to the surface, very reminiscent of a metallic texture. The underside of the wing however is a fairly matt brown colour, both sides being illustrated in Plates 7.1 and 7.2.

The specimen has previously been colorimetrically studied (Wright, 1967; Wright, 1969; Pillai, 1968), although from the latter, quantitative programme no definite conclusions emerged, only that the probable cause of the major part of the colouration was multilayer interference with perhaps some addition from diffraction.

In the former work, Wright discusses the



Plate 7.1 General view of the upper wing surface - Morpho Menelaus.



Plate 7.2 General view of the lower wing surface - Morpho Menelaus.

possible links between the observed colour and interference phenomena with particular emphasis on the best photographs of the structure available at the time. However, it was not possible to specify the relative parts played by interference and diffraction, only to confirm that probably both had important roles in the entire reflection process.

Much has been written on the specimen since the original controversy as to whether the colours were structural or metallic like pigments, the latter view supported by Michelson (1911). Perhaps the most comprehensive and detailed of the early investigations were those of Mason (1927). He describes three distinct types of structure causing iridescence, the first being typified by the Uranidae, the second by the Morpho, and the third by the Entimus.

The work, carried out using optical microscope techniques, visual observation and liquid immersion techniques, is remarkably detailed, although, since the structure was beyond the limit of resolution of the available microscopes, no quantitative confirmation is available of the thin film interference suggestions put forward. However, since much of the observational material is extremely useful, further reference in more detail will be made in the next chapter.

The rest of this chapter will therefore be devoted to both the detailed colorimetric measurements undertaken, and also physical measurements that have been made in the light of the best available microscopic analysis of the material. The following chapter then attempts to correlate these findings in a more theoretical manner.

7.3 The Colorimetric Properties of Morpho Menelaus.

a) Visual Observation.

With such a specimen, whose range of reflected colours is so enormous and so angularly dependent, it is necessary to choose carefully the various measuring configurations in order to obtain the most useful information. Visual observation is thus extremely important and to this end the hemispherical viewer, described by Wright (1969) and illustrated in Figure 7.1, was utilised. A piece of wing, approximately 1 cm square, was mounted in the holder, and located at the centre of curvature of the white hemisphere. It may then be rotated about either a vertical or a horizontal axis.

The specimen was then illuminated by a beam of white light entering through a small hole at the centre of the hemisphere and along the axis of the apparatus. The reflected light from the wing material may then be viewed on the inner wall of the hemisphere and is illustrated in Plate 7.3.

A great dependence on rotation of the specimen was found and, in order therefore to simplify description of the particular angle of rotation, a convenient diagrammatic representation will be used throughout this, and the following, chapter. Reference to Figure 7.2 illustrates the four orthogonal positions of rotation of the wing material in the plane of the paper. The four positions, a, b, c and d, are related to the physical structure, described in the latter part of this chapter, in that the line inside the

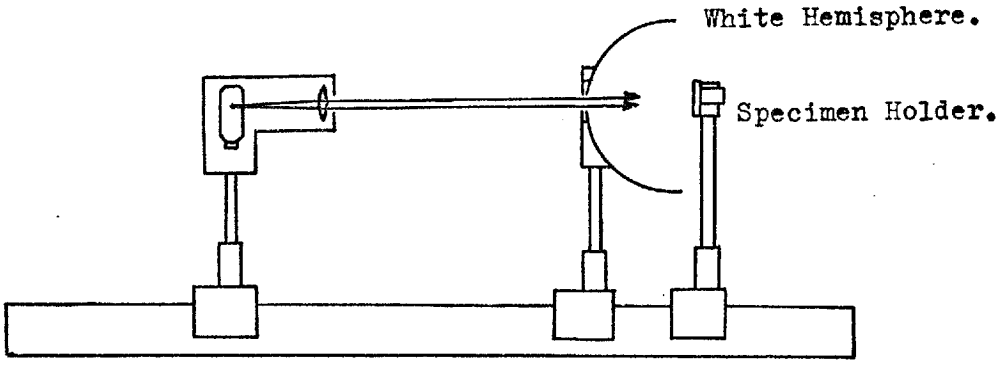


Fig. 7.1. The hemispherical viewer used in studying the polar distribution of reflected light from the Morpho butterfly. (Wright 1969).

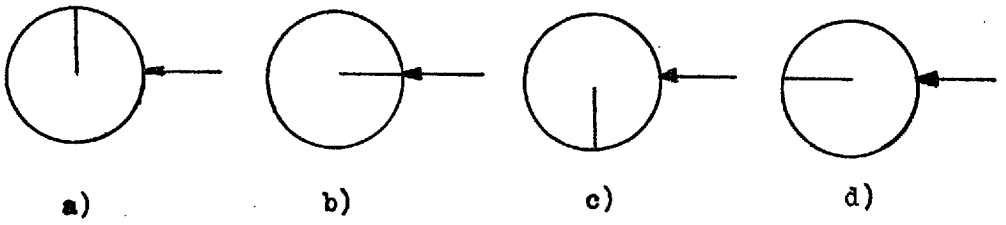


Fig. 7.2. The four possible orthogonal rotation positions of the Morpho sample holder.



Plate 7.3 The angularly reflected light pattern of Morpho Menelaus.

circle represents the direction of the top of the vertical ribs, the direction of the end of the scales being towards the centre point of the circle.

It is now possible to describe the reflected colours, in particular under four positions of rotation and two incident angles.

I) 0° Incidence.

i) Rotations a) and c) - a horizontal band of mainly blue-green reflected light, except at the extreme ends, say larger than 45° viewing, where it is blue-violet in colour. The band lies approximately 10° to 20° above or below the incident beam aperture depending on the particular rotation, above in the case a), below in case c). This would qualitatively agree with the spectral reflection curves quoted by Pillai (1968) at 0° incidence and various angles of collection, assuming this positioning of the sample.

ii) Rotations b) and d) - a similar band, except this time vertically positioned and again offset from the centre. The band in fact rotates with sample rotation.

II) 45° Incidence.

i) Rotations a) and c) - a horizontal band, passing almost through the centre point, blue-green in colour except at the extreme ends where it becomes a blue-violet.

ii) Rotations b) and d) - a vertical blue to blue- violet band at the specular angle, in the case of rotation d), fading into a blue-green colour at angles just less than the specular one.

In general, for positions b) and d), as the angle of incidence increases the colour at the specular angle

moves from a green at 0° to a violet-blue at 45°, and violet beyond.

It may be noted that the band of reflected light always lies at right angles to the rib direction.

b) Measured Spectral Reflection and Transmission Curves.

The colorimetric properties of the wing material are complex, and here the data from a reasonably comprehensive measuring programme on the species menelaus is given, which in turn is amplified in the following chapter with reference to any theoretical interpretation.

The measurements fall into two basic categories, those recorded on the Wright Spectrophotometer, which collects only a small solid angle of reflected flux, about a given angle of collection, and those obtained on a Beckman DK2 Ratio Recording Spectrophotometer (Cahn and Henderson, 1958). This instrument is an integrating spere instrument in which the angle of incidence is normal to the sample surface, and either all, or all the diffusely, reflected light is collected and monitored by means of a magnesium oxide coated integrating sphere and photomultiplier.

Since the colouration was assumed to be due to optical phenomena, results taken at the specular angle and other predetermined angles should be of great assistance in any detailed treatment of the reflection processes responsible. To this end the following data were obtained on the Wright Spectrophotometer.

Rotation is obviously extremely important in the reflection processes of the material, and therefore

a special sample holder was designed for the spectrophotometer. This enabled a circular piece of wing, some centimetre and a half in diameter, to be held taught between two circular metal rings, and the whole could then be rotated through 360° in the plane of the sample surface. The mount fixed on the normal kinematic slide in one of the apertures, whilst the reference - pressed magnesium oxide powder - was located in the other, under the same conditions. By making the rotating part of the holder ring shaped, no immediate backing layer was applied to the material, and therefore any reflections would be entirely due to the sample itself.

The wing material was difficult to mount, mainly due to its delicate, brittle and flaky nature, and since it was felt necessary to mount them as flat as possible many specimens were rejected. The four orthogonal positions a), b), c) and d) already mentioned were marked on the holder by simple microscopic investigation, and a final check by reflected light in the hemispherical viewer, so that a quick visible reference was available to the physical positioning of the sample.

The final monochromatic beam size in the spectrophotometer was reduced to some 5 mm square, the detector aperture restricted to a 5 mm vertical slit to reduce the angular spread, and the following spectral reflection curves measured as previously outlined.

A) Figures 7.3, 7.4, 7.5 and 7.6 illustrate the spectral reflection curves measured under conditions of 45° illumination and 45° viewing with respect to the physical surface

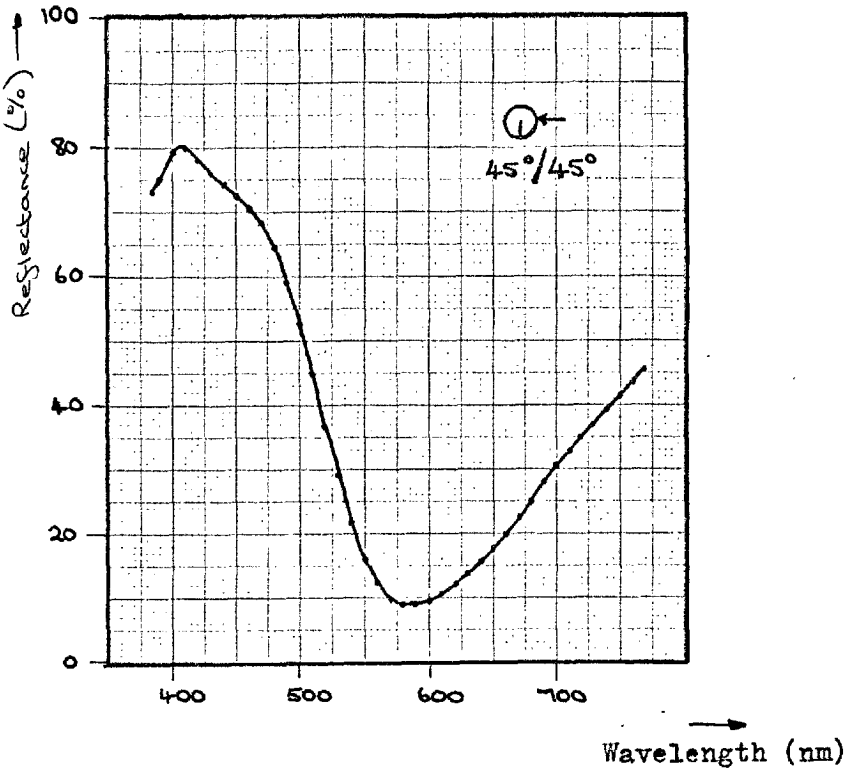


Fig. 7.3 Morpho Menelaus - Spectral reflectance curve for rotation c).

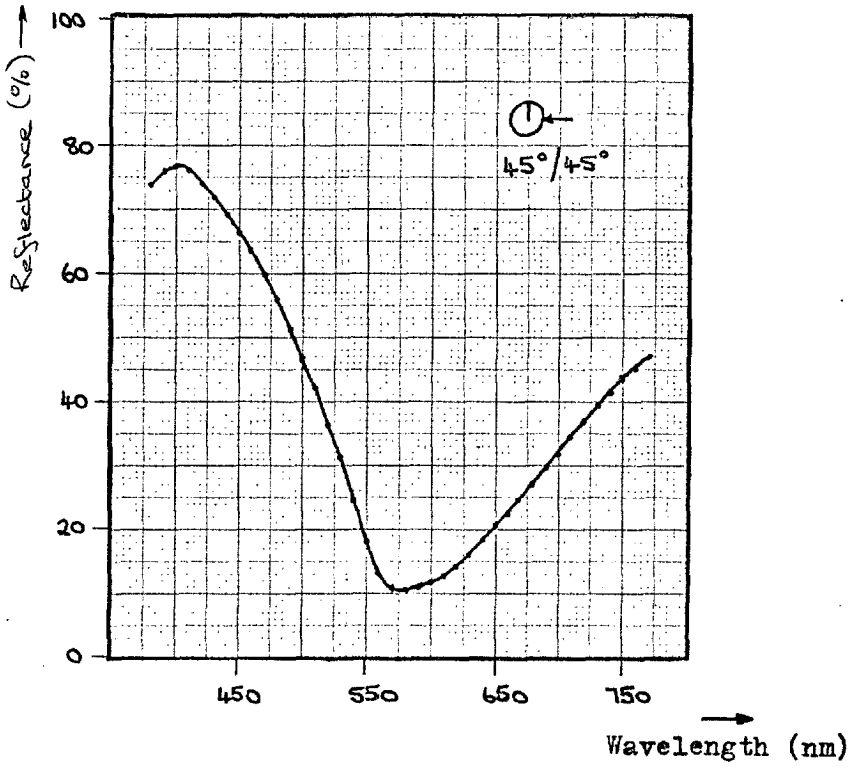


Fig. 7.4 Morpho Menelaus - Spectral reflectance curve for rotation a).

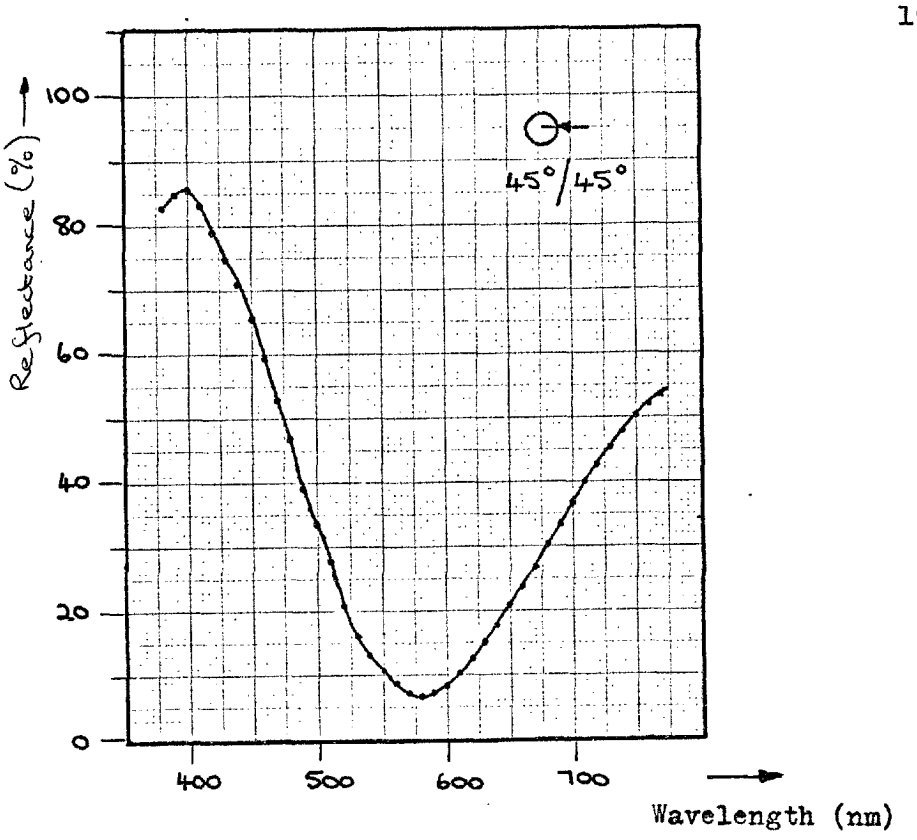


Fig.7.5 Morpho Menelaus - Spectral reflectance curve for rotation b).

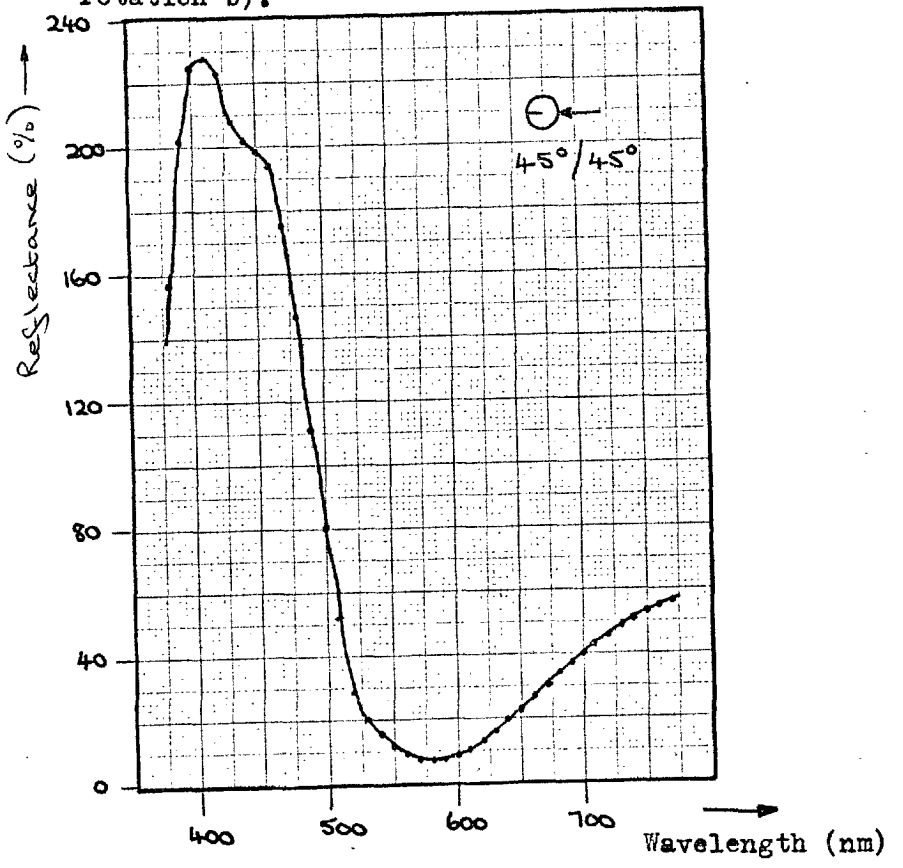


Fig. 7.6 Morpho Menelaus - Spectral reflectance curve for rotation d).

normal. All four curves were obtained at the same central point but at the four different stages of rotation as indicated on the figures.

The curves obtained are remarkably similar at all measured angles of rotation. A peak reflectance between 400 and 420nm falling sharply to a minimum just prior to 600nm and thence rising throughout the rest of the spectrum as far as 770nm. The curve everywhere is smooth with the possible exception of a slight bump at approximately 450nm. The one noticeable difference in the curves is the variation in reflectance value at any given wavelength. This is relatively small except in the case of rotation d), where a peak reflectance almost three times that of the others is observed. At, and beyond, the minimum point however, even this curve conforms to the approximate values of the others. This would possibly point to two independent agents, one responsible for the short wavelength peak, and one for the long wavelength rise. The latter being constant under any given measuring configuration, while the former is extremely dependent on angular rotation.

Intermediate positions of rotation were measured at fewer spectral points and confirmed the general shape at all of them, varying only in absolute value at the short wavelength end. Thus

$$\lambda_{max} \text{ at } 45^{\circ}/45^{\circ} = 400 \text{ to } 420\text{nm}.$$

B) The above measurements were then repeated at arbitrarily spaced points throughout portions of wing, selected from all

four main areas of wing surface on the insect. The data were obtained as those of Chapter 5. A selection of curves around the maximum point is illustrated in Figure 7.7.

The obtained data were again very similar to those previously given, except that a spread in maximum reflectance wavelength was noted from point to point, the extreme case peaking at almost 440nm. Thus it would appear that the exact wavelength distribution does vary somewhat from point to point, as might be expected with such a specimen. Nevertheless this variation is quite small, the general curve shape remaining unaltered above about 500nm, the values being almost identical. Large differences were again found in reflectance value. Thus overall

$$\lambda_{max} \text{ at } 45^{\circ}/45^{\circ} = 400 \text{ to } 440\text{nm}.$$

C) It has been stated earlier that a good deal of polarisation is present in the final monochromatic beam of the Wright instrument and in Chapter 3 a method is given to minimise the effect of this. Since it has been shown in that chapter that surface texture and structure may affect the measured reflectance when polarisation is present, and as it is reasonably likely that the structure of the Morpho wing is instrumental in its colour, it was felt that any such effects on the present results should be avoided where possible. To this end the course of action outlined in that chapter was employed and typical examples of the resulting spectral reflection curves are given in Figures 7.8 and 7.9.

It can be seen that since the curves are,

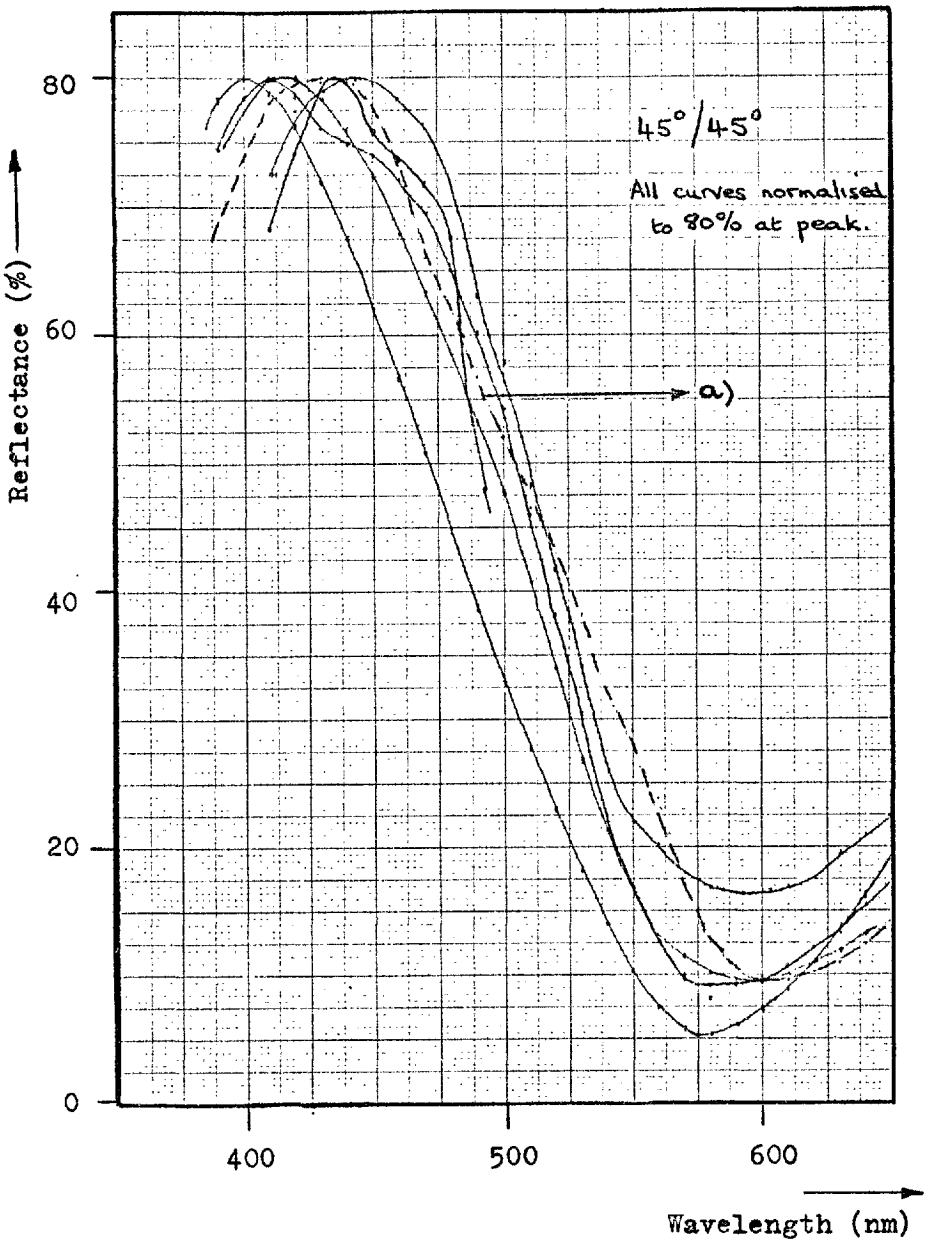


Fig. 7.7. Morpho Menelaus - Selection of spectral reflection curves at various locations over the wing surface, under conditions 45°/45°.

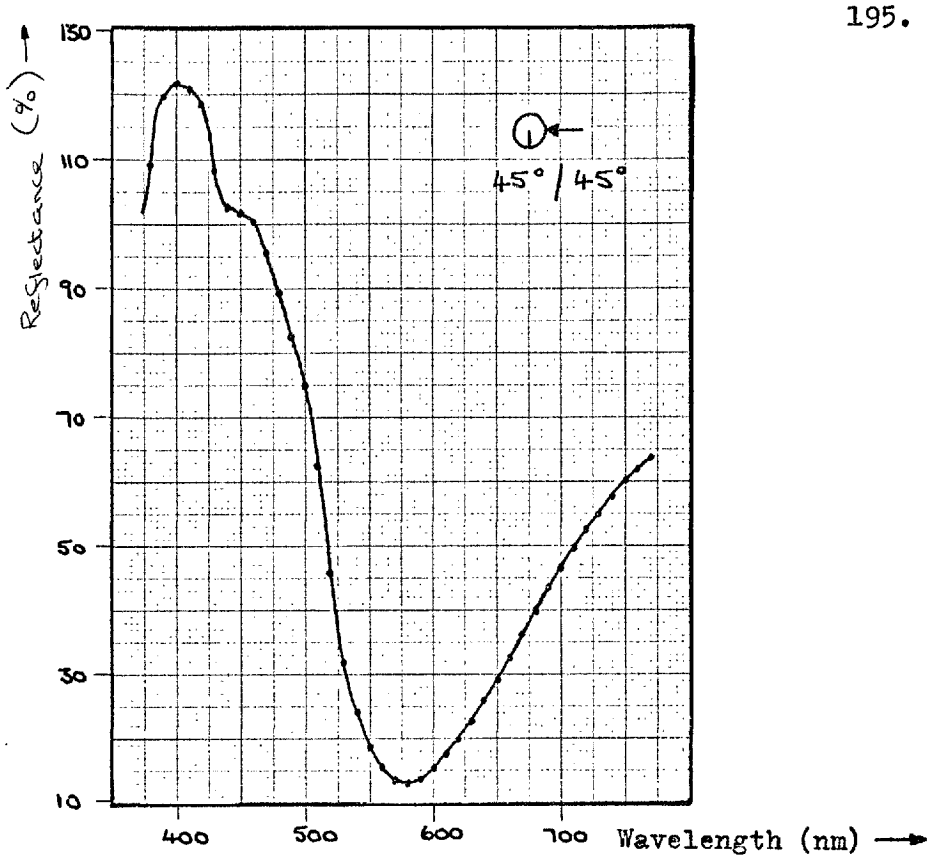


Fig. 7.8 Spectral reflectance for rotation c) with no polarisation present in the system. - Morpho Menelaus.

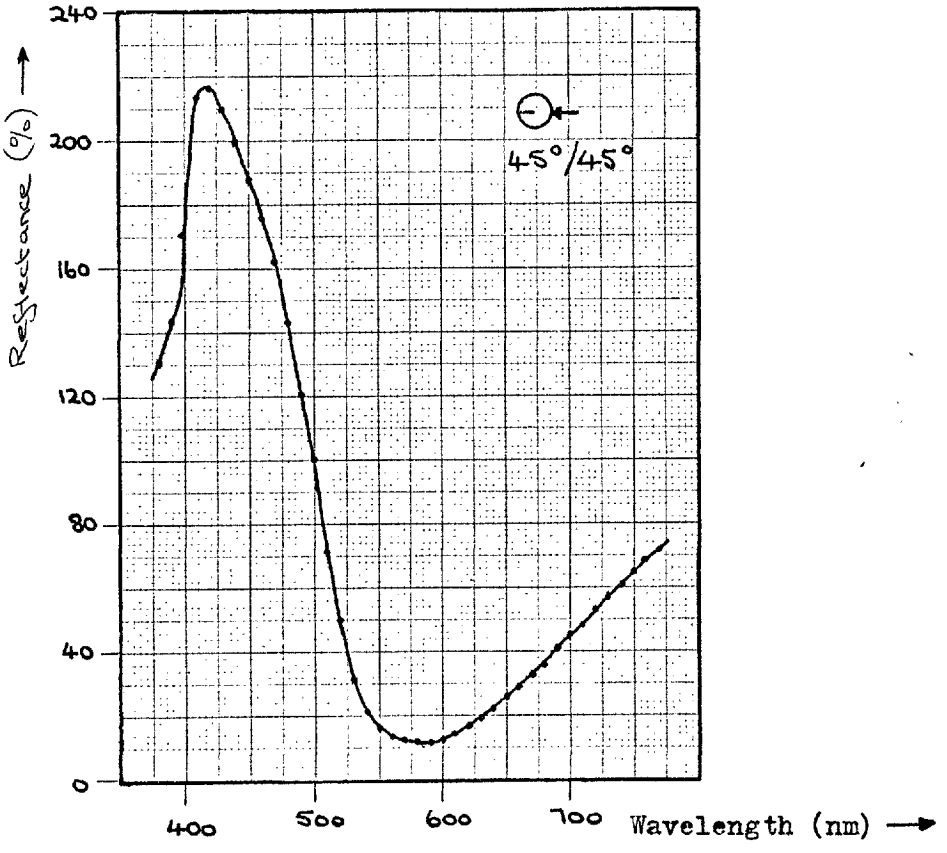


Fig.7.9 Spectral reflectance for rotation d) with no polarisation present in the system. - Morpho Menelaus.

within the spread already indicated, identical to those already given with polarisation present in the system, this appears to have little or no effect here on the spectral distribution of the resulting measurements.

D) To obtain the standard C.I.E. chromaticity coordinates for the material it is necessary to measure under the recommended configuration of normal incidence and 45^{o} collection to avoid as much specular reflection as possible. This was done at several different rotations, and also with all polarisation removed from the measuring system.

Figures 7.10 and 7.11 illustrate the resulting spectral reflectance for two of these particular rotations under $0^{o}/45^{o}$ measuring conditions, while Figures 7.12 and 7.13 represent the same data when all possible polarisation effects were removed.

The curves show a reflectance maximum at approximately 440nm to 445nm in the case of rotation c), and also a), falling via a small plateau at 490nm to a minimum at roughly 620nm and thereupon rising steadily towards the long wavelength end of the spectrum. Position d), and to a lesser degree position b) also, shows little response with only a small gradual rise at both extremes of the visible range.

The latter results would be expected bearing in mind the visual observations, since under this angular arrangement a vertical bar of reflected light was obtained just to either side of the incident beam, a considerable distance from the detector in these measurements. The results

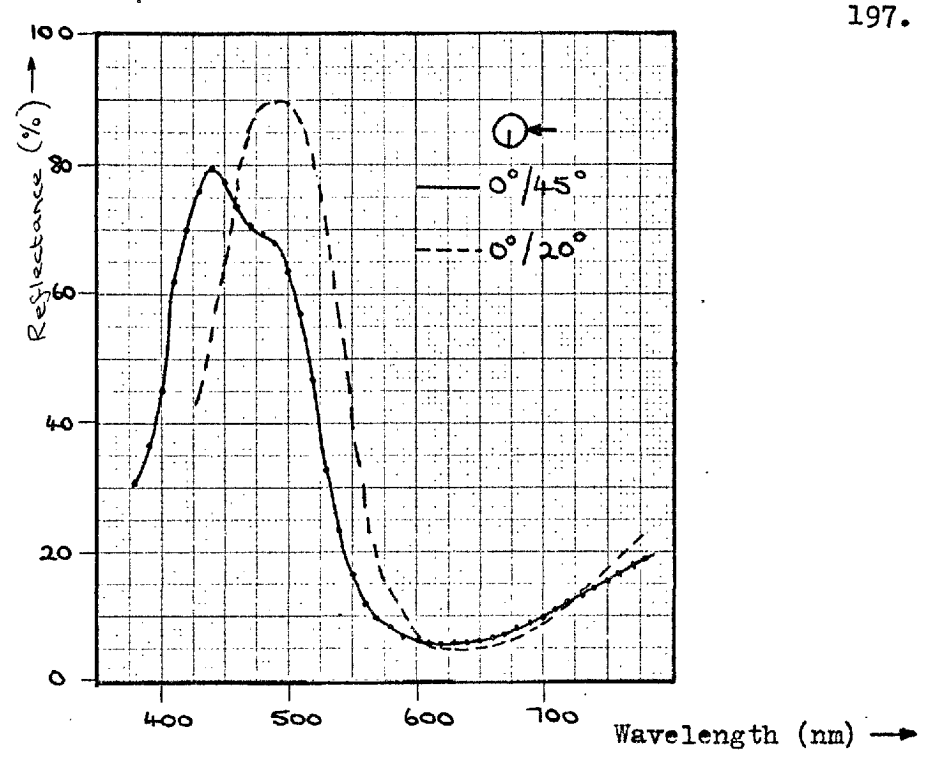


Fig.7.10. Morpho Menelaus - Spectral reflectance for rotation c) under conditions $0^{\circ}/45^{\circ}$.
(Dotted curve measured at $0^{\circ}/20^{\circ}$)

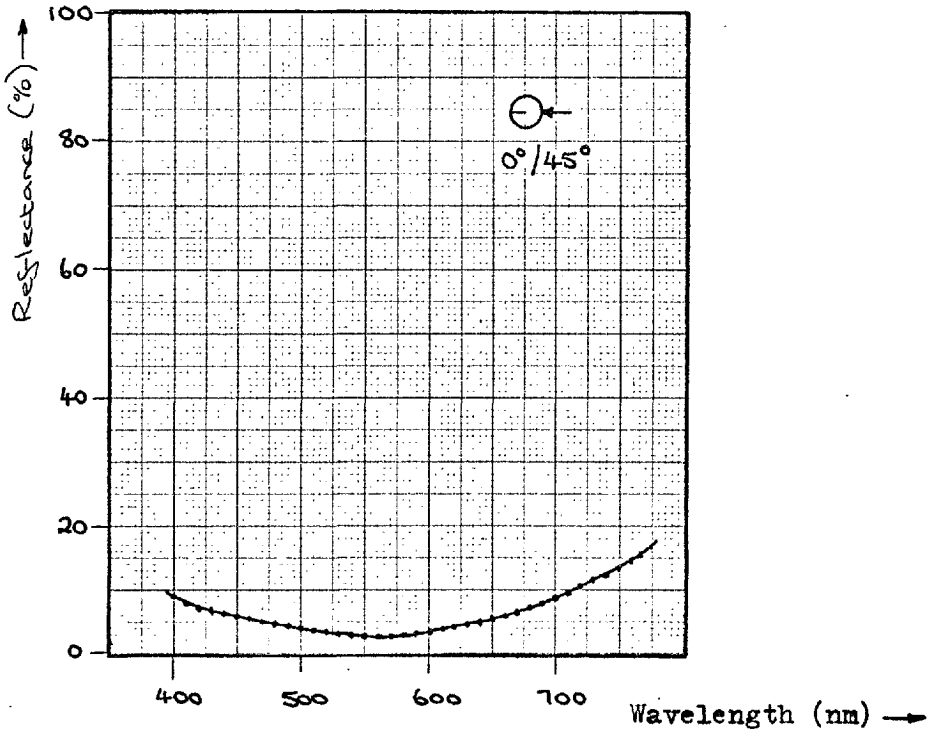


Fig. 7.11. Morpho Menelaus.- Spectral reflectance for rotation d)under conditions $0^{\circ}/45^{\circ}$.

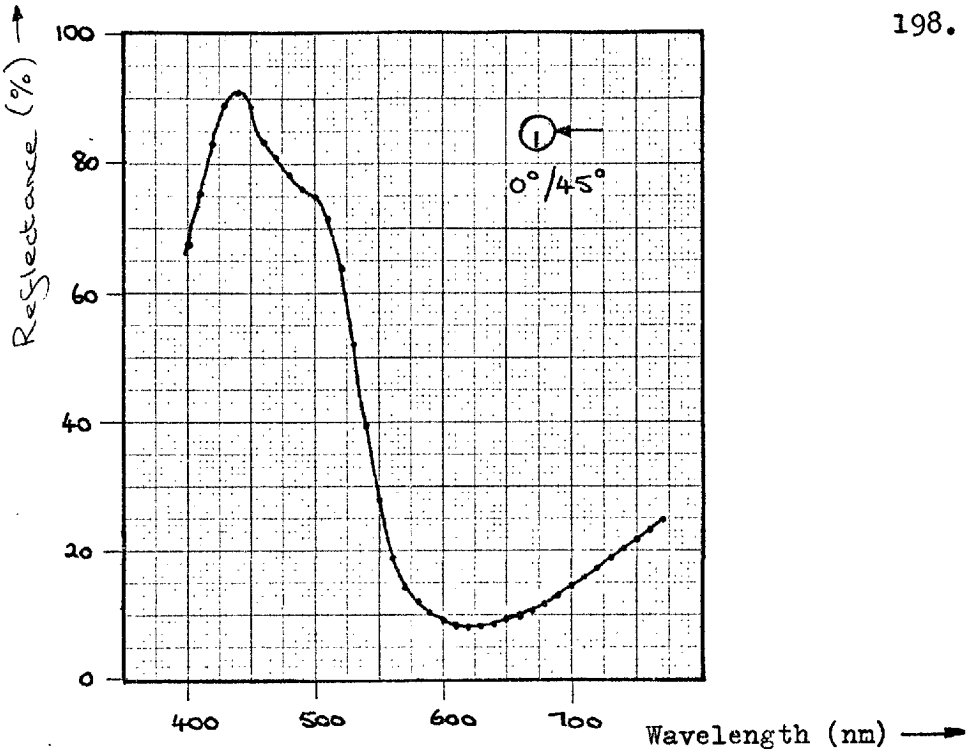


Fig.7.12. Morpho Menelaus - Spectral reflectance for rotation c) with no polarisation present in the system under conditions 0°/45°.

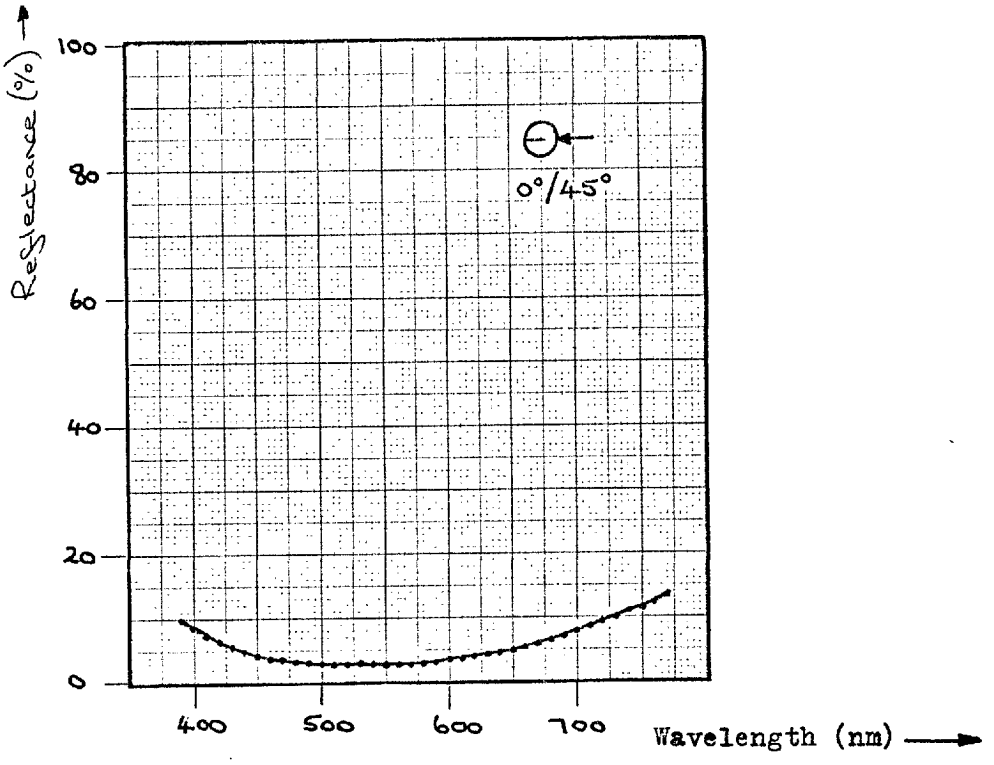


Fig.7.13. Morpho Menelaus - Spectral reflectance for rotation d) with no polarisarion present in the system under conditions 0°/45°.

do indicate however the spectral composition of the more diffusely reflected light at other angles.

Again little obvious difference is noticeable between the curves with or without polarisation present, except that is, for a small difference in overall level.

The chromaticity coordinates with respect to illuminant S_C, calculated from the data of Figure 7.10, were found to be

$$x = 0.1676 \qquad y = 0.1850$$

The figures are, in a sense, misleading however in such specimens, since angular conditions are critical. One might expect, for instance, a more greener hue if the viewing angle were reduced somewhat, from the earlier, visual observations. The identical data, except measured under $0^\circ/20^\circ$ conditions, have been dotted in over Figure 7.10, showing a peak at roughly 490nm and leading to chromaticity coordinates

$$x = 0.1717 \qquad y = 0.2770$$

a movement towards the greener part of the chromaticity diagram. The colour specification of such materials therefore is difficult, except under precisely defined angular conditions, and spectral curves will certainly be more instructive in these particular chapters.

E) The spectral transmission of the sample was similarly measured on the Wright instrument by positioning the detector in the 'straight through' position, directly behind the specimen. The importance of such results was felt to be with reference to any additional substrate material,

which would be in the path of whatever incident light penetrated the full depth of the upper structure.

The results proved difficult to obtain due to the very low levels involved, but are indicated in Figure 7.14. The wing therefore shows negligable transmission up to approximately 600nm, the wavelength where the main minima of the reflection spectra have almost always occurred, and beyond this rises gradually to under 1% at wavelengths longer than 740nm. Thus the material is, to all intents and purposes, opaque, except to the very longest visible wavelengths.

Further angular spectral data measured on the same instrument will be introduced in the next chapter. The remaining colorimetric data were obtained using the Beckman DK2 Spectrophotometer by integrated collection, since this will take reflection at all angles into account.

F) Two main possible modes of measurement are available on such an instrument, namely

i) total - where the specularly reflected beam is included in the integrated output,

and ii) diffuse - where this reflected beam is excluded.

The other important variable in this case is sample rotation. Figure 7.15 shows the spectral reflectance data replotted on a linear wavelength scale for two rotation positions at one location on the wing. Plot A gives the results for a typical rotation a) of the specimen when the scales are vertical, while B represents that of rotation b) when the scales are horizontal. Both were measured under

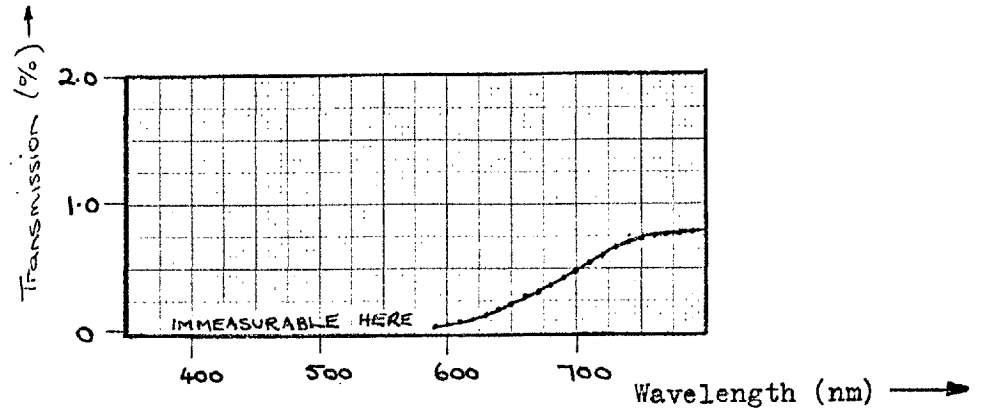


Fig. 7.14. Morpho Menelaus - Spectral transmission through the complete thickness of the wing structure.

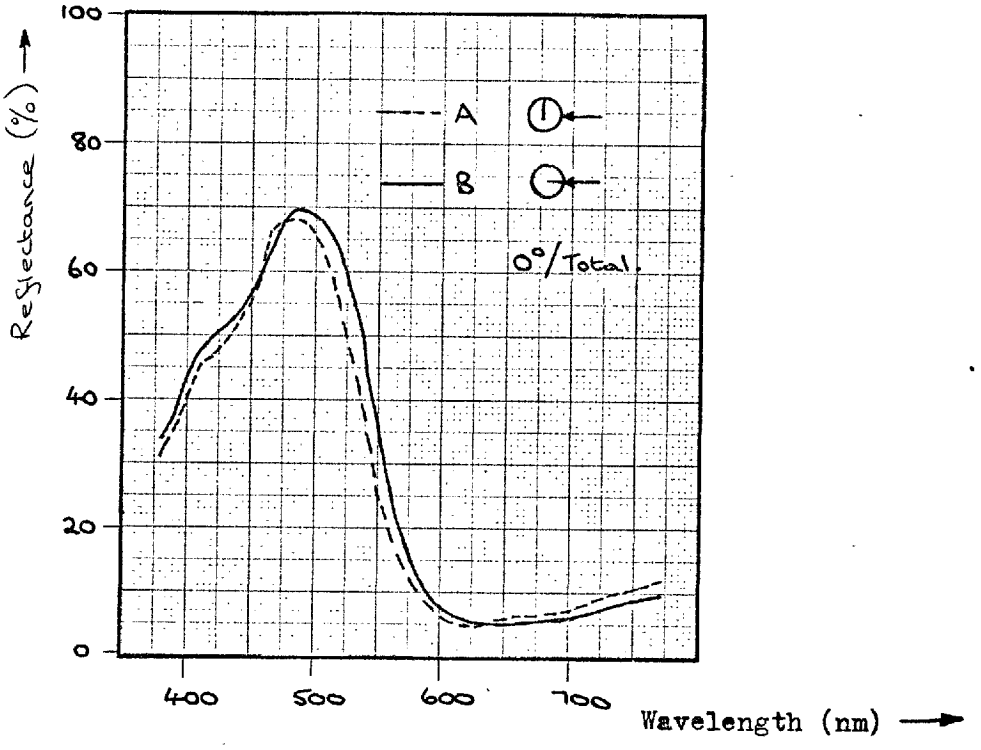


Fig 7.15. Morpho Menelaus - Spectral reflectance of wing material under two rotation conditions, a) and b), measured on Beckman DK2.

total collection conditions.

Figure 7.16 shows the effect of varying the mode of collection from one of total, plot C, to one of diffuse, plot D, at a different location on the sample under rotation condition a).

As might be expected, little variation in general shape is observable under any measuring condition, or, apparently, location. There is a fairly steep rise via a definite step at about 425nm to a broad maximum at approximately 480 to 490 nm. Thereafter the reflectance drops steeply to a minimum at 630nm and continues to rise beyond like the previous sets of data.

This illustrates the effect of including the reflected flux nearer normal to the sample surface which, it has already been established, is more green in colour. The peak shifts therefore to longer wavelengths, maximising at a value for this integrated flux almost equal to that under $0^{\circ}/20^{\circ}$ measuring conditions.

c) Discussion of Results.

Any detailed discussion of results will be left until the next chapter, however it is of interest at this stage to compare the preceding data with the only other available quantitative ones - those of Pillai (1968).

The particular species of Morpho measured is not named, although it is assumed to be menelaus and the spectral reflectance data taken at seven different viewing angles with normal illumination are indicated in Figure 7.17. A gradual peak movement towards longer

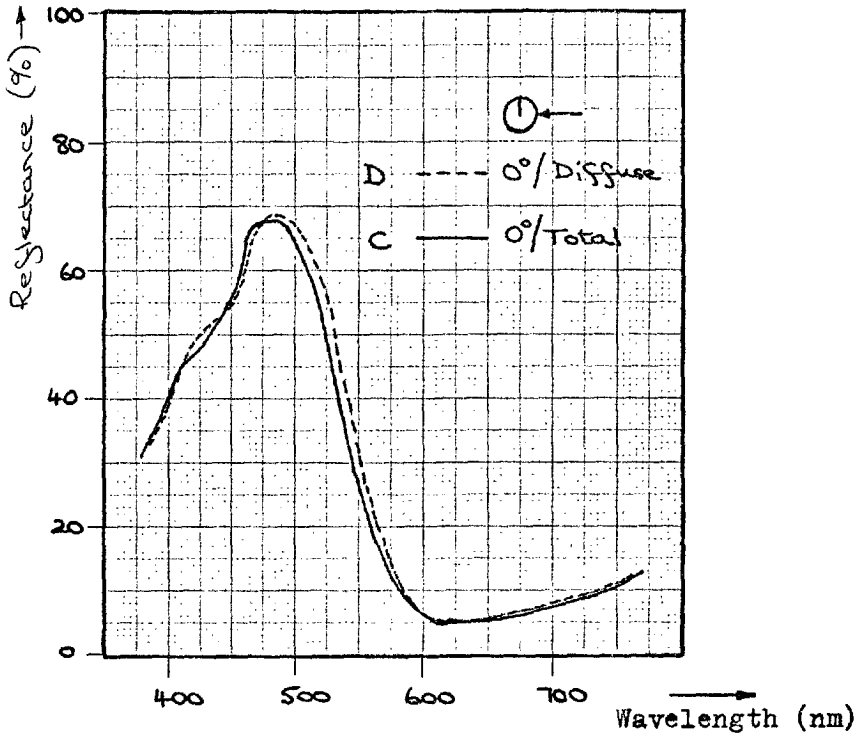


Fig. 7.16. Morpho Menelaus - Spectral reflectance of wing material under two different types of viewing, measured on Beckman DK2.

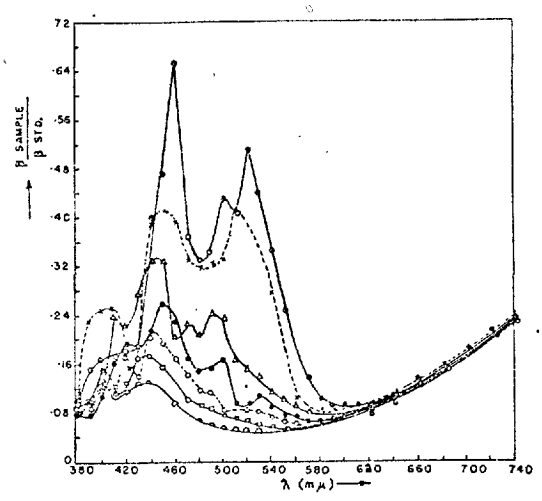


Fig. 7.17. Spectral reflectance curves of the Morpho butterfly wing taken at seven different angles of viewing (35° (•), 40° (+), 45° (Δ), 50° (⊙), 55° (○), 60° (□), and 70° (⌓)) with illumination along the normal. (Pillai 1968)

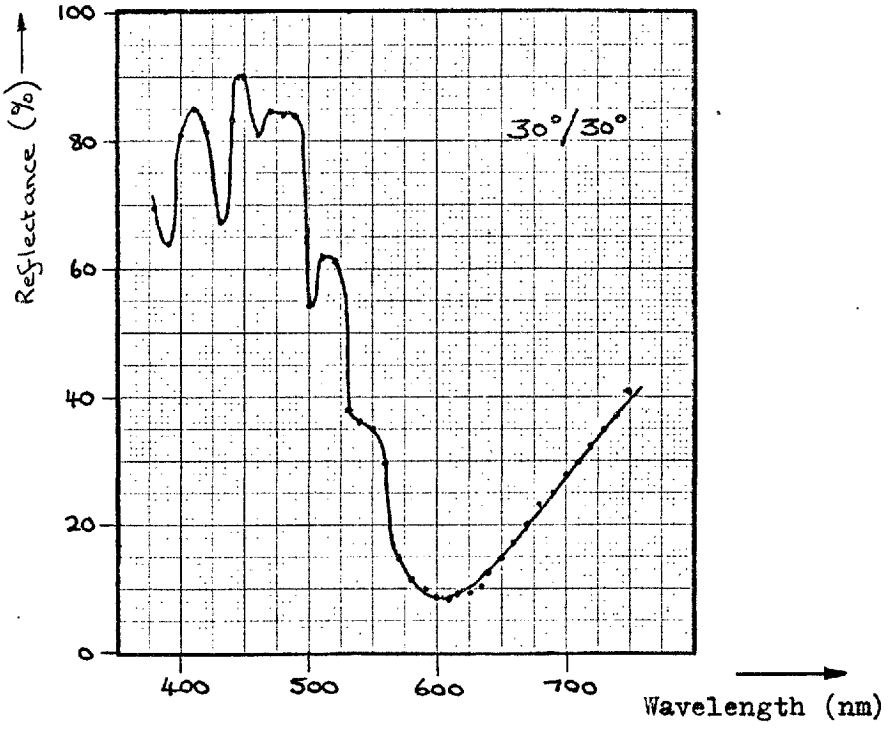


Fig. 7.18. Morpho Menelaus - Spectral reflectance when sample relocation is not exact, under conditions 30°/30°.

wavelength with decreasing viewing angle is readily discernable, a fact certainly borne out by earlier visual observation and also by those measurements taken at 45^{o} and 20^{o} viewing angles.

The absolute values of reflectance are unimportant as has already been discussed since this varies widely with location and rotation. No information is given by Pillai as to the physical orientation of the wing structure under measurement. This is extremely important and it is felt that such data must have been obtained at rotation positions close to c) or a), since the curve has been shown to be almost zero elsewhere.

All the curves of Figure 7.17 show a minimum about 600nm and thereafter a gradual rise to above 20% at the extreme long wavelength end of the spectrum. This is certainly found to be in good agreement with the earlier data of this chapter.

At wavelengths below 600nm however, the data of Pillai and those contained here show certain marked differences. A direct comparison may only be made for one curve, that measured under $0^{o}/45^{o}$ conditions, shown in Figures 7.9 and 7.11. Both sets of data show a peak reflectance at approximately 440nm and on this point are in excellent agreement. To either side of this peak however, Pillai reports secondary maxima of somewhat unpredictable magnitudes, whereas in the results obtained here only a small plateau was found at roughly 490nm, a position of one of the secondary maxima. Since both sets of data were obtained on identical instruments, using similar bandwidths etc., one

must look further for explanations of this difference, beyond measuring conditions.

It has been emphasised elsewhere in this thesis that particular care has been taken in redesigning the sample change lever that exact relocation of any point on the sample is possible, within close limits. The importance of this is indicated by reference to Figure 7.18, a reflectance curve measured at $30^{\circ}/30^{\circ}$ on Morpho menelaus before particular care was taken over exact relocation. It shows wide variations in reflectance for different wavelengths instead of the earlier, smooth curves, and may be compared directly with Figure 8.9 in the next chapter. This would be expected on a sample whose reflectance value changes rapidly and unpredictably with location. The latter fact is certainly appreciated by Pillai since different chromaticity coordinates were obtained at two different points. It is maintained therefore that the so-called secondary maxima of the published data are in fact due to poor sample relocation upon returning from the standard magnesium oxide surface, and as such must be ignored.

This should not be expected to occur at the longer wavelengths since very little variation with either location or measuring configuration has been found here, and this is borne out by reference to Figure 7.17. Under certain conditions it was in fact found necessary to measure first the standard throughout the whole spectral range, followed by the specimen, and again the standard, in order that exact location was maintained. Despite the errors inherent in such a method, due mainly to drifting in the

electronics etc., such results often proved more acceptable on such a sample than the more conventional comparison method.

Apart from this the chromaticity coordinates show reasonable agreement, bearing in mind the variable nature of the material.

7.4 The Physical Properties of the Morpho Butterfly Wing.

Early workers, who believed the striking colours of the Morpho butterfly to be due to optical phenomena rather than pigments, attempted to discover the wing structure, which caused this, by optical microscope studies. Descriptions by Rayleigh (1923), Mason (1927) and others show how much it is possible to discover by these means, results which have been confirmed using a good quality microscope.

The first really detailed treatment of optical microscope studies is that of Mason (1927) who studied many insects, dividing them into three distinct groups. In the case of Morpho, and in particular the species menelaus, he found plane scales lying close to the wing 'like shingles on a roof'. Standing up like vanes upon these scales, he found longitudinal striae 2000 to 3000nm high, separated by less than 1000nm. He also proposed a tilting of the reflecting portion of these vanes to accomodate the angular discrepancies found in specular reflection, this tilting being down towards the root of the scale. Two types of scale are identified - namely outer transparent ones, and under these, further scales of basically the same

construction.

Little or no advance in these remarkably detailed findings was made until the advent of the electron microscope. Anderson and Richards (1942) published photographs of the wing structure of Morpho cypris from a transmission electron microscope which showed far more detail. Figure 7.19 shows the structure of the vanes as deduced from these studies. They found considerable variation in the size of the detailed structure from point to point on the wing, and also found two distinct types of scale - non-iridescent and iridescent - as did Mason.

Each of the vertical vanes was found to have several horizontal mullions, in the case of the iridescent scales twelve from top to bottom of the vane, and for the non-iridescent scales a lesser number. Figure 7.19 illustrates in detail how these were assumed to be arranged, connected to the base of the wing by many 'Y' shaped structures.

Due to the roughness of the upper surface of the vanes it was assumed that the horizontal mullions were inclined to the base, similar to the proposal of Mason, and that the thickness of these mullions, which was finite, increased on approaching the lower ones in the stack. The spacing between such horizontal components was determined to be of the order of 125nm.

A further interesting fact emerged from this work. All previous workers had assumed the material which formed the structure to be chitin, a commonly occurring material, forming the basis of many substances found in nature. Although much evidence had been put forward earlier

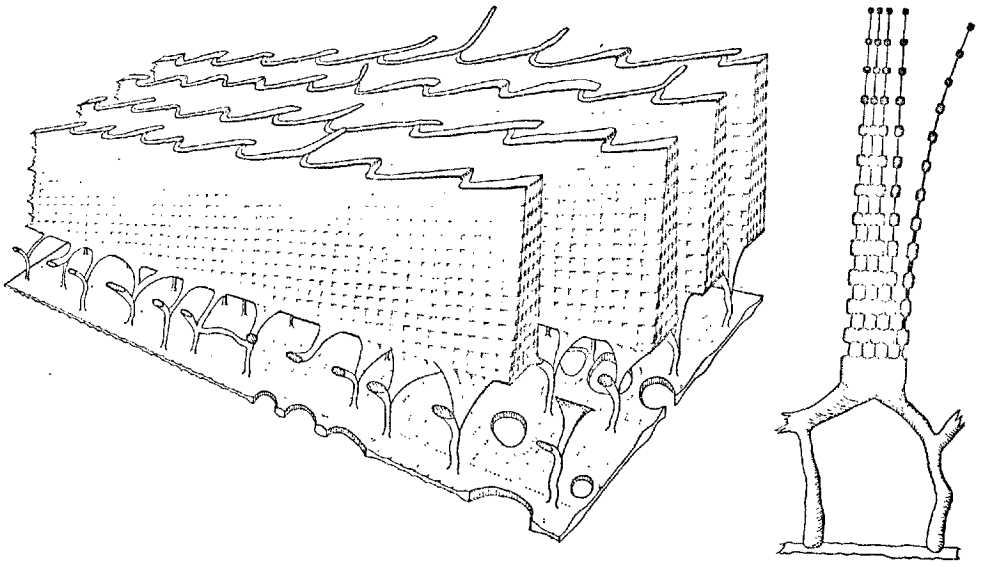


Fig. 7.19. A schematic and idealized reconstruction of a small portion of an iridescent scale. On the right is a cross section of one rib. Morpho cypris. (Anderson and Richards 1942)

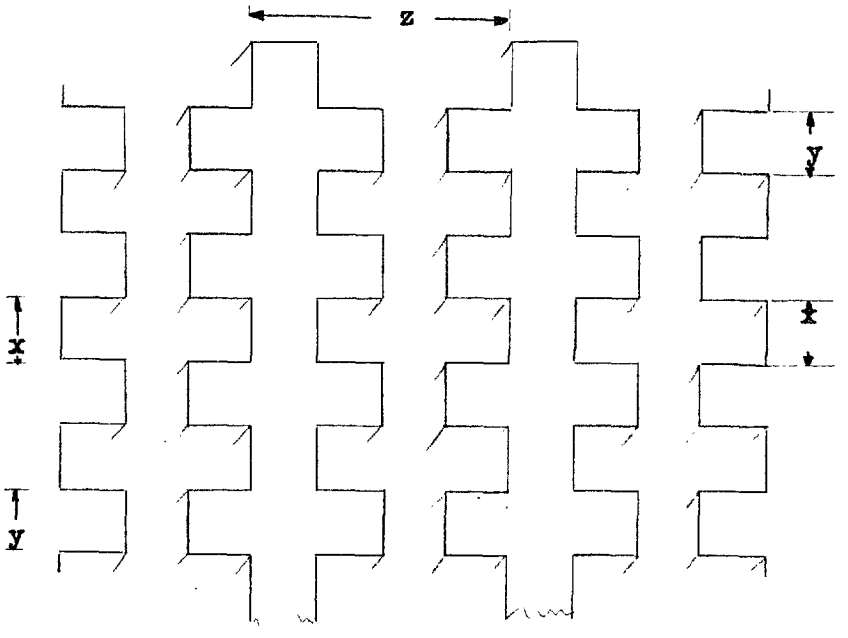


Fig. 7.20. Proposed schematic representation of cross section of genus Morpho wing scales from the photographs of Martin. Two main vertical ribs are shown together with horizontal plates.

to support this, Anderson and Richards feel the material not to be chitin since it completely disintegrated in concentrated KOH in several hours at 160°C, and similarly in NaOH. The exact material is left unknown, however they do suggest it may be composed of certain proteins.

Such was the state of knowledge up to very recently. Martin (1971), in some studies of iridescent materials, covered, amongst other butterflies, the genus Morpho, using a scanning electron microscope. In particular the species menelaus and cypris.

In such work the specimen preparation is difficult, yet critical, and a few of the results of this study are shown in Plates 7.4 to 7.9 inclusive.

Plate 7.4 - This illustrates a general view of the iridescent blue scales of the menelaus overlayed by the top layer of transparent scales, at a magnification of 947 times. The construction of the individual scales is readily discernable, the transparent ones being coarse open structures, while the blue scales consist of fine longitudinal vanes.

Plate 7.5 - At a magnification of 2.07K the tops of the longitudinal vanes are clearly to be seen, in this case for Morpho cypris, showing a remarkably regular series of bands, ending somewhat irregularly at the end of the scale.

Plate 7.6 - This shows a section through the blue scale, the longitudinal vanes disappearing into the photograph. Distortion in these vanes due to the method of sectioning the specimen apparently causes the irregular wavy effect. The photograph, cypris in this case, clearly shows the horizontal substructure of these vanes at a magnification

of 9.3K. Each one therefore consists of a pile of horizontal plates running lengthwise, joined together by a central upright structure. The whole is supported by a forest of connecting branches down to the base, similar to those described by Anderson and Richards. It is believed that this is the positioning of the dark, absorbing pigment, melanin, which is known to exist in the wing.

Plate 7.7 - At right angles to the last photograph, and at a magnification of 19.1K, one obtains in the foreground a side view of these horizontal plates, apparently joined by a small ribbing structure. The plates slope at an angle of approximately 10^{o} to the base as predicted by other workers. Wherever one ends however another begins on top of the vane, thus keeping the total number constant. The subject here is menelaus.

Plate 7.8 - At a magnification of 39K, the menelaus illustrates in detail the construction of the plates. Comparison of this and the final plate show the important difference between the two species, menelaus and cypris, namely the total number of horizontal plates contained on one longitudinal vane. In the case of the menelaus this number is eight, while in the case of cypris it is twelve, again in agreement with Anderson and Richards.

Plate 7.9 - The cypris clearly shows the twelve horizontal plates and also the tendency for the structure to be wider at the base than at the tip of the vane. At a magnification of 21.6K the supporting structure is also clearly visible.

From these and other such excellent photographs it is possible to obtain the dimensions of the detailed structure, and also to know exactly its shape,



Plate 7.4 Morpho Menelaus - General view of the upper wing surface, showing blue scales overlayed by transparent ones. (x947)

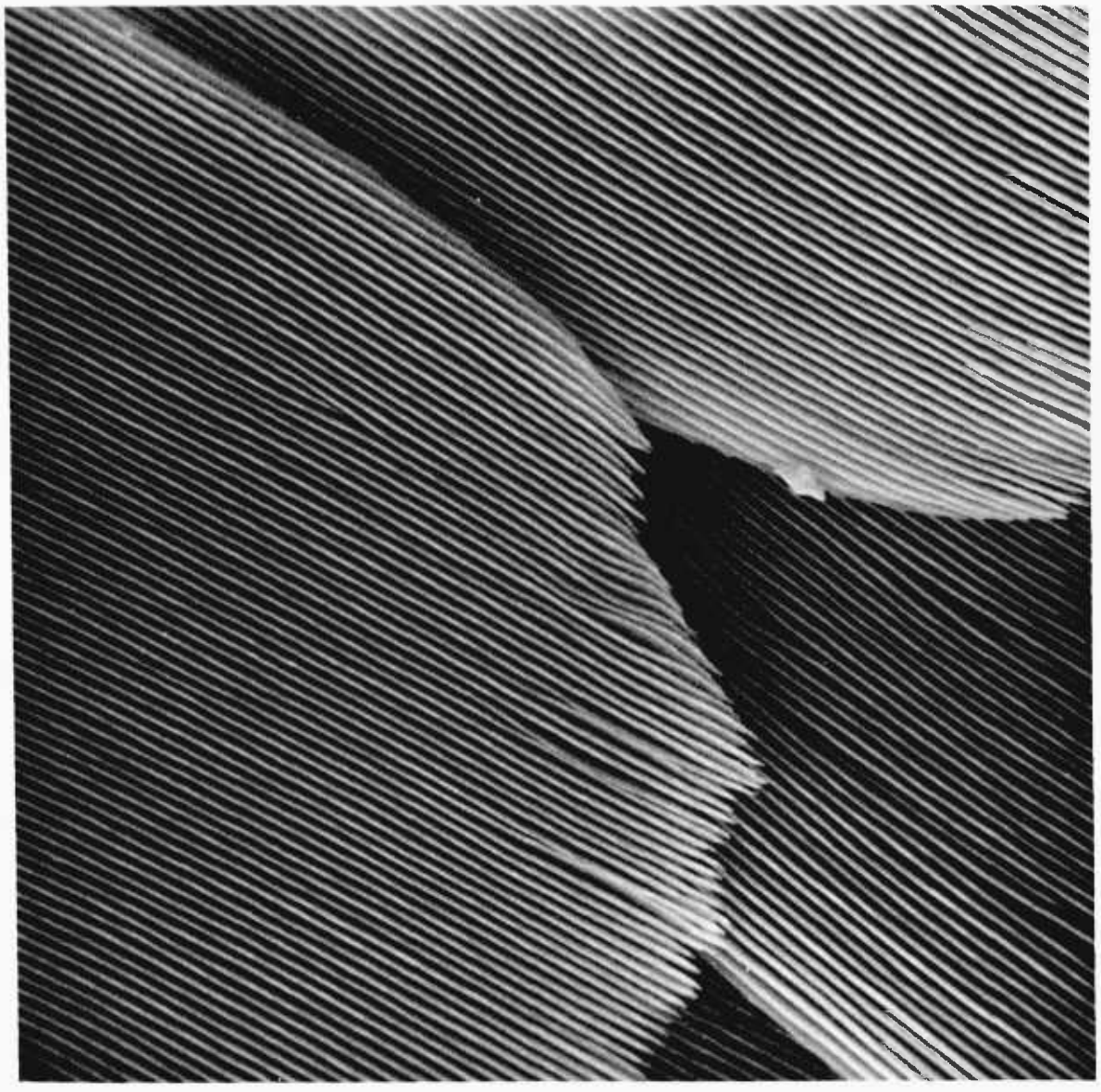


Plate 7.5 Morpho Cypris - Enlarged view of the surface of the blue scales. (x2.07K)

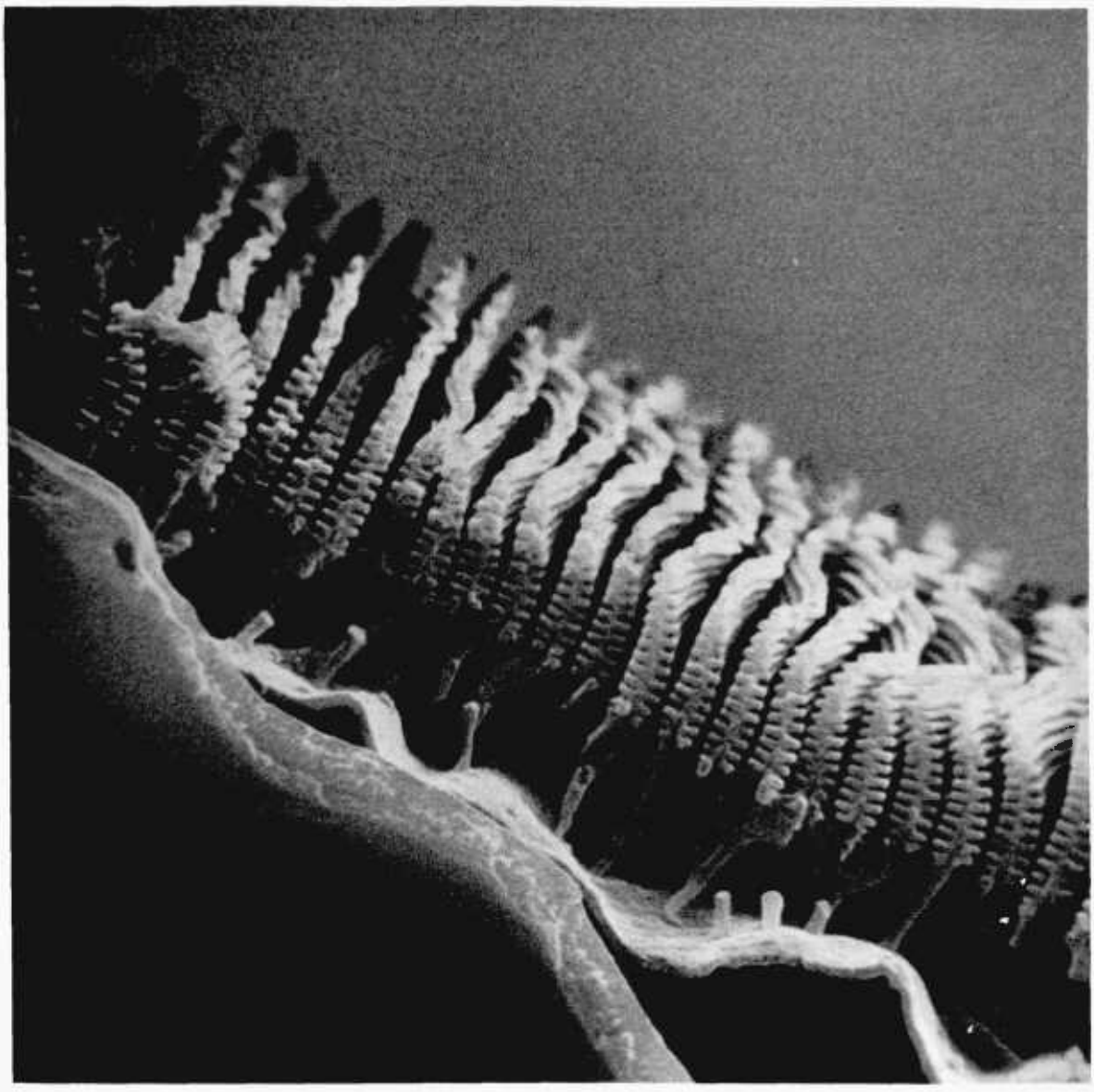


Plate 7.6 Morpho Cypris - Cross section through blue scales.
(x9.3K)

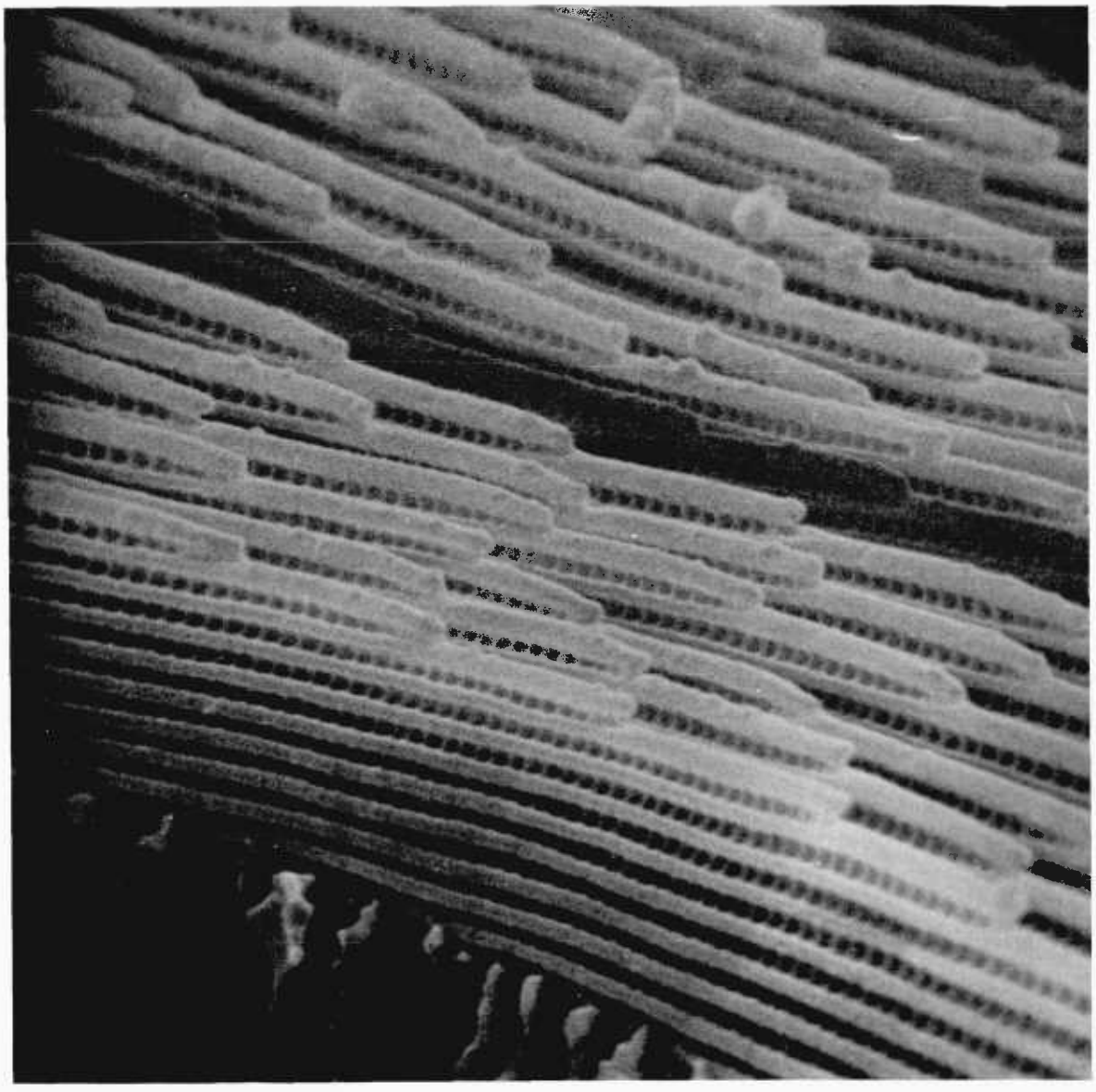


Plate 7.7 Morpho Menelaus - The side structure of the vertical ribs on the blue scale. (x19.1K)

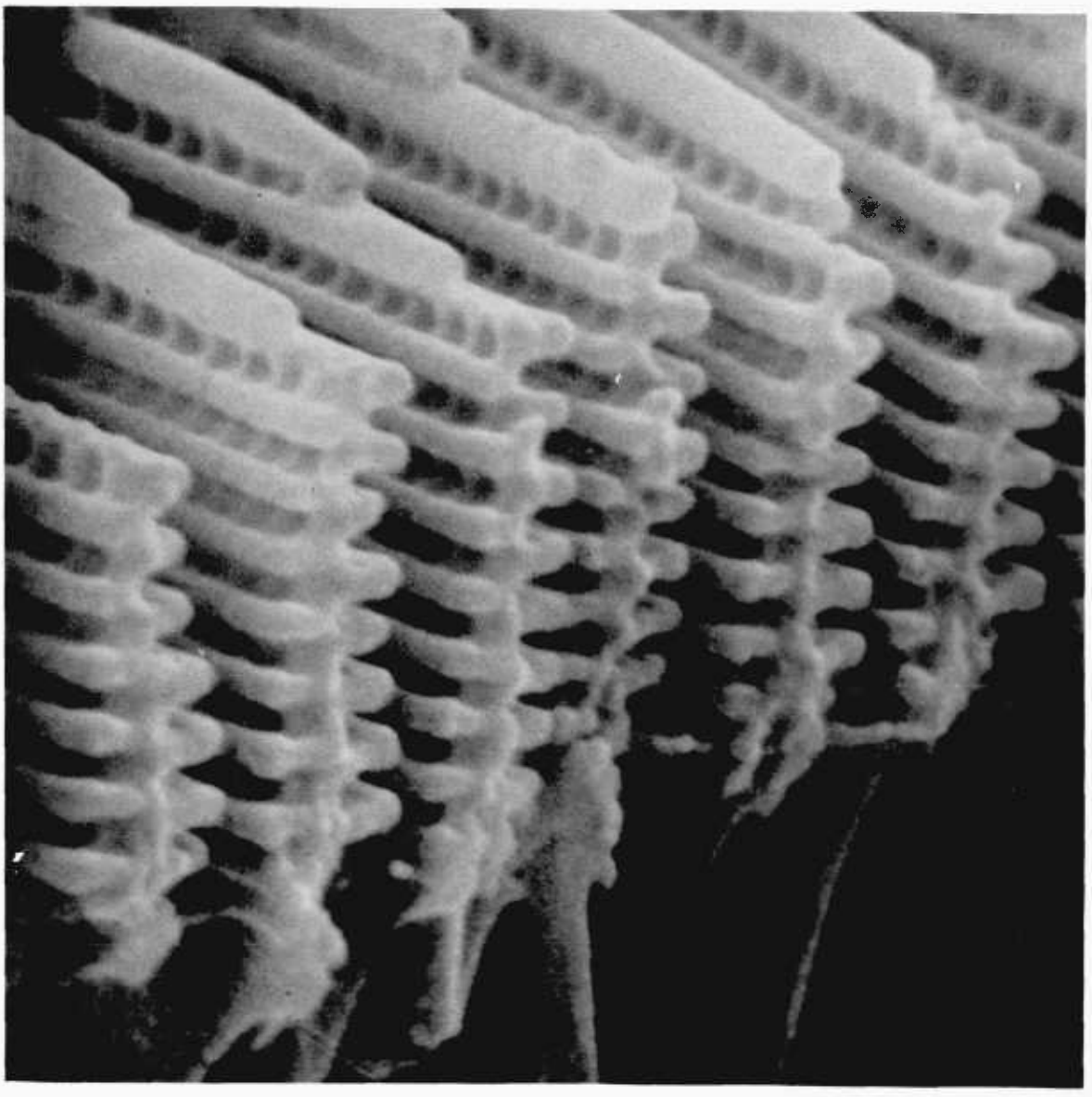


Plate 7.8 Morpho Menelaus - Enlarged cross section through a blue scale. (x39K)

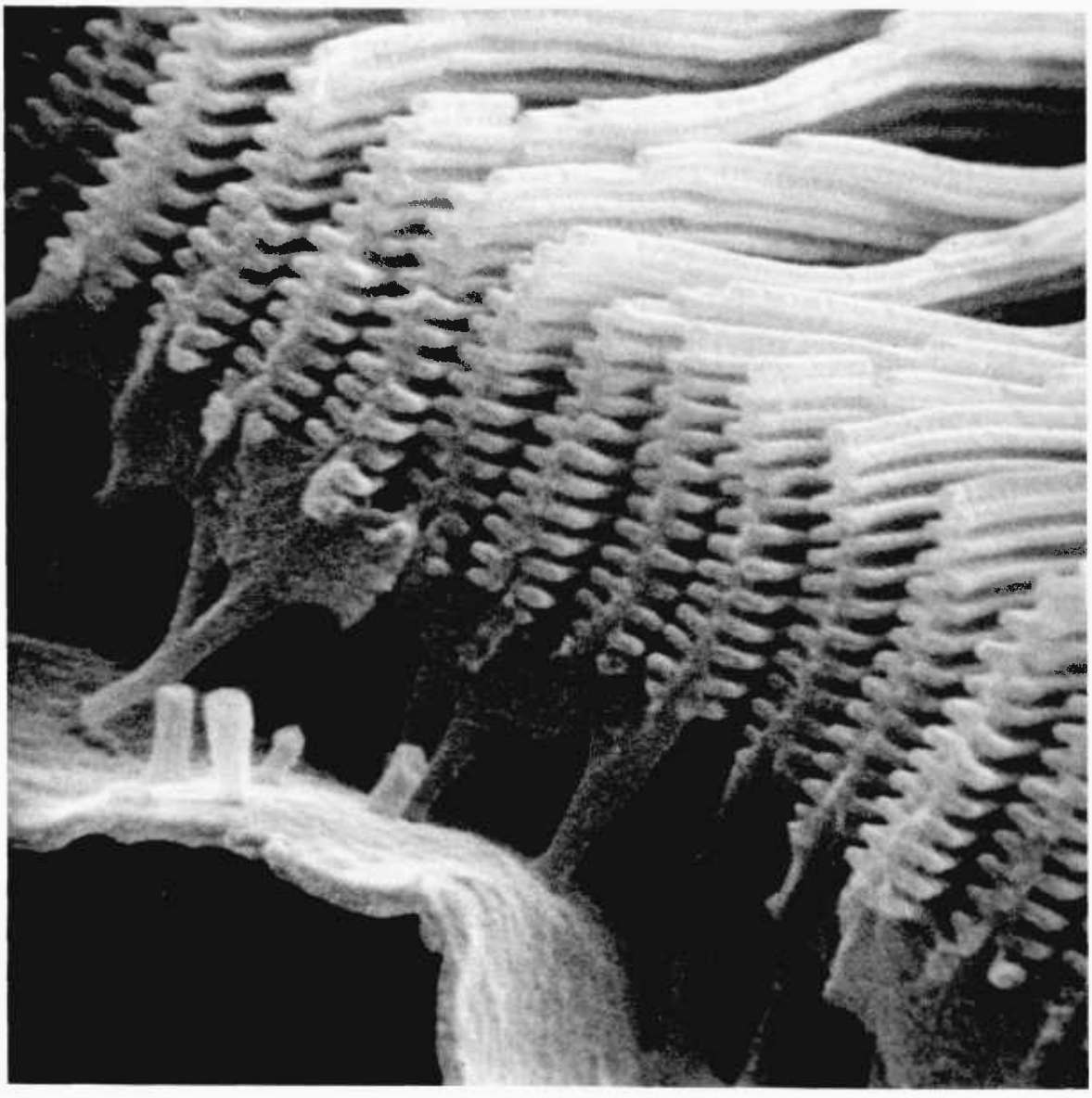


Plate 7.9 Morpho Cypris - Enlarged cross section through a blue scale. (x21.6K)

within of course the limits of the microscope.

Such measurements have been made, and by reference to the somewhat idealised structure of Figure 7.20 the relevant averaged dimensions for Morpho menelaus are:-

$$x = 97\text{nm}$$

$$y = 126\text{nm}$$

$$z = 840\text{nm}$$

The spread in such results is appreciable, partly, no doubt, to the difficulty in assessing the exact boundary between the plates and spaces accurately, but also to the natural variations which are definitely present in the structure.

The standard deviation in these values, obtained from many measurements on two particular photographs, follows below and is typical.

	σ_x	σ_y
Photograph 1	4.1 nm	5.6 nm
Photograph 2	6.8 nm	2.6 nm

What, however, is in less doubt is the unit spacing, or the quantity

$$\sum = x + y$$

since borders are of less importance here.

This quantity seems fairly certain to be of the order of 223nm, however, the problem is discussed further in the following chapter.

Thus the chapter has established the main colorimetric data regarding the material and in the latter part the relevant data concerning its structural shape.

CHAPTER EIGHT.

THEORETICAL INTERPRETATIONS OF THE MORPHO WING STRUCTURE.

It is now necessary to use the extremely detailed knowledge of the wing structure of the Morpho butterfly to interpret and explain the spectral reflectance results obtained in the earlier part of the previous chapter.

Originally the colours were held to be metallic like pigments, however several authors, such as Rayleigh (1919) and Mason (1927), with very detailed reasoning, supported the theory of some type of optical phenomenom, the most likely being some type of multilayer interference or diffraction process. The latter author argued strongly in favour of the interference approach, but all were unable to give definite, quantitative proof since the structure was not resolvable by the optical means at their disposal.

Following the electron microscope photographs of Anderson and Richards (1942) some tentative suggestions were made as to thin layer interference being responsible, but since the structures were only partially identifiable later workers such as Pillai (1968) were still unable to give quantitative proof of this, or the extent to which other optical effects had any bearing.

It is felt however that the photographs obtained by Martin (1971) do in fact show sufficient detail of the fine structure to make a mathematical analysis possible.

8.1 The Case for a Multilayer Interference Approach.

It must be first mentioned that the colours are definitely structural in nature, rather than pigmentary, the colour being maintained down to the individual scale or even vane (Mason, 1927). The material, on being tested by the methods outlined in the previous chapter for determining this difference, leaves no doubt that pigments, other than the base layer of melanin, could not be responsible for the observed colours.

Many factors point to a multilayer interference explanation - certainly the reflections are specular, and the reflected light intensity is high, reminiscent of a many layered stack. The change of hue on increasing the angle of incidence, towards the short wavelength end of the spectrum, is further evidence, and the action of chemical swelling agents and liquids penetrating the structure qualitatively supports such ideas. The effects of physically distorting the structure, polarisation properties and small localised variations all lend weight to such evidence.

Diffraction effects must not be completely ignored. It was earlier stated that a band of reflected light, normal to the longitudinal vanes, is obtained on illumination by collimated light. This immediately suggests a diffraction process also taking place, but in detail two major difficulties are evident. The fact that the incident light may be incident at right angles, or along the striations, and directional, or diffuse, in nature is difficult to reconcile with a diffraction effect, while the order of reflected colours is also incorrect for such a theory. It

has been shown earlier that a violet-blue colour is obtained at the extreme ends of the reflected light, while blue-green colours occupy the centre of the band. This will be mentioned again later.

Thus the evidence seems strong for some type of interference being responsible for the striking colouration, a fact which is further emphasised by reference to the photographs of the previous chapter, showing such regular plates to be responsible for the fine structure of the vertical vanes.

8.2 Determination of the Parameters.

Only the species menelaus will be considered in detail here since it is assumed other species will act likewise by the similarity of construction.

Certain simplifying assumptions are obviously essential in such a complex structure. It is first assumed therefore that the horizontal plates, which make up the substructure of the vertical vanes in Plates 7.6, 7.7, 7.8 and 7.9 of the previous chapter, are continuous in a horizontal plane with no vertical gaps between the striations. This certainly is reasonable since the existing gap is small with respect to the width of any given plate, especially towards the bottom of the stack. At the top, the stacks tend to taper somewhat.

The detailed theory of thin film interference is given in the Appendix, it is sufficient here however to simplify this process in order to ascertain some variables. Undoubtably the most important part of the obtained reflection

curves at 45^{o} incidence and collection is the peak in the blue. The long wavelength end appears to be independent of this part of the curve and due to some other mechanism. This being so, and assuming we ascribe this peak reflectance to a horizontally, infinitely wide multilayer stack of alternately wing material and air, some preliminary calculation allows us more easily to derive the entire theoretical reflection curve.

In Figure 8.1 a basic unit of such a construction is shown - that of a horizontal plate of wing material, followed by a layer of air. Evidence that the gaps are in fact air gaps is fairly strong, since penetration by various liquids, thus changing the reflected colours, is always followed by a gradual restoration of the exact, original colour on evaporation of the liquid. Similarly, the horizontal plates may be crushed up on top of one another by pressure or swollen by particular fluids. When immersed in a liquid, pressure applied to empty scales forces air out of the interior and bubbles may be seen in the surrounding liquid.

The path difference between light reflected specularly at an angle i to the top surface normal and light emerging likewise at an angle i, having been reflected from the second layer of high refractive index material will be given by

$$P.D. = (CE + EF + FD + DB) - AC$$

and the optical path difference

$$O.P.D. = \frac{2ny}{\cos r} + \frac{2x}{\cos i} - (2y.\tan r + 2x.\tan i).\sin i$$

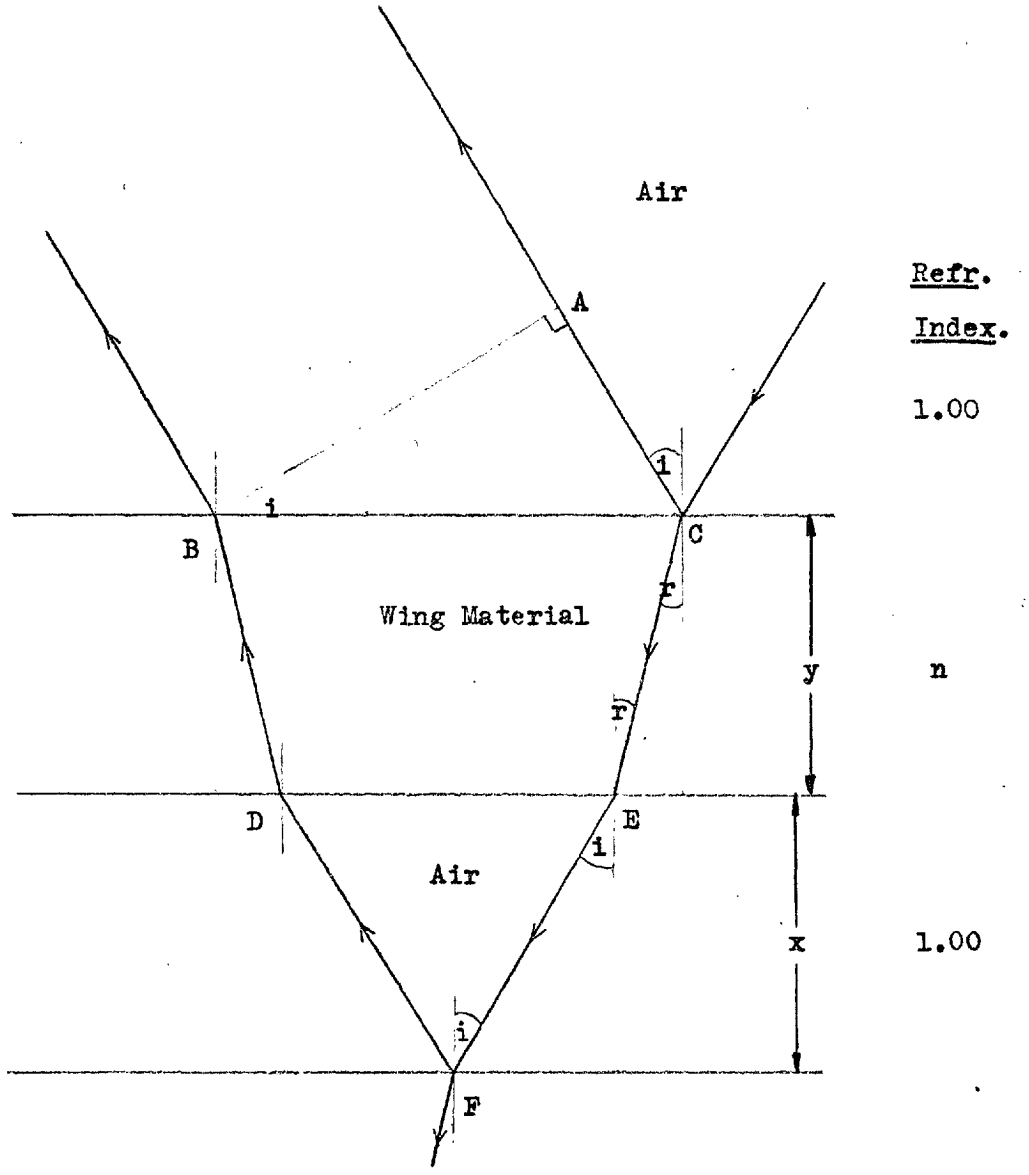


Fig. 8.1. Proposed basic unit of the wing structure.
One layer of wing material, one of air. Morpho.

However

$$n = \sin i / \sin r$$

Thus

$$O.P.D. = \frac{2n^2y}{\sqrt{n^2-\sin^2 i}} + \frac{2x}{\cos i} - \frac{2y\sin^2 i}{\sqrt{n^2-\sin^2 i}} - \frac{2x\sin^2 i}{\cos i}$$

$$= \underline{2y\sqrt{(n^2 - \sin^2 i)} + 2x\cos i}$$

In the more general case where the refractive index of the second layer were m this would become

$$O.P.D. = \underline{2y\sqrt{(n^2 - \sin^2 i)} + 2x\sqrt{(m^2 - \sin^2 i)}}$$

In this case, for constructive interference one must have

$$2y\sqrt{(n^2 - \sin^2 i)} + 2x\cos i = p\lambda_{max} \quad \ldots\ldots\ldots(1)$$

where p is an integer and λ_{max} is the wavelength of peak reflectance.

It has been shown when

$i = 45^\circ$ $\qquad$ $\lambda_{max} = 410nm \longrightarrow 440nm.$

and $\qquad$ $y = 126nm$ $\qquad$ $x = 97nm$

The samples, however, before being placed under the electron microscope had to undergo the evaporation of a thin coat of gold palladium under high vacuum conditions. Because of this such direct measurements may be in error, thus if the thickness of the coating is s nm

$y = (126 - 2s)$ nm $\qquad$ or $y \leqslant 126nm$

and $x = (97 + 2s)$ nm $\qquad$ and $x \geqslant 97nm.$

However the total unit thickness $\sum = (x + y)$ will be unaffected by such considerations and we have

$$\sum = (x + y) = 223 \text{ nm} \quad \ldots\ldots\ldots\ldots(2)$$

Taking n to be i) 1.4 ii) 1.5 iii) 1.6

in value we have from equation (1)

$$\text{i)}\ 2.41\,y + 1.41\,x = \lambda_{max} \quad \ldots\ldots\ldots\ldots(3)$$

$$\text{ii)}\ 2.65\,y + 1.41\,x = \lambda_{max} \quad \ldots\ldots\ldots\ldots(4)$$

$$\text{iii)}\ 2.87\,y + 1.41\,x = \lambda_{max} \quad \ldots\ldots\ldots\ldots(5)$$

The equations are shown plotted in Figure 8.2 for the two extreme values of λ_{max}, namely 410nm and 440nm.

A value for s is difficult to assess, however a fairly typical figure might be of the order of 15nm thick, and thus the value of y could well be as small as say 90 nm and x correspondingly larger.

Turning to the data obtained in Chapter 7 it is now possible to compare these results with those predicted from a thin film interference calculation. Assuming therefore the angular conditions be 45° incidence and 45° viewing, it is possible to make some wavelength comparison with the results of say Figure 7.4 or 7.9, knowing the basic initial data.

A value of 1.4 was given to the refractive index of the wing material, a value within the ranges quoted by the above references. From equations (2) and (3), therefore, knowing λ_{max} to be 410nm, values of

$$x = 128 \text{ nm} \qquad y = 95 \text{ nm}$$

are obtained. It may be noted that this value of x is now in extremely close agreement with that of Anderson and Richards. The final information - the number of high refractive index and low refractive index layers - was determined again from the photographs of the last chapter and found to be

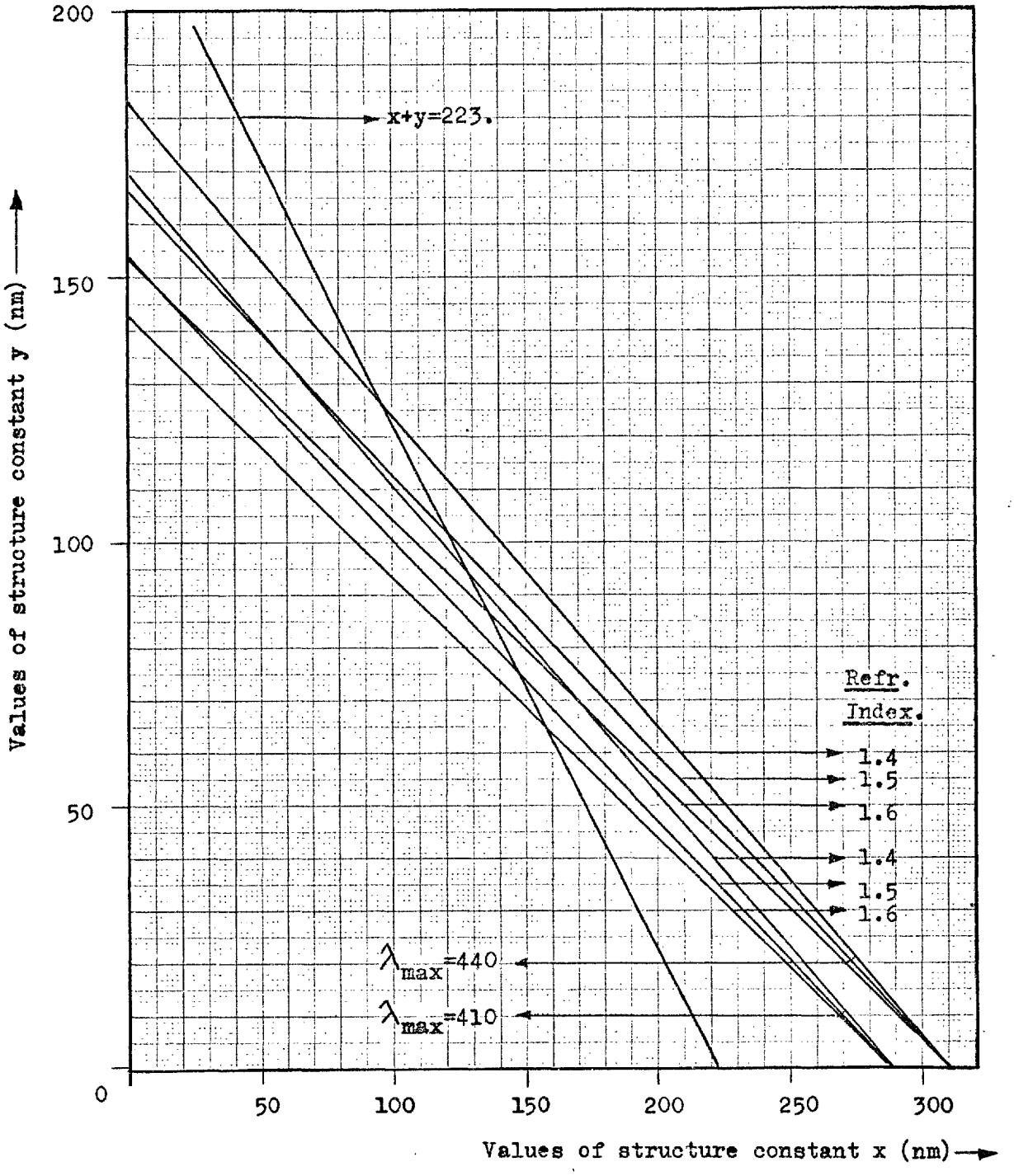


Fig. 8.2. The dependence of peak reflected wavelength (λ_{max}) on the values of structure constants y,x and the refractive index n.

eight of each in the case of menelaus.

The formulae derived in the following Appendix were used to obtain the reflectance at each wavelength throughout the visible spectrum from such a multilayer stack, with no polarisation present in the incident beam. The surrounding medium was assumed to be air (n = 1.00) and the backing material that of the wing (n = 1.40) since this was apparently so from the photographs. The calculation was performed on an I.B.M. 7094 computer due to the lengthy mathematics involved. The results are shown in Figure 8.4, directly following the schematic representation of the system in Figure 8.3.

In assessing the fit of such theoretical results to those measured ones, reference must be made to, say, Figure 7.4 and this has therefore been dotted in, both curves being normalised to the same maximum reflectance value at 410nm.

The general shape of the predicted curve is typical of a multilayer system, showing a series of decreasing secondary maxima on moving from the peak reflected wavelength. This certainly appears to follow the cut-off of the measured curve, falling to a minimum just before 600nm. At longer wavelengths however the theoretical curve shows no marked increase as does the measured one, only an undulating outline of decreasing amplitude.

That the measured curve does not show any of these undulations is not really surprising. In a material of this nature, variations in reflectance are bound to occur for several reasons. Variations have already been found from

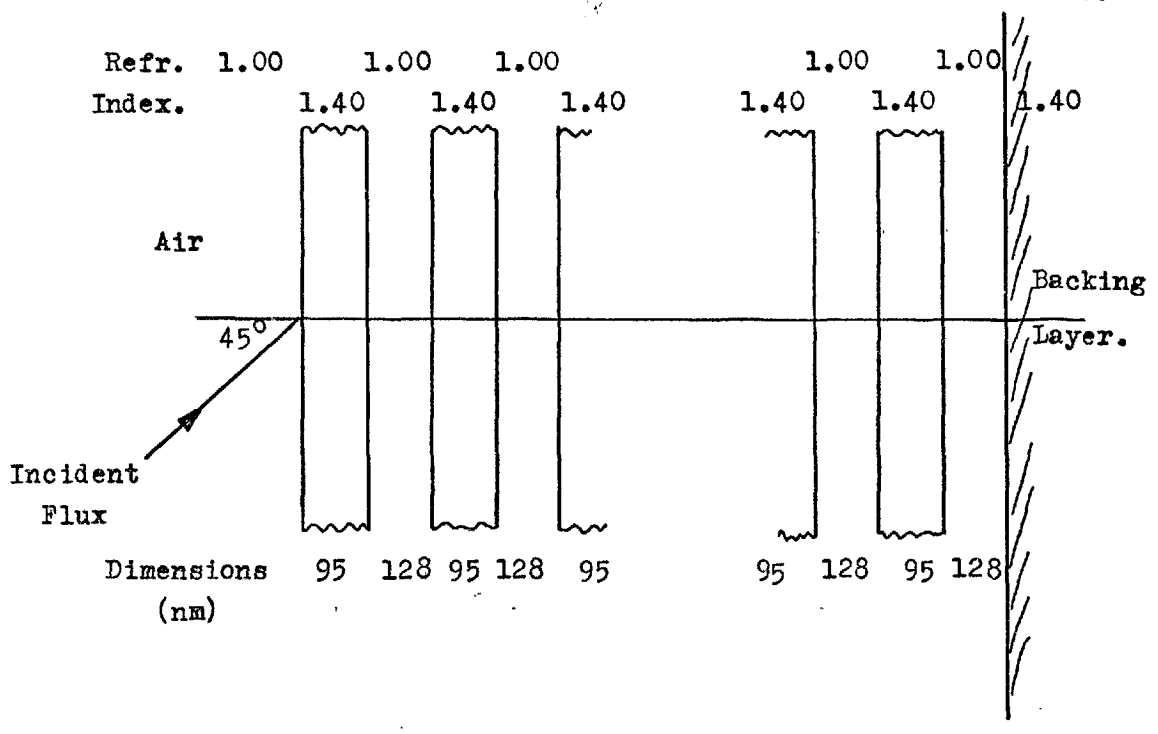


Fig. 8.3. Schematic representation of 16 layer thin film approximation to wing structure of Morpho.

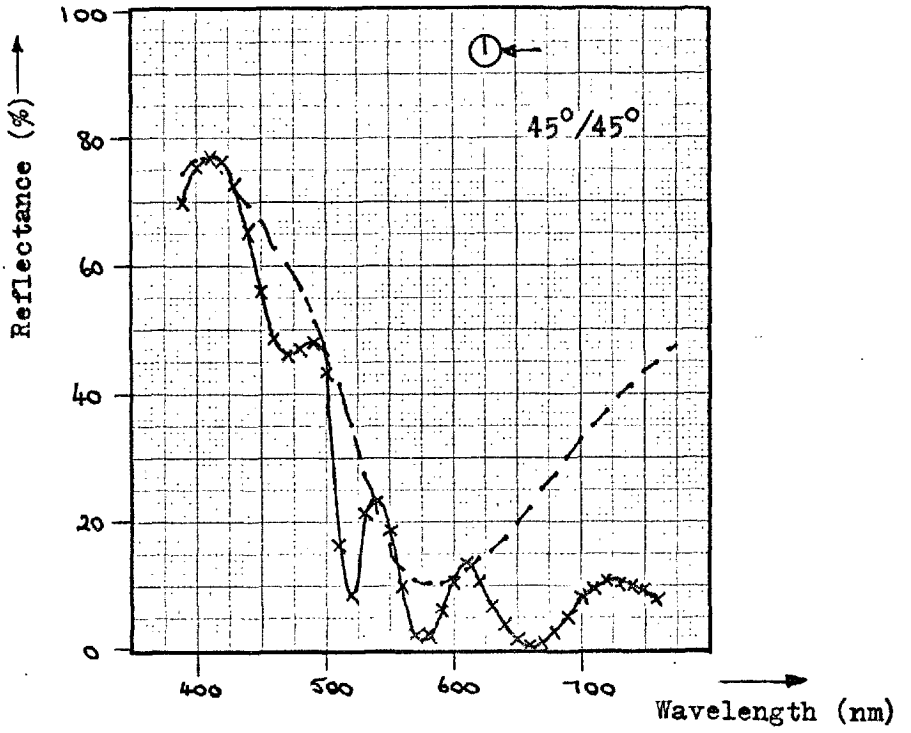


Fig. 8.4. Theoretical spectral reflectance curve for the above multilayer stack (×—×—×) together with the measured one under conditions 45°/45°(← —).

point to point across the surface, and in such a complex structure small changes in structure constants and angular inclination of the scales are almost certain to be present in any measured area. This would have the effect of averaging such changes, resulting in a smoothed reflection curve, which should theoretically pass centrally through the secondary maxima and minima. The last remaining evidence of such maxima in measured curves may be that shown in Figure 7.12 where a slight levelling out of the reflection curve is discernable at wavelengths approximately 60nm longer than that of the maximum.

The predicted reflectance values therefore may be a little low at wavelengths of about 500nm, but overall a reasonably good fit is obtained up to about 600nm. The problem posed by the portion of the curve above 600nm, where an unpredicted rise in reflectance is observed, will be returned to later in this chapter.

The dependence of the shape and absolute reflectance values of such theoretical curves on refractive index of the wing material is critical as simple calculation shows. In quantitative work therefore this value must obviously be determined by measurement. Unfortunately all the above mentioned workers have depended on purely visual assessment, where such a determination was made, and the next section describes how this was done here.

8.3 Determination of the Refractive Index of the Wing Material.

Certainly, up until the work of Anderson and Richards (1942) this material was always assumed to be chitin,

the uncertainty therefore means the refractive index value no longer needs to be that exhibited by other chitinous materials.

In order to determine this accurately, the method of liquid immersion was employed. Clear liquids of varying refractive index were obtained and the wing saturated with each in turn. As the liquid permeates the air spaces of the scale structure, and the refractive index thus increases, so the wing colours change markedly, in the case of acetone (n = 1.36) for example a green-gold colour is present, while for bromo-naphthalene (n = 1.65) all trace of colour disappears leaving only a dull brown. Obviously at the point where only a brown colour remains from the underlying melanin pigment the refractive index of the liquid must be identical to that of the wing material, thus eliminating any possible multilayer reinforcement.

A small piece of diffusely reflecting opal glass was mounted in a glass cell, containing liquid, on the kinematic slide of the spectrophotometer. The opal had previously been calibrated for reflectance against a magnesium oxide standard throughout the visible spectrum and was used as a substandard during the experiment. It thus overcame any effect of glass wall or liquid on the measurements of the wing material which was mounted on a rigid frame and similarly immersed at the other aperture of the slide. Therefore it was possible to vary the liquids and repeat the reflectance measurements for many refractive indices. The geometry used was normal incidence and 45° collection to avoid any specular reflection from the glass

walls. Certainly a $45^{\circ}/45^{\circ}$ arrangement would have been preferable, however this would necessitate mounting the samples at some acute angle to the cell walls to avoid this specular reflection, and the available room was not sufficient to permit this with accuracy.

The reflectance spectra for the wing immersed in three of the liquids used are illustrated in Figure 8.5, together with the corresponding curve measured in air for comparison. The three liquids are ethyl alcohol (n = 1.36), carbon tetrachloride (n = 1.46) and benzene (n = 1.50).

As the intermediate refractive index increases from 1.00 to 1.36 so the reflection maximum shifts to approximately 575nm and is accompanied by a reduction to about one tenth its former size. On increasing the index the peak moves to a slightly longer wavelength and reduces somewhat further in size, until at a value of 1.50 is non existent, to the accuracy of the experiment, leaving only a fairly flat curve of around 1 - 2% reflectance. At this point therefore the refractive index of the wing has been matched and for menelaus

$$\underline{n = 1.50}$$

Further accuracy on this figure would be somewhat misleading since all such liquids will, in some degree, tend to swell the wing structure, leading to inaccuracies. This may be observed as the organic liquids evaporate from the scale and the colour is restored, the liquid contained between the plates disappearing quickly, while that absorbed into the material itself takes a

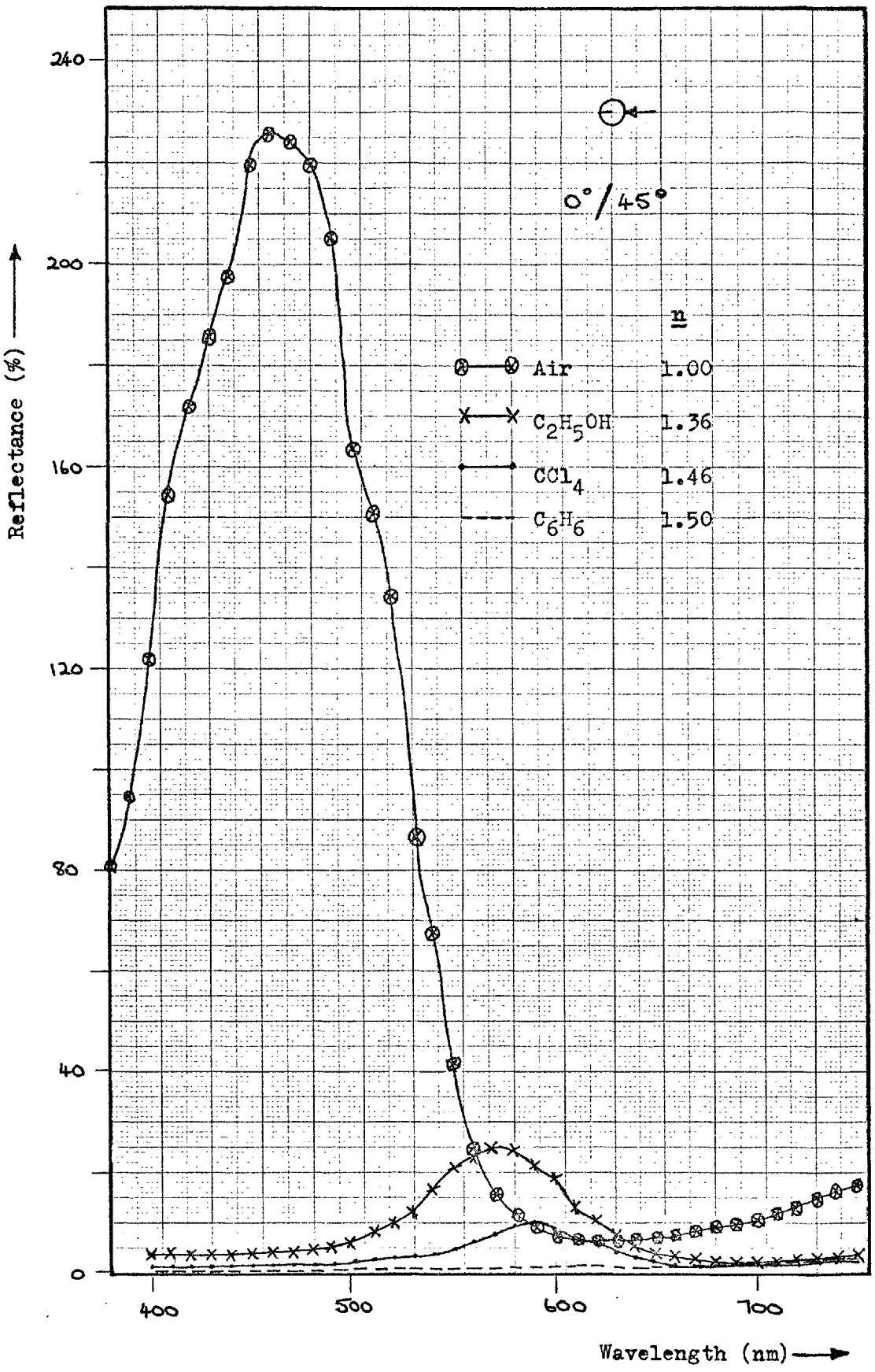


Fig. 8.5. Morpho Menelaus - Spectral reflectance curves when immersed in fluids of varying refractive index.

considerably longer time. Where possible, such effects were kept to a minimum, by the choice of liquid, in order that the quoted results be as accurate as possible.

The result falls within the limits quoted by such workers as Mason (1927) and Rayleigh (1919), however is slightly less than the value calculated by Merritt (1925). The latter worker also obtained typical dimensions for a possible structure, which at the time of the work was completely unknown, and this too is in some error, so little weight must therefore be given to the corresponding value of refractive index.

8.4 Comparison of Measured and Theoretical Reflection Curves for Simple Specular Reflection.

Since there is a certain amount of variation between measured curves, the criterion of comparing curves whose peak reflectance wavelengths coincide was developed. Thus since the refractive index of the wing material

$$n = 1.50$$

we have from equations (2) and (4)

$$y = 95\text{nm} \qquad x = 128\text{nm}$$

to give a reflectance maximum at approximately 430nm. This should then be compared with the curve a) in Figure 7.7. The theoretical curve for such a physical arrangement was calculated as before and is shown, together with the equivalent measured one, in Figure 8.6. Both are again normalised at peak values.

Once more the fit is good up to just above 600nm, following more closely the average of the undulating

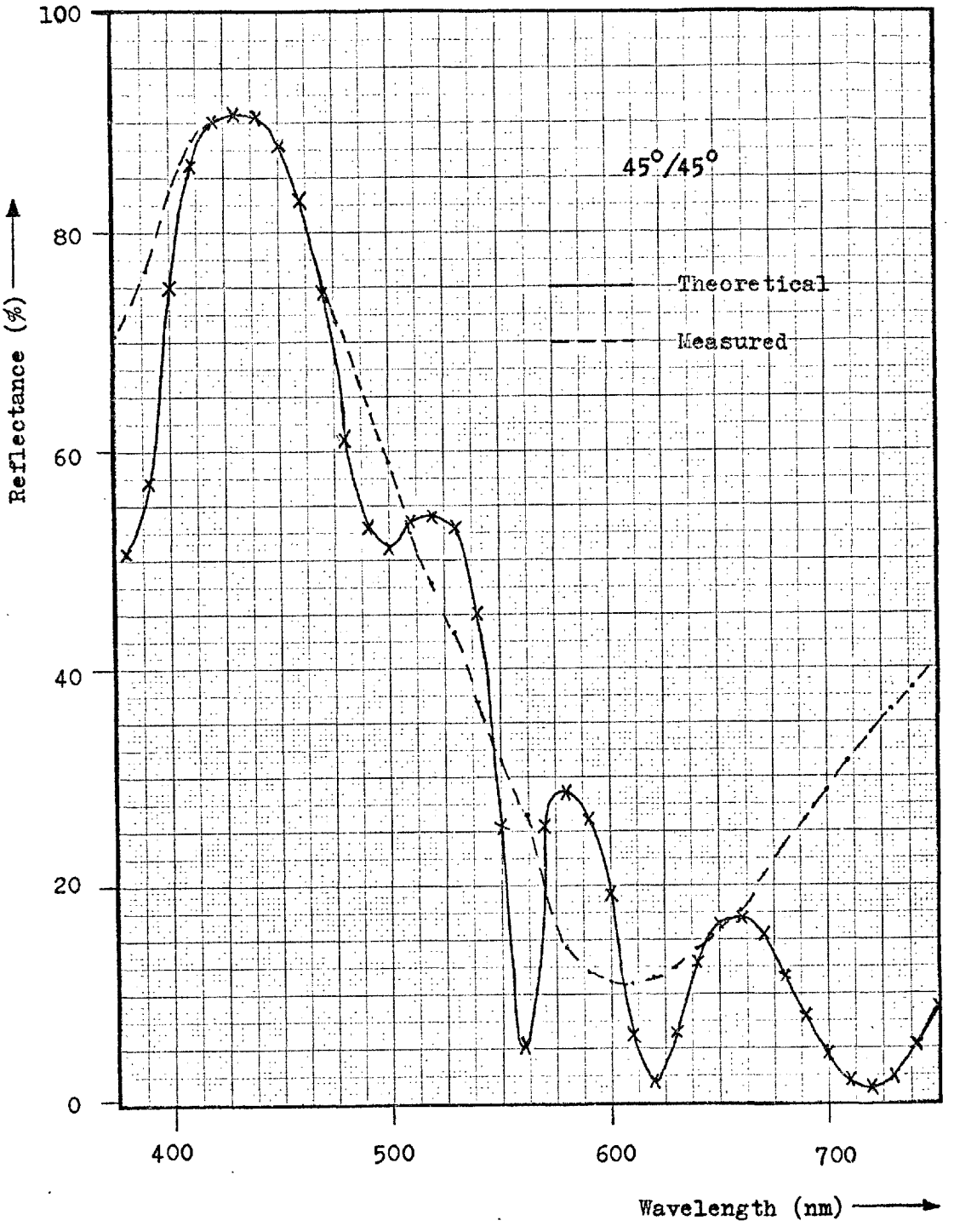


Fig. 8.6. Morpho Menelaus - Theoretical thin film curve (x—x) using the values x=128nm, y=95nm and n=1.50, compared with a measured curve at 45°/45°. (—·—·—)

secondary maxima as might be expected. Above 600nm however the measured curve rises steadily from some 10% reflection to something nearer 40% at 750nm. This is clearly in disagreement with the predicted theoretical curve.

One possible reason for this anomaly would be that these particular wavelengths were reflected quite strongly from the underlying melanin pigment - the only pigment known to be present. This would explain the apparent difference, discussed earlier, between the lower wavelength peak, which varies considerably in shape and size with position and orientation, and this long wavelength portion which remains fairly constant over wide measuring configurations.

To check this theory the wing was mounted facing the opposite direction to earlier measurements and the spectral reflectance of the back surface measured under conditions of 45° incidence and 45° collection.

The actual reflection of this light is, however, more likely to originate at the base of the scales themselves where considerable quantities of melanin are known to be present, thus any light penetrating the scale structure would partly be absorbed and partly reflected from this area.

Measurements of such areas are difficult, however it was found that the scales could be readily removed by fixing 'Sellotape' over the top of the wing surface and almost immediately removing it with extreme care. This removed the scales from their sockets and by means of trial and error, eventually an area sufficiently large

could be removed for measurement. The scales of course retained their distinguishing blue colour, and the reverse side - the melanin base - could then be readily measured using a monochromatic spot some 1 mm square. Finally the spectral reflectance of the area from which the scales had been removed was similarly measured. The results are illustrated in Figure 8.7 for a $45^{\circ}/45^{\circ}$ configuration.

All the obtained curves show the same tendency to remain fairly flat up to about 550nm, after which a gradual increase in reflectance occurs up to the extreme long wavelengths measured. The effects of specular reflection from the 'Sellotape' backing were investigated for the case (b), since it was felt that this should indicate most nearly the true reflectance of the melanin layer. Only a flat spectral response was obtained from the 'Sellotape' alone, and therefore curve (b) should be accurate.

Variations in overall level of the three plots would be expected, since different levels of the melanin backing layer are being investigated. The similarity in shape does verify the presence of a pigment which reflects at long wavelengths. This also explains the shape of the curve obtained in Figure 7.13, since away from the direct specular reflection and the observed band of reflected colours, only this pigmentary reflection should be obtained, together with any scattered wavelengths.

Thus the two distinct parts of the reflection curve seem to fit quite closely the predicted values throughout the visible spectrum under specular conditions and at this particular angle of incidence.

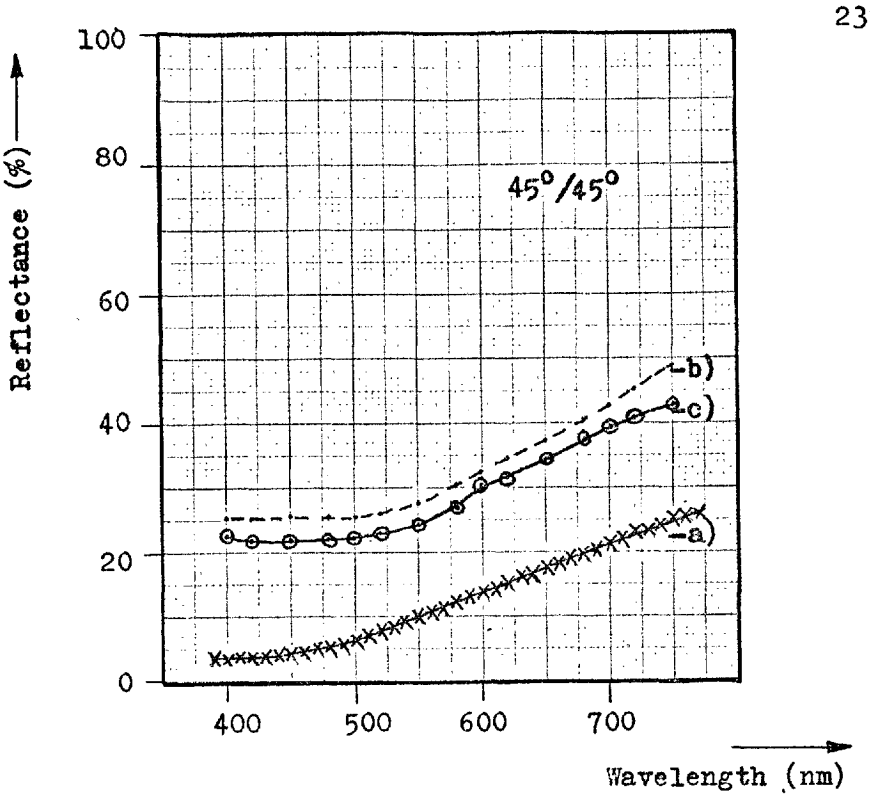


Fig. 8.7. Morpho Menelaus - Spectral reflectance curves for a) rear of wing surface, b) rear of the scales and c) the bed of the scales. $45^{\circ}/45^{\circ}$.

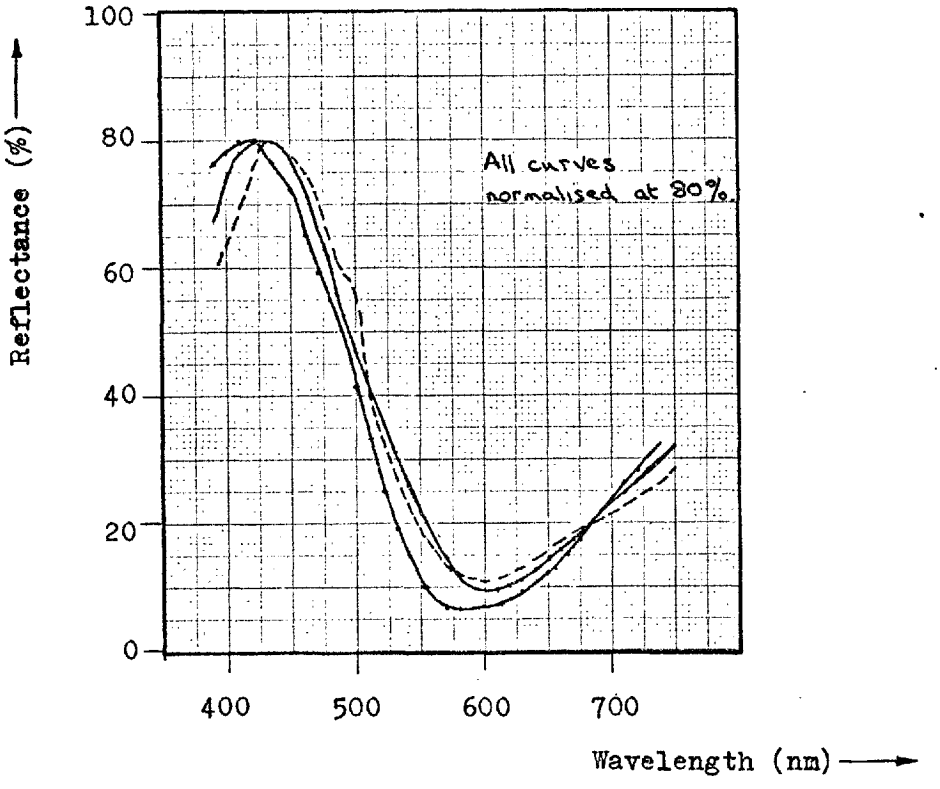


Fig. 8.8. Morpho Menelaus - Spectral reflectance of the wing material under conditions $45^{\circ}/45^{\circ}$ with respect to the horizontal plates of the vertical ribs.

8.5 The Orientation of the Horizontal Layers to the General Scale Surface.

It has already been stated in the preceding chapter that the bright reflected band of light observed in the hemispherical viewer was deflected some 10^{o} to 20^{o} from the incident beam, and rotated at this angular separation about the centre as the wing was rotated. This certainly seems to be due to the observed inclination to the base layer of the horizontal plates, which make up the longitudinal striations, an angle of approximately 10^{o}. This would therefore lead to a deflection of almost 20^{o} in the reflected light. Since the direction of the deflection is always towards the roots of the scales, the evidence seems overwhelming.

Such an inclination of the substructure was predicted by early workers (Mason, 1927) purely from the evidence of the reflected light properties, and the photographs of Martin (1971) do bear this out.

However, this does raise an interesting point in that the wing surface should not be used for angular reference but in fact the horizontal plates themselves.

In an attempt to measure this inclination more accurately the wing was mounted at 45^{o} incidence in the spectrophotometer. By setting to each wavelength in turn and scanning the photomultiplier around the surface at various angles of collection, it was possible to measure the position of specular reflection accurately. On doing this at the positions b) and d) indicated by Figure 7.2 the difference between angular readings for each position should be some

four times the angular dip of the plates.

The wavelength region was restricted to that part of the spectrum where the interference properties were important, since at longer wavelengths relatively small effects should be, and are, apparent because these reflections do not appear in the main, to come from the horizontal plates.

An average value of some 8.5° was obtained by this method, in good agreement with the 10° estimated from the photographs.

The measurements of spectral reflectance were then remade using the plates themselves as the reference level for the wing material. This was done by setting the detector at right angles to the incident beam and placing the wing surface at approximately 36.5° to the incident beam in position b) and 53.5° in position d). The measuring configuration should then be $45^{\circ}/45^{\circ}$ in both cases. The measurements were finally repeated at angles up to 2° either side of these values.

The results obtained were almost identical to those illustrated in Figure 7.7 of the previous chapter, showing the same type of spread in peak value - more dependent on location than anything else. The only obvious difference was the slight shift in the average peak reflection wavelength to the 430 - 440nm region, illustrated in Figure 8.8, giving a typical curve very much as the measured one in Figure 8.6.

It must be assumed therefore that over quite

small angular changes the most obvious variable of the multilayer enhancement process, namely the wavelength of the reflection maximum, is somewhat 'smoothed out' by:-

i) the scattering and diffusion which inevitably takes place in such a material,

ii) spurious reflections from the vertical striations, and iii) the finite angular spread of the detector aperture about the nominal angular setting.

8.6 The Angular Specular Reflection Properties.

If the multilayer process outlined above is entirely responsible for the observed reflected colours exhibited by the wing material the angular variation of measured, specularly reflected light should obey defined rules. For instance, with decreasing angle of incidence the reflected light maxima should occur at increasingly long wavelengths.

The reflectance of the wing material from the menelaus was therefore measured under conditions of 30° incidence and 30° viewing angle to the normal of the horizontal plates. The required angles to the actual surface were obtained as they were in the preceding section.

The results are illustrated for the complete visible spectrum in Figure 8.9, together with the similar theoretical curve obtained by using the techniques outlined in the Appendix and the structure constants outlined and obtained above.

Agreement between the two curves is now no longer as good as in the $45^{\circ}/45^{\circ}$ configuration. The

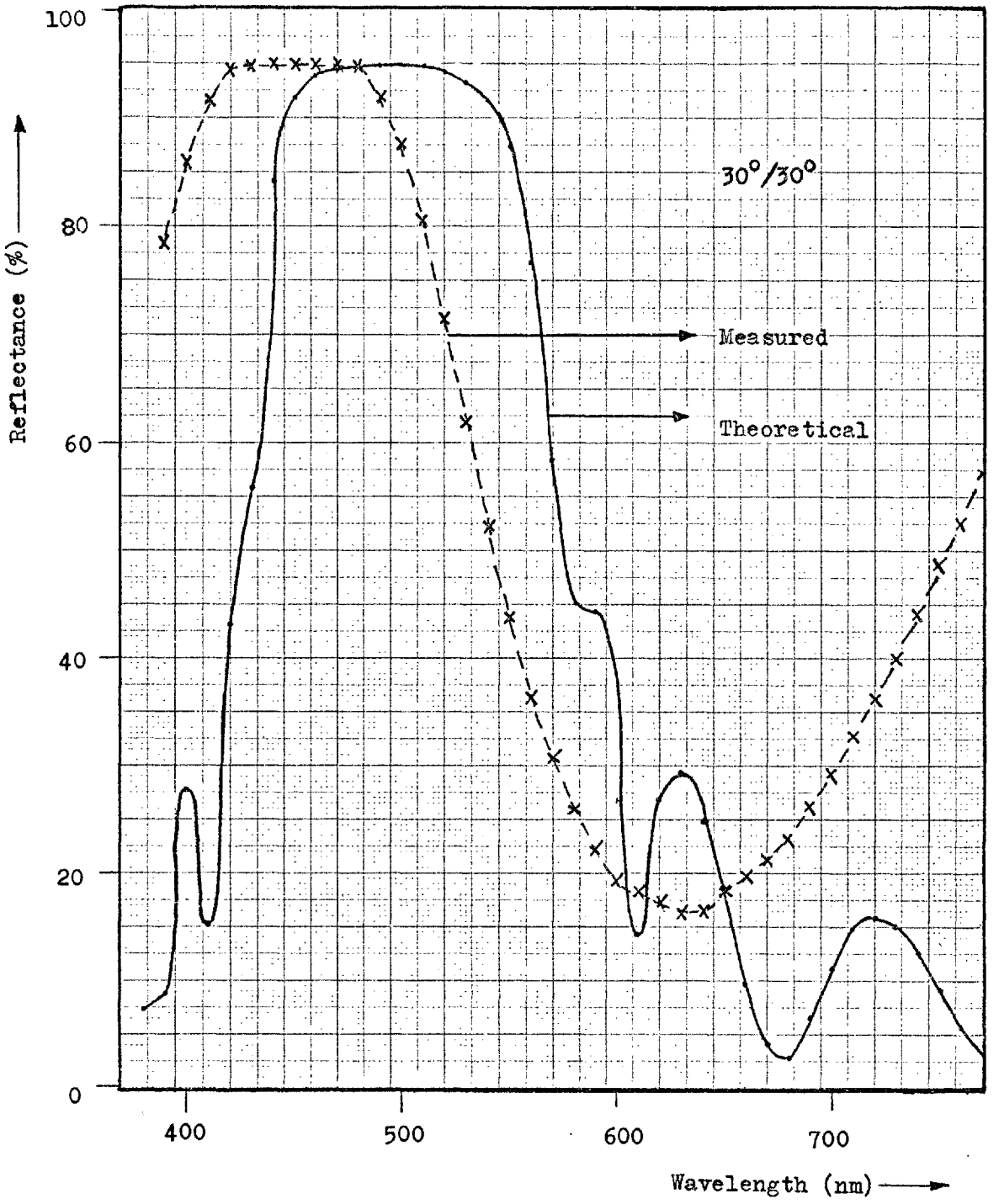


Fig. 8.9. Morpho Menelaus - Comparison of theoretical and measured spectral reflectance curves under conditions 30°/30°.

wavelength peak in the blue has moved to approximately 460nm while the predicted peak occurs at a somewhat longer wavelength of 490nm. There is still a marked increase in the measured curves at the red end of the spectrum, due presumably to the melanin pigment.

An important point in comparison, however, is the overall shape of the low wavelength peak, a place where agreement should be good if interference were entirely responsible. Both curves are remarkably similar in shape, both being considerably wider and flatter than their counterparts at $45^{\circ}/45^{\circ}$.

It would appear therefore that the major error is that the peak intensity wavelength occurs at a wavelength shorter than the theory would suggest for the given angular shift.

To obtain a complete measure of this deficiency in agreement, the specular reflection properties of menelaus were measured about either side of the peak reflectance wavelength, at several angles of incidence, and the wavelength at these maxima obtained graphically from the average of some six curves. All angles quoted are with respect to the horizontal plates of the substructure rather than the scale surface.

The results are illustrated here in column 2 of Table 8.1.

The measured value of λ_{max} is quoted to 5nm since some difficulty was found in assessing this with greater accuracy. This was mainly because

i) large variations occurred in the value from point

to point over the surface, similar to the results obtained at $45^{\circ}/45^{\circ}$ earlier, and

ii) many of the obtained curves had extremely flat maxima as illustrated in Figure 8.9, and the position of the exact peak was difficult to pin point.

TABLE 8.1.

Angle of Incid.	λ_{max}(nm).	Predicted λ_{max}(nm).
0°	485	541
7.5°	480	538
15°	480	528
22.5°	465	512
30°	460	491
45°	420	430
60°	390	361

The results at the extreme ends of the angular range are somewhat unreliable, those at 60° being so since the peak occurs too low in the violet to be able to measure the lower wavelength fall, and those at 0° and 7.5° due to the measuring techniques employed. To obtain such data under a $0^{\circ}/0^{\circ}$ configuration say, it was found necessary to use a mirror with a small hole in the centre to direct the reflected flux from the sample to the detector. The monochromatic beam was incident on the sample through the small central hole.

In column 3 the predicted wavelength of maximum reflectance is given, derived from equation (1)

$$2y\sqrt{(n^2 - \sin^2 i)} + 2x\cos i = p.\lambda_{max}.$$

The values were those used earlier for $45^\circ/45^\circ$ results, namely:-

$y = 95nm$ $x = 128nm$ $n = 1.50$ $p = 1$

Certainly the increasing value of λ_{max} when measured at progressively smaller angles is in agreement with the theoretical results, however the discrepancies between the two sets of data in columns 2 and 3 increase to quite large values as normal incidence is approached.

It is important therefore to ascertain whether this effect may be due to some inaccuracy in the structure constants used, or to some further optical phenomena occurring together with the multilayer interference which has been shown to be present.

Disregarding the extreme angular results, and using those at say 15°, 30° and 45° we obtain from equation (1.)

$$2.95\,y + 1.93\,x = 480 \quad \ldots\ldots \text{a) at } 15^\circ$$
$$2.83\,y + 1.73\,x = 460 \quad \ldots\ldots \text{b) at } 30^\circ$$
$$2.65\,y + 1.41\,x = 420 \quad \ldots\ldots \text{c) at } 45^\circ$$

since both the angle i and the refractive index n are known accurately.

Solving each pair of quadratic equations in turn we have

	y = 160nm	x = 4nm	from a) and b)
	y = 141nm	x = 33nm	from a) and c)
and	y = 132nm	x = 50nm	from b) and c)

Fairly large variations in these values would be expected since they are very dependent on the value of λ_{max}, a figure not known with sufficient accuracy. We cannot therefore take the large spread in predicted values of y and x to be indicative of a failure to produce a set of structure constants which would fit the measured data.

The results do nevertheless indicate values of

$$y \approx 140\text{nm} \qquad x \approx 40\text{nm}$$

for these constants, values which could not possibly be correct since when summed do not produce a sufficiently large dimension, and even from a visual estimate of the photographs the value of y - the thickness of the horizontal plate - is not three to four times the value of x - the gap between these plates.

It is therefore felt that some further optical process may also be present which in some form modifies the existing predicted data to reduce this peak wavelength shift with decreasing angle of incidence. It must be borne in mind that a part of the effect must be in assessing the peaks of both types of curve - measured and theoretical - which are both very flat and very wide.

Visual observations by Anderson and Richards (1942) confirm this smaller than expected shift in wavelength maxima. They deduced from their first electron microscope photographs that whatever substructure was present increased

in thickness the nearer the position was to the base, and that in some form this may explain their observations. It is now clear from the photographs illustrated earlier that such theories are untenable, since, within the accuracy already stated, no apparent increase in thickness of, what is now known to be, horizontal plates, occurs on approaching the bottom of the stack.

It is difficult to deduce the possible root of this discrepancy, however certain points emerge in the following sections.

8.7 The Polar Spectral Reflection Properties of the Wing Material.

Figures 8.10, 8.11 and 8.12 illustrate the polar reflection curves obtained from the wing material at different wavelengths by Pillai (1968). Although the present investigation does not agree with the measurements in the right hand quadrant, at the true specular angle, as is indicated in Figures 7.3 to 7.6 of the previous chapter, a significant point arises from the three polar plots.

In the plane of measurement a marked peak is obtained in the left hand quadrant, at angles about the incident one, at all wavelengths. The presence of such a peak has been confirmed, although in detail somewhat different to that of Pillai in both spectral content and position. No rotational position is defined by this author.

Morpho menelaus was measured, by reflection, at angles about the incident one of 45^{o} to the surface normal at the four orthogonal rotation positions indicated

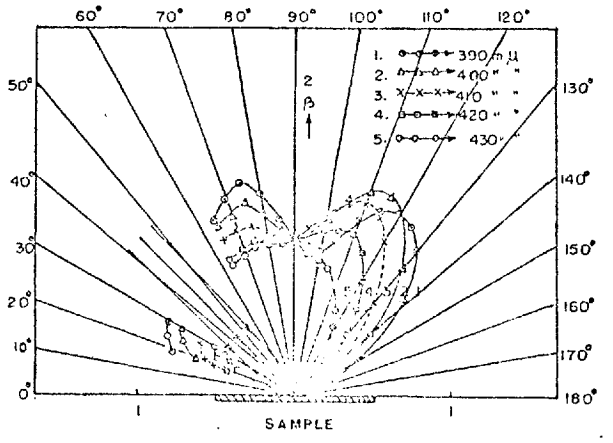


Fig. 8.10 Polar reflectance curves of the Morpho butterfly wing for wavelengths 390, 400, 410, 420 and 430nm. (Pillai, 1968).

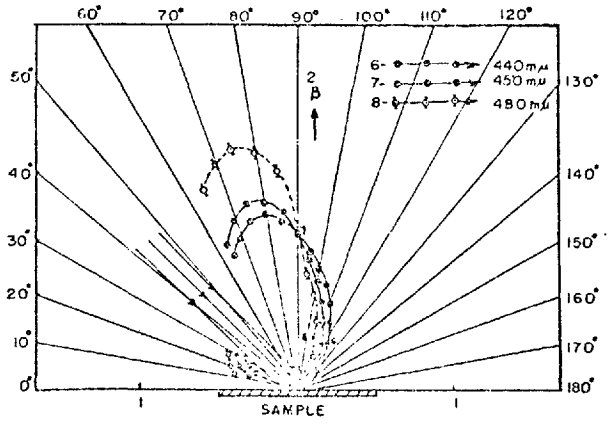


Fig. 8.11 Polar reflectance curves of the Morpho butterfly wing for wavelengths 440, 450 and 480nm. (Pillai, 1968).

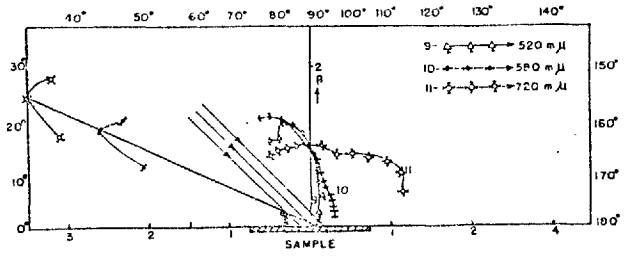


Fig. 8.12 Polar reflectance curves of the Morpho butterfly wing for wavelengths 520, 580 and 720nm. (Pillai, 1968).

in Figure 7.2. Under rotations b) and d) no reflectance above that of the red melanin reflection was discernable. However under rotations a) and c), where the vertical ribs were perpendicular to the plane of measurement, a definite peak was obtained close to the incident direction. It is not possible to measure with ease in the vicinity of the incident angle since the detector obstructs the incoming light beam some 15° to 20° either side of the nominal incident angle. The reflected peak however increased in magnitude on approaching this 45° incident angle from both directions and by interpolation appeared to be at that angle.

It is felt that the results of Pillai may not be true peaks at angles around 70° but more likely present because of some obstruction of the incident beam in the Wright instrument by the detector at angles nearer the incident one than this, leading to inaccurate measurements.

The spectral composition of this back reflected peak was measured as close to the incident angle as possible (60° to the surface normal, in the same quadrant as the incident beam), and is illustrated in Figure 8.13. The curve is remarkably similar to those obtained earlier under a $45^{\circ}/45^{\circ}$ configuration, showing a peak at approximately 440nm followed by a fall in reflectance to about 600nm and a gradual increase thereafter. The slight change in peak wavelength may be due to the 15° error in collecting angle.

The reflectance curve for the multilayer stack, derived and shown in Figure 8.6, would therefore fit closely this spectral reflectance curve and is shown

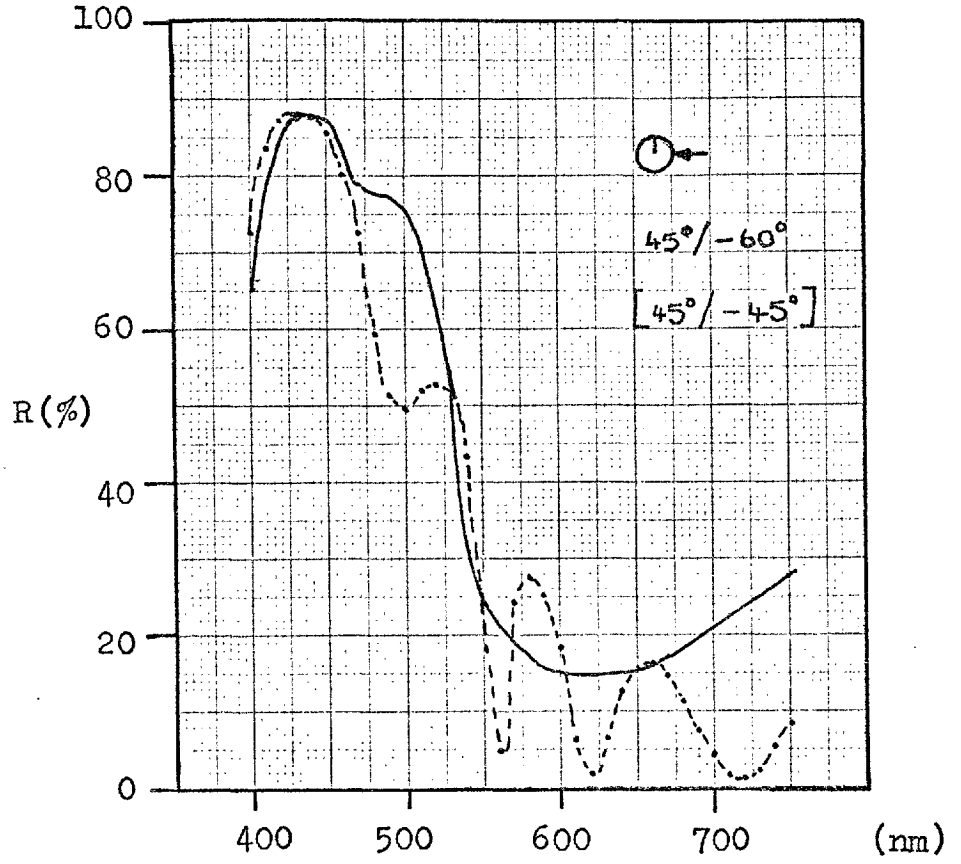


Fig. 8.13 Morpho menelaus - Comparison of spectral reflectance curves i) measured (———) and ii) theoretical (---) at 45°/ -60° - the 'specular' back reflection.

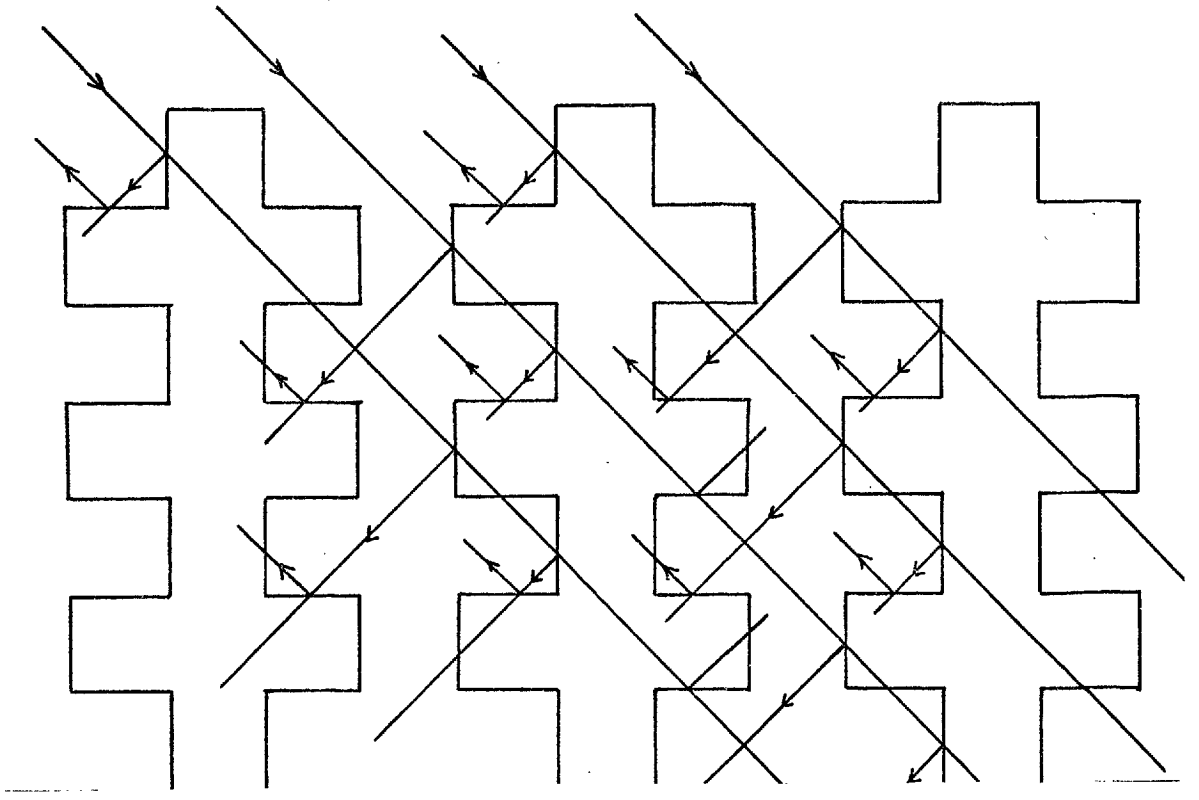


Fig. 8.14 Simple schematic diagram showing the origin of the back reflected, specular peak.

dotted over Figure 8.13, the red component being obtained as before from the underlying melanin pigment.

The importance, other than purely structural, of the vertical ribs now becomes apparent. It is proposed that the incident light on the material is partially reflected by the vertical ribs so that, after sufficient reflections, an appreciable proportion of this light is incident upon the multilayer at an angle identical to the incoming one but on the opposite side of the surface normal, as illustrated diagramatically in Figure 8.14. This would lead to reinforcement by multilayer interference giving for 45° incidence a spectral reflectance as that shown in Figure 8.13 back along the incoming beam direction.

One therefore predicts, and observes, a peak reflectance both in the pure specular direction and the reverse specular direction - that is, back along the incident beam, whose spectral distributions are identical, and equal to the theoretical multilayer curve, as shown, for positions a) and c). For positions b) and d) no reinforced, back reflected component should be measurable since here the vertical ribs are parallel to the plane of measurement and take no part in the process. Therefore the material acts as a straightforward multilayer stack with no vertical structuring and an interference peak should only be recorded at the true specular angle.

This difference between rotation a) and c), and b) and d) has been noted above, all producing a specular, reinforced reflection while only the two former rotations produce this marked back reflection. It must also be

mentioned that Figure 7.6 shows a marked increase in reflectance value at the specular angle of rotation d) over those of a) and c) where a good deal of the incident light is back reflected.

Thus polar reflectance curves similar to those of Figure 8.10 are obtained at rotations a) and c) showing two distinct 'specular' peaks together with appreciable intensities at other angles. It is now clearer why a band of reflected light was observed visually, for, together with the suggestions of the next section, the above proposals, following the inevitable scatterings which will be present, lead to the formation of a distinct band of reflected light.

8.8 The Reflected Light from Morpho Menelaus on Complete Angular Integration.

From the visual description given earlier of the reflected light from the wing material it is clear that a considerable amount of light is present at angles other than the specular one. Since this light forms a band of reflected wavelengths at 90° to the longitudinal striations of the scales, as shown in Plate 7.5, some type of diffraction process is immediately suggested.

In the past, workers have tended to dismiss the presence of any diffraction processes since they do not fit the observed wavelengths reflected at various angles. Mason (1927), in a summary of the findings of several authors, emphasizes the points that for an ordinary grating there will be an uncoloured reflection at the specular angle where all wavelengths are in phase, and that the longer wavelengths

should be diffracted over the wider angles. No such uncoloured reflection is obvious for the Morpho and it has already been described that a blue-violet colour is found at extreme angles and a green-blue colour nearer normal incidence. Diffraction theory and the observed reflected light from the Morpho do not therefore seem to be compatible at first sight.

It would appear however that all the preceding workers have assumed a reflection grating for the scale structure, which certainly does not seem to fit the measured data. A somewhat different approach will be used here.

In a measurement such as that made on the Beckman spectrophotometer the incident light is normal to the material while the entire reflected flux is integrated, by means of a whitened sphere, over all angles. To obtain a close fit to such a curve an extremely detailed knowledge of the optical processes involved in the production of the reflected colours is called for. This then presents an excellent test for such processes which produce responses at angles other than the specular one.

It will here be assumed that some diffraction does occur at the surface of the scale, the longitudinal striations are certainly placed at such distances apart for this to be possible. Each diffracted component at a particular wavelength and order of diffraction is now incident upon the multilayer stack beneath, already described in detail earlier. Dependent on the exact angle of incidence on the stack, no longer necessarily 0^{o}, the particular

wavelengths will be reinforced, or not, as the case may be. This spread in angles of incidence will then produce many wavelengths emergent from the stack at a whole range of angles - giving rise to the aforementioned band of colours.

It would appear reasonable that such wavelengths would tend to be reinforced in particular at the blue and blue-green regions of the spectrum, since the stack is certainly more 'attuned' to this part. This again is borne out in observation by the predominantly blue-green band obtained.

Such proposed properties of the material would not affect the earlier results to any great extent since there the collection was almost purely specular - in effect the zero order of the above process - and thus the calculations, which take into account only wavelengths incident at the prescribed angle, should be almost completely correct.

A computer programme was written which would calculate the overall reflected light at each wavelength from such a system. Each wavelength at 10nm intervals throughout the spectrum was taken in turn, and the angles of each order of diffraction about the normal, positive or negative, calculated up to 90^{o} from the grating equation

$$d.(\sin I + \sin\Theta) = q.\lambda$$

where d is the diffraction grating constant, I and Θ the angles of incidence and diffraction respectively and q the order number.

Each wavelength at its various possible angles

of incidence on the stack was then traced through the thin film programme used earlier, together with the zero order for each wavelength, or that at 0°, Before these could simply be added together however, allowance for the diffraction envelope for such components had to be made.

It is known (see for example Longhurst (1964)) that for a grating consisting of a number of slits N, each of width a, separated by elements of width b, the intensity distribution for light incident at an angle I to the grating is given by

$$\text{Intensity} = (\sin\alpha/\alpha)^2 \cdot (\sin N\beta/\beta)^2$$

where

$$\alpha = \frac{\pi a (\sin\theta - \sin I)}{\lambda}$$

and

$$\beta = \frac{\pi (a + b) (\sin\theta - \sin I)}{\lambda}$$

θ being the angle of the diffracted beam to the normal. The term

$$(\sin\alpha/\alpha)^2 = \frac{\sin^2(\pi a (\sin\theta - \sin I) / \lambda)}{(\pi a (\sin\theta - \sin I) / \lambda)^2}$$

is that describing the overall envelope containing the intensity curve. This therefore is the important term in the present analysis.

Obviously $a + b = d = z$, the quantity defined in the previous chapter, all that remains is to

determine the ratio of a to b. The exact value is difficult to determine from the photographs, since the structure is not very well defined at the surface of each striation owing to the way in which each stack ends. From the evidence of the best possible photographs of this area it was assumed that the gap and the structure were of approximately equal dimensions and therefore

$$a = 420\text{nm}.$$

The whole was run on a C D C 6400 computer and the total effect at each wavelength summed. This should then be comparable with results obtained on the Beckman since all light reflected from the material will have been summed at each wavelength.

Figure 8.15 presents the results of such a calculation at 0° incidence and total collection, together with the spectral reflection curve calculated purely from multilayer interference techniques at 0° incidence.

Figure 8.16 then compares the curve, with diffraction present in the system, with the measured Beckman curve under conditions of total collection. All plots have been normalised to the peak value of the measured data.

The former figure illustrated the typical multilayer curve at this angle - a very wide, flat-topped peak extending from about 490nm to some 610nm with the usual secondary maxima. By including the diffraction effects, a function is obtained whose maximum is greatly sharpened and moved to the extreme short wavelength end of the earlier one, namely 490nm. Secondary maxima are still discernable, although are now somewhat erratic in occurrence.

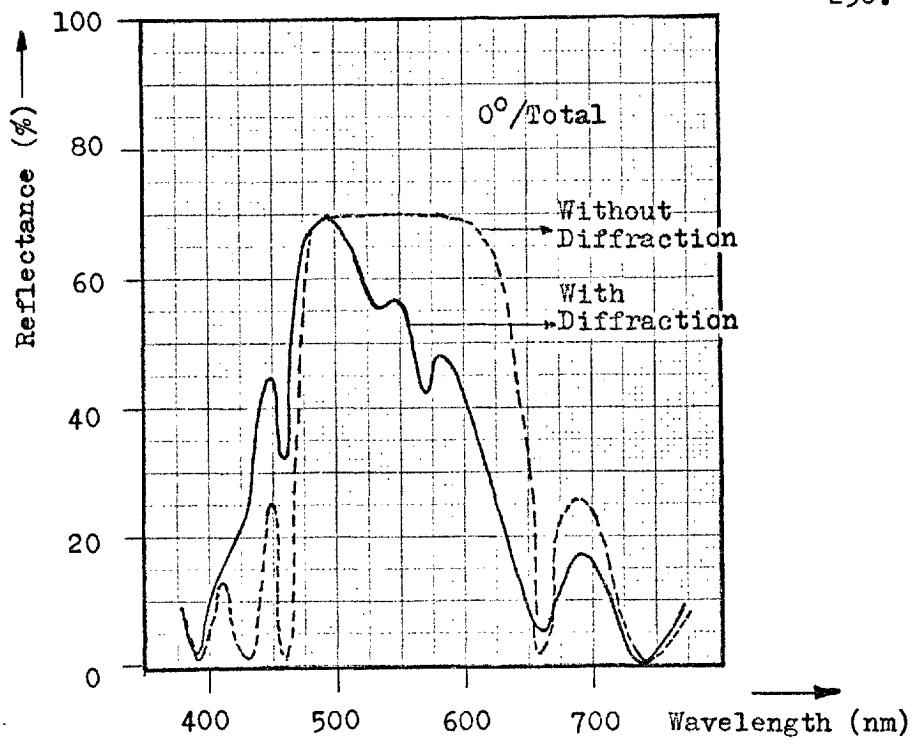


Fig. 8.15. Comparison of spectral, reflected light from a 16 layer thin film stack i) without diffraction (----), ii) with diffraction present (———).

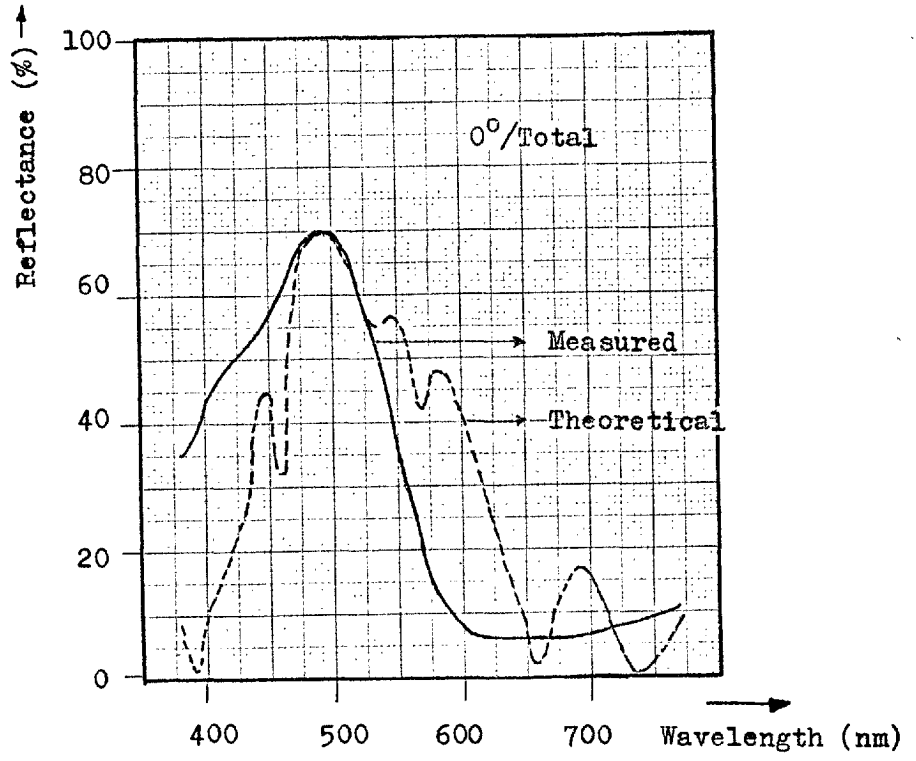


Fig. 8.16. Morpho Menelaus - Comparison of spectral reflectance curves for measured (0°/Total) and a 16 layer stack with diffraction at the top surface.

On comparing the measured curve with this proposed one in Figure 8.16, certainly the peak reflectance wavelength is extremely well predicted, unlike the theoretical value obtained without diffraction present in the system. The extreme blue-violet end is somewhat higher in the measured case than the predicted one although a predicted secondary maximum at 445nm does appear to coincide with a slight plateau on the measured curve.

The reverse is true at the other side of the peak, in the green wavelength region. The cut-off for the predicted curve is not really sharp enough, although both plots reach a minimum point at roughly the same wavelength. Beyond this, the measured curve does not show quite as large a rise as in the specular measuring cases, because, owing to the total angular measurement, proportionally there is a great deal more reflected light at other wavelengths. As before, one would not expect any predictions in this region to be completely accurate.

The theoretical curve would colorimetrically therefore appear to predict too large an amount of green-yellow component, while reducing the blue content too greatly. Overall, however, the curve shows a great improvement over the simple thin film results and, considering the complexity of the process, and the variations present in the system, it is felt that the fit is good, particularly the peak reflectance predictions.

It is concluded that such diffraction processes are likely to be present, together with the apparent multilayer interference. Such a selective diffracting system

appears to reflect only up to about 550nm to any extent, and maximally around 490nm - typical of the observed band of colours. The typical diffracted angle for these blue-green wavelengths is 35° to the normal and this may explain the central part of the band being blue-green in colour. The extreme ends of the band, which are a deep blue-violet colour, may then be due to the second order diffraction, which although absent for a value of 'a' of 420nm, that is

$$a = d/2 = z/2$$

would be present at other values. A good deal of error may, as explained earlier, be present in this figure. Certainly the only second order wavelengths are those at the extreme blue-violet end of the spectrum at angles of approximately 70° to the normal. Some blurring of this reflected light would naturally be expected over some angular range due to the scatterings etc. which must take place.

Thus an explanation of the apparently anomalous band effect is furnished - one which apparently agrees with observed results and diffraction theory. Some doubt is placed upon the value of the structure constant 'a' however.

By making the same type of calculation at say 45° incidence it is possible to make some prediction of the peak reflectance values at non-specular angles, since at such angles the collection should basically be that of the diffracted components at those angles. The computations predict a slight wavelength peak shift towards longer wavelengths for measurement at $45^{\circ}/0^{\circ}$ compared with those at $45^{\circ}/45^{\circ}$ for instance. This is shown to be correct upon measurement. Specular measurements and their predicted

theoretical curves are not affected by such ideas however as long as the detector aperture is small.

8.9 Morpho Menelaus in a Medium of Increased Refractive Index.

As a final check on the multilayer analysis a value of 1.36 was inserted in place of the value 1.00 for the refractive index of the spacing medium between horizontal plates. This would therefore duplicate the case of the menelaus wing immersed in ethyl alcohol - a liquid of refractive index 1.36.

For an angle of incidence of 45^{o} a shift in peak reflectance to a little under 600nm was obtained with an accompanying reduction in peak intensity to some one tenth of the original value in air. Although for a strict comparison it is necessary to measure the wing at specular angle when immersed, and this has earlier been explained to be difficult, the results given in Figure 8.5 are close enough to such a configuration for the accuracy of such a prediction to be verified.

Similar agreement was found for a value of the spacing index of 1.46, a comparison with measurement in carbon tetrachloride, and together these confirm again the overall correctness of the theory.

8.10 Chromaticity Coordinates.

Little emphasis has been placed so far upon chromaticity coordinates or other colorimetric methods. Their use in general is very limited here since the measuring conditions are in complete disagreement with established

proceedure, and far more information is contained in the spectral reflectance curve. A brief indication of typical values may be instructive and Figure 8.17 compares values at $45^{o}/45^{o}$ for two sets of curves, those peaking at 410nm and those at 425nm, for the actual measured values and the predicted ones. Some discrepancy is obvious between paired sets, however the spread in such results over the wing surface would more than encompass the area outlined. The fit therefore is good colorimetrically.

Turning to the other pair of points, these represent the similar measured and theoretical values for 0^{o}/Total collection, including the diffraction effect in the theoretical point. A much larger difference is obvious, this being due to the increased amount of green and decreased amount of blue in the predicted curve, such a fit is therefore not as good colorimetrically as the previous one.

8.11 The Properties of Morpho Cypris.

In the last section of the previous chapter the essential difference between the species of Morpho according to Martin (1971) was shown to be the number of horizontal plates in each vertical stack. For menelaus the number is eight and for cypris, twelve. This therefore provides a further test of the theory since the two species are almost identical in structure apart from this and the same optical processes must create the brilliant iridescent colours of each grouping.

To this end a specimen of the species cypris was mounted in the Wright Spectrophotometer and the spectral

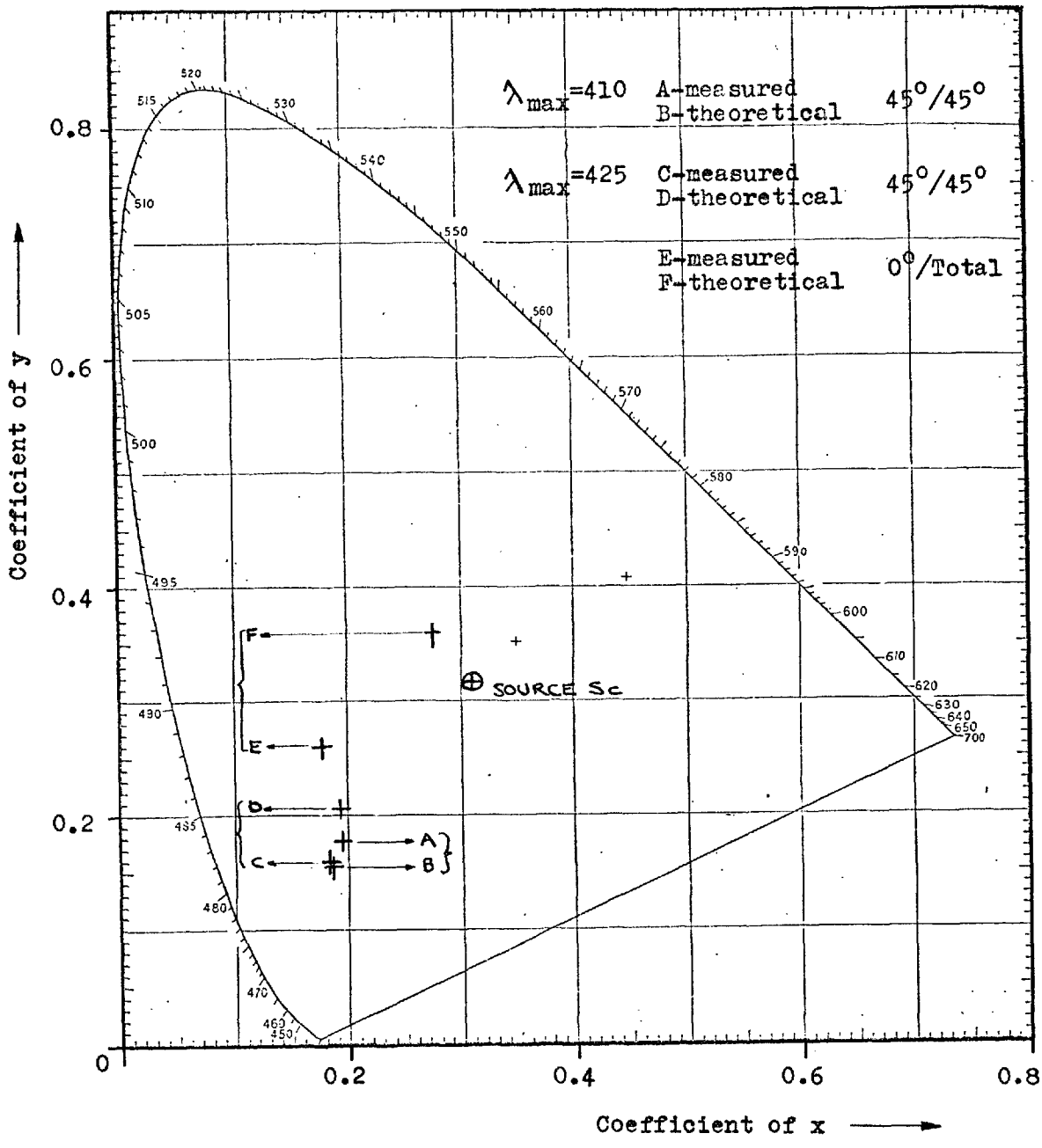


Fig. 8.17. Morpho Menelaus - Chromaticity coordinates of various spectral reflectance curves given earlier.

reflectance measured under $45^{\circ}/45^{\circ}$ configuration. The results are indicated in Figure 8.18 together with the data obtained on the menelaus under the same conditions. Figure 8.19 shows the difference in theoretical curves at 45° incidence for identical parameters, the only exception being the number of layers has been altered from 16 to 24 to correspond to the change from menelaus to cypris.

The important theoretical difference between a stack of 16 layers and one of 24 is the increased height of the maximum in the latter case, together with a marked sharpening of the entire curve around the peak - effectively reducing its half-width. The maximum remains at the same wavelength however, marked differences occurring in secondary peaks.

Turning to the measured curves, the same trend is immediately apparent. The peak intensity for cypris has increased and the width of the high reflecting zone has decreased markedly. The former observation, however, is not necessarily valid since the absolute intensity varies so much from location to location that this may just be coincidence. The second point is correct and certainly significant. Beyond the minimum at long wavelengths the presence of melanin is again detected following much the same trends as the menelaus.

The refractive index of the wing material for cypris was checked as with menelaus and found to be indistinguishable in value from the latter. The photographs of the structure do seem to indicate slightly different dimensions to those already quoted for the horizontal plates

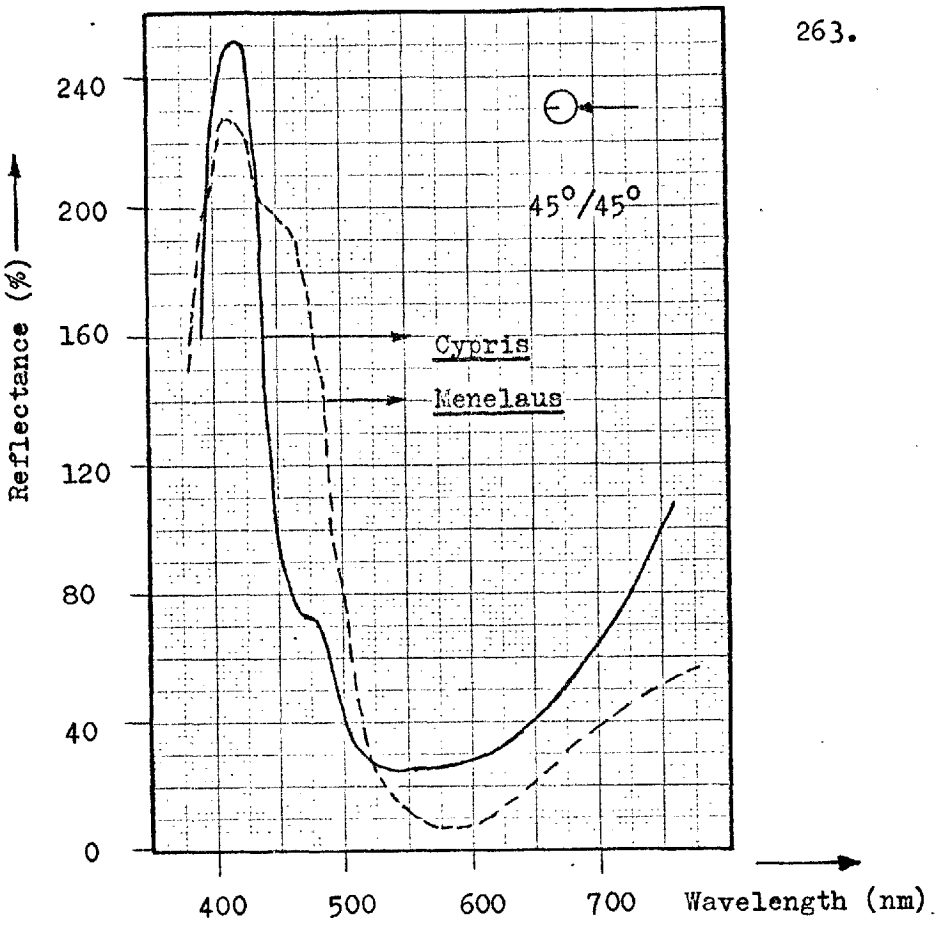


Fig. 8.18. Morpho cypris/menelaus - Comparison of spectral reflectance curves for both species under conditions 45°/45°.

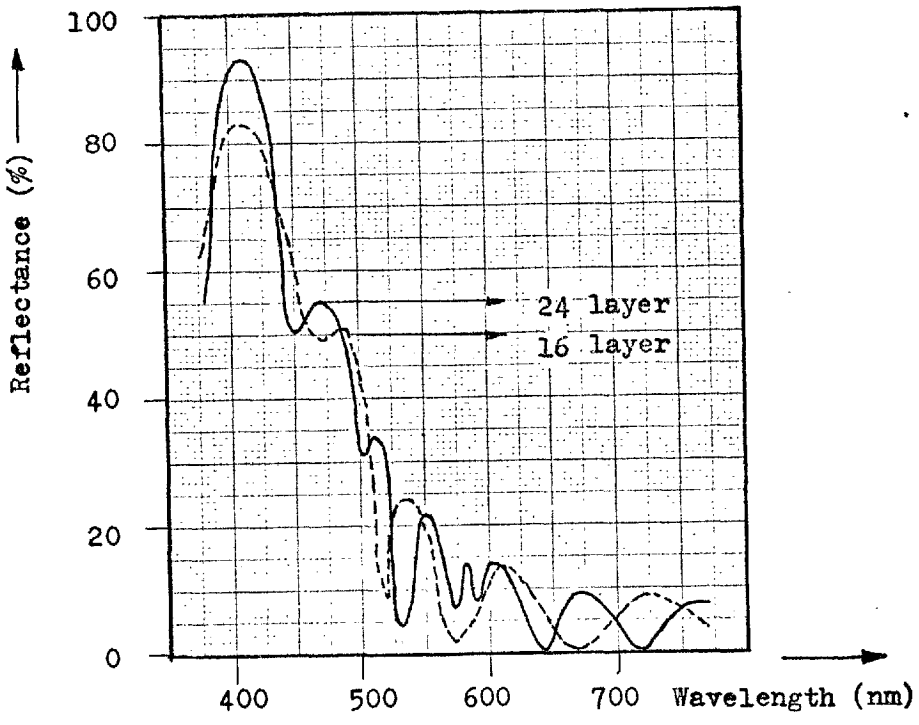


Fig. 8.19. Comparison of spectral reflectance obtained from i) 24 layer stack (——), and ii)16 layer stack (----)

and air gaps in the case of *cypris*. The relevant ones were therefore measured carefully and values for the dimensions y - the plates - and x - the air gaps - were obtained, which tended to indicate that both were of the same order, approximately 100 to 105nm each.

Using these new dimensions the spectral reflection for a 24 layer stack of alternate indices 1.50 and 1.00 was calculated for an incident angle of 45°. This is shown together with the corresponding measured curve in Figure 8.20.

The fit around the peak of the reflectance curve is good and the fall above this is also well predicted. Reflectance values around 475nm are predicted at too high a level, but there is clear evidence at this point of a secondary bump on the measured curve corresponding to a secondary maximum on the theoretical plot. The minimum is reasonably clearly predicted, followed by the usual rise at the long wavelength end due to pigmentary reflection from the melanin present beneath the structure.

On the bases evolved, the fit of the two curves appears to be good and to confirm the general theory.

Finally Figure 8.21 shows the spectral reflectance of *cypris* measured by total angular integration on the Beckman spectrophotometer together with the theoretical curve obtained from the interference plus diffraction theory outlined above. The structure dimensions used here were 100nm for both y and x. As before the fit is reasonable, the maximum being well predicted at some 20nm shorter wavelength than the equivalent one for *menelaus*. The fall

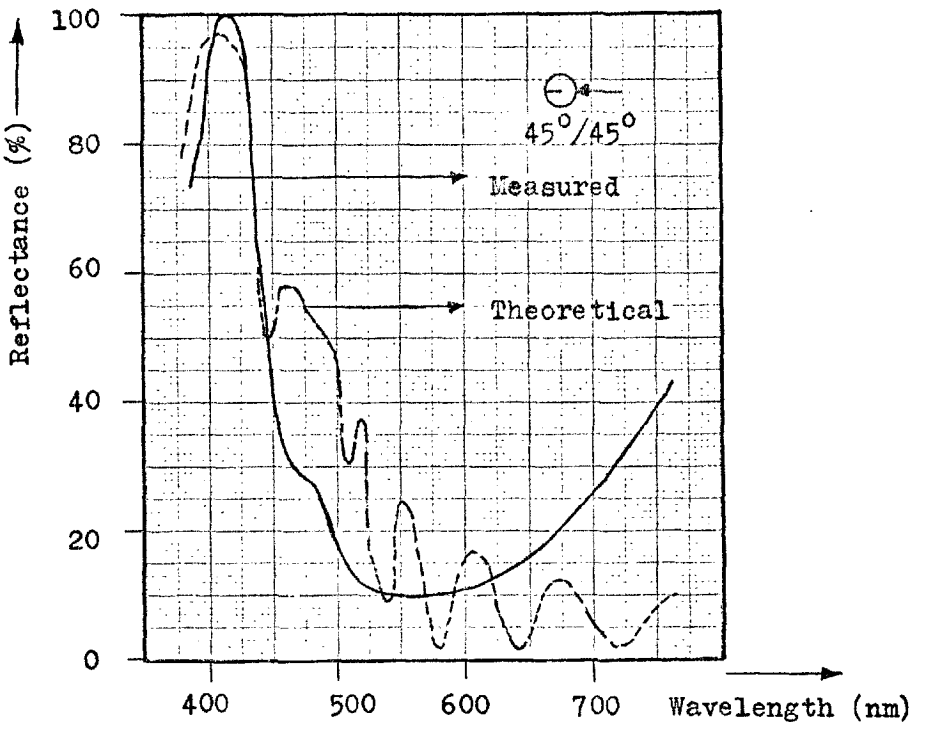


Fig. 8.20. Morpho cypris - Comparison of spectral reflectance curves i) measured (——) and ii) theoretical (---) (x=y=100nm, n=1.50) at 45°/45°.

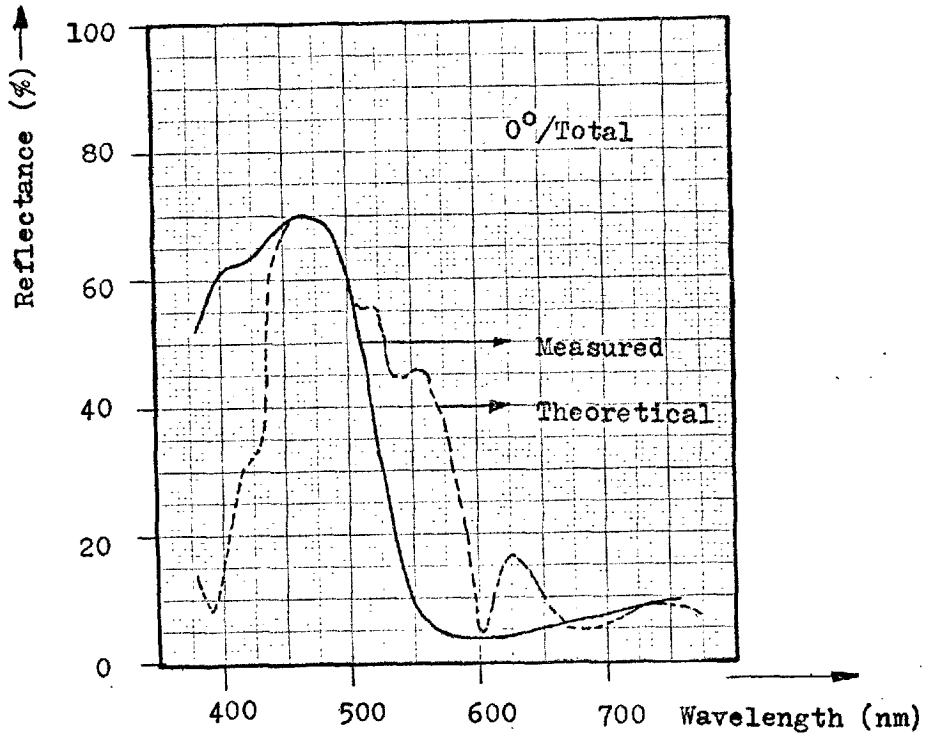


Fig. 8.21. Morpho cypris - Comparison of spectral reflectance curves i) measured (——) and ii) theoretical with diffraction included (----) at 0°/Total. Dimensions as above.

to the long wavelength minimum is in some error as before, but the minimum is itself well predicted. The maxima have again been normalised to the measured one.

It is therefore concluded that the theory predicts the reflection properties of a second species of Morpho, having a slightly different structure. This is taken as further evidence in support of such ideas.

8.12 Conclusions.

Many of the light reflecting properties of the wing material of Morpho butterflies have been measured, particularly those of the species menelaus and also cypris. The spectral composition of such light at various angles of incidence and collection has been given, together with point to point variations, and visual observations.

The known physical properties of the material have been discussed, and by measurements from the best available electron microscope photographs, and determination of the refractive index of the material, a reasonably complete picture of the physical structure has been given.

The complexity of such a small structure inevitably means that some variation in the dimensions of the basic unit is bound to be present. This was certainly observed on the photographs available, and presumably such variations must occur on an even greater scale on selecting points at numerous locations over the wing area, rather than the field of one photograph. The photographs and the spectral reflectance results describe entirely different specimens of the same species, making the possibility of

differences in such dimensions even greater.

Such a spread in structure constants is reflected in the measurements described, especially with measuring location, however very definite types of spectral reflectance curve have emerged.

Because of this it has been possible to put forward a theoretical interpretation of the basic cause of this reflected colour which is not in the main part pigmentary.

A small pigmentary reflection is obtained at long wavelengths due to the presence of melanin beneath the wing structure. Superimposed upon this are apparently the effects of both multilayer interference and diffraction. It is thought that light incident upon the wing is first diffracted by the regular striations and upon transmission through the surface is incident at all angles of diffraction on the multilayer system beneath. Some diffracted wavelengths are therefore reinforced, whilst others undergo destructive interference. The specular reflection will, in wavelength distribution, be independent of the diffraction since it represents the zero order, but will still undergo selection by the multilayer stack. The presence of vertical ribbing has been shown under certain orientations to cause a reversal of a certain proportion of the incident light, causing it to be incident on the multilayer stack at an angle directly opposite to the incident one. Thus a back reflected, spectrally selective, peak of light is obtained whose distribution is governed, as with the true specular one, by the structure constants of the material.

This together with the diffraction effects

explains the band of reflected colours formed, at normal incidence, at right angles to the scale striations, and together with the inevitable scatterings and dimension variations in such a structure explains the relatively constant luminance over this band, since a good deal of the incident flux is present in the various angular orders.

The theory seems to predict well the measured distribution of reflected light from the wing material, especially maxima shapes, peak reflectance and minima wavelengths - the pigmentary melanin reflection explaining the discrepancies at the red end of the spectrum. Such agreement was usually found to fall well within the spread of results obtained under any one measuring configuration.

By measuring firstly only specularly reflected light and then the total, angular, integrated flux, it was possible to establish separately the presence of both interference and diffraction.

Such a doubly selective system explains the major objections to a diffraction theory and the specific points regarding white reflected light at the specular angle and an apparent angular reversal of diffracted colours along the band in the hemispherical viewer.

Perhaps the least successful agreement was obtained for the angular variation in peak reflected wavelengths. Exact angular measuring conditions were difficult to obtain since it was found that the physical surface was not parallel to the top surface of the multilayer structure, but despite this agreement in the wavelength of peak reflectance was not good although predictions regarding the

overall shape of such curves remained excellent. This could be explained by errors in physical parameters, although the ones obtained from the measured peaks did not seem at all possible in practice. Strangely the dimensions obtained for cypris, approximately 100nm for both x and y, would predict a peak reflectance wavelength movement almost that measured on menelaus - namely 410nm to just below 500nm for an angular change of 45^{o} to 0^{o} under specular conditions. Considering the possible error on λ_{max} derived from such flat peaked curves this may well be significant. Only one sample of menelaus is present in all the available photographs, attempts at others not meeting as yet with the same detailed success. It is therefore possible that the obtained structure dimensions are not typical and that in practice the mean of such dimensions lies more closely to those of the cypris, similarly measured. The accuracy of microscope calibration has been checked at some 2%, however a further small error may be included due to the sectioning being other than at right angles to the plane of the photograph. Similarly, the extent to which a complete cover of gold palladium is obtained deep within the structure is difficult to assess.

A smaller value for the refractive index of the wing material would explain the results to some extent although again this was found by careful measurement and is in agreement with other workers observations.

There remains the possibility of further optical phenomena, such as selective scatterings within the material, being responsible for this, but it is difficult to be precise on this point. The presence of the transparent

scales which overlayed the blue ones cannot entirely be overlooked, their structure is similar to the iridescent scales but of a much coarser nature. In detail it is difficult to predict their purpose however.

Already suggestions have been made (Martin, 1971) that further structuring, at present unresolvable, may exist within the horizontal plates.

Despite this, the processes outlined above are held to be responsible for almost the entire reflected light, the variations in which tend to suggest to the observer a very smooth, glossy, almost metallic texture. Undoubtably this is because of the very high proportion of incident light reflected from such a structure, and its amazing angular variation.

There remains only the implications of such material. Already it is used widely for decoration and so on, although were it possible to manufacture such structures one would have a very durable, non-fading medium. The process would be extremely difficult, however, and the end product probably very fragile, although the individual wing scales in practice are extremely strong, it appears the method of laying these to the wing is the weaker point.

APPENDIX.

THE BASIC THEORY OF THIN FILMS.

Listing of Symbols Used.

$\underline{E}$ The electric vector in the electromagnetic field.

$\underline{H}$ The magnetic vector in the electromagnetic field.

$\underline{i},\underline{j},\underline{k}$ Unit vectors along the x-,y- and z- axes respectively.

λ Wavelength.

c Velocity of light in vacuo.

t Time.

n Refractive index.

$\underline{D}$ The electric displacement.

$\underline{B}$ The magnetic induction.

μ The magnetic permeability.

ε The dielectric constant.

Method.

Assume a plane electromagnetic wave of large extent to be moving as shown in Figure A.1, with relevant components E_x, E_z, H_y, towards a boundary at an angle ϕ.

Thus:-

$$\underline{E} = (E_x.\underline{i} + E_z.\underline{k}) \exp i.\frac{2\pi}{\lambda}(ct - n(\sin\phi.x + \cos\phi.z))$$

and

$$\underline{H} = H_y.\underline{j} \exp i.\frac{2\pi}{\lambda}(ct - n(\sin\phi.x + \cos\phi.z))$$

We also have from Maxwells Equations (M.K.S. units)

$$\text{curl } \underline{H} = \underline{J} + \frac{\partial \underline{D}}{\partial t} \qquad \underline{D} = \varepsilon\varepsilon_o\underline{E}$$

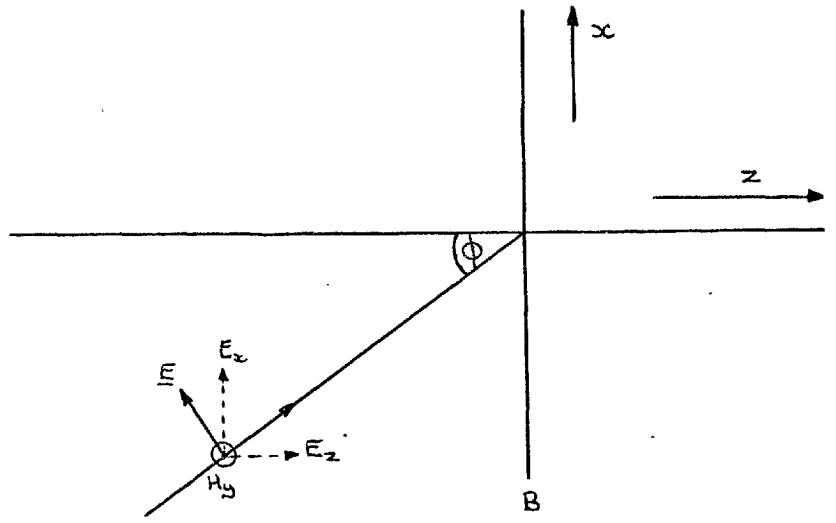


Fig. A.1. Electromagnetic wave moving towards a boundary B at an angle ϕ. (p-polarization.)

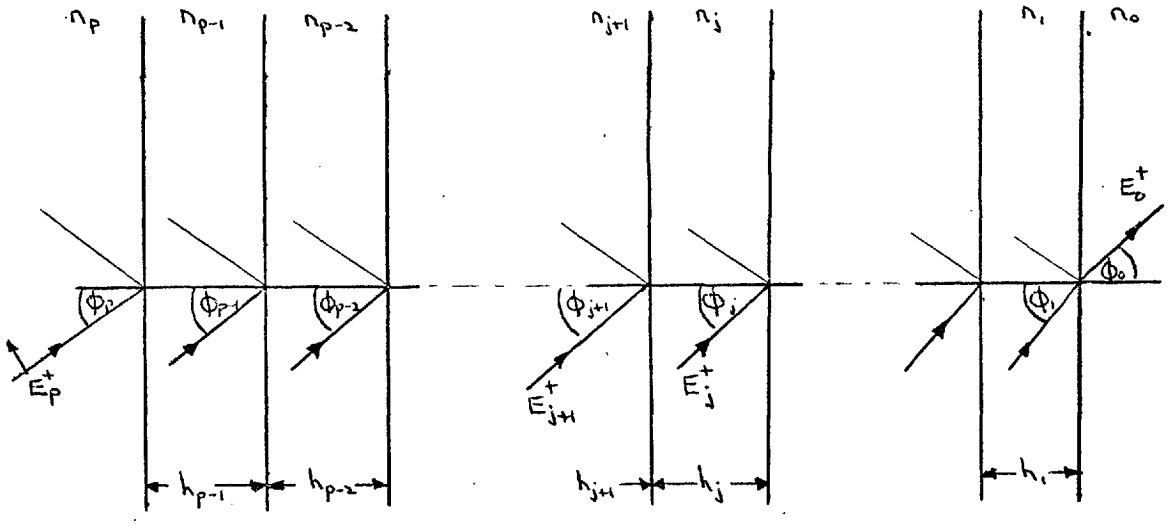


Fig. A.2. Notation used in multilayers. (p-polarization.)

where $\mathcal{E}$ = dielectric constant : $\underline{J}$ = the electric current density and $\mathcal{E}_o = \frac{1}{36} \cdot 10^{-9}$ farad / metre.

Restricting ourselves to dielectric materials : $\underline{J} = 0$

$$\therefore \text{curl } \underline{H} = \frac{\partial \underline{D}}{\partial t}$$

$$\mathcal{E}\mathcal{E}_o \frac{\partial E_x}{\partial t} = \frac{\partial H_z}{\partial y} - \frac{\partial H_y}{\partial z}$$

$$c \cdot \frac{2\pi i}{\lambda} \cdot \mathcal{E}\mathcal{E}_o E_x = H_y \cdot n \cdot \cos\phi \cdot i \frac{2\pi}{\lambda}$$

Now $n = \sqrt{\mathcal{E}\mu}$ and for most materials $\mu \sim 1$

$$\therefore n^2 = \mathcal{E}$$

Substituting above:-

$$H_y^+ = \sqrt{\frac{\mathcal{E}_o}{\mu_o}} \cdot \frac{n E_x^+}{\cos\phi}$$

since $c = 1/\sqrt{\mathcal{E}_o \mu_o}$ in free space.

(+ signs represent the beam moving along the z- direction, reflected beam z is negative and signs are -)

We therefore obtain

$$H_y^- = - \sqrt{\frac{\mathcal{E}_o}{\mu_o}} \cdot \frac{n E_x^-}{\cos\phi}$$

Both are for p-polarisation, for s-polarisation we have

$$\underline{E} = - E_y \underline{i} \exp \frac{2\pi i}{\lambda} (ct - n (\sin\phi . x + \cos\phi . z))$$

$$\underline{H} = (H_x \underline{i} + H_z \underline{k}) \exp \frac{2\pi i}{\lambda} (ct - n (\sin\phi . x + \cos\phi . z))$$

Again from Maxwells Equations

$$- \frac{\partial \underline{B}}{\partial t} = \text{curl } \underline{E} \qquad \text{and} \qquad \underline{B} = \mu\mu_o \underline{H}$$

$$-\mu\mu_o \frac{\partial H_x}{\partial t} = \frac{\partial E_z}{\partial y} - \frac{\partial E_y}{\partial z}$$

From this we obtain, similarly to above, that for s-polarisation

$$H_x^+ = \sqrt{\frac{\varepsilon_o}{\mu_o}}\, n\, E_y^+ \cos\phi$$

$$\text{and} \quad H_x^- = -\sqrt{\frac{\varepsilon_o}{\mu_o}}\, n\, E_y^- \cos\phi$$

We therefore define $\underline{H} = \sqrt{\varepsilon_o / \mu_o} \cdot u\, \underline{E}$

where

$u = n / \cos\phi$ for p-polarisation

$u = n \cdot \cos\phi$ for s-polarisation

$$\text{and} \quad \underline{H}^{\pm} = \pm \sqrt{\frac{\varepsilon_o}{\mu_o}}\, u\, \underline{E}^{\pm}$$

Referring to Figure A.2 we have a typical multilayer stack of varying refractive indices n_j and thicknesses h_j with a beam incident at an angle ϕ.

All the angles ϕ may be found from Snell's Law

$$n_{j+1} \sin\phi_{j+1} = n_j \sin\phi_j$$

The electric field is continuous across a boundary and at any time $\underline{E}$ at each boundary is the resultant of all the transmitted and reflected parts at that boundary.

Obviously $\underline{E}_0^- = 0$

Now between the two interfaces, separated by a distance h, a phase difference will occur in the exponential term since x and y remain constant while $z \longrightarrow z \pm h$.

Thus the term

$$\exp \frac{2\pi i}{\lambda} (ct - n (\sin\phi.x + \cos\phi.z))$$

becomes $$\exp \frac{2\pi i}{\lambda} (ct - n (\sin\phi.x + \cos\phi.(z \pm h)))$$

This phase difference we may write as $\exp(ig_j)$

$$\text{where } g_j = \frac{2\pi}{\lambda} n_j h_j \cos\phi_j.$$

Thus the phase factor for a positive going wave will be multiplied by $\exp(ig_j)$ while the negative going phase factor will be multiplied by $\exp(-ig_j)$. Therefore the total electric vector $\underline{E}$ at the boundary between n_{j+1} and n_j is

$$\underline{E}^+_{j+1} + \underline{E}^-_{j+1} = \underline{E}^+_j \exp(ig_j) + \underline{E}^-_j \exp(-ig_j) \quad \ldots\ldots(A)$$

Since $$\underline{H}^{\pm} = \pm \sqrt{\frac{\varepsilon_o}{\mu_o}} \cdot u \underline{E}^{\pm}$$

and writing a similar equation for the magnetic vectors

$$\underline{H}^+_{j+1} + \underline{H}^-_{j+1} = \underline{H}^+_j \exp(ig_j) + \underline{H}^-_j \exp(-ig_j)$$

we have

$$u_{j+1} (\underline{E}^+_{j+1} - \underline{E}^-_{j+1}) = u_j (\underline{E}^+_j \exp(ig_j) - \underline{E}^-_j \exp(-ig_j)) \quad \ldots(B)$$

we also have the boundary conditions

$$\underline{E}^-_0 = 0 \qquad \text{and} \qquad g_0 = 0$$

Electromagnetic radiation is a form of energy transport, and so far only electric and magnetic amplitudes have been considered. The energy associated with the wave is what is normally observed physically and the rate of flow of energy across unit area is given by the Poynting Vector

$$\underline{P} = \underline{E} * \underline{H}$$

Now E_x is of the form $E_{0x} \exp i(\omega t - kz)$ whose real part is $E_{0x} \cos(\omega t - kz)$.

Similarly $H_y = H_{0y} \cos(\omega t - kz)$

$$\therefore \underline{P} = \underline{E} * \underline{H} = |\underline{E}| \cdot |\underline{H}| \cos^2(\omega t - kz)$$

The mean value of this is

$$\underline{P} = \tfrac{1}{2} |\underline{E}| \cdot |\underline{H}|$$

due to the rapid oscillations and $\underline{H} = \sqrt{\varepsilon_0/\mu_0}\ u\ \underline{E}$

$$\therefore \underline{P} = \tfrac{1}{2} |\underline{E}|^2\ u \sqrt{\varepsilon_0/\mu_0} \qquad \text{.....(C)}$$

If $\underline{A}$ be the incident electric vector at a boundary, and $\underline{R}$ the reflected one from the same boundary, the reflection factor

$$= \frac{\text{reflected power}}{\text{incident power}} = \frac{\tfrac{1}{2} |\underline{R}|^2\ u\sqrt{\varepsilon_0/\mu_0}}{\tfrac{1}{2} |\underline{A}|^2\ u\sqrt{\varepsilon_0/\mu_0}} = \frac{|\underline{R}|^2}{|\underline{A}|^2} \qquad \text{.....(D)}$$

Therefore for p-polarisation

$$E_x = \hat{\underline{E}} \cos\phi \qquad \text{and} \qquad E_z = \hat{\underline{E}} \sin\phi$$

$\therefore$ Total electric vector

$$\hat{\underline{E}} = E_x / \cos\phi$$

$$\underline{A} = \hat{\underline{E}}_p^+ = \underline{E}_p^+ / \cos\phi_p$$

$$\underline{R} = \hat{\underline{E}}_p^- = \underline{E}_p^- / \cos\phi_p$$

$$\therefore \text{The reflection coefficient} = \frac{|\underline{R}|^2}{|\underline{A}|^2} = \left| \frac{\underline{E}_p^-}{\underline{E}_p^+} \right|^2$$

This also holds for s-polarisation.

We now have the basic information and can derive the relevant methods of calculating the reflection coefficients of a general thin film stack.

$$\underline{E}_j = \underline{E}_j^+ + \underline{E}_j^- \quad \text{by definition}$$

$$\text{and } \underline{H}_j = \underline{H}_j^+ + \underline{H}_j^- = u_j (\underline{E}_j^+ - \underline{E}_j^-)$$

By solving these we have

$$\underline{\underline{E}_j^{\pm} = \tfrac{1}{2} (\underline{E}_j \pm \underline{H}_j / u_j)} \qquad \text{.....(E)}$$

$$\underline{E}_{j+1} = \underline{E}_{j+1}^+ + \underline{E}_{j+1}^- = \underline{E}_j^+ \exp(ig_j) + \underline{E}_j^- \exp(-ig_j) \quad \text{from (A)}$$

Substituting from (E) we have

$$\underline{E}_{j+1} = \tfrac{1}{2}(\underline{E}_j + \underline{H}_j/u_j) \exp(ig_j) + \tfrac{1}{2}(\underline{E}_j - \underline{H}_j/u_j) \exp(-ig_j)$$

$$= \underline{E}_j((\exp(ig_j)+\exp(-ig_j))/2) + \frac{\underline{H}_j}{u_j}((\exp(ig_j)-\exp(-ig_j))/2)$$

$$\therefore \underline{\underline{E}_{j+1} = \underline{E}_j \cos g_j + \frac{\underline{H}_j}{u_j} i \sin g_j} \qquad \text{.....(F)}$$

Also $\underline{H}_{j+1} = \underline{H}_{j+1}^+ + \underline{H}_{j+1}^- = u_{j+1}(\underline{E}_{j+1}^+ - \underline{E}_{j+1}^-)$

$$= u_j \underline{E}_j^+ \exp(ig_j) - u_j \underline{E}_j^- \exp(-ig_j)$$

$$= \frac{u_j}{2}(\underline{E}_j + \frac{\underline{H}_j}{u_j}) \exp(ig_j) - \frac{u_j}{2}(\underline{E}_j - \frac{\underline{H}_j}{u_j}) \exp(-ig_j)$$

$$\underline{H}_{j+1} = u_j \underline{E}_j((\exp(ig_j)-\exp(-ig_j))/2) + \underline{H}_j((\exp(ig_j)+\exp(-ig_j))/2)$$

$$\therefore \underline{\underline{H}_{j+1} = i u_j \underline{E}_j \sin g_j + \underline{H}_j \cos g_j} \qquad \text{.....(G)}$$

Equations (F) and (G) may be represented by the matrices:-

$$\begin{pmatrix} \underline{E}_{j+1} \\ \underline{H}_{j+1} \end{pmatrix} = \begin{pmatrix} \cos g_j & \frac{i}{u_j} \sin g_j \\ i\, u_j \sin g_j & \cos g_j \end{pmatrix} \begin{pmatrix} \underline{E}_j \\ \underline{H}_j \end{pmatrix}$$

or

$$\begin{pmatrix} \underline{E}_{j+1} \\ \underline{H}_{j+1} \end{pmatrix} = M_j \begin{pmatrix} \underline{E}_j \\ \underline{H}_j \end{pmatrix}$$

Also

$$\begin{pmatrix} \underline{E}_j \\ \underline{H}_j \end{pmatrix} = M_{j-1} \begin{pmatrix} \underline{E}_{j-1} \\ \underline{H}_{j-1} \end{pmatrix}$$

and therefore

$$\begin{pmatrix} \underline{E}_{j+1} \\ \underline{H}_{j+1} \end{pmatrix} = M_j \cdot M_{j-1} \begin{pmatrix} \underline{E}_{j-1} \\ \underline{H}_{j-1} \end{pmatrix}$$

In general

$$\begin{pmatrix} \underline{E}_p \\ \underline{H}_p \end{pmatrix} = M_{p-1} M_{p-2} \cdots M_{j+1} M_j \cdots M_2 M_1 \begin{pmatrix} \underline{E}_1 \\ \underline{H}_1 \end{pmatrix}$$

Thus intermediate values of $\underline{E}$ and $\underline{H}$ are not required and

$$\begin{pmatrix} \underline{E}_1 \\ \underline{H}_1 \end{pmatrix} = \begin{pmatrix} \cos g_0 & \frac{i}{u_0} \sin g_0 \\ i\, u_0 \sin g_0 & \cos g_0 \end{pmatrix} \begin{pmatrix} \underline{E}_0 \\ \underline{H}_0 \end{pmatrix}$$

but

$$g_0 = 0 \quad \text{also} \quad \underline{E}_0 = \underline{E}_0^+ + \underline{E}_0^- \quad \text{and} \quad \underline{E}_0^- = 0 \qquad \underline{E}_0 = \underline{E}_0^+$$

$$H_0 = \underline{H}_0^+ + \underline{H}_0^- = u_0 \underline{E}_0^+ + u_0 \underline{E}_0^- = u_0 \underline{E}_0^+$$

$$\therefore \begin{pmatrix} \underline{E}_1 \\ \underline{H}_1 \end{pmatrix} = \begin{pmatrix} 1 & 0 \\ 0 & 1 \end{pmatrix} \begin{pmatrix} \underline{E}_0^+ \\ u_0 \underline{E}_0^+ \end{pmatrix}$$

By expanding the above matrix

$$\underline{E}_1 = \underline{E}_0^+$$

$$\underline{H}_1 = u_0 \underline{E}_0^+$$

Thus we may write in general:-

$$\begin{pmatrix} \underline{E}_p \\ \underline{H}_p \end{pmatrix} = M_{p-1} \cdots\cdots\cdots M_1 \begin{pmatrix} 1 \\ u_0 \end{pmatrix} \underline{E}_0^+$$

Thus each film in the stack is represented by its own matrix, making computations on repetitive systems much more straightforward.

Let us now assume we can write

$$\begin{pmatrix} \underline{E}_p \\ \underline{H}_p \end{pmatrix} = M \begin{pmatrix} 1 \\ u_0 \end{pmatrix} \underline{E}_0^+$$

where matrix

$$M = \begin{pmatrix} m_{11} & im_{12} \\ im_{21} & m_{22} \end{pmatrix}$$

Now

$$\underline{E}_p = (m_{11} + im_{12}u_0)\, \underline{E}_0^+$$

$$\underline{H}_p = (im_{21} + m_{22}u_0)\, \underline{E}_0^+$$

By definition

$$\underline{E}_p = \underline{E}_p^+ + \underline{E}_p^-$$

$$\underline{H}_p = \underline{H}_p^+ + \underline{H}_p^- = u_p (\underline{E}_p^+ - \underline{E}_p^-)$$

$$\underline{E}_p = \underline{E}_p^+ + \underline{E}_p^- = (m_{11} + im_{12}u_0)\, \underline{E}_0^+$$

.....(H)

and $\underline{H}_p = u_p (\underline{E}_p^+ - \underline{E}_p^-) = (im_{21} + m_{22}u_0) \underline{E}_0^+$

.....(I)

From u_p.(H) + (I) we have

$$2u_p\underline{E}_p^+ = ((m_{11}u_p + m_{22}u_0) + i(m_{12}u_0u_p + m_{21})) \underline{E}_0^+$$

and from u_p.(H) - (I) we have

$$2u_p\underline{E}_p^- = ((m_{11}u_p - m_{22}u_0) + i(m_{12}u_0u_p - m_{21})) \underline{E}_0^+$$

Therefore we obtain the reflection coefficient

$$= \left| \frac{\underline{E}_p^-}{\underline{E}_p^+} \right|^2 = \left| \frac{(m_{11}u_p - m_{22}u_0) + i(m_{12}u_pu_0 - m_{21})}{(m_{11}u_p + m_{22}u_0) + i(m_{12}u_pu_0 + m_{21})} \right|^2$$

.....(J)

We may similarly obtain the transmission coefficient

$$= \left| \frac{\underline{E}_0^+}{\underline{E}_p^+} \right|^2 = \left| \frac{2\,u_p}{(m_{11}u_p + m_{22}u_0) + i(m_{12}u_pu_0 + m_{21})} \right|^2$$

.....(K)

Thus by finding the matrix M_j for each film, and therefore the entire matrix M, it is possible to substitute the elements of this matrix in equations such as (J) and (K) to derive the properties of the stack.

For the menelaus let W = wing material and A = air.

$$M_W = \begin{pmatrix} \cos g_W & \frac{i}{u_W} \sin g_W \\ i\, u_W \sin g_W & \cos g_W \end{pmatrix}$$

$$\text{and } M_A = \begin{pmatrix} \cos g_A & \frac{i}{u_A} \sin g_A \\ i\, u_A \sin g_A & \cos g_A \end{pmatrix}$$

where $g_W = \frac{2\pi}{\lambda} n_W h_W \cos \phi_W$: $g_A = \frac{2\pi}{\lambda} n_A h_A \cos \phi_A$.

Finally

$$\underline{M = (M_W \cdot M_A)^8}$$

and for <u>cypris</u>

$$\underline{M = (M_W \cdot M_A)^{12}}$$

Obviously for such spectral calculations computer methods are necessary.

(General treatment of certain thin film theory is to be found in Born and Wolf (1970), Weinstein (1954) and Macleod (1969).)

REFERENCES.

ANDERSON T.F. and RICHARDS A.G. (1942) J. Applied Physics, 13, 748.

BARKAS W.W. (1939) Proc. Phys. Soc. 51, 274.

BARTLESON C.J. (1959) Phot. Sci. Eng., 3, 114.

BARTLESON C.J. and BRAY C.P. (1962) Phot. Sci. Eng., 6, 19.

BECKMANN P. and SPIZZICHINO A. (1963) The Scattering of Electromagnetic Waves from Rough Surfaces. Pergamon.

BENNETT H.E. and PORTEUS J.O. (1961) J. Opt. Soc. Am., 51, 123.

BILLMEYER F.W., LEWIS D.L. and DAVIDSON J.G. (1971) Color Eng., 9, 31.

BILLMEYER F.W. and MARCUS R.T. (1969) Applied Optics, 8, 763.

BLET-TALBOT D. (1955) Rev. d'Opt., 34, 579.

BORN M. and WOLF E. (1970) Principles of Optics. Pergamon. 4th Edition.

BOSHOFF M.C. (1957) Ph.D. Thesis. University of London.

BRODERSEN S. (1954) J. Opt. Soc. Am., 44, 22.

BUC G.L. and STEARNS E.I. (1945) J. Opt. Soc. Am., 35, 521.

CAHN L. and HENDERSON B.D. (1958) J. Opt. Soc. Am., 48, 380.

CHINMAYANANDAM T.K. (1919) Phys. Rev., 13, 96.

COMMISSION INTERNATIONALE DE L'ECLAIRAGE. (1931) Compte Rendu, p19.

COMMISSION INTERNATIONALE DE L'ECLAIRAGE. (1959) Compte Rendu, Report of Committee E - 1.3.1.

COMMISSION INTERNATIONALE DE L'ECLAIRAGE. (1963) Compte Rendu, Report of Committee E - 1.3.1.

COMMISSION INTERNATIONALE DE L'ECLAIRAGE. (1967) Compte Rendu, Report of Committee E - 1.3.1.

CRAWFORD B.H. (1971) Private Communication.

DE KERF J.L.F. (1958) J. Opt. Soc. Am. 48, 334.

EBERHARDT W.H. (1950) J. Opt. Soc. Am. 40, 172.

EVANS R.M. (1959) Eye, Film, and Camera in Color Photography. Wiley.

EVANS R.M. (1946) British Patent 660,099. U.S. Patent 2,571,697.

FOX D.L. (1953) Animal Biochromes and Structural Colours. C.U.P.

GIBSON K.S. (1949) Spectrophotometry, N.B.S. Circular, 484.

GIBSON K.S. and KEEGAN H.J. (1938) J. Opt. Soc. Am., 28, 372.

GORDON-SMITH G.W. (1952) Proc. Phys. Soc. B, 65, 275.

GRANVILLE W.C. and JACOBSON E. (1944) J. Opt. Soc. Am., 34, 382.

GRASSMANN H. (1853) Poggendorffs Ann., 89, 69.

GREENEWALT C.H., BRANDT W. and FRIEL D.D. (1960) J. Opt. Soc. Am., 50, 1005.

GUILD J. (1931) Phil. Trans. Roy. Soc. A, 230, 149.

HARDY A.C. and YOUNG F.M. (1949) J. Opt. Soc. Am., 39, 265.

HARRISON V.G.W. (1950) J.O.C.C.A., 36, 569.

HEIDENREICH R.D. (1942) Phys. Rev., 62, 291.

HUNT R.W.G. (1965) J. Opt. Soc. Am., 55, 1540.

HUNT R.W.G. (1967) The Reproduction of Colour. Fountain Press. 2nd Edition.

HUNTER R.S. (1937) J. Research Natl. Bur. Stds., 18, 19, Rp 958.

HUNTER R.S. and JUDD D.B. (1939) A.S.T.M. Bull. 97, 11.

JUDD D.B. (1930) J. Research Natl. Bur. Stds. 4, 515.

JUDD D.B. and WYSZECKI G. (1963) Color in Business, Science and Industry. Wiley. 2nd Edition.

KEEGAN H.J., SCHLETER J.C. and JUDD D.B. (1962) J. Research Natl. Bur. Stds., 66A, 203.

LONGHURST R.S. (1967) Geometrical and Physical Optics. Longmans. 2nd Edition.

MACADAM D.L. (1951) J. Soc. Mot. Pic. Tel. Eng., 56, 487.

MACADAM D.L. (1953) J. Opt. Soc. Am., 43, 533.

MACADAM D.L. (1954) J. Opt. Soc. Am., 44, 713.

MACLEOD H.A. (1969) Thin-Film Optical Filters. Hilger.

MARTIN B. (1971) Private Communication - to be published.

MASON C.W. (1927) J. Phys. Chem., 31, 321.

MERRITT E. (1925) J. Opt. Soc. Am., 11, 93.

MICHELSON A.A. (1911) Phil. Mag., 21, 554.

MIDDLETON W.E.K. and SANDERS C.L. (1951) J. Opt. Soc. Am., 41, 419.

MILLER W.H., BERNARD C.D. and ALLEN J.L. (1968) Science, 162, 760.

NIMEROFF I. (1952) J. Research Natl. Bur. Stds., 48, 441. Rp 2335.

NIMEROFF I. (1953) J. Opt. Soc. Am., 43, 531.

OPTICAL SOCIETY OF AMERICA (1953) Committee on Colorimetry, The Science of Color, Thomas Y. Crowell Co., New York.

PERRY J.W. (1958) Nature, 181, 1704.

PILLAI P.K.C. (1968) J. Opt. Soc. Am., 58, 1019.

POLYANSKII V.K. and RVACHEV V.P. (1966) Optics and Spectroscopy, 20, 391.

PRESTON J.S. (1929-30) Trans. Opt. Soc. (London), 31, 15.

RAYLEIGH LORD (1919) Phil. Mag., 37, 98.

RAYLEIGH LORD (1923) Proc. Roy. Soc. A, 103, 233.

RICHTER M. (1955) J. Opt. Soc. Am., 45, 223.

ROBERTSON A.R. (1965) Ph.D. Thesis. University of London.

ROBERTSON A.R. and WRIGHT W.D. (1965) J. Opt. Soc. Am., 55, 694.

SANDERS J.V. (1964) Nature, 204, 1151.

SCHRODINGER E. (1925) Sitz. Akad. Wiss., Wien, Abt. 11a, 134, 471.

SHIPLEY T. and WALKER G.L. (1956) J. Opt. Soc. Am., 46, 1052.

SPERANSKAYA N.I. (1959) Optics and Spectroscopy, 7, 424.

STILES W.S. (1955) Optica Acta, 2, 168.

STILES W.S. and BURCH J.M. (1959) Optica Acta, 6, 1.

TELLEX P.A. and WALDRON J.R. (1955) J. Opt. Soc. Am., 45, 19.

TOPORETS A.S. (1964) Optics and Spectroscopy, 16, 54.

VALYUS N.A. (1966) Stereoscopy, Focal Press.

WEINSTEIN W. (1954) Vacuum, 4, 3.

WRIGHT W.D. (1928-29) Trans. Opt. Soc., 30, 141.

WRIGHT W.D. (1941) Proc. Phys. Soc., 53, 93.

WRIGHT W.D. (1948) J. Brit. Kinemat. Soc., 13, 1.

WRIGHT W.D. (1954) Optica Acta, 1, 102.

WRIGHT W.D. (1957) Nature, 179, 179.

WRIGHT W.D. (1959) J. Opt. Soc. Am., 49, 384.

WRIGHT W.D. (1964) Symp. Colour and Life. (Inst. Biology, London, 1964), pp 1-11.

WRIGHT W.D. (1967) The Rays are not Coloured. Hilger.

WRIGHT W.D. (1969) The Measurement of Colour. Hilger.

WYSZECKI G. and STILES W.S. (1967) Color Science. Wiley.

ACKNOWLEDGEMENTS.

I wish to express my thanks to Prof. W.D. Wright for suggesting this research project and for constant advice and encouragement throughout the period of this study.

Similar thanks are also extended to all members of the Applied Optics Section, Imperial College, and in particular Dr. B.H. Crawford, Dr. L. Planskoy and Dr. K.H. Ruddock for both introducing the art of colour measurement to me and many helpful discussions during the course of the research.

I am also greatly indebted to Mr. B. Martin and the Electron Microscope Unit of the British Museum (Natural History) for permission to reproduce their excellent photographs in Chapter Seven and use them to determine necessary parameters for the work.

The work has been supported by a grant from the Science Research Council which is gratefully acknowledged.

Finally, my thanks to my wife, Ann, to whom all this was always obvious.

Corrigenda.

Page 86 Scale of Photograph Omitted - Each sample is 28mm square.

Page 167 Line 11 - Figure 6.6 should read Figure 6.11.

Page 169 Line 26 - Continued to read

(..... Such a comparison, especially in a coordinate system as visually non-linear as the x-y space, is only valid in an application such as the present one where the comparison of colour difference is made within a small area of colour space), ... and in the direction of one particular variable, e.g. excitation purity.

Page 188 Line 16 - integrating spere should read integrating sphere.

Additional References.

BARTLESON C.J. and BRENEMAN E.J. (1967) Phot. Sci. Eng., 11, 254

BRENEMAN E.J. (1962) Phot. Sci. Eng., 6, 172.

HUNT R.W.G. (1950) J. Opt. Soc. Am., 40, 362.

HUNT R.W.G. (1952) J. Opt. Soc. Am., 42, 190.

HUNT R.W.G. (1967) The Reproduction of Colour, Fountain Press, 2nd Edition, pp 325-326.

HUNT R.W.G. (1969) Brit. Kinemat., Sound and Tel. J., 51, 268.